



NATIONAL TECHNICAL UNIVERSITY OF ATHENS  
SCHOOL OF NAVAL ARCHITECTURE AND MARINE ENGINEERING

# **MODULAR THERMODYNAMIC SIMULATION OF THE CLOSED CYCLE PERIOD FOR A CYLINDER OF A LARGE MARINE DIESEL ENGINE**

DIPLOMA THESIS

**ELEFThERIOS DEDES**

SUPERVISOR: PROFESSOR NIKOLAOS KYRTATOS

JULY 2009

## Contents

List of Figures.....	3
List of Tables.....	6
Acknowledgements.....	7
1 Introduction.....	8
2 Mathematical Equations .....	11
2.1 Gas Properties .....	11
2.2 Open Thermodynamic System .....	16
2.3 Valve .....	21
2.4 Compressor .....	25
2.5 Intercooler (Heat Exchanger) .....	29
2.6 Turbine .....	32
2.7 Combustion Model S Curve.....	38
2.8 Heat Transfer Elements.....	40
2.8.1 Conduction .....	40
2.8.2 Convection.....	41
2.8.3 Radiation.....	43
2.9 Cylinder Geometry .....	46
2.10 Geometrical Energy Loss .....	51
3 Simulation Blocks.....	53
3.1 Block Library .....	54
3.2 Major Blocks .....	55
3.2.1 Turbocharger and Intercooler blocks .....	55
3.2.2 Inlet and Exhaust Valve Blocks .....	59
3.2.3 Open Thermodynamic System and Gas Properties Block .....	63
3.2.4 Fixed Fluid and Gas Properties Block.....	65
3.2.5 Cylinder Heat Transfer Block .....	66
3.2.6 Combustion Block.....	68
3.2.7 One Cylinder Block .....	69
3.2.8 Eight cylinders block .....	70
4 Simulation Results .....	71
4.1 Test examples.....	71
4.1.1 Two gas containers connected through a valve .....	71
4.1.2 Heat Transfer.....	75

4.1.3	Cylinder Geometry .....	81
4.1.4	Compressor and Intercooler test .....	88
4.1.5	Turbine test .....	92
4.2	One cylinder engine example .....	96
5	Conclusions.....	117
6	References .....	118
Appendices .....		119
—	Appendix A .....	120
—	Appendix B.....	132
	Complete engine example.....	132
—	Appendix C.....	140
—	Appendix D .....	141

## List of Figures

Fig. 2-1 Block: Gas Properties .....	15
Fig. 2-2 Block: Open Thermodynamic System .....	20
Fig. 2-3 Block: Valve.....	24
Fig. 2-4 Block: Compressor .....	28
Fig. 2-5 Block: Intercooler.....	31
Fig. 2-6 Block: Turbine .....	36
Fig. 2-7 Turbine Sub block 1 .....	37
Fig. 2-8 Turbine sub block 2.....	37
Fig. 2-9 Block: S - Curve Combustion.....	39
Fig. 2-10 Block: conduction Heat Flux Block.....	41
Fig. 2-11 Block: Convection Heat Transfer .....	42
Fig. 2-12 Block: Radiation Heat Transfer .....	46
Fig. 2-13 Basic length, angle and torque developed to crankshaft due to gas forces .....	47
Fig. 2-14 Block: Cylinder Geometry .....	50
Fig. 2-15 Typical cylinder arrangement .....	50
Fig. 2-16 Block: Geometrical Energy Loss.....	52
Fig. 3-1 Simulink Block Library with 19 elements.....	54
Fig. 3-2 Block: Compressor .....	56
Fig. 3-3 Block: Intercooler.....	57
Fig. 3-4 Block: Turbine .....	58
Fig. 3-5 Turbocharger Major Block .....	58
Fig. 3-6 Inlet Valve's Equivalent area vs crankshaft's Angle .....	60
Fig. 3-7 Block: Inlet Valve .....	60
Fig. 3-8 Exhaust Valve's Equivalent area vs crankshaft's Angle.....	61
Fig. 3-9 Block: Exhaust Valve .....	62
Fig. 3-10 Major Block: Gas Properties and Open Thermodynamic System.....	64
Fig. 3-11 Major Block: Fixed Fluid and Gas Properties .....	65
Fig. 3-12 Cylinder and Exhaust Valve heat transfer implementation .....	66
Fig. 3-13 Cylinder Heat Transfer major block.....	67
Fig. 3-14 Block: S - Curve Combustion.....	68
Fig. 3-15 One cylinder major block.....	69
Fig. 3-16 MAN 8K90MC-C6 Cylinders .....	70
Fig. 4-1 Configuration of mass flow through a valve.....	71
Fig. 4-2 Temperature mass and pressure of container one .....	73
Fig. 4-3 Temperature, mass and specific burned fuel mass fraction of container two.....	74
Fig. 4-4 Pressure, mass flow and enthalpy change rate of container two .....	74
Fig. 4-5 Cross Section of configuration of heat transfer through wall .....	75
Fig. 4-6 Block Representation of the Example.....	78
Fig. 4-7 Heat flux and temperature at capacitors A, B and heat sink and temperature difference .....	79
Fig. 4-8 Heat flux due to conduction and convection and temperature difference from convection block.....	79
Fig. 4-9 Heat flux elements and total at capacitors A, B and heat Sink.....	80
Fig. 4-10 Configuration of piston connected to crankshaft.....	81

Fig. 4-11 Geometry and Energy Loss Elements test .....	84
Fig. 4-12 Pressure loss elements at pressure loss block.....	85
Fig. 4-13 Friction heat, temperature and cylinder's torque and polar inertia .....	85
Fig. 4-14 Upper cylinder: volume change rate, volume, linear velocity and linear position...	86
Fig. 4-15 Lower cylinder: volume change rate, volume, linear velocity and linear position...	86
Fig. 4-16 Crankshaft's angular velocity, angular position and angular position based on engine's cycle.....	87
Fig. 4-17 Compressor and heat exchanger coupled between an infinite volume gas and a gas container .....	88
Fig. 4-18 Compressor Intercooler fitted between infinite volume and gas container .....	89
Fig. 4-19 temperature, pressure, mass increase and Enthalpy change rate of gas container	90
Fig. 4-20 Intercooler's downstream temperature, pressure and mass flow to container .....	91
Fig. 4-21 Compressor's Pressure Ratio, mass flow, efficiency and Torque absorbed .....	91
Fig. 4-22 Configuration of turbine fitted between gas container and infinite volume .....	92
Fig. 4-23 Turbine connected to finite and infinite volumes .....	92
Fig. 4-24 Turbine swallowing capacity map versus pressure ratio.....	93
Fig. 4-25 Turbine stagnation to static isentropic efficiency map .....	93
Fig. 4-26 Temperature, Pressure and Entrapped Mass drop of gas container 1 .....	94
Fig. 4-27 Enthalpy change rate, mass flow to container 1, mean and Actual Temperature Increase .....	95
Fig. 4-28 Turbine's mass flow, efficiency and torque developed .....	95
Fig. 4-29 One cylinder engine configuration .....	96
Fig. 4-30 Simulation temperature (top) and pressure of cylinder.....	98
Fig. 4-31 Inlet port (top) and exhaust valve mass flow to or from cylinder .....	99
Fig. 4-32 Cylinder developed torque (top) and moment of inertia.....	100
Fig. 4-33 Cylinder trapped mass (top) and equivalence ratio .....	101
Fig. 4-34 Instantaneous volume of cylinder (top) and burning fuel rate of combustion .....	101
Fig. 4-35 Simulated temperature (top) and pressure of cylinder (75%) .....	103
Fig. 4-36 Torque (top) and polar inertia developed by cylinder (75%) .....	104
Fig. 4-37 Inlet port (top) and exhaust valve mass flow to or from cylinder (75%).....	104
Fig. 4-38 Trapped mass and equivalence ratio inside cylinder (75%) .....	105
Fig. 4-39 Simulation temperature (top) and pressure of cylinder (50%) .....	106
Fig. 4-40 Inlet port (top) and exhaust valve mass flow to or from cylinder (50%).....	107
Fig. 4-41 Cylinder developed torque (top) and moment of inertia (50%).....	107
Fig. 4-42 Cylinder trapped mass (top) and equivalence ratio (50%) .....	108
Fig. 4-43 Temperature (top) and pressure traces for different combustion parameters .....	109
Fig. 4-44 Temperature (top), pressure traces for different combustion constants .....	110
Fig. 4-45 Torque developed per cycle (top) and moment of inertia .....	111
Fig. 4-46 greater detail (top) of figure Fig. 4-45 .....	112
Fig. 4-47 Mass flow from inlet port (top) and exhaust valve .....	112
Fig. 4-48 Trapped mass inside cylinder (top) and equivalence ratio.....	113
Fig. 4-49 Details of Fig. 4-48 (top) and equivalence ratio .....	113
Fig. 4-50 Temperature (top) and pressure trace for one cylinder, for different values of injected fuel.....	114

Fig. 4-51 Temperature (top) and pressure trace for one cylinder, for different values of clearance volume .....	115
Fig. 4-52 greater detail of Fig. 4-51 .....	115
Fig. 0-1 Engine Configuration .....	132
Fig. 0-2 Heat Transfer area versus piston position for convection HTB2 .....	135
Fig. 0-3 Heat Transfer area versus piston position for convection HTG2.....	136
Fig. 0-4 Heat Transfer area versus piston position for conduction HTA3 .....	136
Fig. 0-5 Heat Transfer area versus piston position for convection HTB2 .....	136
Fig. 0-6 Heat Transfer area versus crankshaft position between the exhaust valve disk and cylinder head EVA2.....	137
Fig. 0-7 MAN 8K90MC-C6 implementation .....	139

## List of Tables

Table 3-1 Simulation groups.....	53
Table 4-1: Container and Valve Data.....	72
Table 4-2: Carbon Steel Properties.....	75
Table 4-3 Alusil Properties.....	76
Table 4-4 Water Properties .....	76
Table 4-5 Heat Transfer Block Data .....	77
Table 4-6 Heat Capacitors Data.....	77
Table 4-7 Geometry and Heat Capacitor Data .....	83
Table 4-8 Geometry loss and Pressure of Cylinder's Volume Data .....	83
Table 4-9 Data for Open thermodynamic system, fixed fluid and geometry of the container	89
Table 4-10 Dimensions of MAN NA70/TO9098 Turbocharger .....	89
Table 4-11 Data used in the example.....	93
Table 4-12 Phase of phenomenon versus crank angle.....	97
Table 4-13 Inlet and exhaust manifold temperature, pressure at 90% load .....	102
Table 4-14 Inlet and exhaust manifold temperature and pressure at 75% load measured <sup>3</sup>	103
Table 4-15 Inlet and exhaust manifold temperature, pressure at 50% load .....	106
Table 4-16 Constant sets for combustion model .....	109
Table 4-17 Constant values for parametric runs at 75% load .....	110
Table 4-18 Combustion constants and fuel injected per cycle .....	114
Table 4-19 Combustion constants and clearance volume of cylinder .....	114
Table 0-1 Developed S - Functions .....	120
Table 0-2 Inlet Plenum geometry and gas properties.....	132
Table 0-3 Exhaust Plenum geometry and gas properties.....	133
Table 0-4 Heat transfer Convection Data for Exhaust Casing .....	133
Table 0-5 Exhaust Casing heat capacitor Data and Ambient Air's properties.....	134
Table 0-6 Intake Ambient Air conditions.....	134
Table 0-7 Exhaust Ambient Air conditions .....	134
Table 0-8 Crank shafts Data.....	135
Table 0-9 Abbreviation for Heat Transfer Elements.....	137
Table 0-10 Data used in radiation heat flux Blocks .....	137
Table 0-11 Data used in the conduction heat flux controllers .....	137
Table 0-12 Data used in the convection heat flux controllers .....	138
Table 0-13 Data used in the heat capacitors.....	138
Table 0-14 Data used in the Open Thermodynamic system Block representing cylinder ....	138

## **Acknowledgements**

The author wishes to acknowledge Professor N. Kyrtatos for the supervision, the knowledge provided and the useful remarks and corrections that helped the current thesis move forward in a correct manner.

Also, Dr. G. Papalamprou for the guidance, the review and remarks at all stages of the development.

Finally, the staff of Laboratory of Marine Engineering, Dr. M. Ioannou, Mr. T. Stelios, Dr. N. Alexandrakis, Mr. S. Tzanos and Mr. S. Glaros, who provided the necessary information which this diploma thesis required, for the simulation of one cylinder of the 8K90MC-C6 marine Diesel engine manufactured by MAN diesel.



# 1 Introduction

In our days, when environmental protection and low petroleum consumption are the top priorities of an engine manufacturer, the design and construction of fully optimized engines is required and therefore simulation plays a significant role in marine industry. The simulation is significant for evaluating the system during design stages and also in the long run, when the tuning process takes place in the orientation of optimization. It is also important for obtaining experience in the operation behavior of the real construction (engine in this case) with the minimum environmental and economical impact. Simulation also aids in designing, adjusting and applying control systems (in the implemented model) and uses the mathematical model of the system's dynamic behavior for optimizing the operation of the individual subsystems. Most importantly, it optimizes the system as unit, using higher level optimizing criteria such as, total fuel consumption, emissions, operating cost and maintenance. The simulation also allows the better utilization of the propulsion system in a manner that does not affect the reliability by finding the optimized spot between the latter and performance.

The use of simulation provides insight and deeper understanding of the physical processes that are being modeled. As interaction is made, simulation allows researchers to see the effects in the system. Thus, it is easier to find, correct, and change features in order to optimize the system. As complex models are used in practice, modelers require ways of abstracting their models and having the ability to traverse levels of abstraction. The abstraction is an important design approach to break a system into hierarchical levels. In this thesis, the use of the term simulation is synonymously equal to computer simulation.

The tools generally used for simulation are divided in three categories. The first category is the programming languages such as FORTRAN, C, C++. The second category is the simulation packages like Matlab - Simulink and the older platform named ACSL. In the third category belong the multidimensional analysis packages like FEM (Finite Element Method).

Simulink is a software package for modeling, simulating, and analyzing dynamic systems. It supports linear and nonlinear systems, modeled in continuous time, sampled time, or a hybrid of the two. Systems can also be multirate, i.e. have different parts that are sampled or updated at different rates. For modeling, Simulink provides a graphical user interface (GUI) for building models as block diagrams. With this interface, the models are drawn easily. With 'drag and drop', in contrast with conventional simulation packages that formulate differential equations and difference equations in a compiled language or program. Simulink includes a comprehensive block library of sinks, sources, linear and nonlinear components, and connectors. Also user blocks can be constructed and put into the user libraries.

FEM (sometimes referred to as finite element analysis) is a numerical technique for finding approximate solutions of partial differential equations (PDE) as well as of integral equations. The solution approach is based either on eliminating the differential equation completely (steady state problems), or rendering the PDE into an approximating system of ordinary differential equations, which are then numerically integrated using standard techniques such as Euler's method, Runge-Kutta, etc.

In solving partial differential equations, the primary challenge is to create an equation that approximates the equation to be studied, but is numerically stable, meaning that errors in the input data and intermediate calculations do not accumulate and cause the resulting output to be meaningless. There are many ways of doing this, all with advantages and disadvantages. The Finite Element Method is a good choice for solving partial differential equations over complex domains (like cars and oil pipelines), as well as cases of domain changes (as during a solid state reaction with a moving boundary), when the desired precision varies over the entire domain, or when the solution lacks smoothness. In the shipping industry, engine manufacturers utilized this method in order to forecast thermal and mechanical stress, dynamic charge, vibration and noise in mechanical pieces inside the burning chamber of the engine's cylinder.

This thesis uses the MATLAB®/Simulink® platform, to implement a marine propulsion system that uses a marine Diesel Engine. The model methods that have been proposed in order to implement internal combustion engines are the thermodynamic models and the fluid dynamic models. The difference between the two models is found at the basic equations that describe the structure of the model, are obtained using the conservation of mass law or from a full analysis of the motion of the fluid inside the engine (Kyrtatos, 1993). The thermodynamic models are also known as zero dimensional models because they do not utilize the geometrical data of the fluid motion inside the control plenums due to the fact that implementation of the fluid flow does not exist. For the needs of the model, zero dimensional models were used. The latter have several advantages over the higher order modes and can be very useful even if in nowadays plenty computational power is available. A zero dimensional model is easy to build, has fewer degrees of freedom to evaluate, meaning less state variables and parameters that may cause problems in solving the equations, requires less known data that have to be inserted manually and is easier to adapt for warning or failure operation compared to higher order models.

This thesis uses the model of emptying and filling methods (Heywood, 1988), (Kyrtatos, 1993). The gas containers for inlet and exhaust are simulated as finite volumes where the gas mass changes as a function of time. The inlet and exhaust systems can be implemented as one volume (each one) or like a group of volumes, with restrictions of flow (e.g. valves, filters). Each volume afterwards is considered as control volume (open system with constant volume) which contains gas in a steady condition in each time step. The conservation of mass and energy laws, plus the additional information for the mass flow, from and to each volume, are utilized to specify the condition of the gas in each control volume. Such models can be used for time variable phenomena, which they do not have major variances inside the volume that each control volume describes. These models cannot describe the change of pressure and other gas properties that can be observed due to dynamic phenomena inside the inlet and exhaust gas containers.

The target of this thesis is to elaborate on a methodology for the simulation of a marine diesel propulsion installation, with focus on an easy extendable manner with adequate accuracy. The methodology of the present thesis elaborates on the work of Lambropoulos (Lambropoulos, 2000). The simulation platform proposed in this work is suitable for the evaluation of the feasibility design in the early stages, the fine tuning of the design and as an

aid of taking operational decisions. Also, it can be used as part of an intelligent onboard controller for making higher level optimizations by evaluating the performance of the marine Diesel engine, with economical, technical and environmental advantages.

Future work is required towards two main areas: the integration of building blocks that will lead to a complete engine and the utilization of more complex mathematic equations that represent the engine operation more accurately.

This diploma thesis is divided in three chapters.

Chapter 2 contains the mathematical equations that implement from thermodynamic point of view the engine, using the emptying and filling method, which was described above.

In chapter 3 the simulation major engine blocks are presented. The building blocks (here after, blocks) are divided into groups based on their functionality.

Chapter 4 contains the results of test examples that were performed in order to validate the blocks that form a marine Diesel Engine. Results from the simulation of a two stroke one cylinder marine diesel engine, type MAN DIESEL K90MC-C6, are also presented in this chapter.

## 2 Mathematical Equations

The mathematical equations governing each block of the current thesis are presented in this chapter. The blocks that are represented are the following:

- Gas Properties
- Open Thermodynamic System
- Valve
- Compressor
- Intercooler (Heat Exchanger)
- Turbine
- Combustion model S curve
- Heat transfer elements
  - Conduction
  - Convection
  - Radiation
- Cylinder Geometry
- Geometrical Energy Loss

The equations are contained in an s – function block, which the simulation platform utilizes in order to perform the necessary calculations. S-functions (system-functions) provide a powerful mechanism for extending the capabilities of the Simulink® environment. An S-function is a computer language description of a Simulink block written in programming languages like MATLAB®, C, C++, or FORTRAN that is provided in an easy to modify, template. S-functions follow a general form and can accommodate continuous, discrete and hybrid systems (Mathworks, 2002). An S- Function represents a general Simulink block with input vector  $u$ , output vector  $y$ , and state vector  $x$ , consisting of continuous and discrete states. Every S – Function must include code to set the initial values of all elements of the state vector and to define the sizes of the input vector, the output vector and the continuous (or discrete in other cases) components of the state vector (Dabney & Harman, 2004).

The S – Function code for the mathematical equations is presented in Appendix A.

### 2.1 Gas Properties

In this section the governing equations used for calculating the working gas properties are presented. It is assumed that the mixture is homogenous and that the combustion products are in thermodynamic equilibrium. Thus the specific internal energy  $u$  of the gas is a function of temperature, pressure and equivalence ratio

$$u = f_u(T, p, \phi) \quad (2.1.1)$$

When the change rate of the specific internal energy is not available, it can be rewritten using partial derivatives

$$\dot{u} = \frac{\partial u}{\partial T} \cdot \dot{T} + \frac{\partial u}{\partial p} \cdot \dot{p} + \frac{\partial u}{\partial \phi} \cdot \dot{\phi} \quad (2.1.2)$$

Gas constant R is also a function of temperature, pressure and equivalence ratio. Thus

$$R = f_R(T, p, \phi) \quad (2.1.3)$$

When the change rate of gas constant is not available, it can be calculated using partial derivatives

$$\dot{R} = \frac{\partial R}{\partial T} \cdot \dot{T} + \frac{\partial R}{\partial p} \cdot \dot{p} + \frac{\partial R}{\partial \phi} \cdot \dot{\phi} \quad (2.1.4)$$

It is also known that specific heat at constant volume ( $c_v$ ) and at constant pressure ( $c_p$ ) is

$$C_v = \frac{\partial u}{\partial T} \quad (2.1.5)$$

$$C_p = \frac{\partial h}{\partial T}$$

Specific enthalpy for one mol of gas is equal to

$$h = u + R \cdot T \quad (2.1.6)$$

The derivation of the above equation with temperature

$$\frac{\partial h}{\partial T} = \frac{\partial u}{\partial T} + \frac{\partial(R \cdot T)}{\partial T} \quad (2.1.7)$$

But

$$\frac{\partial(R \cdot T)}{\partial T} = \frac{\partial R}{\partial T} \cdot T + R \quad (2.1.8)$$

Thus

$$\frac{\partial h}{\partial T} = \frac{\partial u}{\partial T} + \frac{\partial R}{\partial T} \cdot T + R \quad (2.1.9)$$

According to equation (2.1.5), equation (2.1.9) can be written as

$$c_v = c_p + \frac{\partial R}{\partial T} \cdot T + R \quad (2.1.10)$$

The isentropic coefficient  $\gamma$  will be

$$\gamma = \frac{c_p}{c_v} \quad (2.1.11)$$

Substituting equation (2.1.11) to (2.1.10) it is found that

$$c_v = \frac{1}{\gamma-1} \cdot \left( \frac{\partial R}{\partial T} \cdot T + R \right) \quad (2.1.12)$$

or

$$c_p = \frac{\gamma}{\gamma-1} \cdot \left( \frac{\partial R}{\partial T} \cdot T + R \right) \quad (2.1.13)$$

when the term

$$\frac{\partial R}{\partial T} \cdot T \quad (2.1.14)$$

is small comparing to the others, therefore it can be neglected and the equations are similar to the ones of the ideal gas.

In order to use the above mentioned method to calculate the gas properties, functions  $u = f_u(T, p, \phi)$  and  $R = f_R(T, p, \phi)$  are required. Here  $f_R$  and  $f_u$  are obtained using curve fitting of the gas properties for various values of temperature, pressure and equivalence ratio.

The calculation method for lean air/ fuel mixtures ( $\phi < 1.0$ ) were taken from Krieger and Borman (Borman & Krieger, 1966), obtained by curve fitting the equilibrium data of Newhall and Starkman (Newhall & Starkman, 1963), while the properties for rich mixtures products ( $1.0 < \phi < 1.6$ ) were obtained by curve fitting data published by the General Electric Company.

### **Lean mixture**

Assuming the fact that no dissociation takes place ( $T < 1333$  K), specific energy  $u$  and gas constant  $R$  are calculated using the following expressions

$$u = K_1(T) - K_2(T) \text{ [kJ / kg]} \quad (2.1.15)$$

where

$$K_1(T) = 0.692 \cdot T + 39.17 \cdot 10^{-6} \cdot T^2 + 52.9 \cdot 10^{-9} \cdot T^3 - 228.62 \cdot 10^{-13} \cdot T^4 + 277.58 \cdot 10^{-17} \cdot T^5 \quad (2.1.16)$$

$$K_2(T) = 3049.39 + 5.7 \cdot 10^{-2} \cdot T + 9.5 \cdot 10^{-5} \cdot T^2 - 21.53 \cdot 10^{-9} \cdot T^3 + 200.26 \cdot 10^{-14} \cdot T^4 \quad (2.1.17)$$

The gas constant  $R$  is equal to

$$R = 0.285 - 0.02 \cdot \phi \text{ [kJ / Kg} \cdot \text{K]} \quad (2.1.18)$$

For  $T > 1333$  K dissociation effects cannot be neglected and the specific internal energy and gas constant are given by

$$u = u_0 + 2.326 \cdot e^C \quad (2.1.19)$$

C is equal to

$$C = C_1 + C_2 + C_3 \quad (2.1.20)$$

where

$$C_1 = 10.4166 + 7.85125 \cdot \phi - 3.71257 \cdot \phi^3 \quad (2.1.21)$$

$$C_2 = \left( -27.00107 - 28.5087 \cdot \phi - 17.30375 \cdot \phi^3 \right) \cdot \frac{1800}{T} \quad (2.1.22)$$

$$C_3 = (0.154226 \cdot \phi^3 - 0.38656 \cdot \phi - 0.10329 + (0.21289 \cdot \phi - 0.026574) \cdot \frac{1800}{T}) \cdot \ln(14.5 \cdot p) \quad (2.1.23)$$

while R is equal to

$$R = R_0 + 4.1868 \cdot e^{A \cdot 10^{-3}} \quad (2.1.24)$$

where  $R_0$  is the gas constant as calculated from equation (2.1.18) and A is equal to

$$A = \left( 11.98 - 45.796 \cdot \frac{1800}{T} - 0.4354 \cdot \ln(14.5 \cdot p) \right) \cdot \phi + 0.2977 \cdot \ln(\phi) \quad (2.1.25)$$

### **Rich mixture ( $1.0 < \phi < 1.6$ )**

*For  $\phi > 1.0$  and  $T < 1333$  K specific energy will be equal to*

$$u = -2888.78 + 595.25 \cdot (\phi - 1) + 0.66854 \cdot T + 2.71304 \cdot 10^{-4} \cdot T^2 - 7.40325 \cdot 10^{-8} \cdot T^3 + 0.25107 \cdot (\phi - 1) \cdot T \quad (2.1.26)$$

*For  $\phi > 1.1$  and  $T > 1333$  K specific energy will be equal to*

$$u = -3466.2 + 903.84 \cdot (\phi - 1) + 0.65898 \cdot T - 3.79924 \cdot 10^{-4} \cdot T^2 - 8.23288 \cdot 10^{-8} \cdot T^3 \quad (2.1.27)$$

*For  $\phi > 1.1$  and  $T > 1333$  K specific energy will be equal to*

$$u = u_1 + 14.2029 \cdot (T - 1388.89)^{4.5371} \cdot \frac{11 - 10 \cdot \phi}{p^{0.46024}} \quad (2.1.28)$$

In all above sub cases the gas constant R will be equal to

$$R = 0.22751 + 0.063438 \cdot \phi - 3.33005 \cdot 10^{-5} \cdot \phi^2 \quad (2.1.29)$$

The equivalent ratio  $\phi$  is calculated from the burned fuel mass fraction  $\xi$  and the stoichiometric fuel to air ratio  $(F/A)_{st}$ , thus

$$\phi = \frac{\xi}{(1-\xi) \cdot (F/A)_{st}} \quad (2.1.30)$$

The derivative of equation (2.1.30) is the equivalence ratio change rate, so

$$\dot{\phi} = \frac{\dot{\xi}}{(1-\xi)^2 \cdot (F/A)_{st}} \quad (2.1.31)$$

The viscosity of air is calculated (Heywood, 1988) over temperature range of 500 K up to 4000 K and for pressure from 1 bar to 100 bar using the following correlation

$$\mu_{air} = 3.3 \cdot 10^{-7} \cdot T^{0.7} \quad (2.1.32)$$

The viscosity as a function of temperature of hydrocarbon differs from that of air. Including the correction for  $\phi=0$  up to  $\phi=4$ , on the viscosity of hydrocarbon – air combustion products, the correlation is given below as

$$\mu = \frac{\mu_{air}}{1 + 0.027 \cdot \phi} \quad (2.1.33)$$

Fig. 2-1 represents the block for gas properties in MATLAB/ Simulink.

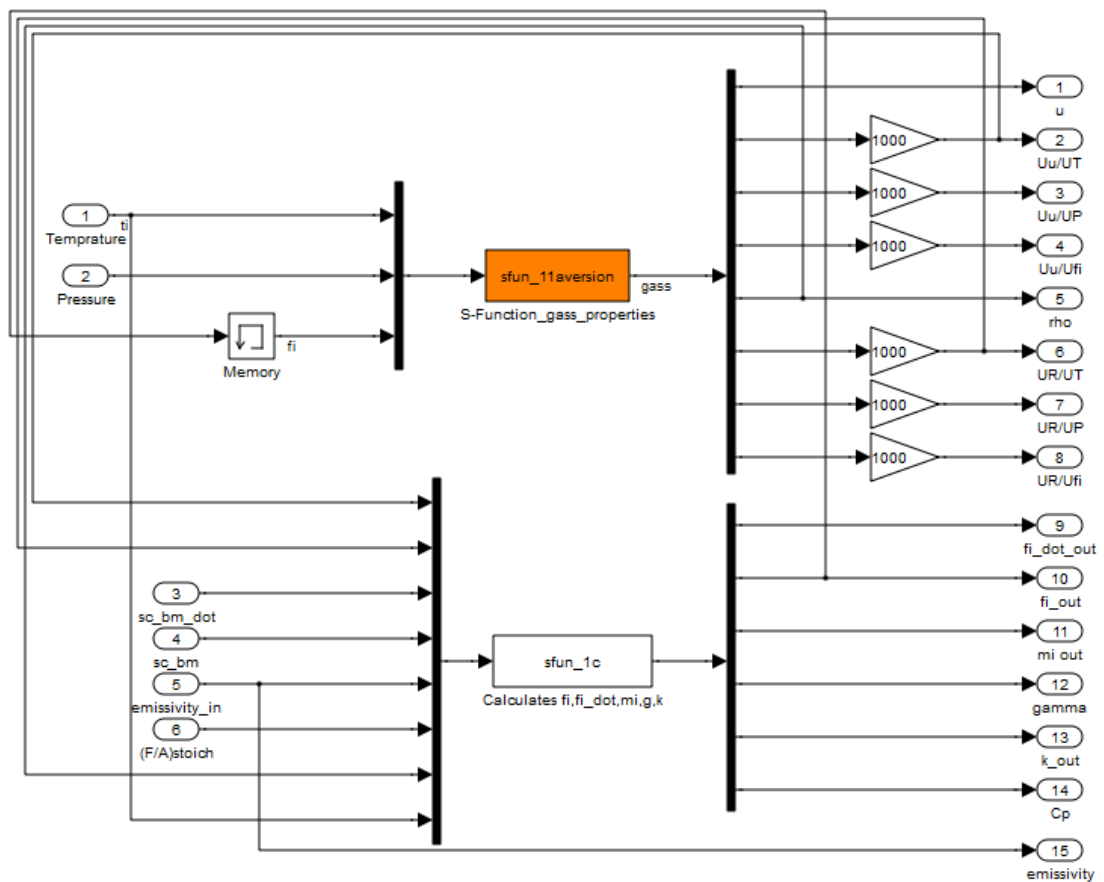


Fig. 2-1 Block: Gas Properties



## 2.2 Open Thermodynamic System

In this section the equations for the open thermodynamic system are presented. The laws of mass and energy conservation are applied. This modeling approach is appropriate when the gas inside the open system boundary can be assumed uniform in composition and state at each point in time and when the state and mixture composition vary with time due to heat transfer, work transfer and mass flow across the boundary and boundary displacement.

The law of mass conservation is

$$\dot{m} = \sum_{i=1}^n \dot{m}_i \quad (2.2.1)$$

where  $\dot{m}_i$  is the individual mass rate exchange to the system. The instantaneous mass of the open thermodynamic system will be

$$m = \int_0^t \dot{m} dt + m_{ic} \quad (2.2.2)$$

where  $m_{ic}$  is the mass contained in the open thermodynamic system at  $t=0$  (initial mass).

The equivalence ratio  $\phi$  is given also from

$$\phi = \frac{m_f / m_a}{\left( m_f / m_a \right)_{st}} \quad (2.2.3)$$

while

$$(F / A) = \frac{m_f}{m_a} \quad (2.2.4)$$

As a result

$$\phi = \frac{F / A}{(F / A)_{st}} \quad (2.2.5)$$

For the specific instantaneous burned fuel mass fraction,  $\xi$ , of the open thermodynamic system, we have

$$\xi = \frac{m_f}{m} = \frac{m_f}{m_a + m_f} \quad (2.2.6)$$

by performing the appropriate calculations using equation (2.2.3) – (2.2.6) the equation (2.1.30) in section of gas properties is constructed.

$$\xi = \int_0^t \dot{\xi} + \xi_{ic} \quad (2.2.7)$$

where  $\xi_{ic}$  is the initial burned fuel mass fraction that was contained in the open thermodynamic system at  $t=0$ .

### Pressure Calculation

In order to evaluate the pressure of the working gas inside the container, the ideal gas equation is applied

$$P \cdot V = m \cdot R \cdot T \quad (2.2.8)$$

or

$$p = \frac{m \cdot R \cdot T}{V} \quad (2.2.9)$$

The time derivative of the above equation will be

$$\dot{p} = \frac{m \cdot R}{V} \cdot \dot{T} + \frac{m \cdot T}{V} \cdot \dot{R} + \frac{R \cdot T}{V} \cdot \dot{m} - \frac{m \cdot R \cdot T}{V^2} \cdot \dot{V} \quad (2.2.10)$$

The gas constant  $R$  is a function of temperature, pressure and equivalent ratio  $R = f_R(T, p, \phi)$ . By substituting equation (2.1.4) to (2.2.10) it is obtained

$$\dot{p} = \frac{m \cdot R}{V} \cdot \dot{T} + \frac{m \cdot T}{V} \cdot \left( \frac{\partial R}{\partial T} \cdot \dot{T} + \frac{\partial R}{\partial p} \cdot \dot{p} + \frac{\partial R}{\partial \phi} \cdot \dot{\phi} \right) + \frac{R \cdot T}{V} \cdot \dot{m} - \frac{m \cdot R \cdot T}{V^2} \cdot \dot{V} \quad (2.2.11)$$

substituting the terms

$$\frac{m \cdot R \cdot T}{V^2} = \frac{p}{V} \quad (2.2.12)$$

in the equation (2.1.11) the latter takes the following shape

$$\left( 1 - \frac{p \cdot \partial R}{R \cdot \partial p} \right) \cdot \dot{p} = \left( \left( \frac{1}{T} + \frac{\partial R}{R \cdot \partial T} \right) \cdot \dot{T} + \frac{\partial R}{R \cdot \partial \phi} \cdot \dot{\phi} + \frac{1}{m} \cdot \dot{m} - \frac{1}{V} \cdot \dot{V} \right) \cdot p \quad (2.2.13)$$

Setting the following terms to constants

$$A = \left( 1 - \frac{p \cdot \partial R}{R \cdot \partial p} \right) \quad (2.2.14)$$

$$B = \left( \frac{1}{T} + \frac{\partial R}{R \cdot \partial T} \right) \quad (2.2.15)$$

$$C = \frac{\partial R}{R \cdot \partial \phi} \cdot \dot{\phi} + \frac{1}{m} \cdot \dot{m} - \frac{1}{V} \cdot \dot{V} \quad (2.2.16)$$

Equation (2.2.13) becomes

$$A \cdot \dot{p} = (B \cdot \dot{T} + C) \cdot p \quad (2.2.17)$$

and by solving for  $\dot{p}$

$$\dot{p} = \frac{(B \cdot \dot{T} + C) \cdot p}{A} \quad (2.2.18)$$

### **Temperature Calculation**

The energy conservation law for the open thermodynamic system will be

$$\dot{U} = \dot{Q} - \dot{W} + \dot{H} \quad (2.2.19)$$

where  $\dot{U}$  is the gas internal energy change rate,  $\dot{Q}$  is the heat flux entering or leaving the system,  $\dot{W}$  is the work that the system produces or absorbs and  $\dot{H}$  is the total enthalpy of the gas entering or leaving the system per time. It is also known that

$$\dot{U} = \dot{u} \cdot m + u \cdot \dot{m} \quad (2.2.20)$$

The total heat flux entering or leaving the system is the sum of the heat transfer through the boundaries of the system

$$\dot{Q} = \sum_{i=1}^n \dot{Q}_i + \sum_{j=1}^n \dot{Q}_j \quad (2.2.21)$$

The power produced or absorbed by the system is

$$\dot{W} = p \cdot \dot{V} \quad (2.2.22)$$

The total enthalpy of the gas entering or leaving the system will be

$$\dot{H} = \sum_{i=1}^n (h_i \cdot \dot{m}_i) \quad (2.2.23)$$

By combining equations (2.2.20) – (2.2.23) it is obtained

$$\dot{u} \cdot m + u \cdot \dot{m} = \sum_{i=1}^n \dot{Q}_i + \sum_{j=1}^n \dot{Q}_j - p \cdot \dot{V} + \sum_{i=1}^n (h_i \cdot \dot{m}_i) \quad (2.2.24)$$

As it is mentioned in the previous chapter the specific internal energy of the gas is a function of temperature, pressure and equivalence ratio. By substituting equation (2.1.2) to (2.2.24) then

$$\left( \frac{\partial u}{\partial T} \cdot \dot{T} + \frac{\partial u}{\partial p} \cdot \dot{p} + \frac{\partial u}{\partial \phi} \cdot \dot{\phi} \right) \cdot m + u \cdot \dot{m} = \sum_{i=1}^n \dot{Q}_i + \sum_{j=1}^n \dot{Q}_j - p \cdot \dot{V} + \sum_{i=1}^n (h_i \cdot \dot{m}_i) \quad (2.2.25)$$

In order to simplify the above equation

$$D = \sum_{i=1}^n \dot{Q}_i + \sum_{j=1}^n \dot{Q}_j - p \cdot \dot{V} + \sum_{i=1}^n (h_i \cdot \dot{m}_i) \quad (2.2.26)$$

And now it is written as

$$\left( \frac{\partial u}{\partial T} \cdot \dot{T} + \frac{\partial u}{\partial p} \cdot \dot{p} + \frac{\partial u}{\partial \phi} \cdot \dot{\phi} \right) \cdot m + u \cdot \dot{m} = D \quad (2.2.27)$$

By substituting the pressure change rate using the final simplified equation and by rearranging the term, it is obtained for  $\dot{T}$

$$\dot{T} = \frac{\frac{D - u \cdot \dot{m}}{m} - \frac{\partial u}{\partial p} \cdot \frac{C}{A} \cdot p - \frac{\partial u}{\partial \phi} \cdot \dot{\phi}}{\frac{\partial u}{\partial T} + \frac{\partial u}{\partial p} \cdot \frac{B}{A} \cdot p} \quad (2.2.28)$$

The instantaneous gas temperature of the open thermodynamic system is the integration of equation (2.2.28), thus

$$T = \int_0^t \dot{T} dt + T_{ic} \quad (2.2.29)$$

where  $T_{ic}$  is the initial temperature of the open thermodynamic system at  $t=0$ .

An open thermodynamic system, in order to be connected requires the calculation of Prandtl number and Reynolds number. Thus

$$Pr = \frac{c_p \cdot \mu}{k} \quad (2.2.30)$$

while the Reynolds number  $Re$  will be

$$Re = \frac{\rho \cdot w \cdot L}{\mu} \quad (2.2.31)$$

where  $\rho$  is the gas density,  $w$  is the mean velocity of the gas,  $L$  is the characteristic length,  $\mu$  is the viscosity coefficient and  $c_p$  is the specific heat capacity of gas. The gas density is calculated from

$$\rho = \frac{m}{V} \quad (2.2.32)$$

In order to calculate the average gas velocity, a semi experimental method is proposed from Woschni (Metz, Urben, & Steiger, 1967) modified for swirl phenomenon, thus

$$w = C_1 \cdot \bar{S}_p + C_2 \cdot u_s + C_3 \cdot \frac{V_d \cdot T_r}{p_r \cdot V_r} \cdot (p - p_m) \quad (2.2.33)$$

Where  $V_d$  is the displaced volume,  $p$  is the instantaneous pressure of the cylinder,  $p_r$ ,  $V_r$ ,  $T_r$  are the fluid pressure, volume and temperature at some reference state, and  $p_m$  is the motored cylinder pressure at the same crank angle as  $p$ .  $U_s$  is given from the equation

$$U_s = \frac{B \cdot \omega_p}{2} \quad (2.2.34)$$

where  $\omega_p$ , is the rotation speed of the paddle wheel, used to measure the swirl velocity. The constants  $C_1$ ,  $C_2$ ,  $C_3$  are specific to the period of engine cycle. Thus

For the gas exchange period:

$$C_1 = 6.18 \quad C_2 = 0.417 \quad C_3 = 0.0 \quad (2.2.35)$$

For the compression period:

$$C_1 = 2.28 \quad C_2 = 0.308 \quad C_3 = 0.0 \quad (2.2.36)$$

For the combustion and expansion period:

$$C_1 = 2.28 \quad C_2 = 0.308 \quad C_3 = 3.24 \cdot 10^{-3} \quad (2.2.37)$$

Fig. 2-2 represents the implemented open thermodynamic system in MATLAB/Simulink.

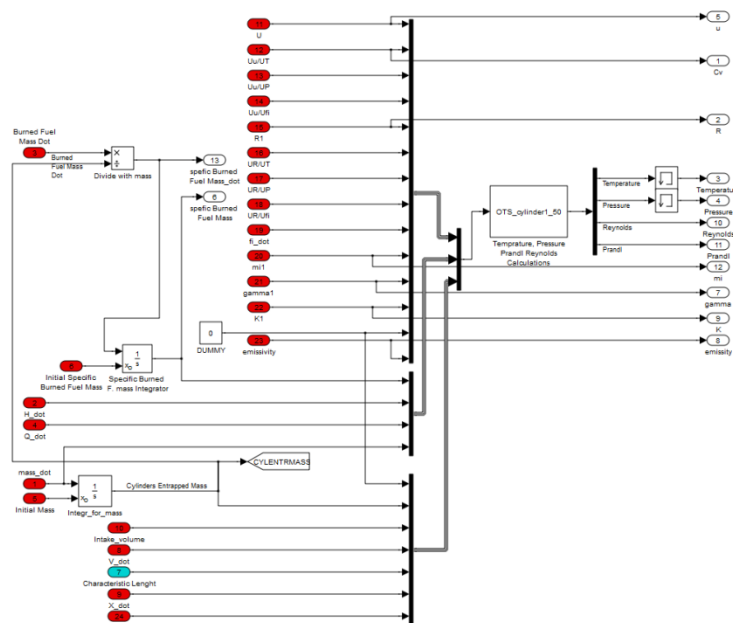


Fig. 2-2 Block: Open Thermodynamic System

## 2.3 Valve

This section presents the equations for mass flow through a restriction.

The flow is assumed steady and isentropic. The mass flow through a restriction is given as a function of the condition of the gas upstream and downstream the restriction. As the flow is assumed isentropic, no heat transfer is taking place due to the fact that no friction is present. In order to obtain the real flow, an effective cross – sectional area  $A_E$  is used instead of the reference area which is usually the minimum geometrical cross – sectional area  $A_G$ . For this purpose, the discharge coefficient is introduced, given by the following relationship

$$C_D = \frac{A_E}{A_G} \quad (2.3.1)$$

Thus the effective area required to calculate the real flow is

$$A_E = C_D \cdot A_G \quad (2.3.2)$$

The  $C_D$  value is obtained experimentally or approximated using statistic data obtained through restrictions with the same geometry and flow conditions. The conditions applied before (upstream) the restrictions are dynamic, meaning the kinetic energy of the gas is also included, therefore stagnation conditions are applied. After the restriction (downstream) gas properties are static.

For an isentropic flow the stagnation temperature of the gas  $T_0$  before the restriction is related to the conditions at the other points of the flow with the equation

$$T_0 = T + \frac{c^2}{2 \cdot c_p} \quad (2.3.3)$$

where  $c$  is the topical velocity of the gas and  $c_p$  is the specific heat for constant pressure. Also it is known that

$$\frac{T}{T_0} = \left( \frac{p}{p_0} \right)^{\frac{\gamma-1}{\gamma}} \quad (2.3.4)$$

where  $\gamma$  is the isentropic coefficient and  $p_0$  is the stagnation pressure before the restriction. The Mach number  $M$  is defined as

$$M = \frac{c}{a} \quad (2.3.5)$$

where  $a$  is the speed of sound. Solving equation (2.3.5) for  $c$  gives

$$c = M \cdot a \quad (2.3.6)$$

As the speed of sound is also equal to

$$a = \sqrt{\gamma \cdot R \cdot T} \quad (2.3.7)$$

equation (2.3.6) becomes

$$c = M \cdot \sqrt{\gamma \cdot R \cdot T} \quad (2.3.8)$$

If dissociation effects are neglected, the specific heat at constant pressure  $c_p$  of the gas is equal to

$$c_p = \frac{\gamma}{\gamma - 1} \cdot R \quad (2.3.9)$$

By substituting equation (2.3.9) to (2.3.3) the following equation can be obtained

$$T_0 = T + \frac{M^2 \cdot R \cdot T \cdot (\gamma - 1)}{2 \cdot \gamma \cdot R} \quad (2.3.10)$$

which by rearrangement leads to

$$T_0 = T \cdot \left( 1 + \frac{\gamma - 1}{2} \cdot M^2 \right) \quad (2.3.11)$$

Solving for the fraction  $T/T_0$

$$\frac{T}{T_0} = \left( 1 + \frac{\gamma - 1}{2} \cdot M^2 \right)^{-1} \quad (2.3.12)$$

Combing equations (2.3.12) and (2.3.4) and solving for p

$$p = \left( 1 + \frac{\gamma - 1}{2} \cdot M^2 \right)^{\frac{-\gamma}{\gamma - 1}} \cdot p_0 \quad (2.3.13)$$

The mass flow through a restriction is the product of the gas density  $\rho$ , the geometric equivalent area  $A$  of the restriction and the gas speed  $c$ ; thus

$$\dot{m} = \rho \cdot A \cdot c \quad (2.3.14)$$

and using the ideal gas law and solving for density  $\rho$  it is obtained that

$$\rho = \frac{p}{R \cdot T} \quad (2.3.15)$$

Using equations (2.3.8), (2.3.14) and (2.3.15) the mass flow can be expressed as

$$\dot{m} = \frac{p}{R \cdot T} \cdot A \cdot M \cdot \sqrt{\gamma \cdot R \cdot T} \quad (2.3.16)$$

and by multiplying both terms with  $\gamma$  and by rearranging the equation, mass flow can be written as

$$\dot{m} = \frac{\gamma \cdot A \cdot p}{\sqrt{\gamma \cdot R \cdot T}} \cdot M \quad (2.3.17)$$

By substituting temperature T and pressure p from equations (2.3.13) and the rearranged (2.3.11), mass flow can finally be written as

$$\dot{m} = \frac{\gamma \cdot A \cdot p_0}{\sqrt{\gamma \cdot R \cdot T_0}} \cdot M \cdot \left(1 + \frac{\gamma - 1}{2} \cdot M^2\right)^{\frac{-(\gamma + 1)}{2(\gamma - 1)}} \quad (2.3.18)$$

but solving the equation (2.3.13) for M, it is found that

$$M = \sqrt{\frac{2}{\gamma - 1} \cdot \left[ \left(\frac{p}{p_0}\right)^{\frac{1 - \gamma}{\gamma}} - 1 \right]} \quad (2.3.19)$$

and by substituting equation (2.3.19) to (2.3.18) it is obtained that

$$\dot{m} = \frac{A \cdot p_0}{\sqrt{R \cdot T_0}} \cdot \sqrt{\frac{2 \cdot \gamma}{\gamma} \cdot \left[ \left(\frac{p}{p_0}\right)^{\frac{2}{\gamma}} - \left(\frac{p}{p_0}\right)^{\frac{\gamma + 1}{\gamma}} \right]} \quad (2.3.20)$$

The maximum mass flow occurs when the speed of the gas at the throat reaches the sonic speed where the Mach number is equal to 1. The pressure ratio when this occurs is called critical pressure ratio. While the working pressure ratio remains below this critical ratio the flow is unchoked while above the critical ratio, the flow becomes choked. The pressure ratio at critical speed is (Kyrtatos, 1993)

$$\frac{p}{p_0} = \left(1 + \frac{\gamma - 1}{2}\right)^{\frac{-\gamma}{\gamma - 1}} \quad (2.3.21)$$

or

$$\frac{p}{p_0} = \left(\frac{2}{\gamma + 1}\right)^{\frac{\gamma}{\gamma - 1}} \quad (2.3.22)$$

and so equation (2.3.18) resolves to

$$\dot{m} = \frac{\gamma \cdot A \cdot p_0}{\sqrt{\gamma \cdot R \cdot T_0}} \cdot \left(\frac{2}{\gamma + 1}\right)^{\frac{(\gamma + 1)}{2(\gamma - 1)}} \quad (2.3.23)$$

Equation (2.3.23) is used for sonic flow.



The model of flow through a restriction in MATLAB/Simulink is shown in Fig. 2-3.

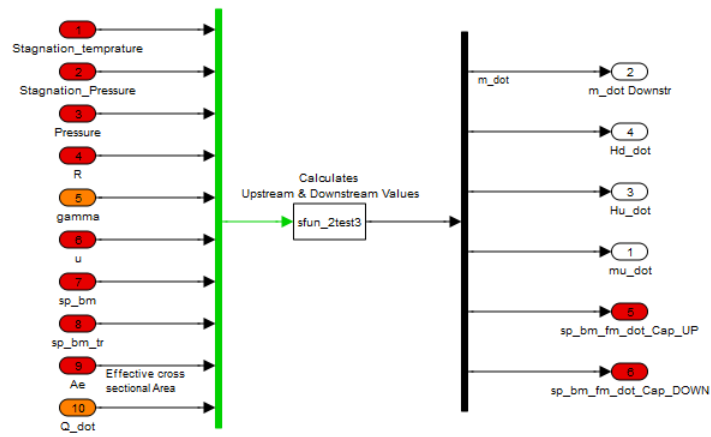


Fig. 2-3 Block: Valve

## 2.4 Compressor

The behavior of compressor is obtained through performance maps that the manufacturer provides. These maps generally relate the mass flow rate through the compressor with the working pressure ratio (fraction of downstream to upstream pressure) and the compressor angular velocity (N will be noted as  $\dot{a}$  from now on) along with the isentropic efficiency ( $\eta_{oi}$ ). The performance maps in most cases are obtained under reference conditions. Thus, in order to obtain these values, equivalent reference mass flow rate and angular velocity must be calculated. The reference mass flow rate  $\dot{m}_{ref}$  and angular velocity  $\dot{a}_{ref}$  are obtained using the following equations

$$\dot{m}_{ref} = \rho_{o1} \cdot \dot{V}_{ref} = \dot{V} \cdot \sqrt{\frac{T_{ref}}{T_{o1}}} \quad (2.4.1)$$

$$\dot{a}_{ref} = \dot{a} \cdot \sqrt{\frac{T_{ref}}{T_{o1}}} \quad (2.4.2)$$

The kinetic energy inside the control volume is neglected; for this reason the stagnation temperature  $T_{o1}$  and stagnation gas pressure  $p_{o1}$  are approximately equal to the static ones for the upstream volume (Watson & Janota, 1982), thus

$$\begin{aligned} T_{o1} &\simeq T_1 \\ p_{o1} &\simeq p_1 \end{aligned} \quad (2.4.3)$$

where  $T_1$  is the static gas temperature in the upstream volume and  $p_1$  is the static gas pressure respectively.

Moreover the stagnation temperature  $T_{o2}$  of the gas entering the downstream volume is not equal to the static one  $T_2$  due to the fact that kinetic energy of the gas cannot be neglected. In order to calculate the stagnation specific enthalpy entering the downstream volume, the stagnation temperature is used. In order to use the performance maps, it is required to have the reference conditions under which the measurements were conducted. Some manufacturers in order to produce maps that can be easily read, are integrating the values to the reference conditions to the map, thus the map flow rate and map angular velocity are available. Thus (Kyrtatos, 1993)

$$\dot{V}_{map} = \dot{V} \cdot \sqrt{\frac{T_{ref}}{T_{o1}}} \quad (2.4.4)$$

$$\dot{a}_{map} = \dot{a} \cdot \sqrt{\frac{T_{ref}}{T_{o1}}} \quad (2.4.5)$$

The reference conditions ( $T_{ref}$  and  $p_{ref}$ ) can be considered properties of the map. Therefore the map flow rate through the compressor will be given from a map in the form

$$\dot{m}_{map} = f_{in} \left( \frac{p_{o2}}{p_{o1}}, \dot{a}_{map} \right) \quad (2.4.6)$$

and the isentropic efficiency accordingly

$$\eta_{oic} = f_{\eta_{oic}} \left( \frac{p_{o2}}{p_{o1}}, \dot{a}_{map} \right) \quad (2.4.7)$$

The actual mass flow rate can now be calculated using the map mass flow value and  $T_{o1}$

thus

$$\dot{m} = \rho_{o1} \cdot \dot{V} = \rho_{o1} \cdot \dot{V}_{map} \cdot \sqrt{\frac{T_{o1}}{T_{ref}}} \quad (2.4.8)$$

The power transfer from the compressor to the gas is  $\dot{W}$ . This power transfer is translated to gas enthalpy increase  $\Delta h_{oa}$ , thus

$$\dot{W} = \dot{m} \cdot \Delta h_{oa} \quad (2.4.9)$$

and

$$\Delta h_{oa} = h_{o2} - h_{o1} \quad (2.4.10)$$

where  $h_{o2}$  and  $h_{o1}$  are the stagnation specific enthalpies of the gas.

The torque absorbed by the compressor is

$$M_c = \frac{\dot{W}_c}{2 \cdot \pi \cdot \dot{a}} \quad (2.4.11)$$

where  $\dot{a}$  is the compressor impeller angular velocity in rotations per second [RPS] provided by the connection with the turbine.

In order to obtain the actual stagnation specific enthalpy change rate  $\Delta h_{oa}$  the stagnation isentropic efficiency  $\eta_{oic}$  is used

$$\Delta h_{oa} = \frac{\Delta h_{oi}}{\eta_{oi}} \quad (2.4.12)$$

where  $\Delta h_{oi}$  is the ideal stagnation enthalpy change for isentropic compression. Assuming constant specific heat under constant pressure  $c_p$  for the gas working range in the compressor, equation (2.4.12) can be rewritten as

$$c_p \cdot \Delta T_{oa} = \frac{c_p \cdot \Delta T_{oi}}{\eta_{oic}} \quad (2.4.13)$$

and by rearranging

$$\Delta T_{oa} = \frac{\Delta T_{oi}}{\eta_{oic}} \quad (2.4.14)$$

where

$$\Delta T_{oi} = \left[ \left( \frac{p_{o2}}{p_{o1}} \right)^{\frac{\gamma_1-1}{\gamma_1}} - 1 \right] \cdot T_{oi} \quad (2.4.15)$$

thus the actual temperature increase will be

$$\Delta T_{oa} = \frac{T_{o1}}{\eta_{oic}} \cdot \left[ \left( \frac{p_2}{p_1} \right)^{\frac{\gamma_1-1}{\gamma_1}} - 1 \right] \quad (2.4.16)$$

The actual stagnation temperature entering the upstream volume is

$$T_{o2} = T_{o1} + \Delta T_{oa} \quad (2.4.17)$$

and the stagnation specific enthalpy of the gas entering the downstream volume will be

$$h_{o2} = u_1 + R_1 \cdot T_{o2} \quad (2.4.18)$$

therefore the stagnation enthalpy change rate entering the downstream volume is

$$\dot{H}_{o2} = \dot{m} \cdot h_{o2} \quad (2.4.19)$$

Accordingly for the upstream volume

$$h_{o1} = u_1 + R_1 \cdot T_{o1} \quad (2.4.20)$$

and

$$\dot{H}_{o1} = -\dot{m} \cdot h_{o1} \quad (2.4.21)$$

In order to calculate the heat exchange that takes place at turbine, properties like the gas temperature, thermal conductivity, radiation, emissivity, Prandtl and Reynolds numbers, are required.

The heat transfer calculation requires the mean gas temperature inside the compressor, thus

$$\bar{T} = T_{o1} + \frac{\Delta T_{oa}}{2} \quad (2.4.22)$$

The thermal conductivity and radiation emissivity are considered constant and are the same with the gas that flows through the compressor. Reynolds number is approximated in the same way as in valve's equations, thus

$$Re = \frac{4 \cdot \dot{m}}{\pi \cdot D_t \cdot \mu_1} \quad (2.4.23)$$

where  $\dot{m}$  is the mass flow through the turbine and  $\mu$  is the viscosity coefficient of the upstream volume. Prandtl number is obtained from

$$Pr = \frac{c_p \cdot \mu_1}{k_1} \quad (2.4.24)$$

where

$$c_p = \frac{\gamma_1}{\gamma_1 - 1} \cdot R_1 \quad (2.4.25)$$

The total burned fuel mass fraction change rate,  $\dot{\xi}$ , for the downstream volume equals to

$$\dot{\xi}_2 = \dot{m} \cdot (\xi_1 - \xi_2) \quad (2.4.26)$$

while the upstream volume is zero, thus

$$\dot{\xi}_1 = 0 \quad (2.4.27)$$

The compressor block in MATLAB/Simulink is illustrated in Fig. 2-4.

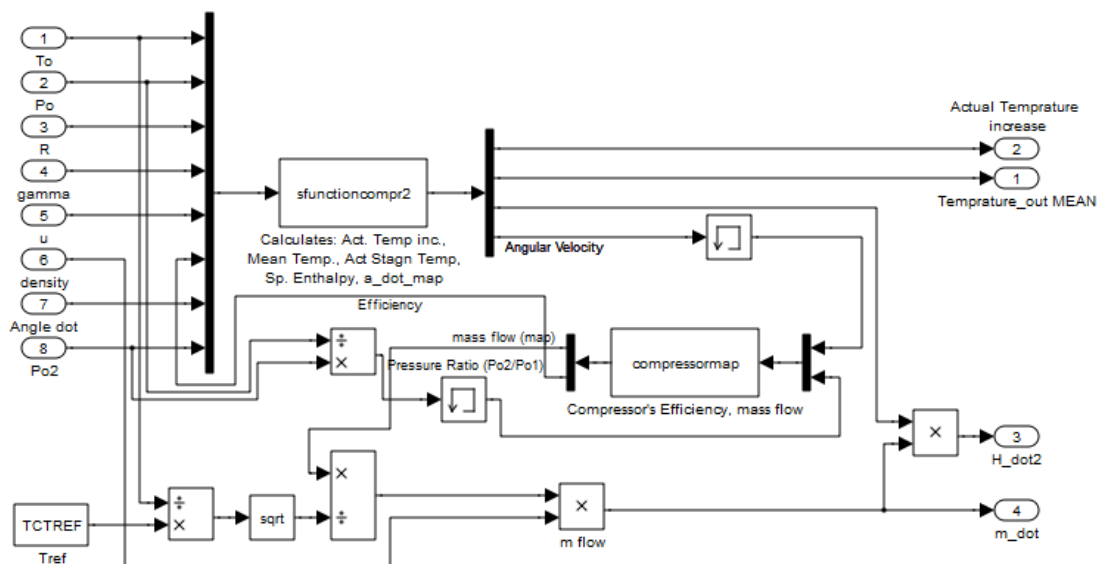


Fig. 2-4 Block: Compressor

## 2.5 Intercooler (Heat Exchanger)

The mathematical equations of intercooler are presented here. The law of conservation of mass is applied thus the mass rate entering and leaving the intercooler is equal to

$$\dot{m}_1 = \dot{m}_2 \quad (2.5.1)$$

The gas entering the system is denoted as 1 condition and leaving the system as 2 condition. The pressure at stage 1 will be equal to stage 2 plus the pressure drop

$$p_1 = p_2 + \frac{\dot{m}_1}{|\dot{m}_1|} \cdot \Delta p \quad (2.5.2)$$

The term  $\frac{\dot{m}_1}{|\dot{m}_1|}$  provides the proper sign according to the flow direction. The pressure drop  $\Delta p$  for a particular heat exchanger is typically a function of the fluid mass rate. The relation between pressure drop and mass rate is provided in most cases by the manufacturer. Thus the pressure drop is provided by a function in the form

$$\Delta p = f_{\Delta p}(\dot{m}_2) \quad (2.5.3)$$

The temperature of the fluid leaving the heat exchanger depends on the temperature of the fluid that enters the heat exchanger, the temperature of the heat exchanging medium (coolant for the intercooler) and the efficiency of the heat exchanger. The efficiency of the later is defined as

$$\eta_\varepsilon = \frac{\Delta h_{\text{act}}}{\Delta h_{\text{max}}} \quad (2.5.4)$$

where  $\Delta h_{\text{act}}$  is the actual heat exchanged and  $\Delta h_{\text{max}}$  is the maximum possible heat that can be exchanged. Also the heat exchange efficiency is provided by the manufacturer in the form of a chart which relates the efficiency with the mass flow rate, thus

$$\eta_\varepsilon = f_\varepsilon(\dot{m}_2) \quad (2.5.5)$$

Assuming having constant specific heat for constant pressure for the temperature range of the fluid inside the heat exchanger, equation (2.5.4) leads to

$$\eta_\varepsilon = \frac{c_p \cdot (T_1 - T_2)}{c_p \cdot (T_1 - T_w)} = \frac{T_1 - T_2}{T_1 - T_w} \quad (2.5.6)$$

and by solving (2.5.6) for  $T_1$

$$T_1 = T_2 \cdot (1 - \eta_\varepsilon) + \eta_\varepsilon \cdot T_w \quad (2.5.7)$$

The heat exchanged through the heat exchanger walls  $\dot{Q}_w$  will be equal to

$$\dot{Q}_w = \dot{m}_1 \cdot c_p \cdot (T_1 - T_2) \quad (2.5.8)$$

The law of energy conservation applies so

$$\dot{Q}_2 = -\dot{Q}_w \quad (2.5.9)$$

$c_p$  can be calculated from the following equation

$$c_p = \frac{\gamma_2}{\gamma_2 - 1} \cdot R_2 \quad (2.5.10)$$

The phenomenon inside the heat exchanger is isenthalpic thus, the enthalpy change rate will pass unchanged from state 1 to state 2, thus

$$\dot{H}_2 = \dot{H}_1 \quad (2.5.11)$$

Also, since the composition of the fluid does not change inside the heat exchanger the burned fuel mass fraction of state 2 will be equal to the one of state 1, thus

$$\xi_1 = \xi_2 \quad (2.5.12)$$

This also means that the total burned fuel mass fraction change rate of state 2 will be equal to the one of stage 1, thus

$$\dot{\xi}_1 = \dot{\xi}_2 \quad (2.5.13)$$

The specific internal energy of the fluid  $u_1$  will be equal to the one in state 2, plus the specific internal energy difference due to temperature and pressure change. Although the internal energy depends on both temperature and pressure, due to the fact that depends little to pressure and the pressure drop inside the heat exchanger is negligent, then the specific internal energy will change only due to temperature difference, thus

$$\Delta u = c_v \cdot (T_1 - T_2) \quad (2.5.14)$$

where  $c_v$  is the specific heat of the working fluid at constant volume and is equal to

$$c_v = \frac{1}{\gamma_2 - 1} \cdot R_2 = \frac{c_p}{\gamma_2} \quad (2.5.15)$$

thus the specific internal energy of the fluid  $u_1$  is

$$u_1 = u_2 + c_v \cdot (T_1 - T_2) \quad (2.5.16)$$

Also the mass density of the fluid  $\rho_1$  is equal to

$$\rho_1 = \frac{p_1}{R_2 \cdot T_1} \quad (2.5.17)$$

Finally the gas constant  $R$ , the ratio of specific heats  $\gamma$ , the thermal conductivities  $k$ , the absolute gas viscosity  $\mu$  and the radiation emissivity  $\epsilon$  of the gas, are assumed constant.

$$\begin{aligned}
 R_1 &= R_2 \\
 \gamma_1 &= \gamma_2 \\
 \mu_1 &= \mu_2 \\
 k_1 &= k_2 \\
 \epsilon_1 &= \epsilon_2
 \end{aligned}
 \tag{2.5.18}$$

This assumption does not introduce significant error. The block representation of intercooler in MATLAB/Simulink is shown in Fig. 2-5.

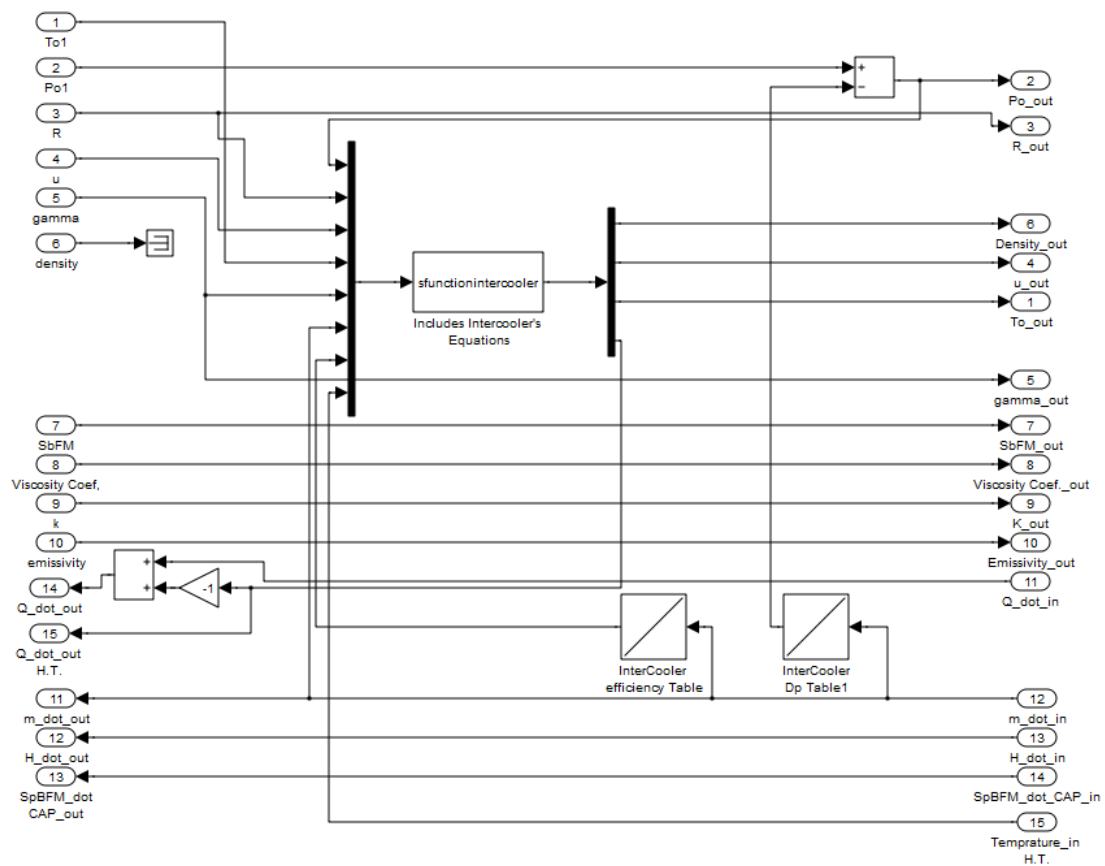


Fig. 2-5 Block: Intercooler



## 2.6 Turbine

In this section the mathematical equation for the Turbine are presented. The mathematical model of the turbine requires the solution of coupled equations. The equation coupling cannot be avoided since turbine as like as the compressor model, includes maps (which are available in the form of an array and cannot directly solved in an uncoupled form). That's why memory block is used in order to start the equation sequence.

As already stated the behavior of the turbine is usually obtained through two maps. The first, represents the swallowing capacity (mass flow rate) of the turbine to the working pressure ratio  $p_{o1}/p_2$ , (Watson & Janota, 1982). These maps generally relate the mass flow rate through the compressor with the working pressure ratio  $p_{o1}/p_2$  (1 refers to the upstream and 2 to the downstream) and the compressor angular velocity  $N$  along with the isentropic efficiency  $\eta_{oit}$ . The performance maps that are produced directly from the test facilities of the manufacturers, are obtained under reference conditions of gas temperature and pressure ( $T_{ref}, p_{ref}$ ). The reference mass flow rate  $\dot{m}_{ref}$  is generally obtained from the following equation

$$\dot{m}_{ref} = \dot{m} \cdot \frac{p_{ref}}{p_{o1}} \cdot \sqrt{\frac{T_{o1}}{T_{ref}}} \quad (2.6.1)$$

Turbine maps use the stagnation to static pressure ratio<sup>1</sup> since the kinetic energy leaving the system is considered as a loss. In order to calculate the downstream static pressure  $p_2$  the velocity of the gas leaving the turbine, must be determined. In order to use the performance maps the reference conditions under which the measurements were conducted, are required. Some manufacturers in order to produce maps that can be easily read are integrating the values to the reference conditions of the map, thus the map flow rate according to the manufacturer of the selected turbine is

$$\dot{m}_{map} = \dot{m} \cdot \sqrt{T_{REF}} \quad (2.6.2)$$

Each manufacturer has a different approach in representing the values. The map mass flow rate though, will be given for the turbine from the map in the following form

$$\dot{m}_{map} = \dot{f}_m \left( \frac{p_{o1}}{p_2} \right) \quad (2.6.3)$$

and the isentropic efficiency  $\eta_{oit}$  accordingly

$$\eta_{oit} = f_{\eta_{oit}} \left( \frac{p_{o1}}{p_2}, \frac{U}{C} \right) \quad (2.6.4)$$

The actual mass flow can now be calculated using the map mass flow, using the equation

---

<sup>1</sup> In contrast the compressor maps use the pressure to stagnation pressure ratio since the kinetic energy of the upstream volume is ignored (case of ambient air) while the kinetic energy of the gas leaving the compressor is not lost.

$$\dot{m} = \dot{m}_{map} \cdot \frac{1}{\sqrt{T_{REF}}} \quad (2.6.5)$$

The term  $U/C$  is the turbine blade speed ratio and is defined as the turbine wheel tip linear velocity  $C$  for a radial flow turbine<sup>2</sup> to the velocity that would be achieved by the gas if following an isentropic expansion from the inlet conditions, to the pressure at the exit from the turbine  $C$ , thus

$$\frac{U}{C} = \frac{\pi \cdot D_t \cdot \dot{a}}{\sqrt{2 \cdot \Delta h_{ois}}} \quad (2.6.6)$$

where  $D_t$  is the turbine diameter,  $\dot{a}$  is the turbine wheel angular velocity and  $\Delta h_{ois}$  is the stagnation to static specific enthalpy difference when the gas follows isentropic expansion. Assuming constant specific heat this leads to

$$\Delta h_{ois} = c_p \cdot \Delta T_{ois} \quad (2.6.7)$$

By combining equation (2.6.6) and (2.6.7) is obtained

$$\frac{U}{C} = \frac{\pi \cdot D_t \cdot \dot{a}}{\sqrt{2 \cdot c_p \cdot \Delta T_{ois}}} \quad (2.6.8)$$

Where  $c_p$  is obtained from the following equation

$$c_p = \frac{\gamma_1}{\gamma_1 - 1} \cdot R_1 \quad (2.6.9)$$

and  $\Delta T_{ois}$  is equal to

$$\Delta T_{ois} = T_{o1} - T_{s2} \quad (2.6.10)$$

where  $T_{s2}$  is the downstream static temperature for isentropic expansion (s is for isentropic). In order to obtain  $T_{s2}$  the expression for isentropic expansion between the pressure and temperature of the expanded gas is used, thus

$$\frac{p_{o1}}{p_2} = \left( \frac{T_{o1}}{T_{s2}} \right)^{\frac{\gamma_1}{\gamma_1 - 1}} \quad (2.6.11)$$

solving (2.6.11) for  $T_{s2}$  leads to

$$T_{s2} = T_{o1} \cdot \left( \frac{p_{o1}}{p_2} \right)^{\frac{1 - \gamma_1}{\gamma_1}} \quad (2.6.12)$$

---

<sup>2</sup> Or the wheel linear velocity at its mean height in the case of the axial flow turbine

In order to obtain the static downstream pressure  $p_2$ , the following expression is used which relates the static and stagnation pressures of a gas

$$p_2 = p_{o2} \cdot \left( \frac{T_2}{T_{o2}} \right)^{\frac{\gamma_1}{\gamma_1 - 1}} \quad (2.6.13)$$

It is also known that

$$\Delta T_{oa} = T_{o1} - T_{o2} \quad (2.6.14)$$

and

$$\Delta T_{oa} = \eta_{oit} \cdot \Delta T_{oi} \quad (2.6.15)$$

where

$$\Delta T_{oi} = T_{oi} \cdot \left[ 1 - \left( \frac{p_{o1}}{p_{o2}} \right)^{\frac{1-\gamma_1}{\gamma_1}} \right] \quad (2.6.16)$$

thus  $T_{o2}$  is equal to

$$T_{o2} = T_{o1} + \eta_{oit} \cdot T_{oi} \cdot \left[ 1 - \left( \frac{p_{o1}}{p_{o2}} \right)^{\frac{1-\gamma_1}{\gamma_1}} \right] \quad (2.6.17)$$

The downstream static temperature  $T_2$  required in (2.6.13) can be calculated from the downstream stagnation temperature  $T_{o2}$  from the following equation

$$T_2 = T_{o2} - \frac{u_d^2}{2 \cdot c_p} \quad (2.6.18)$$

where  $u_d$  is the gas velocity exiting the diffuser.  $u_d$  can be calculated by

$$u_d = \frac{\dot{m}}{A_d \cdot \rho_d} \quad (2.6.19)$$

Where  $A_d$  is the cross section area of the diffuser and  $\rho_d$  is the density of the gas exiting the diffuser. This density can be calculated by approximation using the stagnation condition after the diffuser, thus

$$\rho_d = \frac{p_{o2}}{R_1 \cdot T_{o2}} \quad (2.6.20)$$

Combining (2.6.19) and (2.6.20)

$$u_d = \frac{\dot{m} \cdot R_1 \cdot T_{o2}}{A_d \cdot P_{o2}} \quad (2.6.21)$$

The mechanical power delivered by the turbine is calculated from the following equation

$$\dot{W}_t = \dot{m} \cdot c_p \cdot \Delta T_{oa} \quad (2.6.22)$$

and the torque developed to the turbine is

$$M_t = \frac{\dot{W}_t}{2 \cdot \pi \cdot \dot{\alpha}} \quad (2.6.23)$$

The stagnation specific enthalpy of the gas entering the downstream volume is

$$h_{o2} = u_1 + R_1 \cdot T_{o2} \quad (2.6.24)$$

The stagnation enthalpy change rate entering the downstream volume is given from the following relationship

$$\dot{H}_{o2} = \dot{m} \cdot h_{o2} \quad (2.6.25)$$

Accordingly for the upstream volume, the stagnation specific enthalpy of the gas is

$$h_{o1} = u_1 + R_1 \cdot T_{o1} \quad (2.6.26)$$

The stagnation enthalpy change rate entering the upstream volume is given from the following relationship

$$\dot{H}_{o2} = -\dot{m} \cdot h_{o1} \quad (2.6.27)$$

In order to calculate the heat exchange that takes place at turbine, the gas temperature, thermal conductivity, radiation, emissivity, Prandtl and Reynolds numbers, are required.

The heat transfer calculation requires the mean gas Temperature inside the turbine, thus

$$\bar{T} = T_{o1} + \frac{T_{o1} - T_2}{2} \quad (2.6.28)$$

The thermal conductivity and radiation emissivity are considered constant and are the same to the gas' that flows through the turbine. The Reynolds number is approximated the same way as in compressor equations, thus

$$Re = \frac{4 \cdot \dot{m}}{\pi \cdot D_t \cdot \mu_{us}} \quad (2.6.29)$$

where  $\dot{m}$  is the mass flow through the turbine and  $\mu$  is the viscosity coefficient of the upstream volume (us). The Prandtl number is obtained from the following equation

$$Pr = \frac{c_p \cdot \mu_{us}}{k_{us}} \quad (2.6.30)$$

where

$$c_p = \frac{\gamma_{us}}{\gamma_{us} - 1} \cdot R_{us} \quad (2.6.31)$$

The total burned fuel mass fraction change rate for the downstream volume equals to

$$\dot{\xi}_2 = \dot{m} \cdot (\xi_1 - \xi_2) \quad (2.6.32)$$

while the upstream volume is zero, thus

$$\dot{\xi}_1 = 0 \quad (2.6.33)$$

The models of Turbine block and subblocks in MATLAB/Simulink, are shown in Fig. 2-6, Fig. 2-7 and Fig. 2-8.

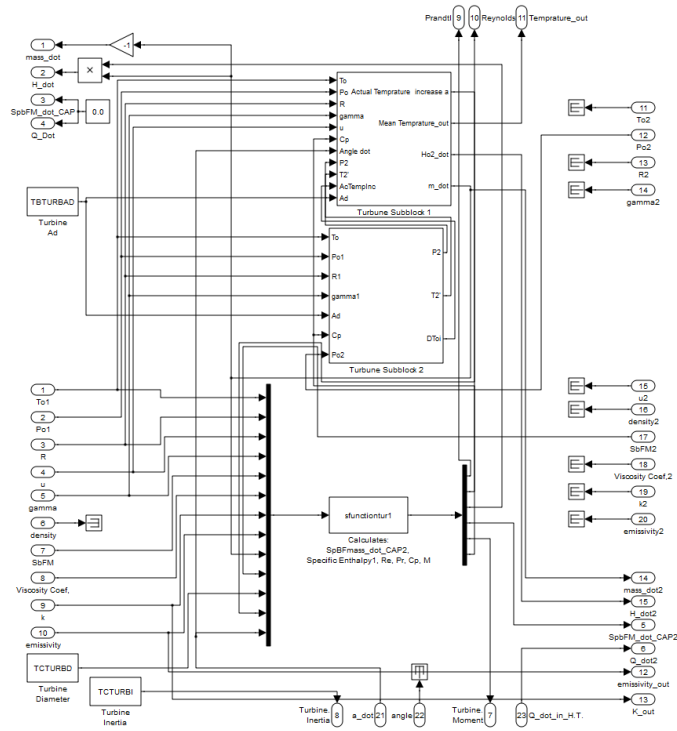


Fig. 2-6 Block: Turbine

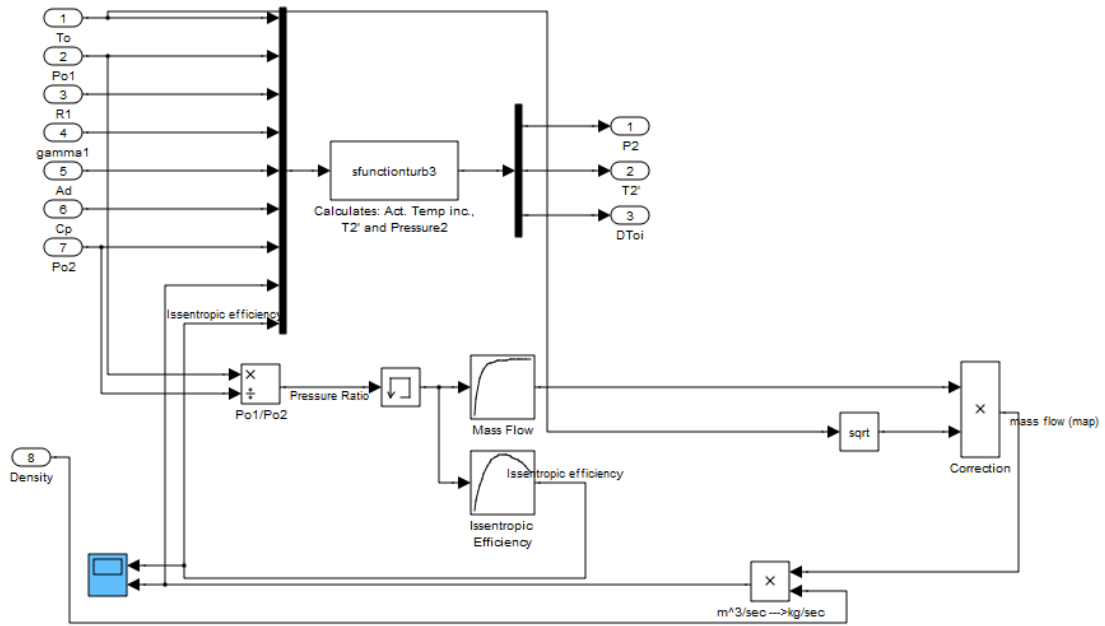


Fig. 2-7 Turbine Sub block 1

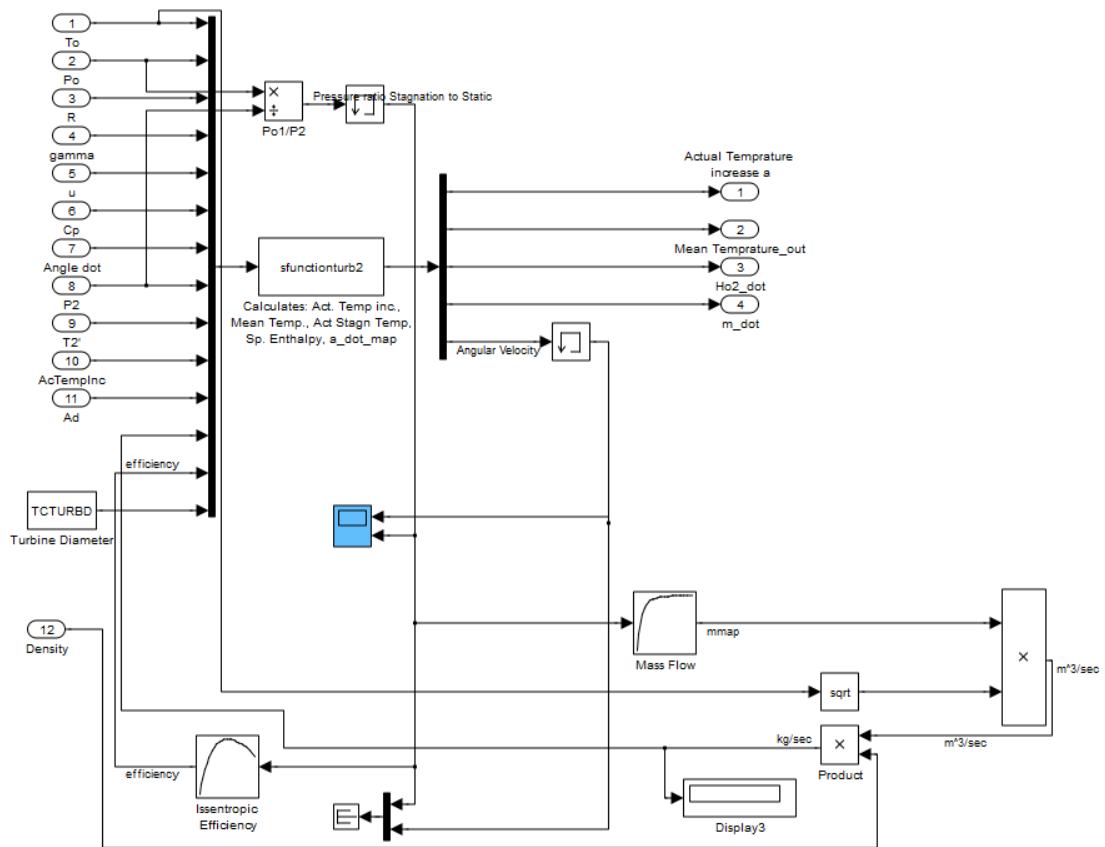


Fig. 2-8 Turbine sub block 2

## 2.7 Combustion Model S Curve

In this chapter the S – curve ( $f_s$ ) is presented as an implementation approach for the accumulated burned fuel during direct fuel injection in a cylinder.

For convenience, the time derivative of the s – curve is used. The later has the advantage that the time integral is equal to unity, thus by multiplying  $\dot{f}_s$  with the fuel mass injected results in the fuel burning rate.

The basic form of the S – Curve is

$$f_s = 1 - e^{-C_1 \cdot x^{C_2}} \quad (2.7.1)$$

where x is the S – Curve parameter taking values in the range [0,1] and  $C_1, C_2$  are constants defining the shape of the S – Curve. For the purpose of using  $f_s$  for modeling the accumulated burned fuel, during a single fuel injection in Diesel engines, the x parameter is substituted with the term

$$\frac{\alpha - \alpha_r}{\Delta\alpha} \quad (2.7.2)$$

where  $\alpha$  is the instantaneous angular position of the crankshaft,  $\alpha_r$  is the reference angle where the fuel burning starts and  $\Delta\alpha$  is the duration of the burning fuel expressed in crankshaft angle. So the S – Curve equation takes the form

$$f_s = 1 - e^{-C_1 \cdot \left(\frac{\alpha - \alpha_r}{\Delta\alpha}\right)^{C_2}} \quad (2.7.3)$$

and by differentiating for the time the equation (2.7.3) and by rearranging the following equation is obtained

$$\dot{f}_s = e^{-C_1 \cdot \left(\frac{\alpha - \alpha_r}{\Delta\alpha}\right)^{C_2}} \cdot C_1 \cdot C_2 \cdot \left(\frac{\alpha - \alpha_r}{\Delta\alpha}\right)^{C_2-1} \cdot \frac{d\left(\frac{\alpha - \alpha_r}{\Delta\alpha}\right)}{dt} \quad (2.7.4)$$

$\alpha_r$  varies slowly over time, thus it can be assumed as constant with a negligible error

$$\dot{f}_s = e^{-C_1 \cdot \left(\frac{\alpha - \alpha_r}{\Delta\alpha}\right)^{C_2}} \cdot C_1 \cdot C_2 \cdot \left(\frac{\alpha - \alpha_r}{\Delta\alpha}\right)^{C_2-1} \cdot \frac{\dot{\alpha} - 0}{\Delta\alpha} \quad (2.7.5)$$

and finally by rearranging

$$\dot{f}_s = C_1 \cdot C_2 \cdot \frac{\dot{\alpha}}{\Delta\alpha} \cdot e^{-C_1 \cdot \left(\frac{\alpha - \alpha_r}{\Delta\alpha}\right)^{C_2}} \cdot \left(\frac{\alpha - \alpha_r}{\Delta\alpha}\right)^{C_2-1} \quad (2.7.6)$$

Where  $\alpha$  is the instantaneous angular position [-],  $\dot{\alpha}$  is the instantaneous angular speed [ $s^{-1}$ ],  $\alpha_r$  is the reference angular position (starting point) [-],  $\Delta\alpha$  is s –curve angular length [-] and  $C_1, C_2$  are constants [-].

The implementation of the combustion block in MATLAB/Simulink is shown in Fig. 2-9.

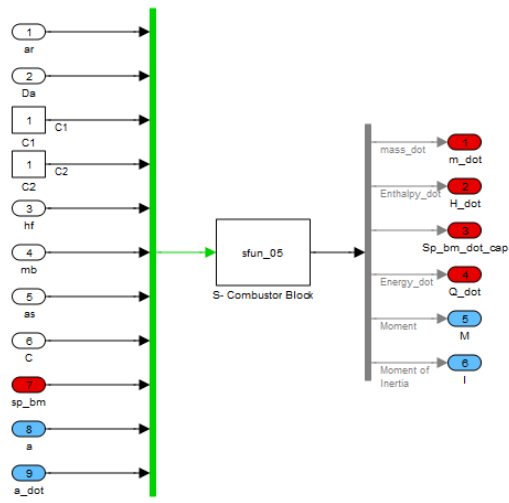


Fig. 2-9 Block: S - Curve Combustion



## 2.8 Heat Transfer Elements

In order to create a model that describes suitably the heat transfer between two or more masses, three blocks are modeled that describe the three ways of heat transfer, conduction, convection and radiation. Each of these blocks contains the factors that equations need to calculate the heat flux between the elements that are connected.

### 2.8.1 Conduction

The conduction heat Flux Block illustrates the heat transfer between two masses using the Fourier law for calculating the heat flux amount. The equation which calculates the heat flux requires certain geometry data, named, contact area of the two masses, the shape factors of each mass. Plus physical and thermal properties of the materials are needed which are provided by the female connections of the block, shown in Fig. 2-10. The conduction block is used only for solid masses accumulating heat, which eventually ends in heat Transfer between them.

The amount of heat flux passed between two masses is given from the Fourier Law. The equation shows the simplest case of heat exchange between two flat walls of different materials having thermal conductivities  $k_1$  and  $k_2$  respectively and with contact area  $A_c$ . Thus:

$$\dot{Q}_{cd(2-1)} = \frac{K_1}{\delta_1} \cdot A_c \cdot (T_c - T_1) = \frac{K_2}{\delta_2} \cdot A_c \cdot (T_2 - T_c) = -\dot{Q}_{cd(1-2)} \quad (2.8.1)$$

Where:

$\delta_1$  and  $\delta_2$ : are the distance between the center of each wall and the contact area. Typically is assumed that is the half of the wall thickness.

$T_c$ : is the absolute temperature of the contact area.

The quantities  $1/\delta_i$ , where  $i$  is the number of the material are the shape factors with respect to the contact area. Therefore, the equation (1.1) can be rewritten as follow:

$$\dot{Q}_{cd(2-1)} = S_1 \cdot A_c \cdot (T_c - T_1) = S_2 \cdot A_c \cdot (T_2 - T_c) = -\dot{Q}_{cd(1-2)} \quad (2.8.2)$$

From the above equation is found that:

$$k_1 \cdot S_1 \cdot A_c \cdot T_c - k_1 \cdot S_1 \cdot A_c \cdot T_1 = k_2 \cdot S_2 \cdot A_c \cdot T_2 - k_2 \cdot S_2 \cdot A_c \cdot T_c \quad (2.8.3)$$

By solving for the absolute temperature  $T_c$  of the contact area it is found that

$$T_c = \frac{k_2 \cdot S_2 \cdot T_2 + k_1 \cdot S_1 \cdot T_1}{k_1 \cdot S_1 + k_2 \cdot S_2} \quad (2.8.4)$$

And now by combining equations (2.6.1) and

$$\dot{Q}_{cd(2-1)} = L \cdot A_c \cdot (T_2 - T_1) \quad (2.8.5)$$

$$\dot{Q}_{cd(2-1)} = k_1 \cdot S_1 \cdot A_c \cdot (T_c - T_1) = L \cdot A_c \cdot (T_2 - T_1) \quad (2.8.6)$$

and by substituting in equation (2.6.4) and solving for L

$$L = \left[ \frac{K_1 \cdot S_1 \cdot K_2 \cdot S_2}{K_1 \cdot S_1 + K_2 \cdot S_2} \cdot T_2 - \frac{K_1 \cdot S_1 \cdot K_2 \cdot S_2}{K_1 \cdot S_1 + K_2 \cdot S_2} \cdot T_1 \right] \cdot \frac{1}{T_2 - T_1} \quad (2.8.7)$$

By eliminating  $T_1$  and  $T_2$  from the equation (2.6.7)

$$L = \frac{K_1 \cdot S_1 \cdot K_2 \cdot S_2}{K_1 \cdot S_1 + K_2 \cdot S_2} \quad (2.8.8)$$

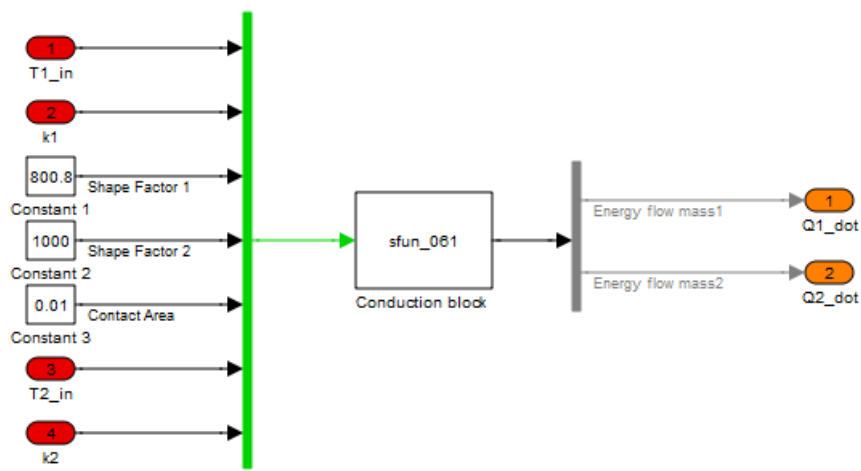


Fig. 2-10 Block: conduction Heat Flux Block

## 2.8.2 Convection

The convection heat flux block is an element that controls the heat flux between two masses that accumulating heat, using the Newton law for calculation the heat flux amount. As seen in Fig. 2-11, the required information for heat flux calculation are the contact area and geometry shape factor. Certain constants are also required for the calculation of convection coefficient  $h$  while physical and thermal properties of the materials are provided from the connection with other blocks.

The heat flux passed between a solid and a fluid mass through convection is given from the Newton Law. The following equations model a simple case of a flat wall and a fluid, having thermal conductivities  $k_s$  and  $k_f$  respectively and with a contact area  $A_c$ . The heat flux exchanged will be

$$\dot{Q}_{cv(2-1)} = \frac{k_s}{\delta_s} \cdot A_c \cdot (T_c - T_s) = h \cdot A_c \cdot (T_f - T_c) = -\dot{Q}_{cv(1-2)} \quad (2.8.9)$$

Where  $T_c$  is the absolute temperature of the contact area and  $\delta_s$  is the half thickness. Shape factor is equal to

$$S_s = \frac{1}{\delta_s} \quad (2.8.10)$$

Thus equation (2.6.9) can be rewritten as

$$\dot{Q}_{cv(2-1)} = S_s \cdot A_c \cdot (T_c - T_s) = h \cdot A_c \cdot (T_f - T_c) \quad (2.8.11)$$

Heat flux can also be calculated using L

$$\dot{Q}_{cv(2-1)} = L \cdot h \cdot A_c \cdot (T_f - T_c) \quad (2.8.12)$$

by combing equations (2.6.9) and (2.6.12) and solving for L it is found that

$$L = \frac{K_s \cdot S_s \cdot h}{K_s \cdot S_s + h} \quad (2.8.13)$$

the absolute temperature of contact area will be

$$T_c = \frac{k_s \cdot S_s \cdot T_s + h \cdot T_f}{k_s \cdot S_s + h} \quad (2.8.14)$$

Where

$$h = \frac{Nu \cdot k_f}{D} \quad (2.8.15)$$

$$Nu = \alpha \cdot Re^b \cdot Pr^c \quad (2.8.16)$$

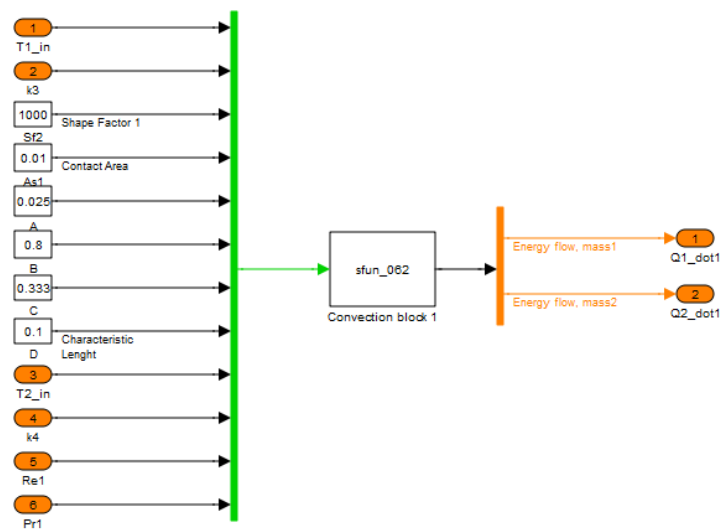


Fig. 2-11 Block: Convection Heat Transfer

### 2.8.3 Radiation

The radiation heat flux controller is an element which controls the heat transfer between two masses using the Steffan - Boltzman law for calculating the heat flux amount. The configuration of the block is shown in Fig. 2-12. Certain geometry data are required for the calculation named radiation shape factor and Contact area.

According to theory of Steffan - Boltzman, the total energy density emitted from a black body is proportional to the fourth power of absolute temperature. Thus

$$E_b = \sigma \cdot T^4 \quad (2.8.17)$$

Where,  $E_b$  is the energy radiated per unit time and area (power density) by the ideal radiator,  $\sigma$  is the Steffan – Boltzman constant and it is equal to

$$\sigma = 5.669 \cdot 10^{-8} W / m^2 \cdot K \quad (2.8.18)$$

When heat flux takes place from 1 to 2, the following equation models the phenomenon

$$E_{b1} \cdot A_2 \cdot F_{(1-2)} \quad (2.8.19)$$

Where  $F_{(1-2)}$  is the radiation shape factor and illustrates the fraction of energy leaving the surface one and reaches the surface two. As mentioned above the two surfaces are black meaning that all radiation is absorbed and the net heat power exchange is given by

$$\dot{Q}_{rd(1-2)} = E_{b1} \cdot A_1 \cdot F_{(1-2)} - E_{b2} \cdot A_2 \cdot F_{(2-1)} \quad (2.8.20)$$

If the two surfaces have the same temperature, meaning that no heat exchange takes place, the equation (2.6.20) leads to

$$E_{b1} = E_{b2} \quad (2.8.21)$$

And eventually to

$$A_1 \cdot F_{(1-2)} = A_2 \cdot F_{(2-1)} \quad (2.8.22)$$

By combing equations (2.6.20) – (2.6.21), the net heat exchange for black bodies is

$$\dot{Q}_{rd(1-2)} = A_1 \cdot F_{(1-2)} \cdot (E_{b1} - E_{b2}) = A_2 \cdot F_{(2-1)} \cdot (E_{b2} - E_{b1}) \quad (2.8.23)$$

The radiation heat flux is easy to calculate assuming that black bodies are invoked. Since a part of the amount is absorbed by the materials meaning that energy can be reflected back and forth between the heat exchanging surfaces, a more complex system will be described in order to model the real physical system. Therefore, the irradiation  $G$  and radiosity  $J$  terms are used. Irradiation is the total radiation incident upon a surface per unit time and per unit area. The radiosity is the sum of the energy and the energy reflected when no energy is transmitted through the material.

$$J = \varepsilon \cdot E_b + r \cdot G \quad (2.8.24)$$

Where  $r$  is the reflectivity of the surface and  $\varepsilon$  is the emissivity which is defined as the ratio of actual heat radiated density  $E$  and the theoretical black body heat radiated density  $E_b$

$$\varepsilon = \frac{E}{E_b} \quad (2.8.25)$$

The reflectivity is given by

$$r = 1 - \varepsilon \quad (2.8.26)$$

Now by substituting the equations (2.6.25) and (2.6.25) to (2.6.24) it is obtained

$$J = \varepsilon \cdot E_b + (1 - \varepsilon) \cdot G \quad (2.8.27)$$

The net energy leaving the surface is the difference of the above elements (irradiation and radiosity)

$$\frac{\dot{Q}_{rd(b-s)}}{A_r} = J - G = \varepsilon \cdot E_b + (1 - \varepsilon) \cdot G - G = \varepsilon_b \cdot (E_b - G) \quad (2.8.28)$$

where  $A_r$  is the surface of radiating body. By substituting  $G$  from the equation (2.6.27) equation (2.6.28) can be rewritten as follows

$$\frac{\dot{Q}_{rd(b-s)}}{A_r} = \varepsilon \cdot \left( E_b - \frac{J - \varepsilon \cdot E_b}{1 - \varepsilon} \right) \quad (2.8.29)$$

by simplifying and rearranging

$$\frac{\dot{Q}_{rd(b-s)}}{A_r} = \varepsilon \cdot \frac{E_b - J}{1 - \varepsilon} \quad (2.8.30)$$

or alternately

$$\frac{\dot{Q}_{rd(b-s)}}{A_r} = \frac{E_b - J}{(1 - \varepsilon) / (\varepsilon \cdot A_r)} \quad (2.8.31)$$

Examining the equation (2.6.31) it is found that if the denominator of the right side is considered as the surface resistance to radiation heat transfer, the numerator a potential difference and the heat flow of the current, then a network can be created similar to electrical systems.

The total radiation leaving the system one and reaching system two is

$$J_1 \cdot A_1 \cdot F_{(1-2)} \quad (2.8.32)$$

Versa

$$J_2 \cdot A_2 \cdot F_{(2-1)} \quad (2.8.33)$$

The net interchange is equal to

$$\dot{Q}_{rd(1-2)} = (J_1 - J_2) \cdot A_1 \cdot F_{(1-2)} = (J_1 - J_2) \cdot A_2 \cdot F_{(2-1)} \quad (2.8.34)$$

Knowing that

$$A_1 \cdot F_{(1-2)} = A_2 \cdot F_{(2-1)} \quad (2.8.35)$$

The surface resistance of surface one is

$$\dot{Q}_{rd(b-1)} = \frac{E_{b1} - J_1}{(1 - \varepsilon_1) / (\varepsilon_1 \cdot A_1)} \quad (2.8.36)$$

Accordingly for surface two

$$\dot{Q}_{rd(2-b)} = \frac{J_1 - E_{b2}}{(1 - \varepsilon_2) / (\varepsilon_2 \cdot A_2)} \quad (2.8.37)$$

Using the conservation law for energy and by eliminating the J, equation (2.6.34) can be rewritten as follows

$$\dot{Q}_{rd(b-1)} = \dot{Q}_{rd(2-b)} = \frac{E_{b1} - E_{b2}}{\left( \frac{(1 - \varepsilon_1)}{\varepsilon_1 \cdot A_1} + \frac{1}{(A_1 \cdot F_{(1-2)})} + \frac{(1 - \varepsilon_2)}{\varepsilon_2 \cdot A_2} \right)} = \dot{Q}_{rd(1-2)} \quad (2.8.38)$$

By substituting  $E_{b1}$  and  $E_{b2}$  from the above equation

$$\dot{Q}_{rd(1-2)} = \frac{\sigma \cdot (T_1^4 - T_2^4)}{\left( \frac{(1 - \varepsilon_1)}{\varepsilon_1 \cdot A_1} + \frac{1}{(A_1 \cdot F_{(1-2)})} + \frac{(1 - \varepsilon_2)}{\varepsilon_2 \cdot A_2} \right)} \quad (2.8.39)$$

Which is the final equation used for calculating the heat exchanged between two surfaces due to radiation.

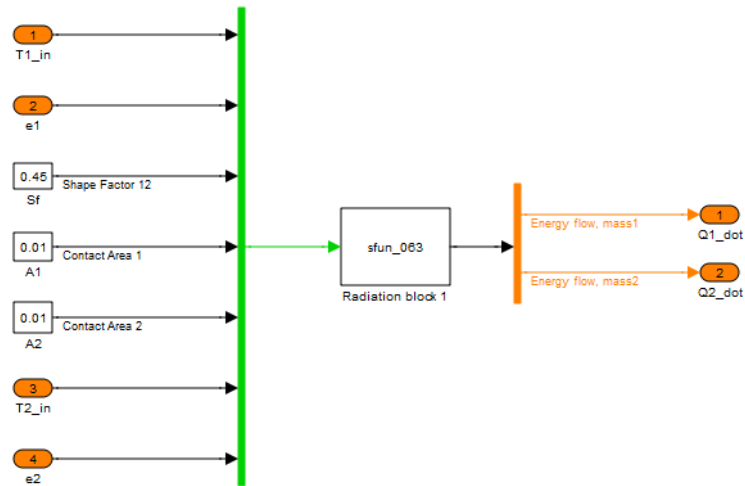


Fig. 2-12 Block: Radiation Heat Transfer

## 2.9 Cylinder Geometry

The mathematical equations governing the Cylinder Geometry are presented here. The model incorporates two volumes denoted as upper  $V_U$  and lower  $V_L$ . Both volumes are fully symmetrical and are equally treated. As a result of this, both volumes can be used as combustion chambers independently. The upper volume  $V_U$  at any crank angle position is the sum of the upper clearance volume  $V_{cU}$  and the upper displaced or swept volume  $V_{dU}$  (Kyrtatos, 1993), thus

$$V_U = V_{cU} + V_{dU} \quad (2.9.1)$$

accordingly the lower part  $V_L$  at any crank angle position is the sum of the lower clearance volume  $V_{cL}$  and the lower displaced or swept volume  $V_{dL}$ , thus

$$V_L = V_{cL} + V_{dL} \quad (2.9.2)$$

where the displaced volumes ( $V_{dU}$  and  $V_{dL}$ ) are the product of the piston distance relative position ( $x_U$  and  $x_L$  accordingly) and the cylinder cross section area  $A_{cs}$ . Thus the upper displaced volume  $V_{dU}$  is

$$V_{dU} = A_{cs} \cdot x_U \quad (2.9.3)$$

and

$$V_{dL} = A_{cs} \cdot x_L \quad (2.9.4)$$

The cross section area of the cylinder  $A_{cs}$  is

$$A_{cs} = \pi \cdot \frac{B^2}{4} \quad (2.9.5)$$

where  $B$  is the cylinder bore.

The position of the piston with respect to the upper face of the piston is

$$x_U = r + d \quad (2.9.6)$$

while the piston position with respect the lower face of the piston  $x_L$  is

$$x_L = r - d \quad (2.9.7)$$

where  $r$  is the crank radius and  $d$  is the distance of the piston from the mid – stroke position as shown in Fig. 2-15 and is calculated using the following equation

$$d = l - r \cdot \cos(2 \cdot \pi \cdot a) - E \quad (2.9.8)$$

where  $l$  is the connecting rod length,  $a$  is the crank angle and  $E$  is equal to

$$E = l \cdot \sqrt{1 - \frac{r^2}{l^2} \cdot \sin^2(2 \cdot \pi \cdot a)} \quad (2.9.9)$$

The notation used in the previous equations is shown Fig. 2-13

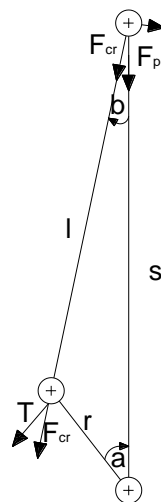


Fig. 2-13 Basic length, angle and torque developed to crankshaft due to gas forces

For simplicity in equations,

$$\begin{aligned} \cos(2 \cdot \pi \cdot a) &= w \\ \sin(2 \cdot \pi \cdot a) &= h \end{aligned} \quad (2.9.10)$$

thus,

$$d = l - r \cdot w - E \quad (2.9.11)$$

So equation (2.9.9) can now be rewritten as



$$E = l \cdot \sqrt{1 - \left(\frac{r \cdot h}{l}\right)^2} \quad (2.9.12)$$

The velocity of the piston with respect to the upper face of the piston is calculated from

$$\dot{x}_U = r \cdot h \cdot 2 \cdot \pi \cdot \dot{a} \cdot \left(1 + \frac{r \cdot w}{E}\right) \quad (2.9.13)$$

where  $\dot{a}$  is the crank angular velocity. As already stated before, the system is symmetrical thus the velocity  $\dot{x}_L$  of the piston with respect to the lower face of the piston is opposite to the  $\dot{x}_U$  thus,

$$\dot{x}_L = -\dot{x}_U \quad (2.9.14)$$

The cylinder upper volume change rate is calculated as the product of the piston velocity with respect to the upper part and the cross section area of the cylinder, thus

$$\dot{V}_U = A_{cs} \cdot \dot{x}_U \quad (2.9.15)$$

The system is symmetrical thus,

$$\dot{V}_L = -\dot{V}_U \quad (2.9.16)$$

The torque developed from (or absorbed by) the cylinder due to the sum of the gas forces Fig. 2-13 acting on the upper and lower faces of the piston  $M_p$  is

$$M_p = T \cdot r \quad (2.9.17)$$

where T is the tangential component of  $F_{cr}$  force and is equal to

$$T = F_p \cdot h \cdot \left(1 + \frac{r \cdot w}{E}\right) \quad (2.9.18)$$

where  $F_p$  is the total force developed from the gas . By combining (2.9.17) and (2.9.18)

$$M_p = F_p \cdot r \cdot h \cdot \left(1 + \frac{r \cdot w}{E}\right) \quad (2.9.19)$$

$F_p$  is given by

$$F_p = A_{cs} \cdot p_U - A_{cs} \cdot p_L = A_{cs} \cdot (p_U - p_L) \quad (2.9.20)$$

where  $p_U$  is the absolute gas pressure developed on the the upper face of the piston and  $p_L$  is the absolute gas pressure developed on the lower face of the piston.

The moving parts of the system piston assembly, connecting rod assembly etc have considerable mass which during one engine cycle accelerate and de – accelerate. The system

can be simplified in two masses. A rotating mass  $m_r$  and a mass moving linearly  $m_l$ . For the purpose of this diploma thesis an equivalent polar moment of inertia of the system is needed. This equivalent polar moment of inertia can be the mean value over one complete crankshaft cycle or the instant value. In order to find the instantaneous equivalent polar moment of inertia of the moving parts the total kinetic energy stored to the system is considered. The total kinetic energy  $K$  of the system using the instantaneous equivalent polar moment of inertia is

$$K = \frac{1}{2} \cdot I_p \cdot (2 \cdot \pi \cdot \dot{a})^2 \quad (2.9.21)$$

The kinetic energy of the rotating mass is

$$K_r = \frac{1}{2} \cdot m_r \cdot (2 \cdot \pi \cdot r \cdot \dot{a})^2 \quad (2.9.22)$$

and the kinetic energy  $K_l$  of the linear moving mass  $m_l$  is

$$K_l = \frac{1}{2} \cdot m_l \cdot \dot{x}^2 \quad (2.9.23)$$

but the sum of the kinetic energies of the rotating and linear moving masses is equal to the total kinetic energy of the system using the instantaneous equivalent polar moment of inertia, thus

$$K = \frac{1}{2} \cdot m_r \cdot (2 \cdot \pi \cdot r \cdot \dot{a})^2 + \frac{1}{2} \cdot m_l \cdot \dot{x}^2 = \frac{1}{2} \cdot I_p \cdot (2 \cdot \pi \cdot \dot{a})^2 \quad (2.9.24)$$

Solving equation (2.9.24) for the polar moment of inertia  $I_p$

$$I_p = \frac{m_r \cdot (2 \cdot \pi \cdot \dot{a})^2 + m_l \cdot \dot{x}^2}{(2 \cdot \pi \cdot \dot{a})^2} = m_r \cdot r^2 + \frac{m_l \cdot \dot{x}^2}{(2 \cdot \pi \cdot \dot{a})^2} \quad (2.9.25)$$

A modification of equation (2.9.25) is needed when the angular velocity takes value equal to zero, when the mentioned equation becomes illegal. In this case the second term has no meaning and can be safely ignored, thus

$$I_p = \begin{cases} m_r \cdot r^2 + \frac{m_l \cdot \dot{x}^2}{(2 \cdot \pi \cdot \dot{a})^2} & \text{if } \dot{a} \neq 0 \\ m_r \cdot r^2 & \text{if } \dot{a} = 0 \end{cases} \quad (2.9.26)$$

The presented model in MATLAB/Simulink is shown in Fig. 2-14 while Fig. 2-15 shows the typical cylinder arrangement.

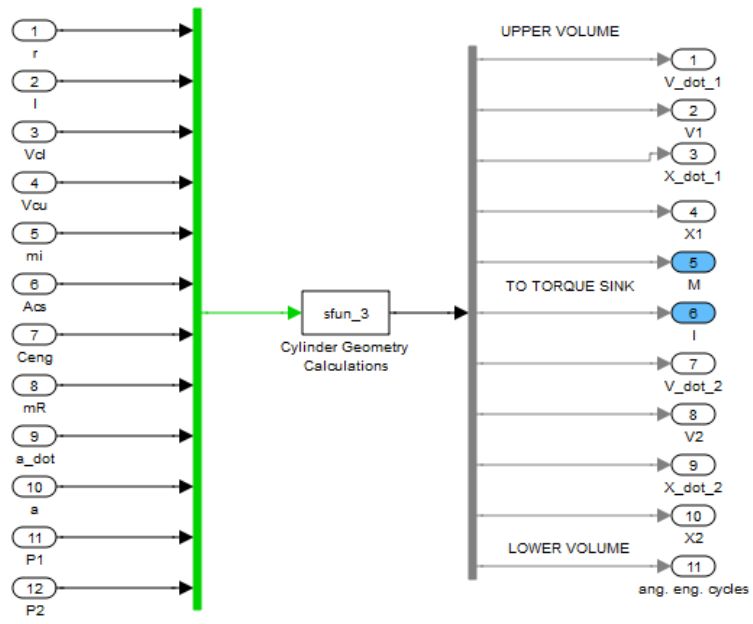


Fig. 2-14 Block: Cylinder Geometry

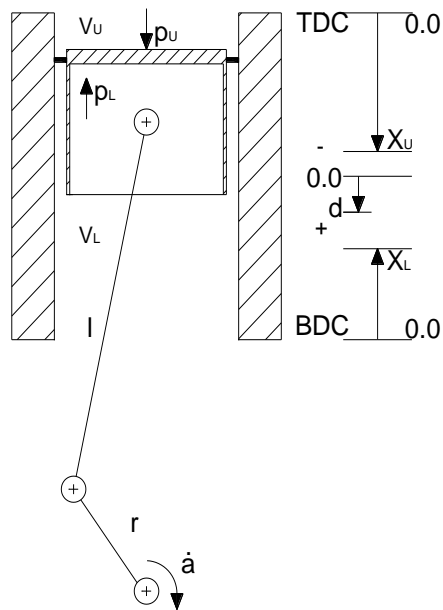


Fig. 2-15 Typical cylinder arrangement

## 2.10 Geometrical Energy Loss

The mathematical equations governing the Geometrical energy loss are presented in this section.

Three terms consist the pressure loss. The first term is the proportional to the total pressure applied and is defined as a percentage of the total pressure applied and is defined as a percentage of the total pressure which is provided to the geometry of the cylinder. This pressure percentage drop is analogous to the mechanical efficiency  $\eta_f$ . The second term is proportional to the linear reference velocity. The third term is equal to a constant pressure drop which is always present (while the linear velocity is not equal to zero) independent of the loading condition. Thus the pressure loss is equal to

$$p_f = \begin{cases} \eta_f \cdot |p_2| + C \cdot |\dot{x}_2| + p_s & \text{if } \dot{x}_2 \neq 0 \\ \eta_f \cdot |p_2| + C \cdot |\dot{x}_2| & \text{if } \dot{x}_2 = 0 \end{cases} \quad (2.10.1)$$

All the above constants and  $p_s$  variable must be positive numbers.

The mechanical power converted to heat is equal to

$$\dot{Q}_f = |\dot{V}| \cdot p_f \quad (2.10.2)$$

It is noted that (2.10.2) is always positive since it represents the heat supplied. The pressure transmitted of state 1 before the pressure loss is equal to

$$p_1 = \begin{cases} p_2 - p_f & \text{if } \dot{x}_2 \geq 0 \\ p_2 - p_f & \text{if } \dot{x}_2 < 0 \end{cases} \quad (2.10.3)$$

The volume change rate and the volume are passing unchanged from the geometrical energy loss model, thus

$$\begin{aligned} \dot{V}_2 &= \dot{V}_1 \\ V_2 &= V_1 \end{aligned} \quad (2.10.4)$$

Also, the linear velocity and linear position are passing unchanged from the geometrical energy loss model, thus

$$\begin{aligned} \dot{x}_2 &= \dot{x}_1 \\ x_2 &= x_1 \end{aligned} \quad (2.10.5)$$

The presentation of the model is shown in Fig. 2-16.

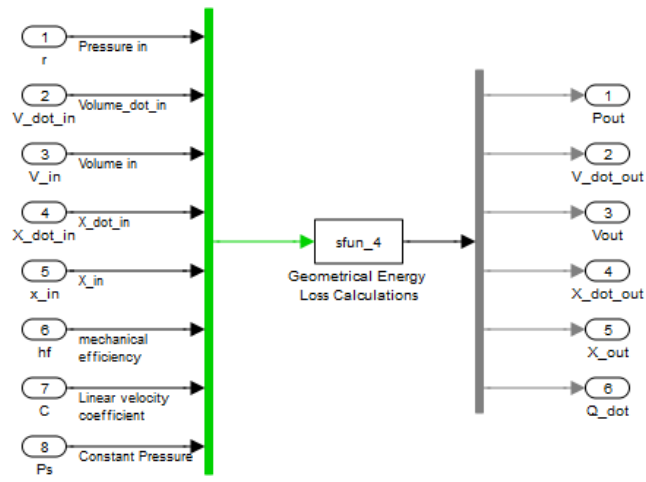


Fig. 2-16 Block: Geometrical Energy Loss

### 3 Simulation Blocks

In this chapter of the diploma thesis, major simulink® blocks are described. The available groups are (Lambropoulos, 2000):

- Thermo – fluid group, which contains all the necessary information about gas properties, the implementation of plenum as laws of thermodynamics and emptying and filling methods
- Geometry group, which contains the equations of cylinder geometry and contains also the link between the thermo – fluid group and the mechanical interface of the system such as torque and angular velocity
- Heat Transfer group, which implements the three ways of heat transfer, such as conduction, convection and radiation. Each of them or combined properly implement the ways of heat flux of the engine

Due to the fact that these blocks contain most of the blocks described in Chapter 2 as mathematical equations blocks, the term major is used in order to describe a group of blocks at a higher level, for engine configuration. In next section, the Simulink® library of the major blocks, or blocks that can be used independently, is presented. Also, each major block is described thoroughly.

In order to construct a simple system, graphical connection of the blocks must be performed. The general idea of connection is with arrows that show the flow of the signals. Therefore, it is clear to the user, which block with which other or others is connected. Table 3-1 groups the various blocks into the library.

Table 3-1 Simulation groups

Group	Blocks
<b>Thermo - fluid</b>	Gas Properties, Fixed Fluid, Open Thermodynamic System, Compressor, Intercooler, Turbine, S – Curve combustion, Turbocharger, MAN NA70/TO78 TC, 8 Cylinders, one cylinder
<b>Geometry</b>	Cylinder Geometry, Geometrical energy Loss, Stiff shaft
<b>Heat Transfer</b>	Conduction, Convection, Radiation, Cylinder Heat transfer

The corresponding S – Functions can be found in Appendix A.

### 3.1 Block Library

A total snapshot of the Simulink block library is shown in Fig. 3-1. Appendix C shows this library in greater detail. The library contains 19 blocks as follows:

- Turbocharger Block
- Inlet and Exhaust Valve Blocks
- Open Thermodynamic and Gas Properties Block
- Fixed Fluid and Gas Properties Block
- Cylinder Heat Transfer Block
- Combustion Block
- One Cylinder Block
- Multiple Connected Cylinders Block

The above blocks are presented in detail in section 3.2.

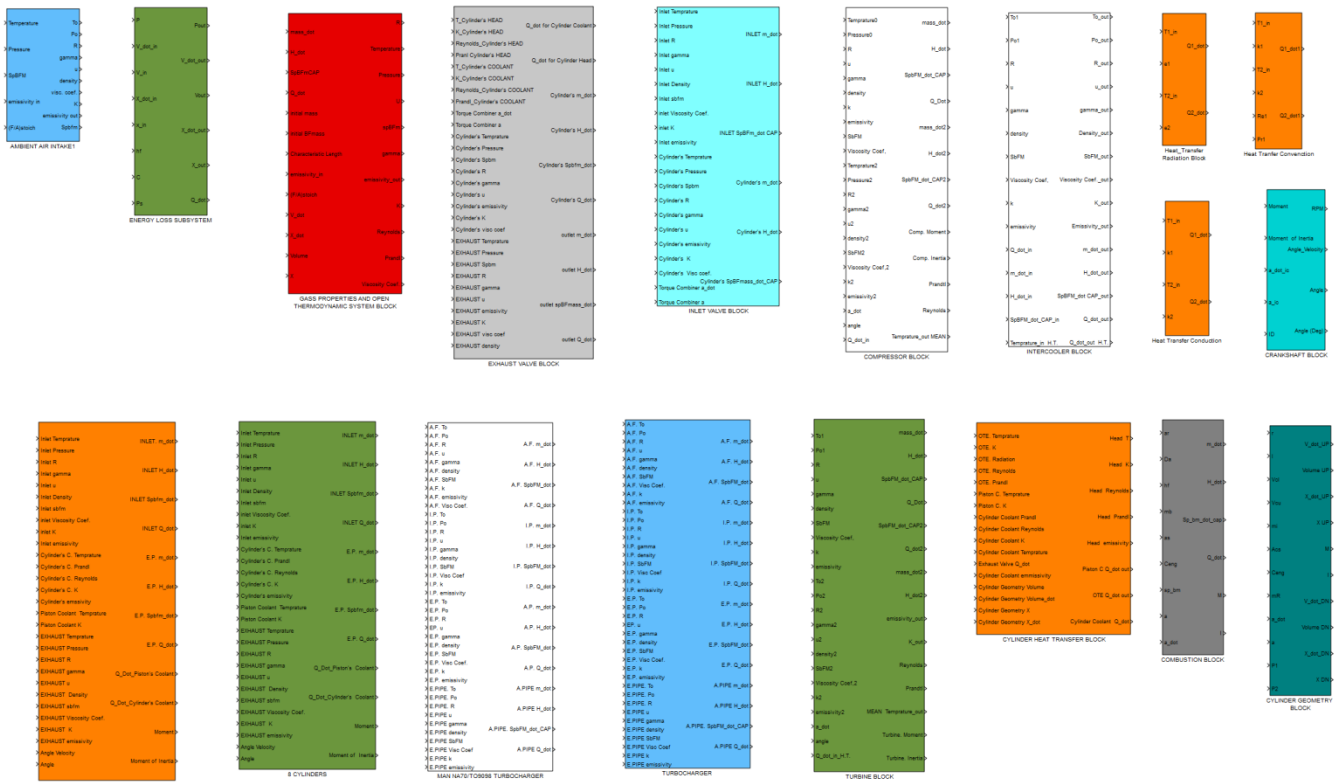


Fig. 3-1 Simulink Block Library with 19 elements

## 3.2 Major Blocks

### 3.2.1 Turbocharger and Intercooler blocks

Various types of exhaust driven turbochargers have been designed for supercharging reciprocating internal combustion engines. A turbocharger consists basically of a compressor and a turbine coupled on a common shaft. The exhaust gases from the engine are directed by the turbine inlet casing on to the blades of the turbine and subsequently discharged to atmosphere through a turbine outlet which compresses the air and directs it to the engine induction manifolds, to supply the engine cylinders with air of higher density than is available to a naturally aspirated engine (Watson & Janota, 1982). The Marine Diesel Engine is equipped with a marine turbocharger that contains also a heat exchanger to cool down the gas after the compression due to the fact that the change of gas pressure after the compressor block also increases the temperature of the gas. Thus in order to provide lower density intake air, an intercooler (heat exchanger using as coolant medium water) is also installed. This text describes a radial compressor, an intercooler and a turbine along with a stiff rotating shaft that form the model of the turbocharger used. The implement engine uses 3 turbochargers manufactured by MAN. The type of turbocharger used is NA70/TO9098.

The compressor is modeled as a standalone unit and the power required to drive the compressor is obtained as already stated, through a shaft. Thus the compressor can obtain power from turbine(s), crankshaft(s) and any combination of them. The compressor behaves as a device controlling the gas mass flow between two control volumes. The gas mass flow rate is depended on the pressure ratio between the control volumes and the compressor speed.

Compressor performance is described using a map (usually obtained from the manufacturer) which provides the mass flow rate through the compressor (at reference states) and the corresponding isentropic efficiency for various pressure ratios and speeds (compressor's angular velocity).

The shaft power required by the compressor is equal to the enthalpy increase of the gas during the compression process. The actual temperature increase is calculated by dividing the ideal enthalpy increase with an efficiency factor called isentropic efficiency of the compressor (due to the fact that compression is not ideal to have isentropic change). Under normal circumstances, the compressor takes the air from the volume with the lower pressure (downstream) and delivers it to the volume with higher pressure (upstream) than the atmosphere. The working pressure ratio is defined as the ratio of the upstream pressure to the downstream pressure of the gas. The mass flow is implemented in the compressor as one way. Thus the gas flows only from upstream to downstream volume. Thus for pressure ratios higher than unity the mass will flow from the volume with the lower pressure to the volume with the higher pressure while in case of pressure ratios lower than unity the mass will flow from the volume with the higher pressure volume towards the lower pressure volume.



In reality heat transfer also occurs in the casing. Thus in order to have a better approach to the real behavior of the compressor, heat transfer is implemented using one heat transfer male interface through which the heat flux is defined externally using heat transfer elements assuming mean gas temperature and thermal conductivities. The heat extracted or added to the gas through heat transfer is then provided to the upstream volume using the female thermo fluid interface (Temperature, pressure, gas constant, viscosity coefficient, specific burned fuel mass fraction, density, internal energy, thermal conductivity and emissivity as inputs).

The compressor is modeled as a subsystem which controls the flow between two control volumes. The compressor block uses the gas state and properties of the two control volumes together with the angular velocity of the compressor in order to calculate the mass flow rate using a map. The compressor block has twenty inputs and eight outputs that provide the aforementioned stated properties. The compressor block is shown in Fig. 3-2.

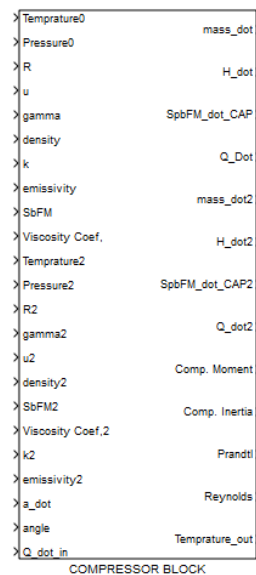


**Fig. 3-2 Block: Compressor**

The compressor is connected to a heat exchanger. This is necessary due to temperature increase of the gas pursuant to pressure increase and is undesirable at this stage. Thus an intercooler achieves lower temperature and thus higher density of the working fluid. The turbocharger block contains an intercooler based on the heat exchanger efficiency. The efficiency is provided by the manufacturer of the intercooler. The intercooler block implements a pipe which exchanges heat with the walls having a fixed one male thermo - fluid interface (mass flow specific Enthalpy change rate, Total Specific Burned fuel mass change rate and Heat flux as outputs), one female thermo – fluid and one female heat interface (Reynolds, Prandtl, emissivity, thermal conductivity, temperature as outputs and Heat flux as input). The intercooler block is shown in Fig. 3-3.

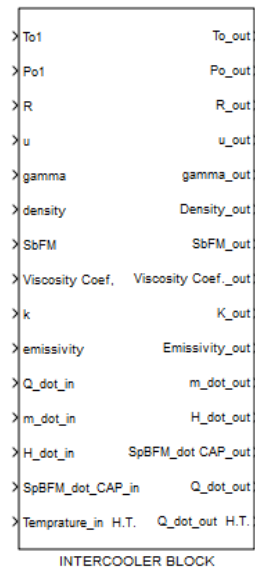


**Fig. 3-3 Block: Intercooler**

The turbines are used to convert gas thermal energy into mechanical rotational energy. Typically turbines are used for driving compressors or for providing extra power to the crankshaft. Turbines used in large marine Diesel engines are typically of the axial flow type whereas in smaller engines often radial flow type is used.

The turbine performance is usually described using two maps. The first map shows the swallowing capacity (mass flow rate) of the turbine while the other gives the efficiency of the turbine. All values of the maps are given in the reference conditions so a correction has to be made (Watson & Janota, 1982).

The power developed from the turbine to the turbine's shaft is equal to the total enthalpy change of the gas. The total enthalpy change is calculated from the ideal enthalpy change calculated with the isentropic efficiency factor, due to the fact that the change is not ideal.

A turbine can also be implemented as an equivalent valve, as the mass swallowing capacity behavior of turbine approaches the characteristic one of valve. Many turbine manufacturers adopt this approach and provide an equivalent area value of a valve instead of the swallowing capacity of the turbine. Since this adaption is not accurate over all the operating area of the turbine, they are forced to provide a correcting factor (usually denoted as  $\alpha_T$ ) in order to compensate this. In this thesis, the swallowing capacity map is used instead of the equivalent area map.

As heat transfer takes place through the turbine casing, it is taken into account in the simulation. Heat transfer is implemented using female and male connections with the appropriate in each case heat transfer blocks. The heat flux here, is provided externally using the female interface (female is considered when the flow of signals is entering the block) and the properties needed by the heat transfer block are provided using the male interface (male is considered when the flow of signal is leaving the block) which sends the

thermal properties. The heat extracted or added to the gas through heat transfer is then provided to the upstream volume using the female thermo – fluid interface.

The turbine is modeled as a subsystem which controls the flow between two control volumes. The turbine block uses the gas state and properties of the two control volumes together with the angular velocity of the turbine in order to calculate the mass flow rate using a swallowing capacity map. Heat transfer is provided externally using mean values of the gas state and properties. The turbine block is equipped with two thermo fluid female interfaces, with mechanical female interface and with one heat transfer male interface. The turbine block is shown in Fig. 3-4 while the whole Turbocharger is shown in Fig. 3-5.



Fig. 3-4 Block: Turbine

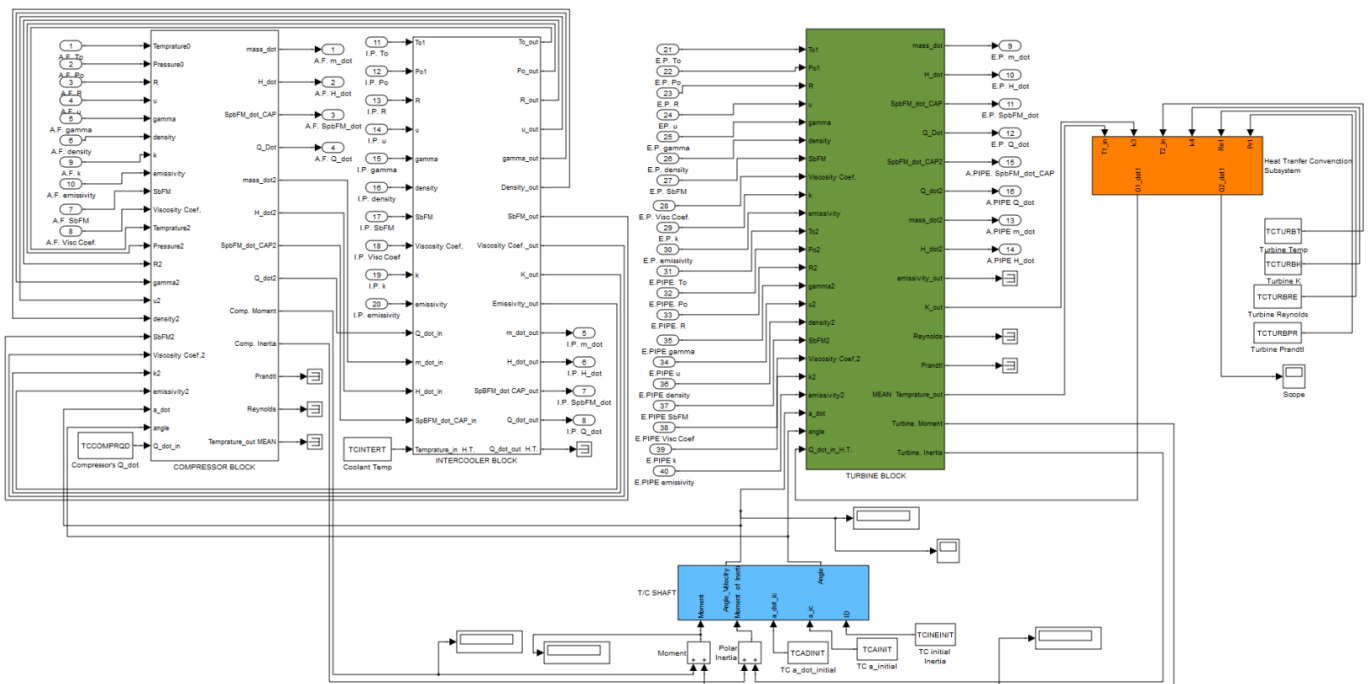


Fig. 3-5 Turbocharger Major Block

### 3.2.2 Inlet and Exhaust Valve Blocks

In many parts of the engine cycle, fluid flows through a restriction. Typical examples of flows through a restriction are the inlet and exhaust valves of the engine, where air flows from the intake manifold through the open inlet valve inside the cylinder plenum and when the combustion occurs, the exhaust gas flows from the cylinder plenum to pass through the open exhaust valve to the exhaust manifold. The gas flow is derived from the equivalent ideal steady state adiabatic and reversible flow (isentropic and frictionless) through a restriction with identical geometry and dimensions. Since the real gas flow behavior depart from the ideal assumption of isentropic flow, an effective area is used instead of the restriction's geometric area for the calculation of the mass flow rate (Heywood, 1988). This correction is done in order to achieve the actual mass flow. Also the assumption that the steady state behavior extends to quasi steady conditions is made.

Since the valve acts between two control volumes as a flow controller, the gas flows from the volume with the higher pressure to the volume with the lower pressure. Therefore as a controller, in valve block, the pressure controls the way of the flow and determines which volume at each time step is considered as upstream or downstream (flow from upstream to downstream).

In most cases, in order to approach the real behavior of a gas passing through a restriction, the occurring heat transfer is taken into account, despite the isentropic gas flow assumption. Heat transfer is considered before and after the restriction using external heat flux blocks, by taking into account the temperature and thermal properties of the gas. The heat extracted or added to the gas through heat transfer is taken into account when the enthalpy of the gas entering the upstream volume is calculated.

In order to implement the engines inlet or exhaust valve, the valve block is used with heat transfer blocks, heat capacitors impellent the material properties that match each metal part the valve has. Therefore, in order to implement the inlet valve, that no heat transfer is taking place, the major block inlet valve is constructed by the valve block that is insulated, thus no heat transfer interface is available and a control element of the equivalent area of the valve ( $A_e$ ) that is provided externally controlled by the crank angle value. The Fig. 3-6 illustrates the equivalent area of the valve versus the crank angle.

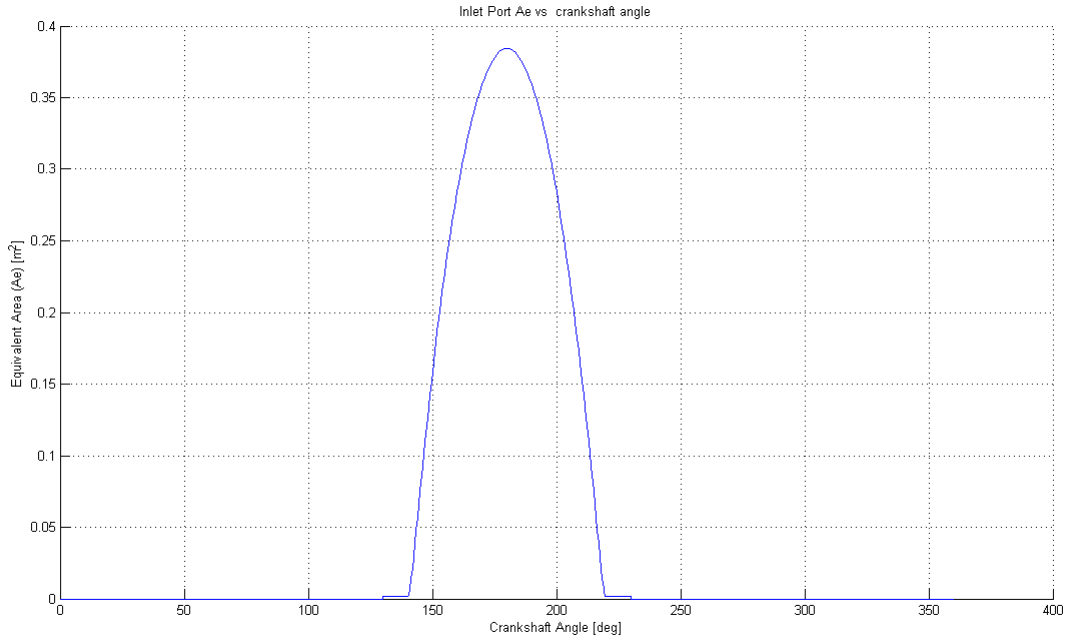


**Fig. 3-6 Inlet Valve's Equivalent area vs crankshaft's Angle**

As already stated the valve is insulated and therefore no heat transfer takes place (heat flux equal to zero). Fig. 3-7 illustrates the Inlet Valve major block.

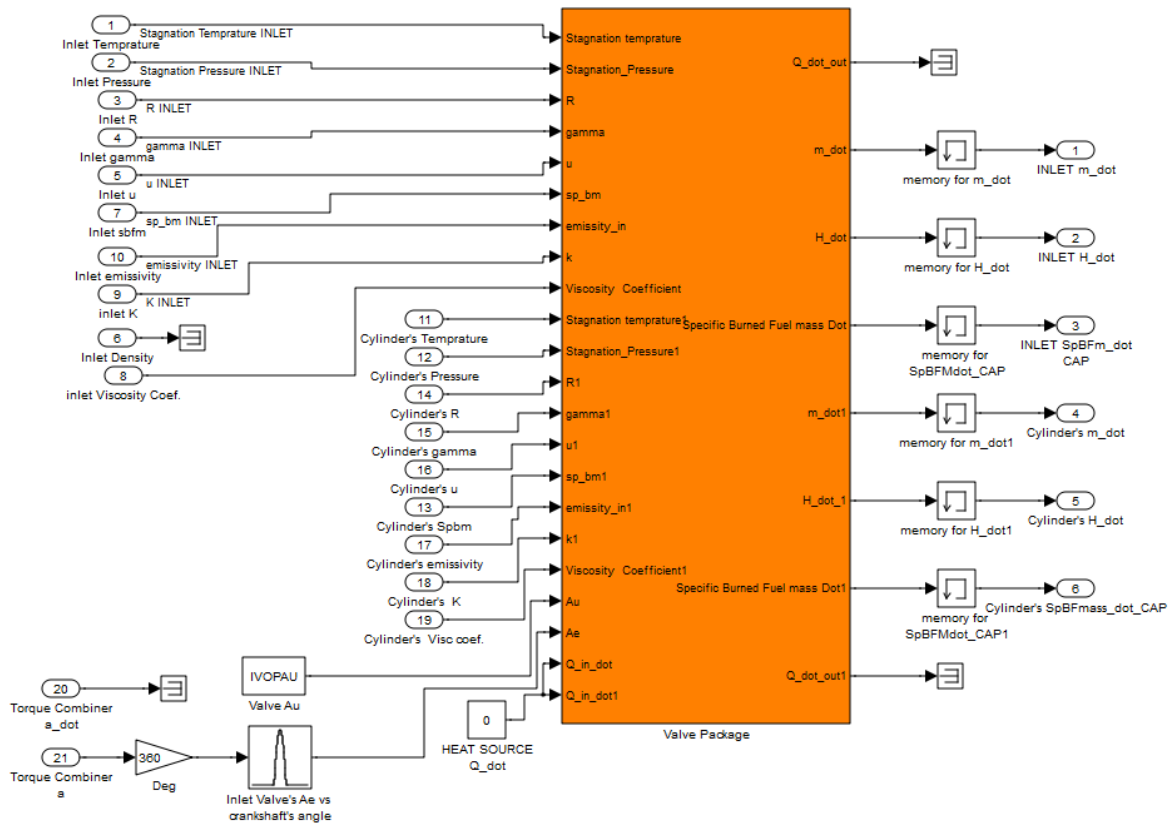


**Fig. 3-7 Block: Inlet Valve**

As is the case of inlet port, the exhaust valve of the cylinder is implemented using again a valve block, with the heat transfer interface and the equivalent area that is provided externally and is controlled by the crankshaft angle. In the exhaust valve, heat transfer cannot be ignored and should be taken into account. The exhaust valve heat transfer includes various heat capacitors and heat flux controllers. Fig. 3-8 shows the equivalent area for the exhaust valve versus crankshaft's angle.

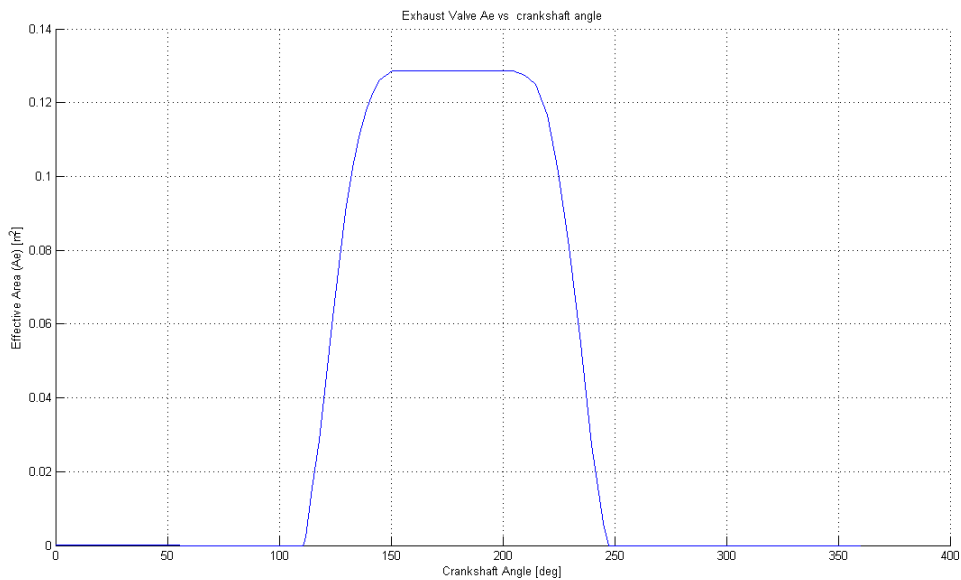


**Fig. 3-8 Exhaust Valve's Equivalent area vs crankshaft's Angle**

When the exhaust valve is open the area used in the conduction heat flux controller, a map of contact area versus the linear position of the piston is used, by the time the contact the valve disk and the cylinder head are no longer in contact, the output of the map is zero. These maps are provided externally and differ for each engine. The modular implementation of the Exhaust valve is shown in Fig. 3-9.

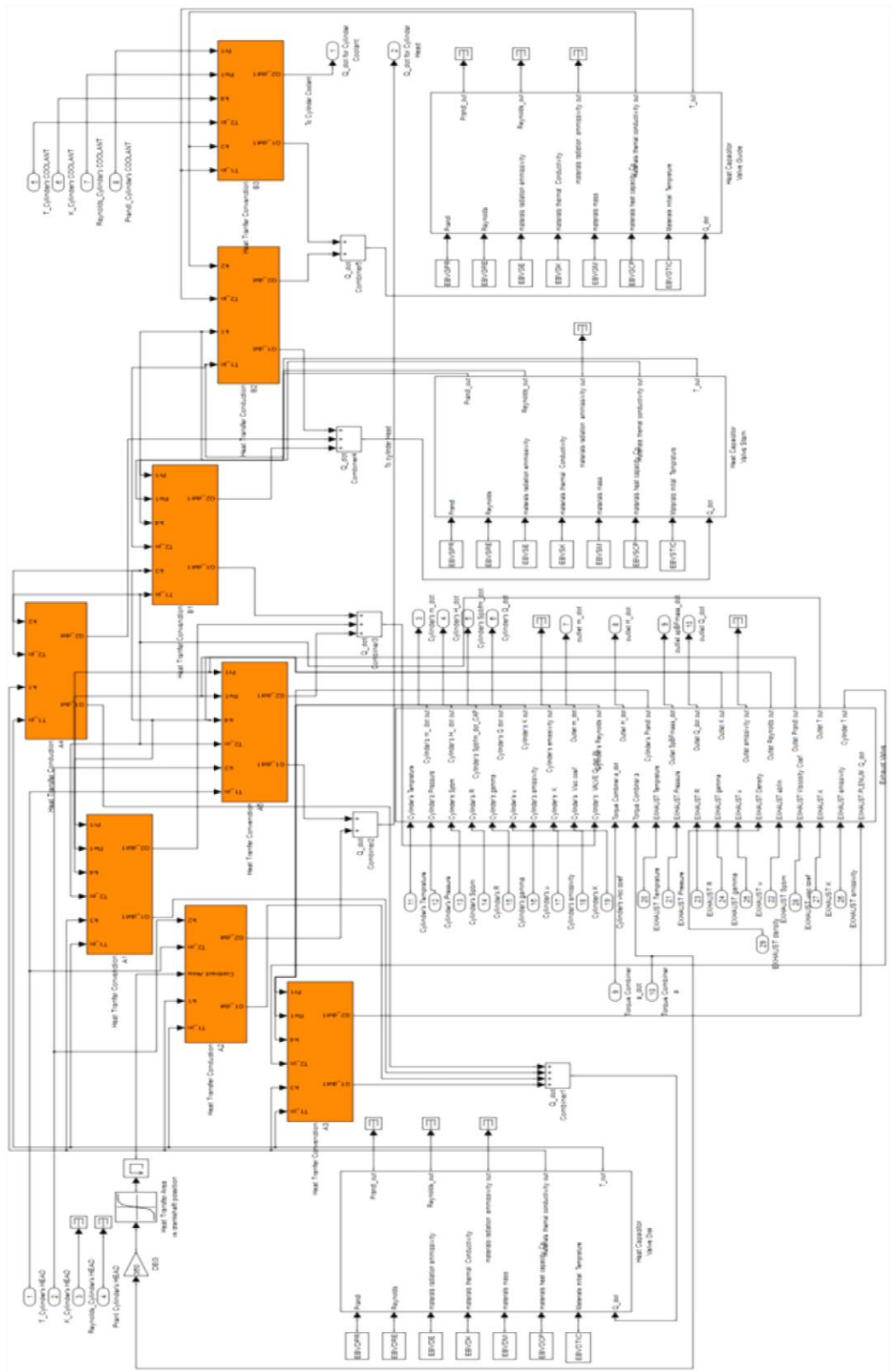


Fig. 3-9 Block: Exhaust Valve

The major block shown in Fig. 3-9, contains inputs that are connected to the jacket cooling system in order to drop the rising temperature due to hot exhaust gas that flow through the exhaust valve to the exhaust manifold.

### 3.2.3 Open Thermodynamic System and Gas Properties Block

This block contains two sub blocks namely, open thermodynamic system and gas properties. Each of these blocks calculates certain variables needed in the operation of the system. The gas properties sub block contains equations contained in (Heywood, 1988) that best describe the properties of the gas mixture contained in a certain volume. From a thermodynamic perspective, each volume (i.e. inlet, outlet or cylinder's volume) is described using the equations of an open thermodynamic system, where laws of thermodynamics are applied.

Therefore, each of these blocks corresponds to simpler ones. The major block "Open Thermodynamic System and gas properties" is shown in Fig. 3-10. It is often required to implement a region of the engine as an open thermodynamic system. Typical examples are the cylinder volume and the intake and exhaust manifolds. This modeling approach is appropriate when the gas inside the open system boundary can be assumed uniform in composition and state at each time step and when the state and mixture composition vary with time due to heat transfer, work transfer and mass flow across the boundary and boundary displacement (Kyrtatos, 1993). Fluid gas is exchanged through the open thermodynamic system boundary. The mass change rate of the fluid flow is controlled externally using the female ports of the block. These ports are connected e.g. with a valve, compressor blocks etc. The mass change rate totals the sum of the individual flow controllers connected to the Open Thermodynamic System. This combined mass is coupled with the Enthalpy change rate, the specific burned fuel mass fraction change rate (the change refers to the entrapped mass inside the control volume) and the heat flux exchanged due to the geometrical openings required in having mass flow. The total properties ( $\dot{H}, \dot{E}$ ) are required since the combined flow of all the flow controllers is used. Using the combined flow simplifies the calculations required.

The Open thermodynamic block consists of twelve inputs and two values that are feed internally from the open thermodynamic system to the gas properties. These values are used also outside the boundaries of the major block.

This block is subject to heat transfer through the boundary walls of the system. The heat flux is provided externally using female and male interface. The gas temperature along with the thermal properties of the material (e.g. thermal conductivity  $\kappa$ , radiation emissivity  $\epsilon$ , Reynolds  $Re$  and Prandtl  $Pr$  numbers) are provided through this interface and the heat flux is calculated externally using heat transfer elements in topology which best suits the system modeled. The heat flux takes place in two stages. The first stage takes place through the openings required for the mass flow in and out of the system and the second part through the boundary walls of the system. The open thermodynamic system's volume  $V$  and volume change rate are also provided externally through the female interface. This allows each time the same major block to implement different plenum (e.g. inlet manifold, or upper and lower volume of the cylinder, due to the motion of the piston). This approach facilitates easy expansion since new geometries can be added with the introduction of a new element. The geometrical information (that each time is provided using the appropriate interface) provides to this major block with the volume and volume change rate along with reference velocity and portion and utilizes the gas pressure in order to convert it to other forms.



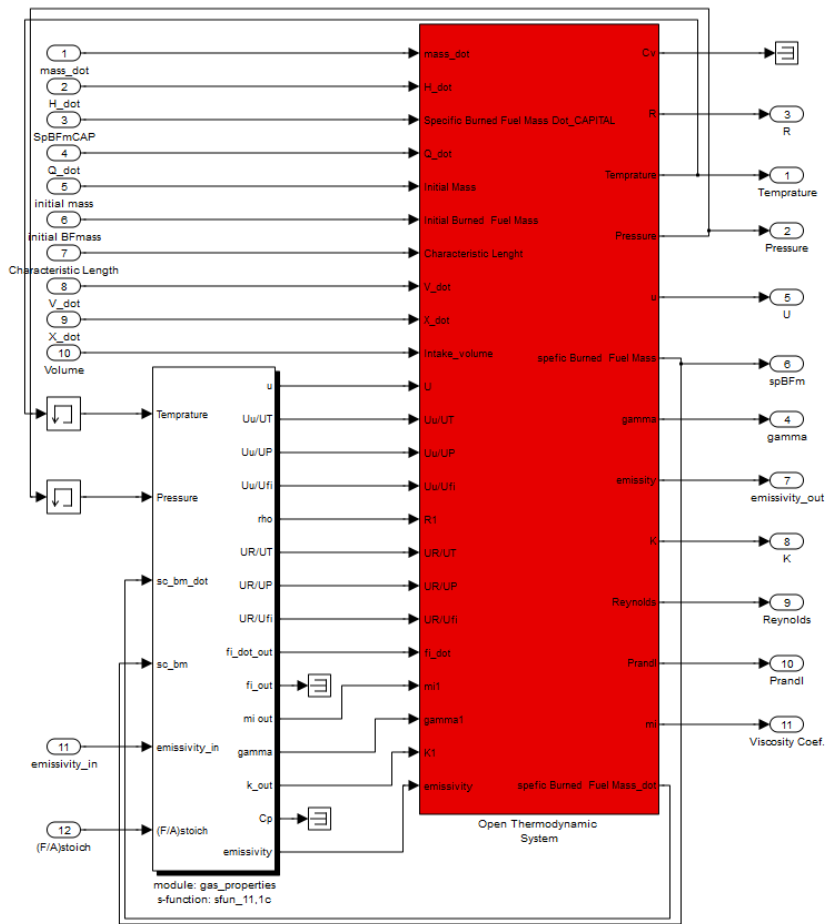


Fig. 3-10 Major Block: Gas Properties and Open Thermodynamic System

### 3.2.4 Fixed Fluid and Gas Properties Block

When implementing a thermodynamic system, it is often useful to investigate the behavior of schemes which although non-existent to nature, are interesting for studying purposes. Such a case is when an element exists which can impose a constant fluid mass flow rate into a thermodynamic volume regardless of the thermodynamic condition (gas temperature, pressure etc.) inside this volume. The flow can be positive or negative, where in the first case the element functions as a gas mass flow generator with constant gas properties, while in the second case the element functions as gas mass sanction device capable of maintaining constant flow rate. In the later case the properties of the gas are taken from the thermodynamic volume the fluid flows. In order to model this behavior the fixed fluid block is introduced. This block is connected to gas properties block and the two of them form the major block fixed fluid and gas properties. The fixed fluid is modeled as a constant mass flow generator with constant properties if the flow is positive and with properties taken from the thermodynamic volume if the flow is negative. This block is used to implement the ambient air conditions, like the intake of the turbocharger or the exhaust gas after the turbine of the turbocharger.

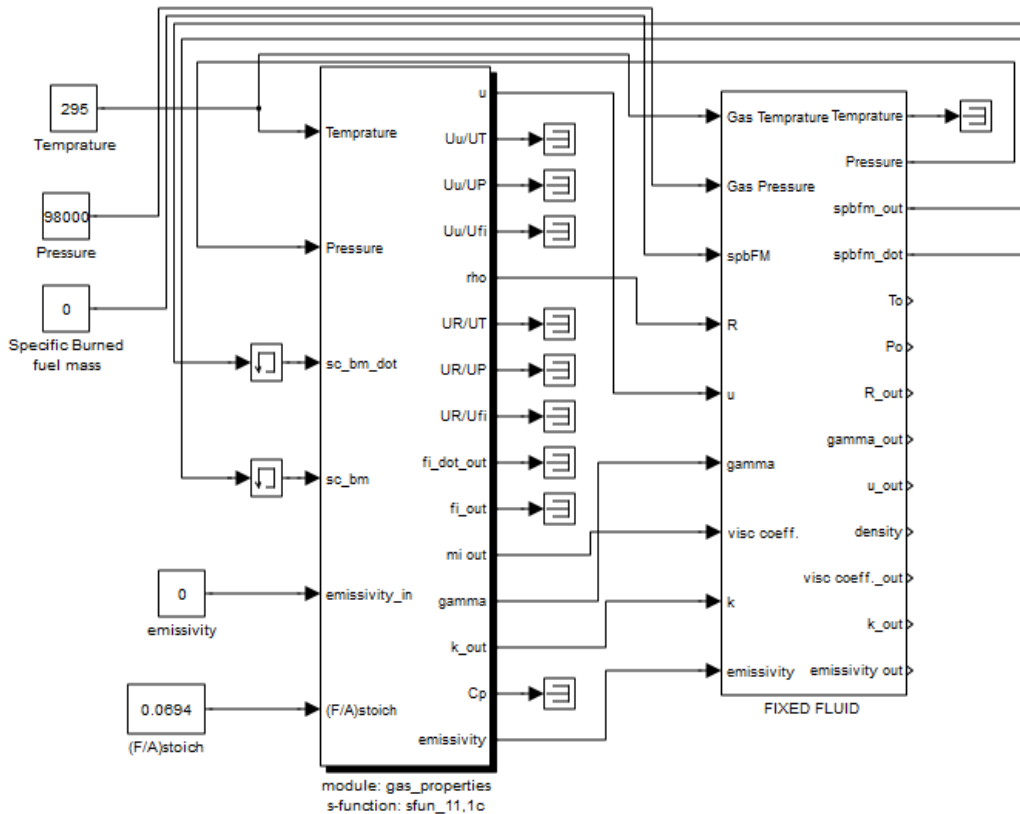


Fig. 3-11 Major Block: Fixed Fluid and Gas Properties

### 3.2.5 Cylinder Heat Transfer Block

In order to implement the heat transfer of the cylinder, all the material that form the cylinder are implemented individually. The head of the cylinder is modeled individually, while the liner is divided in two parts, since the upper part is the one that takes all the heat flux due to the combustion. The piston is also divided in two parts, the piston crown and the piston skirt.

The working fluid is in contact with the head, the upper and lower part of the liner and the piston crown. Each connection is illustrated in Fig. 3-12 . The heat transfer method is illustrated using HTD1,R, HTB1,R, HTG1,R and HTA1,R (convection and radiation heat flux blocks).

The head, upper and lower liner of the cylinder are exchanging heat with the jacket coolant through HTD2, HTG2 and HTG3 respectively (convection heat flux blocks).

The heat developed on the piston crown is rejected to the piston coolant using the HTA2 (convection heat flux controller). Also the exchange between the piston and the cylinder liners through the ring is taken into account using the HTA3 and HTB2 respectively (conduction heat flux block)

The piston crown and piston skirt are exchanging heat through HTA4 (conduction heat flux block).

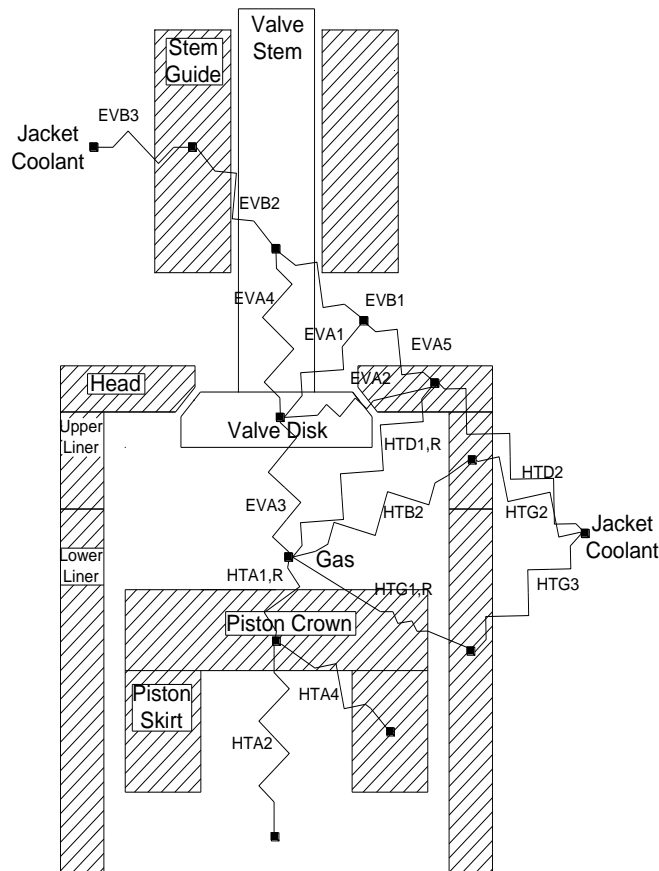


Fig. 3-12 Cylinder and Exhaust Valve heat transfer implementation

Since the piston is changing position due to operation of the engine, the contact area between the working gas and the upper and lower parts of the liner is constantly changing. The contact area is controlled externally using the piston position  $x$  that is provided as an input to the Heat Transfer major block from Geometrical Energy Loss block. The diagrams used to control the area are presented in Appendix B, where the complete engine configuration is described. The implementation of the heat transfer major block is shown in Fig. 3-13.

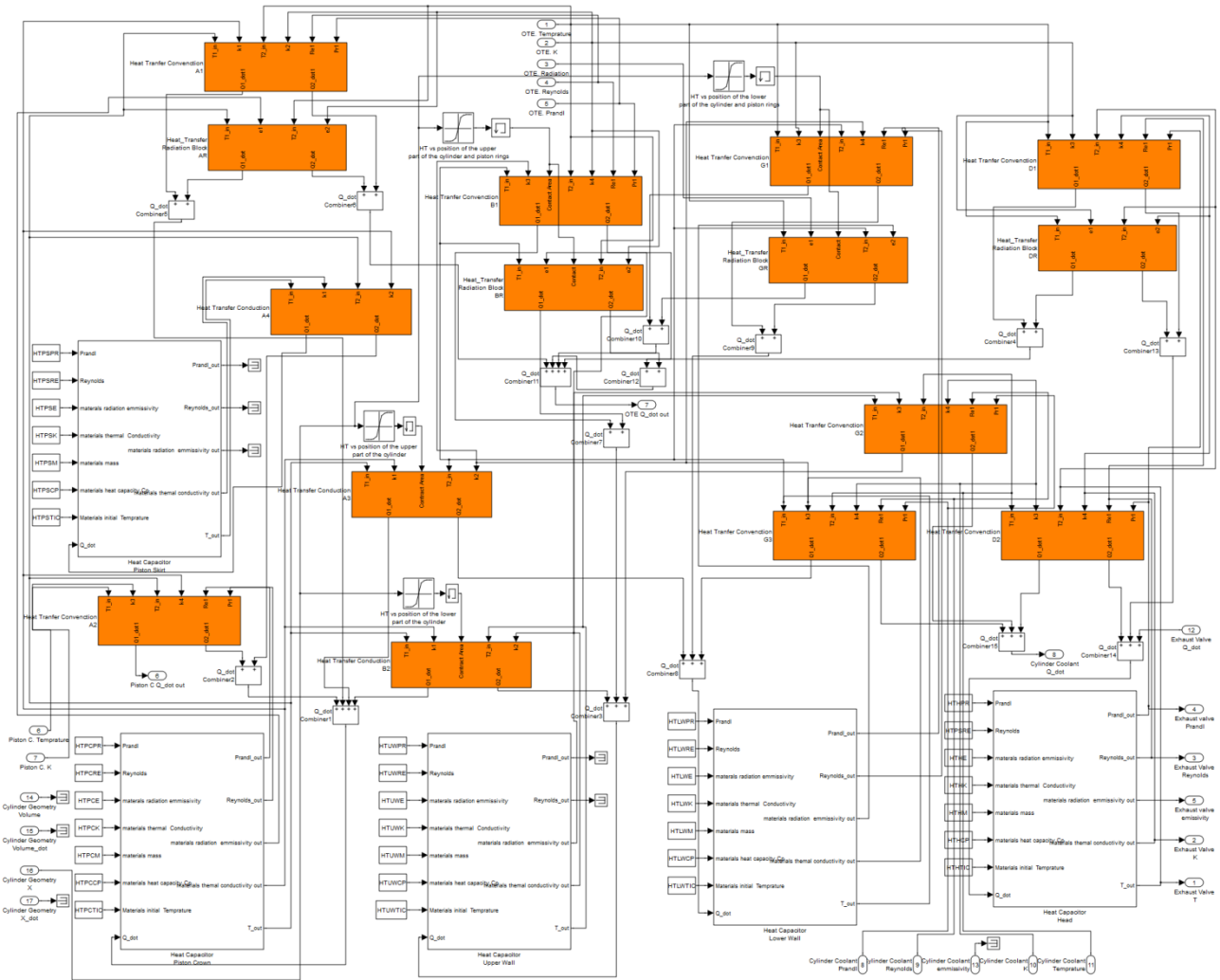


Fig. 3-13 Cylinder Heat Transfer major block

### 3.2.6 Combustion Block

The combustion process normally takes place inside the open thermodynamic system that implements the cylinder volume. In order to have a flexible model, the combustion is an external block. This method is best suited here, because future work may upgrade the combustion model to a more complex one. Following this approach it is also possible to have multiple combustion elements that can be used (modeling two or more injectors with different injection timing).

The model presented here uses the S – Curve method. Taking a close look to the combustion modeling in the empty – filling method, it can be seen that the combustion process is typically a heat release and a mixture composition change. Both the heat release and the mixture composition change can be handled through a thermo - fluid connection so the advantages described above can be obtained.

The S – combustor block is equipped with one female thermo - fluid interface which provides the heat released from the combustion process to the element connected and one female mechanical interface which provides the timing data. The block representation of the S – Combustion Block is shown in Fig. 3-14.

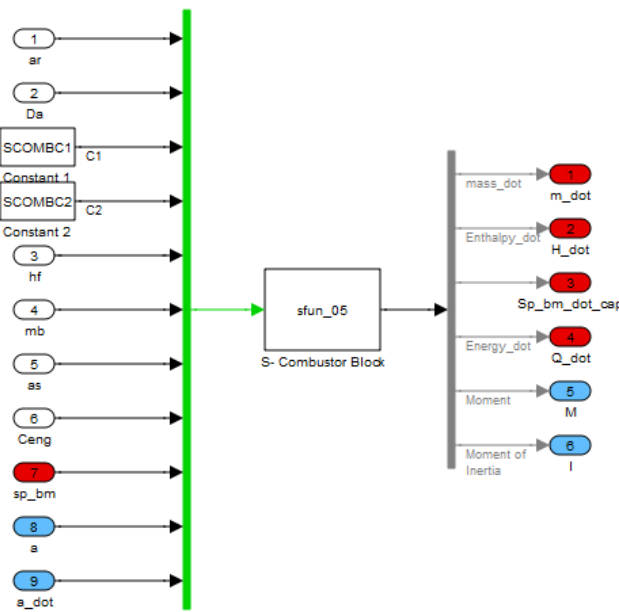


Fig. 3-14 Block: S - Curve Combustion

Outputs 5 and 6 of the block show the mechanical interface (moment, moment of inertia), while input 7 and outputs 1-4 provide connection with the thermo – fluid interface.

### 3.2.7 One Cylinder Block

This block illustrates the complete model of one cylinder of an engine, comprising the piston, the rod the crankshaft, the upper and the lower volume of the cylinder, the liner, the inlet port (or inlet valve if the engine is 4 stroke), the exhaust valve and the combustion model that implements the injector and the combustion process inside the upper volume. Each of these blocks was individually described in the previous sections.

The volumes of the cylinder are assumed as open thermodynamic systems. Inside the open thermodynamic system, gas properties block is connected. In order to establish the connection with the inlet and exhaust manifolds, the use of inlet port (or valve) and exhaust valve is necessary. Due to pressure difference, mass flow occurs, therefore fresh air (meaning rich to oxygen and other substances of atmospheric air) passes inside the cylinder's plenum, where the variable geometry, due to piston movement, is implemented using the geometry block. As already stated in previous chapters, piston rings and other factors are responsible for the existence of friction. The pressure loss due to these factors is implemented and was taken into consideration with the use of geometrical energy loss block. When the block that implements the rotation of the crankshaft axis, sends information about the current degrees of axis angle, certain controllers, open or close the inlet port, the exhaust valve, or give the command to start the combustion of the compressed mixture inside the upper volume (when the piston is located at the top dead center, TDC). The linear position of the piston is also a controller that allows the heat transfer blocks, to understand and calculate the heat flux at all positions of the piston.

All the outputs of the cylinder are connected to the appropriate blocks (e.g. mass flow, enthalpy change rate etc to the inlet and exhaust manifolds or the torque and moment of inertia to the crankshaft interface). At each point of interest, scopes and display screens are connected in order to monitor the whole operation of the cylinder. Fig. 3-15 illustrates the cylinder of a marine 2 stroke Diesel Engine, with Inlet port(s) and Exhaust valve(s) and one beck.

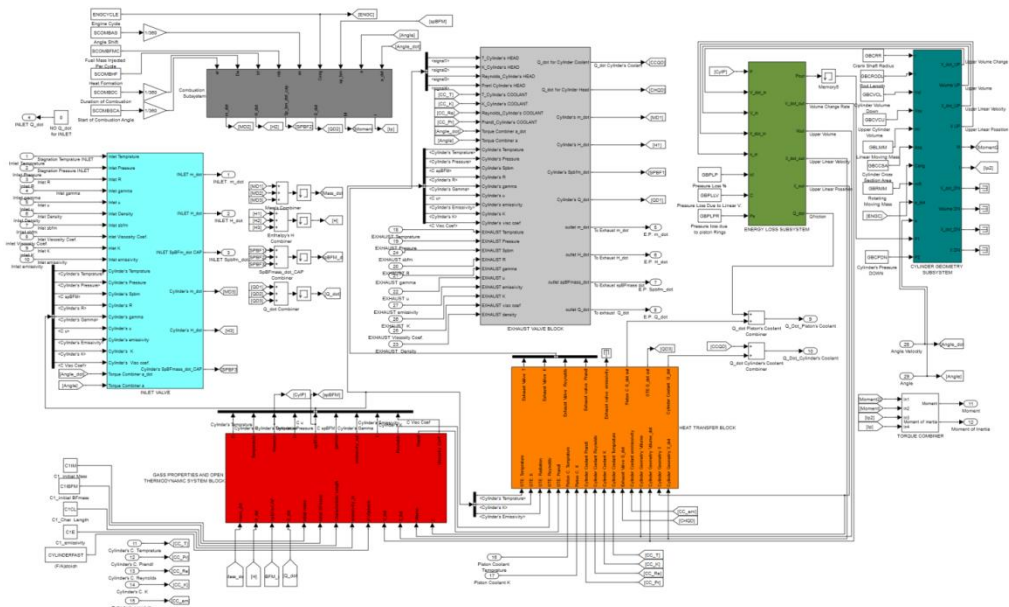


Fig. 3-15 One cylinder major block

### 3.2.8 Eight cylinders block

In a realistic simulation, a multi cylinder engine is simulated. For this case a block for an eight cylinder MAN 8K90MC-C6 library block was developed

Each cylinder is identical to the others in a multi cylinder engine. The only change is the initial crankshaft angle, because of the fact the each cylinder has different firing order and in order to have smooth production of torque and avoid vibrations, so they must have different phase angle. To avoid complex connection, the signals are inserted to a bus that transfers them to each cylinder. Each output of each cylinder is connected to signal combiner blocks that add each e.g. torque to one, that later is send to the appropriate block. The complete illustration of cylinders of the MAN 8K90MC-C6 diesel engine is illustrated in Fig. 3-16.

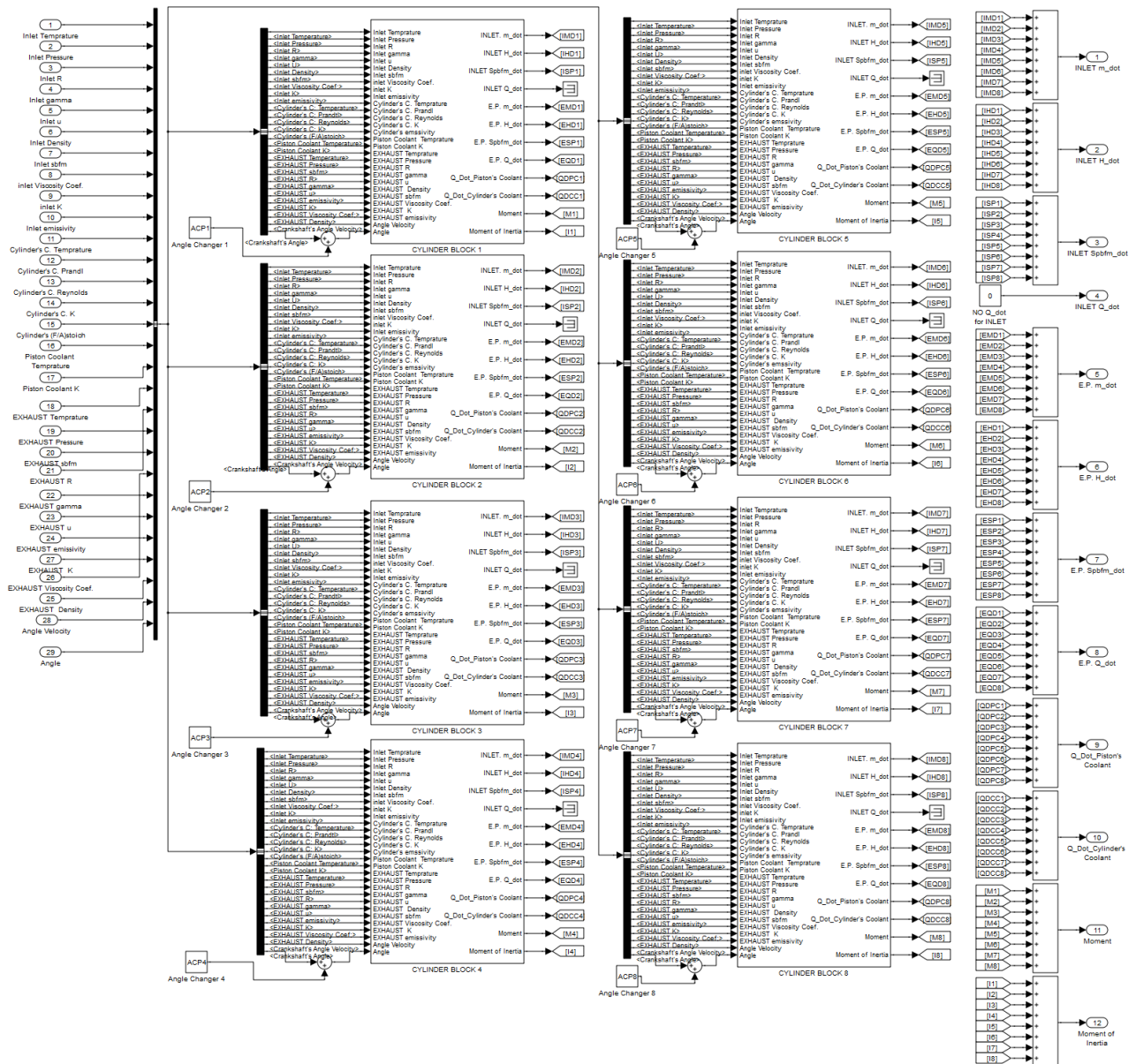


Fig. 3-16 MAN 8K90MC-C6 Cylinders

## 4 Simulation Results

This chapter contains the simulation results of test cases that were implemented in order to validate the results of the equation used in the blocks in chapter 3 and to affirm that these results would be meaningful and describe suitably the physical processes that took place in each component of a real engine. The test cases were set up in a manner that the results compared with already known results from other simulation efforts. As a general comment from these examples, the simulation results were found adequately close to existing and already verified results.

The test case comprises: two containers connected through a valve, heat transfer, cylinder geometry, compressor and intercooler test and turbine test.

After completing the validation of the blocks, a single-cylinder of the marine diesel engine of MAN 8K90MC-C6 was set up using the blocks that were previously checked.

### 4.1 Test examples

In this section four test cases are presented in order to validate the results of the following blocks: gas properties and open thermodynamic system, fixed fluid, valve, compressor, intercooler, turbine, heat transfer blocks (conduction, convection and radiation), geometry block and geometrical energy loss block.

#### 4.1.1 Two gas containers connected through a valve

This is a simple example of a valve fitted between two gas containers. The configuration of the example is shown in Fig. 4-1. The purpose of this example is to validate the results of the blocks: gas properties, open thermodynamic system and valve. In addition, it demonstrates how two fundamental fluid elements can be combined in order to model a physical configuration.

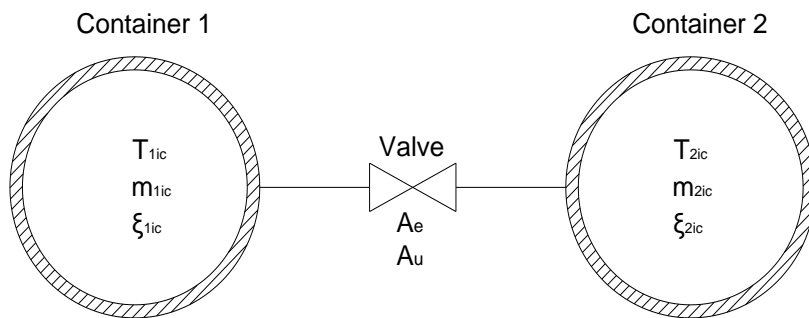


Fig. 4-1 Configuration of mass flow through a valve

The containers are insulated therefore no heat transfer is possible. Containers have also a certain known volume. A valve is fitted between them. The valve has a constant equivalent area and is also insulated.

The two gas containers are modeled using the open thermodynamic system block. Gas properties are given using the appropriate “gas properties” block that provides all the



necessary information. Thus the gas properties element provides the thermodynamic properties of the fluids, a heat source provides the insulation condition (heat flux equal to zero) and geometry source provides the geometry of the container (volume). The data used in the example are shown in Table 4-1.

**Table 4-1: Container and Valve Data**

Container 1	Container 2	Valve
$p_1 = 402970 \text{ N} / \text{m}^2$	$p = 101303 \text{ N} / \text{m}^2$	$A_e = 0.0003 \text{ m}^2$
$m_{ic} = 10 \text{ kg}$	$m_{ic} = 1 \text{ kg}$	$A_u = 0.0006 \text{ m}^2$
$T_{ic} = 400 \text{ K}$	$T_{ic} = 300 \text{ K}$	
$\xi_{ic} = 0.01$	$\xi_{ic} = 0.0$	
$B = 0.0 \text{ m}$	$B = 0.0 \text{ m}$	
$\dot{V} = 0.0 \text{ m}^3 / \text{s}$	$\dot{V} = 0.0 \text{ m}^3 / \text{s}$	
$V = 2.85 \text{ m}^3$	$V = 0.85 \text{ m}^3$	

All heat sources were set to zero due to insulation condition, meaning that no heat flux takes place in this example.

**Block representation of the example**

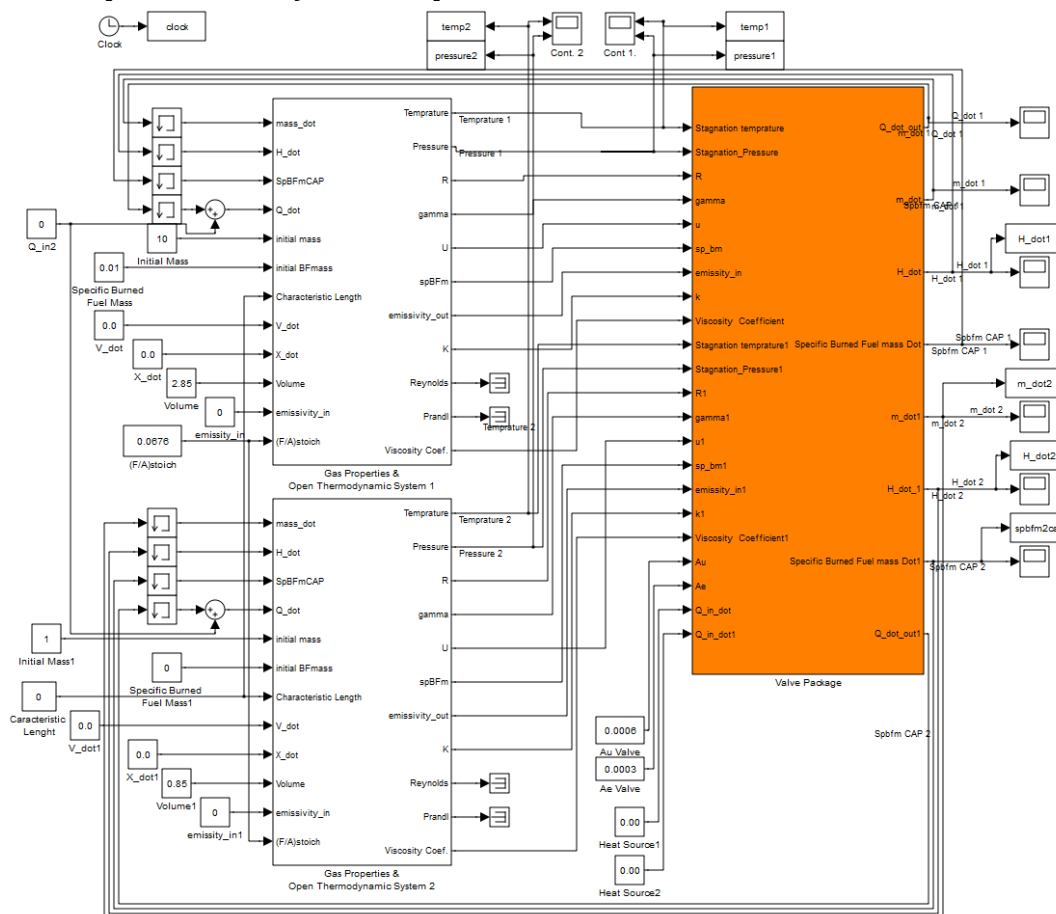


**Fig. 4-1** The two container blocks are connected to each other through a valve

## Results

At time  $t=0$  the mass flow started. Due to pressure difference mass flow occurs from the container with higher pressure (container one) to the container with the lower pressure (container two). The mass flow stops when the two pressures are equal. This condition is met at time 7.3 seconds, when the whole simulation lasts for 10 seconds. Fig. 4-2 shows the temperature, pressure and mass decrease in container one due to mass flow. Fig. 4-3 shows temperature and mass rising. Also the specific burned fuel mass fraction is rising due to the flow from container one to container two. Fig. 4-4 shows the pressure increase, the change of mass flow over time and the enthalpy change rate of container two.

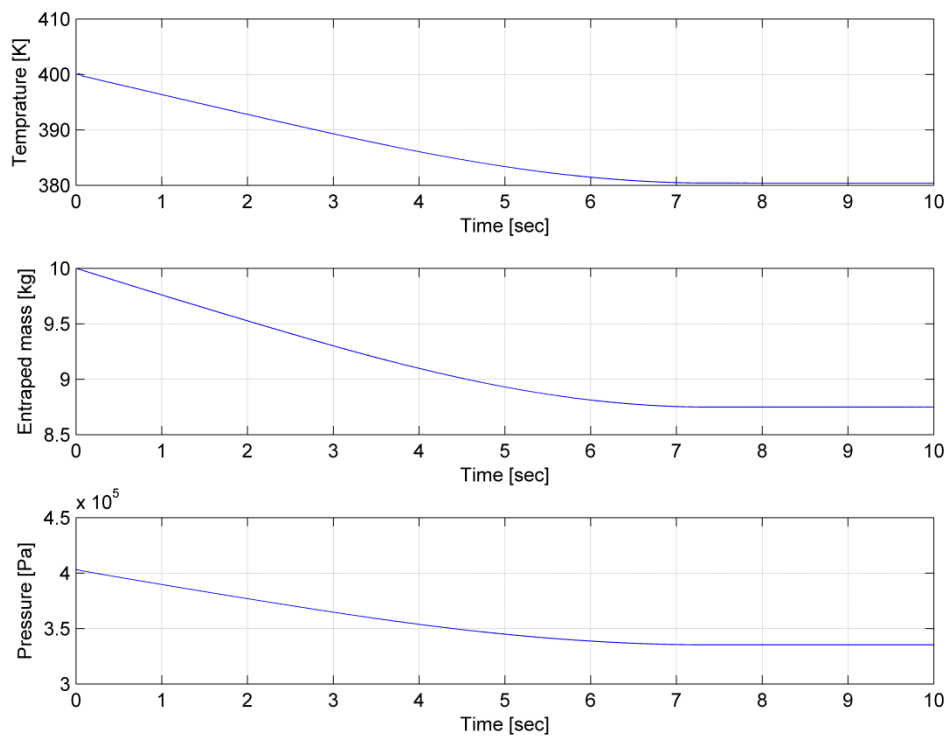


Fig. 4-2 Temperature mass and pressure of container one

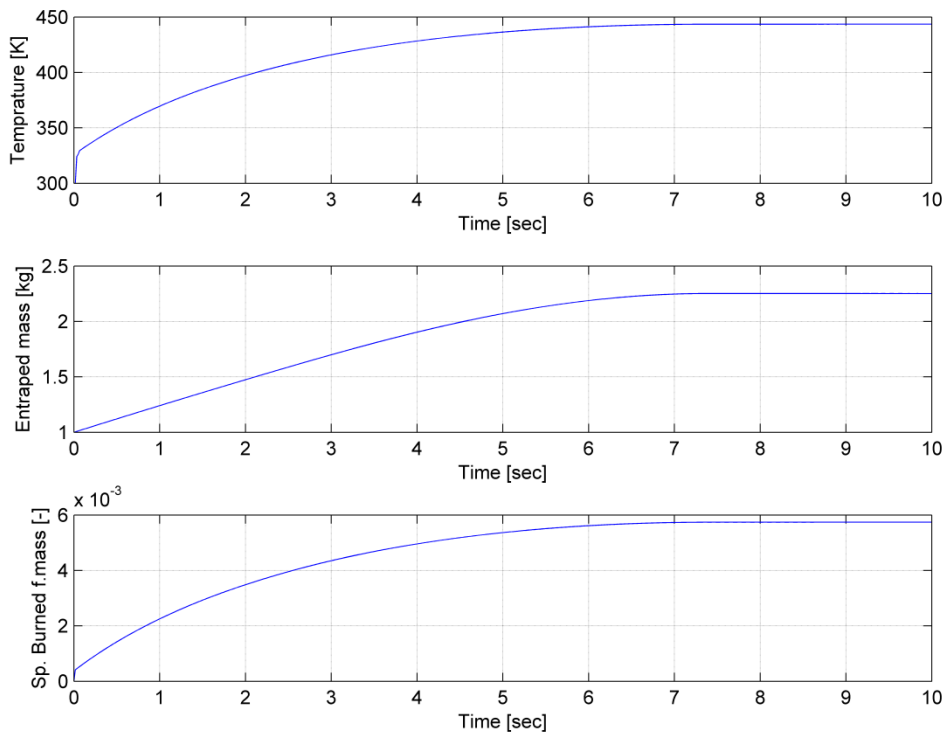


Fig. 4-3 Temperature, mass and specific burned fuel mass fraction of container two

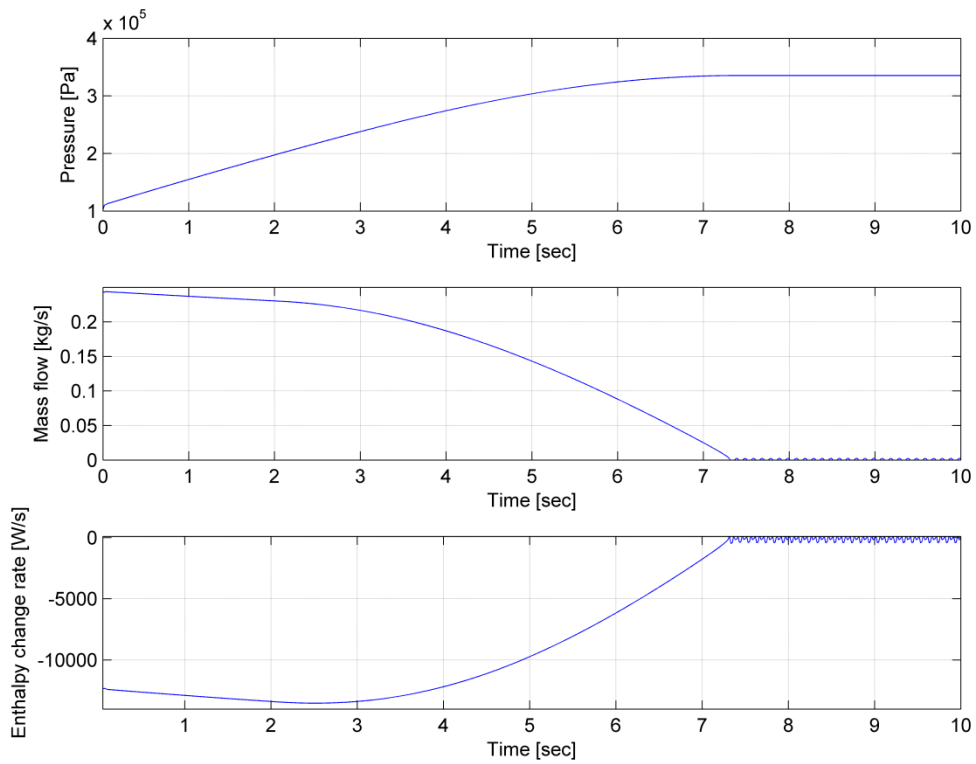


Fig. 4-4 Pressure, mass flow and enthalpy change rate of container two

### 4.1.2 Heat Transfer

A simple example of heat transfer is presented in Fig. 4-5. The configuration on the left side has a constant heat source of 100 W. The wall consists of two materials. Material A is carbon steel (C 0.5%) and material B is alusil (Al 78 – 80%, Si 20 – 22%). To the right hand side of material B, water is flowing at constant temperature. The heat source provides heat power ignoring the temperature of the material that the heat power is applied to.

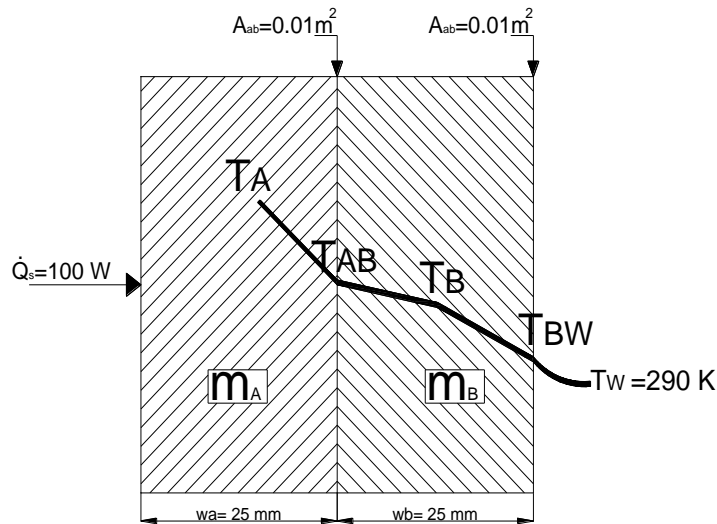


Fig. 4-5 Cross Section of configuration of heat transfer through wall

For the material A the block heat capacitor was used. The wall is rectangular parallelepiped having cross section area  $A_{ab}=0.01\text{m}^2$  and width  $w_a=0.025\text{m}$  which leads to a volume of  $V_a=0.00025$ . The physical and thermal properties of the materials used can be found in Table 4-2. Using these properties, it can be found that

$$m_A = V_A \cdot \rho_A = 1.958 \text{ kg} \quad (4.1.1)$$

Reynolds and Prandtl numbers are set to zero because the material is solid.

Table 4-2: Carbon Steel Properties

Carbon steel (C 0.5%) properties at 290 K	
$\rho_A$	$= 7833.0 \text{ kg} / \text{m}^3$
$c_{pA}$	$= 465.0 \text{ J} / \text{kg}$
$k_A$	$= 54.0 \text{ W} / \text{m} \cdot \text{K}$
$\varepsilon_A$	$= 0.8 \text{ —}$

For the material B a heat capacitor was used also. This wall is also rectangular parallelepiped having the same cross section area as wall A  $A_{bf}=0.01\text{m}^2$  and width  $w_b=0.020 \text{ m}$  which leads to a volume of  $V_b=0.00020 \text{ m}^3$ . The physical and thermal properties of Alusil can be found in Table 4-3. Using these properties the mass of the wall B can be found

$$m_B = V_B \cdot \rho_B = 0.525 \text{ kg} \quad (4.1.2)$$

Reynolds and Prandtl numbers are set to zero because the material is solid.

**Table 4-3 Alusil Properties**

Alusil (Al 78 – 80%, Si 20 – 22%) properties at 290 K	
$\rho_B$	$= 2627.0 \text{ kg} / \text{m}^3$
$c_{pB}$	$= 854.0 \text{ J} / \text{kg}$
$k_B$	$= 161.0 \text{ W} / \text{m} \cdot \text{K}$
$\varepsilon_B$	$= 0.25 \quad -$

The cooling water was assumed as heat sink, meaning that provides a constant temperature and all the heat flux passing to it, is absorbed. The water was considered to have mass flow equal to 45 kg/s. The Reynolds and Prandtl numbers can be obtained using the following equations

$$Re_w = \frac{Y_w \cdot d_f}{\mu_w} \quad (4.1.3)$$

$$Pr_w = \frac{c_{pw} \cdot \mu_w}{k_w} \quad (4.1.4)$$

where  $d_f$  is the characteristic length and equal to 0.1 m.

The properties of water can be found in Table 4-4

**Table 4-4 Water Properties**

Water properties at 290 K	
$\rho_B$	$= 997.4 \text{ kg} / \text{m}^3$
$c_{pB}$	$= 4179 \text{ J} / \text{kg}$
$k_B$	$= 0.604 \text{ W} / \text{m} \cdot \text{K}$
$\varepsilon_B$	$= 0.25 \quad -$
$\mu_f$	$= 0.00098 \text{ kg} / \text{m} \cdot \text{s}$

The heat transfer between wall A and wall B was conduction; therefore a conduction block was utilized. Contact area between the two materials is set to 0.01 m<sup>2</sup>. In order to calculate the shape factors  $\delta_A$  and  $\delta_B$  are required. These two are given from

$$\delta_A = \frac{\omega_A}{2} = 0.00125 \text{ m} \quad (4.1.5)$$

$$\delta_B = \frac{\omega_B}{2} = 0.001m \quad (4.1.6)$$

thus

$$S_A = \frac{1}{\delta_A} = 800.0m^{-1} \quad (4.1.7)$$

$$S_B = \frac{1}{\delta_B} = 1000.0m^{-1} \quad (4.1.8)$$

The heat transfer between wall B and water was convection and radiation; therefore convection and radiation blocks were used. The contact area was set to 0.01 m<sup>2</sup>. For the convection heat flux block the geometry shape factor  $S_s$  was taken equal to  $S_B$ . The a, b, c constants for the calculation of Nusselt number were taken equal to a=0.025, b=0.8 and c=0.333 due to the assumption of turbulent flow while the characteristic length D was set to 0.1 m. For the radiation heat flux block the shape factor was set to 0.45 and the cross section area was taken equal to 0.01 m. The data used in heat transfer blocks are presented in Table 4-5. The data for the heat Capacitors are presented in Table 4-6 as well. As mentioned before, the heat source provides constant heat flux equal to 100 W.

**Table 4-5 Heat Transfer Block Data**

Convection Block Data	Radiation Block Data	Conduction Block Data
$A_c = 0.01 \text{ m}^2$	$A_1 = 0.01 \text{ m}^2$	$A_c = 0.01 \text{ m}^2$
$S_s = 1000 \text{ m}^{-1}$	$A_2 = 0.01 \text{ m}^2$	$S_1 = 800.8 \text{ m}^{-1}$
$D = 0.1 \text{ m}$	$F_{(1-2)} = 0.45 -$	$S_2 = 1000 \text{ m}^{-1}$
$a = 0.025 -$		
$b = 0.8 -$		
$c = 0.333 -$		

**Table 4-6 Heat Capacitors Data**

Heat Capacitor A Block	Heat Capacitor B Block	Heat Sink
$m = 1.958 \text{ kg}$	$m = 0.525 \text{ kg}$	$T_{ic} = 290 \text{ K}$
$c_p = 465.0 \text{ J} / (\text{kg} \cdot \text{K})$	$c_p = 854.0 \text{ J} / (\text{kg} \cdot \text{K})$	$Pr = 6.78 -$
$T_{ic} = 290 \text{ K}$	$T_{ic} = 290 \text{ K}$	$Re = 4592 -$
$Pr = 0.0 -$	$Pr = 0.0 -$	$k = 0.604 \text{ W} / (\text{m} \cdot \text{K})$
$Re = 0.0 -$	$Re = 0.0 -$	$\varepsilon = 0.95 -$
$k = 54 \text{ W} / (\text{m} \cdot \text{K})$	$k = 161 \text{ W} / (\text{m} \cdot \text{K})$	
$\varepsilon = 0.8 -$	$\varepsilon = 0.25 -$	

## Building block representation of the example

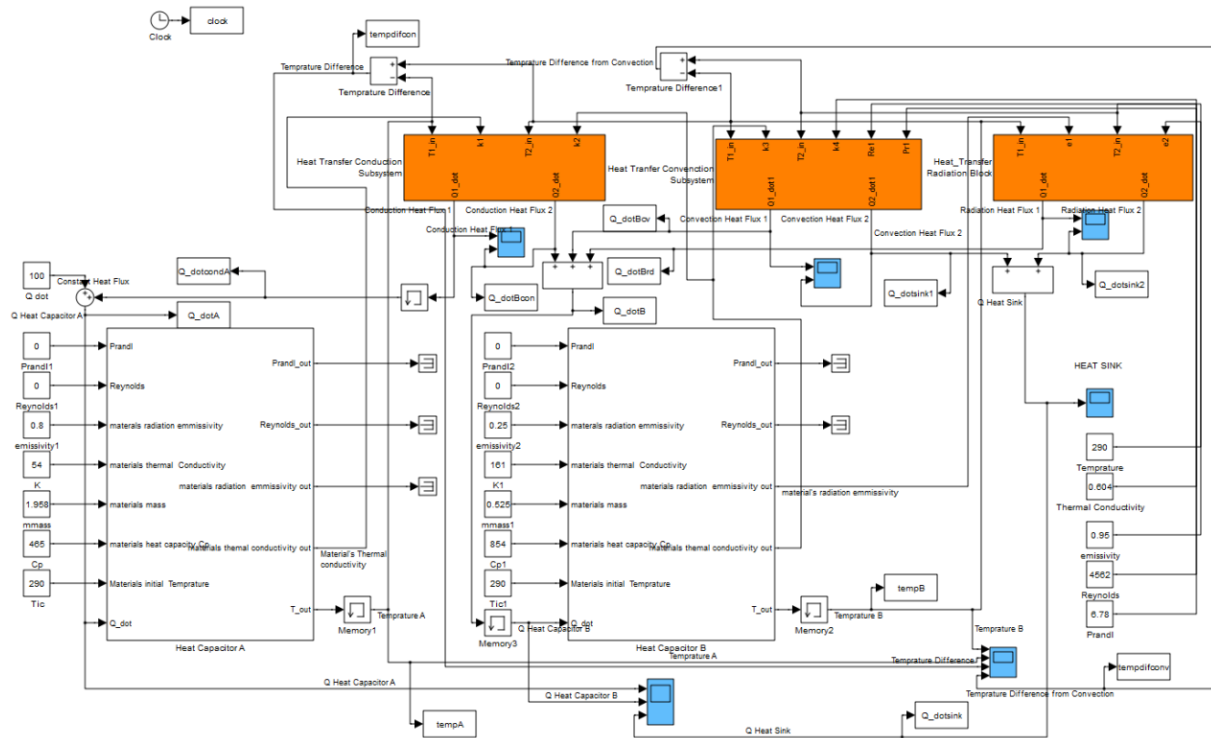


Fig. 4-6 Block Representation of the Example

## Results

The simulation runs for 3600 seconds (one hour). The initial wall temperature was taken equal to 290 K. The heat source provided 100 W constant heat during the simulation. The heat absorbed from heat capacitors and heat sink is presented in Fig. 4-7 - Fig. 4-9. Also, during the simulation, the heat absorbed by the heat capacitors A and B decreases since the temperature of them reaches gradually the equilibrium. On the other hand, the heat absorbed by the heat sink increases with time until it reaches the highest value, which is equal to the heat supplied by the heat source. In Fig. 4-7 the heat flux entering the heat capacitors and water can be seen. Also the temperature rise is illustrated. In the same figure it is shown the temperature difference of conduction and convection for heat capacitor B. In Fig. 4-8 it is shown the amount of Heat flux due to conduction and convection. Also it is illustrated the temperature difference of convection and conduction. In Fig. 4-9, the whole heat flux arriving at heat capacitors A, B and water is presented.

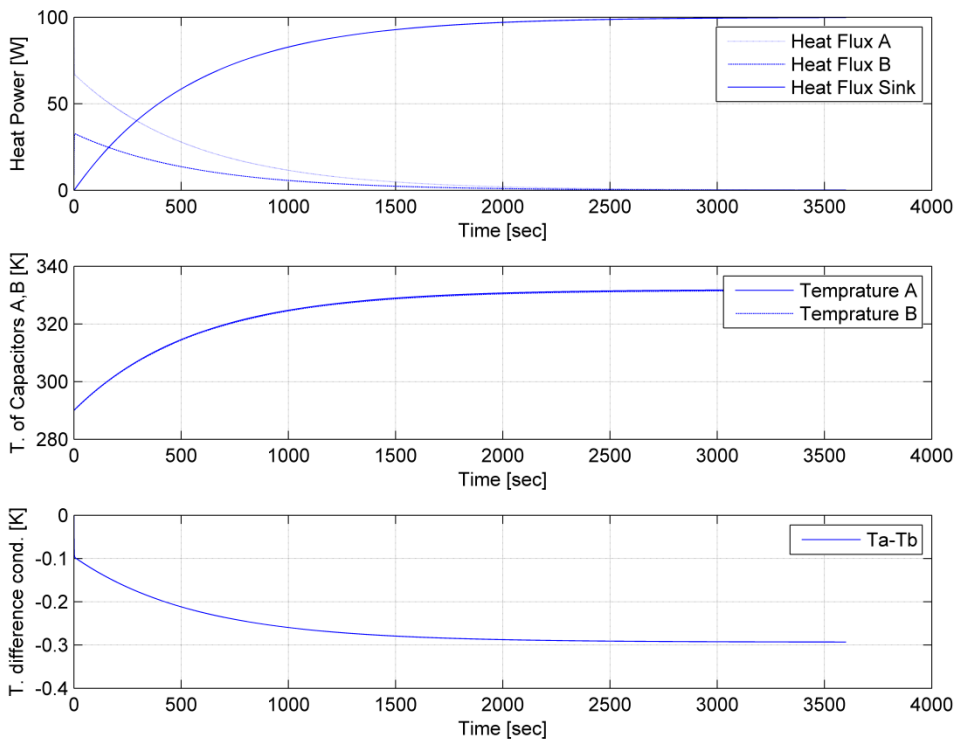


Fig. 4-7 Heat flux and temperature at capacitors A, B and heat sink and temperature difference

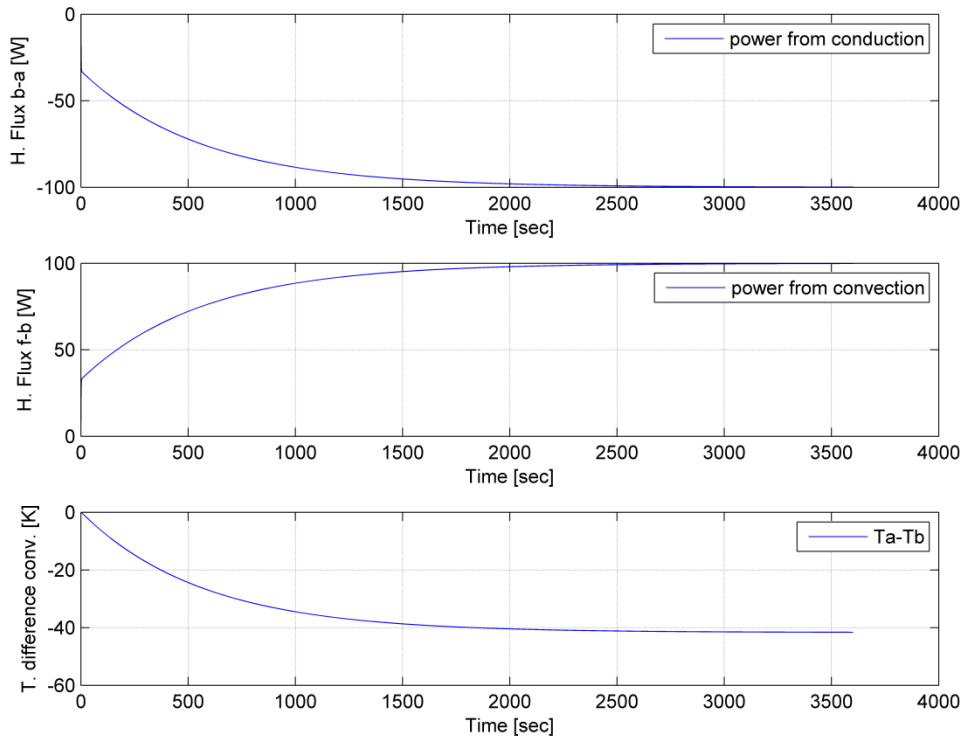
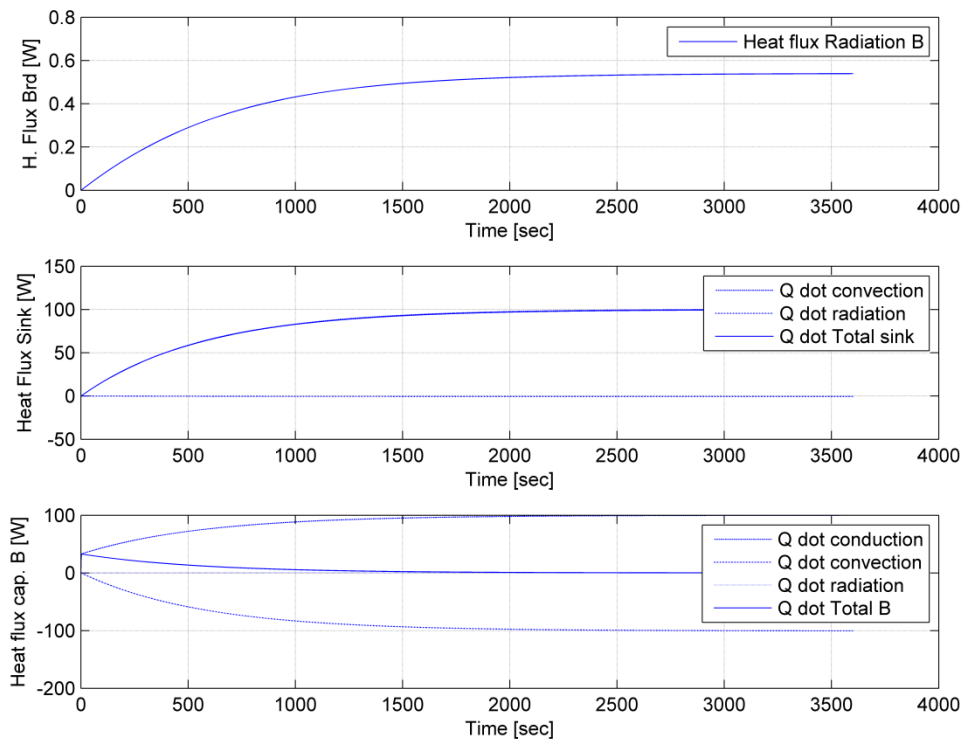


Fig. 4-8 Heat flux due to conduction and convection and temperature difference from convection block





**Fig. 4-9 Heat flux elements and total at capacitors A, B and heat Sink**

### 4.1.3 Cylinder Geometry

In this example a piston inside a cylinder is connected to a rotating shaft. On the top and bottom sides of the piston, constant pressure is applied, while it is rotated by an external rotating torque sink (which models the crankshaft) with constant angular velocity regardless of loading torque value.

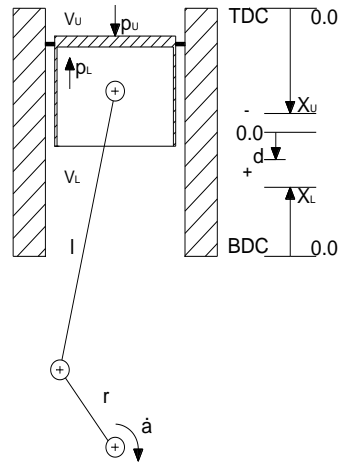


Fig. 4-10 Configuration of piston connected to crankshaft

The purpose of the test is to show how the geometry elements are used and also for validation purposes. Constant pressures are preferred since any implementation faults can be easily identified. The upper pressure models the gas pressure that is applied to the piston due to the weight of mass  $m$  equal to  $p \cdot A_{cs} / g$ , where  $A_{cs}$  is the cylinder cross section area and  $g$  is the gravity acceleration. The lower pressure can be considered to be the atmospheric pressure. The upper pressure is equal to

$$p_U = 1950000 \text{ N / m}^2 \quad (4.1.9)$$

which is approximately equal to the indicated mean effective pressure of a two stroke Diesel Engine. The lower pressure is equal to the atmospheric pressure at sea level

$$p_L = 100000 \text{ N / m}^2 \quad (4.1.10)$$

The cylinder bore  $B$  was set equal to

$$B = 0.9 \text{ m} \quad (4.1.11)$$

the cylinder's cross section area is given by the following equation

$$A_{cs} = \pi \cdot \frac{B^2}{4} = \pi \cdot \frac{0.9^2}{4} = 0.63617 \text{ m}^2 \quad (4.1.12)$$

The crankshaft radius  $r$ , was taken equal to

$$r = 1.275 \text{ m} \quad (4.1.13)$$

and the rod length  $l$ , was set equal to

$$l = 3.5 \text{ m} \quad (4.1.14)$$

In this test the upper and lower compression volumes ( $V_{UL}$  and  $V_{CL}$ ) were set to zero due to the assumption that they are infinite. Thus

$$V_{CU} = V_{CL} = 0 \text{ m}^3 \quad (4.1.15)$$

For the linear moving mass  $m_l$  and rotating mass  $m_r$ , the following values were used

$$m_l = 6000 \text{ kg} \quad (4.1.16)$$

and

$$m_r = 4000 \text{ kg} \quad (4.1.17)$$

The energy loss due to piston ring friction is calculated using a geometry loss block. This energy loss is considered as pressure loss  $p_f$  which consists of three terms. First is the pressure loss as a percentage of the applied pressure. Since the piston rings are pressed against cylinder's walls with a pressure proportional to the applied pressure, the energy loss will be proportional to the applied pressure. The percentage of this pressure was taken equal to

$$\eta_f = 0.02 \quad (4.1.18)$$

Second term is the pressure loss due to piston linear velocity  $\dot{x}_U$ . This pressure loss is proportional to  $\dot{x}_U$  and this is explained by the fact that there is a lubrication layer on the cylinder walls. The value of the pressure loss constant, due to piston linear velocity,  $C_1$  was calculated using an estimation of the pressure loss when the engine rotates at full load where the angular velocity is  $1.5 \text{ s}^{-1}$ . The estimated pressure loss was set equal to  $p_{f2}=100000 \text{ N/m}^2$ . Using the mean piston velocity  $\bar{\dot{x}}_U$ , is obtained from the following relationship

$$\bar{\dot{x}}_U = 4 \cdot \dot{a} \cdot r \quad (4.1.19)$$

By substituting the values to equation (4.1.19) it is obtained that

$$\bar{\dot{x}}_U = 4 \cdot 1.5 \cdot 1.275 = 7.65 \text{ s}^{-1} \quad (4.1.20)$$

The pressure loss constant due to linear velocity is

$$C = \frac{P_{f2}}{\bar{\dot{x}}_U} = 13072 \text{ N / m} \cdot \text{s} \quad (4.1.21)$$

The third term of the pressure loss is taken constant and is produced from the constant pressure that piston rings are applying to the cylinder walls due to their elasticity. This value was taken constant and equal to

$$p_s = 10000 \text{ N} / \text{m}^2 \quad (4.1.22)$$

The crankshaft angular velocity was set initially to  $1.5 \text{ s}^{-1}$  and was kept constant for 2 seconds after that the angular velocity was linearly reduced for 26 seconds to  $-1.5 \text{ s}^{-1}$  and kept there for 4 more seconds till it was linearly increased for other 26 seconds and kept at  $1.5 \text{ s}^{-1}$  for the final 2 seconds of the simulation. Total simulation time 60 seconds (1 minute). The heat dissipated from the geometrical energy loss is used from the heat capacitor block for the calculation of the rise of temperature. In order to calculate the heat due to friction the mass  $m$  and heat capacity at constant pressure  $c_p$  values were set to unity. The initial heat capacitor temperature  $T_{ic}$  was also set to zero for convenience in results. The configuration can be seen in Fig. 4-11. The data used in the example can be found in Table 4-7 and Table 4-8.

**Table 4-7 Geometry and Heat Capacitor Data**

Cylinder Geometry Block		Heat Capacitor Block
$V_{cU} = 0$	$\text{m}^3$	$m = 1 \text{ kg}$
$V_{cL} = 0$	$\text{m}^3$	$c_p = 1 \text{ J} / \text{kg} \cdot \text{K}$
$A_{cs} = 0.6317$	$\text{m}^2$	$T_{ic} = 0 \text{ K}$
$l = 3.5$	$\text{m}$	$Pr = 0 -$
$m_l = 6000$	$\text{kg}$	$Re = 0 -$
$m_r = 4000$	$\text{kg}$	$k = 0 \text{ W} / (\text{m} \cdot \text{K})$
$c = 1$	$-$	$\varepsilon = 0 -$

**Table 4-8 Geometry loss and Pressure of Cylinder's Volume Data**

Geometry Energy loss Block	Upper Cylinder Volume	Lower Cylinder Volume
$\eta_f = 0.02 -$	$p = 1950000 \text{ N} / \text{m}^2$	$p = 10000 \text{ N} / \text{m}^2$
$C = 13072 \text{ N} / \text{m} \cdot \text{s}$		
$p_s = 10000 \text{ N} / \text{m}^2 \cdot \text{s}$		



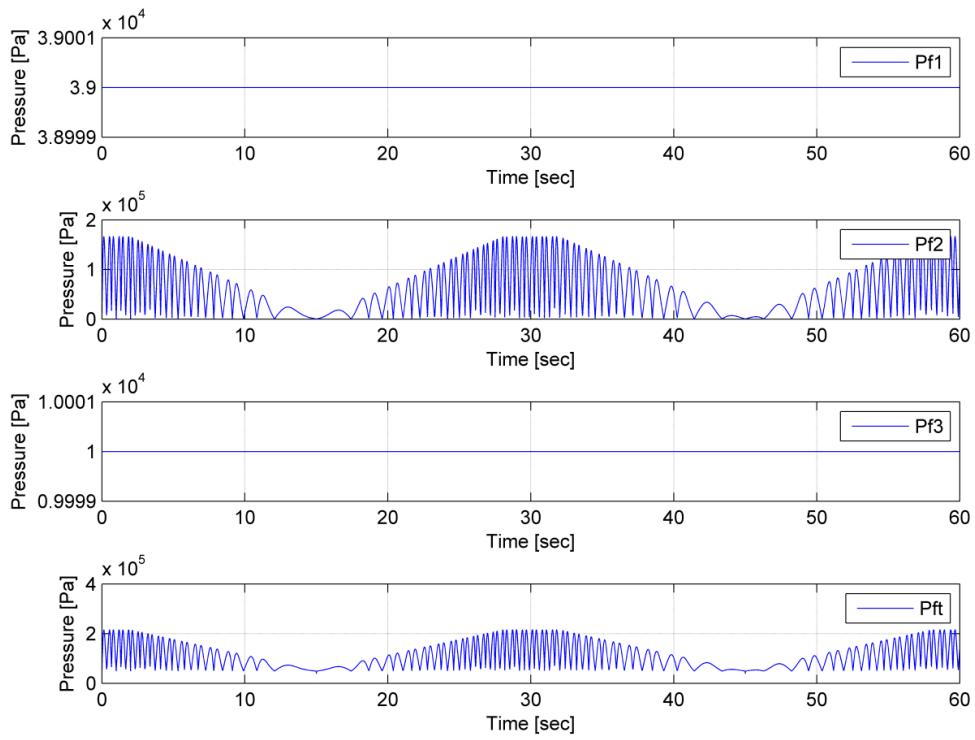


Fig. 4-12 Pressure loss elements at pressure loss block

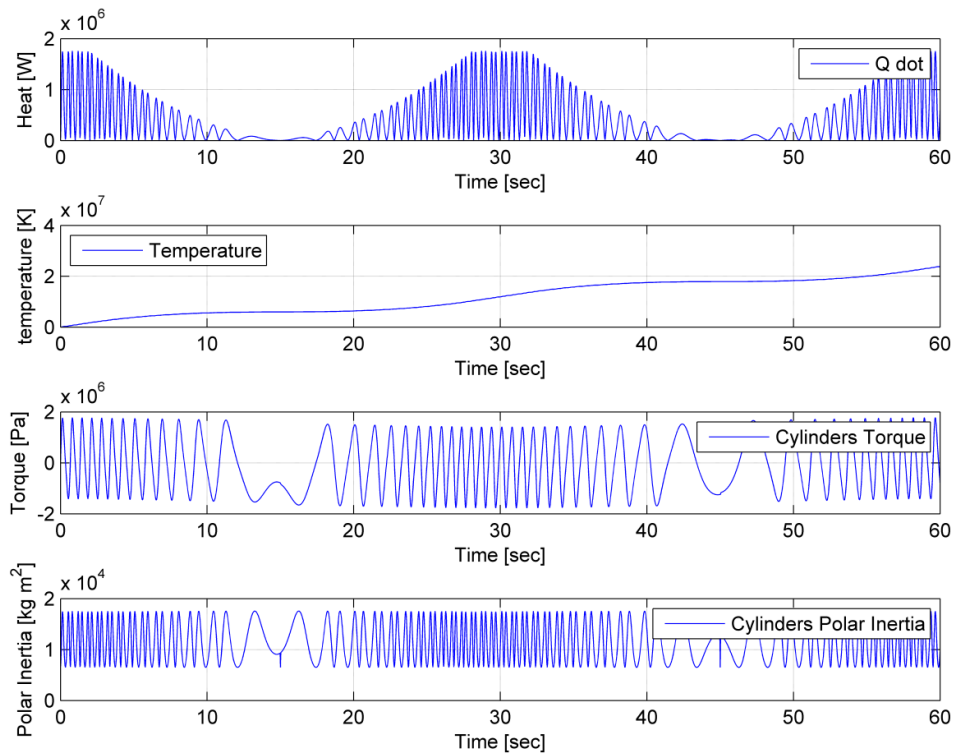
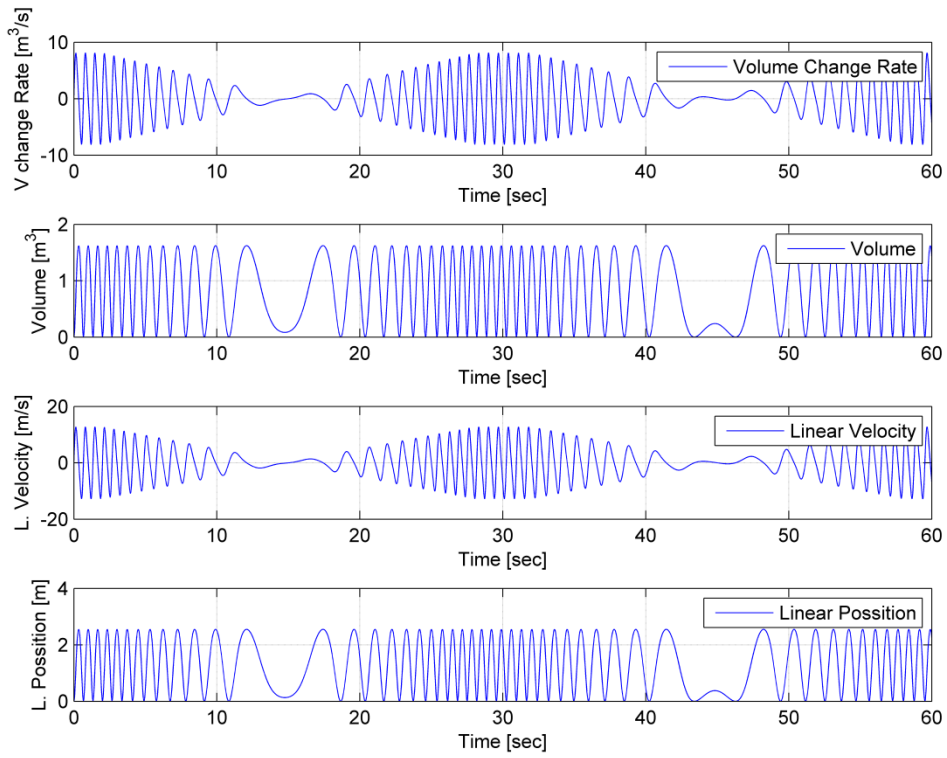
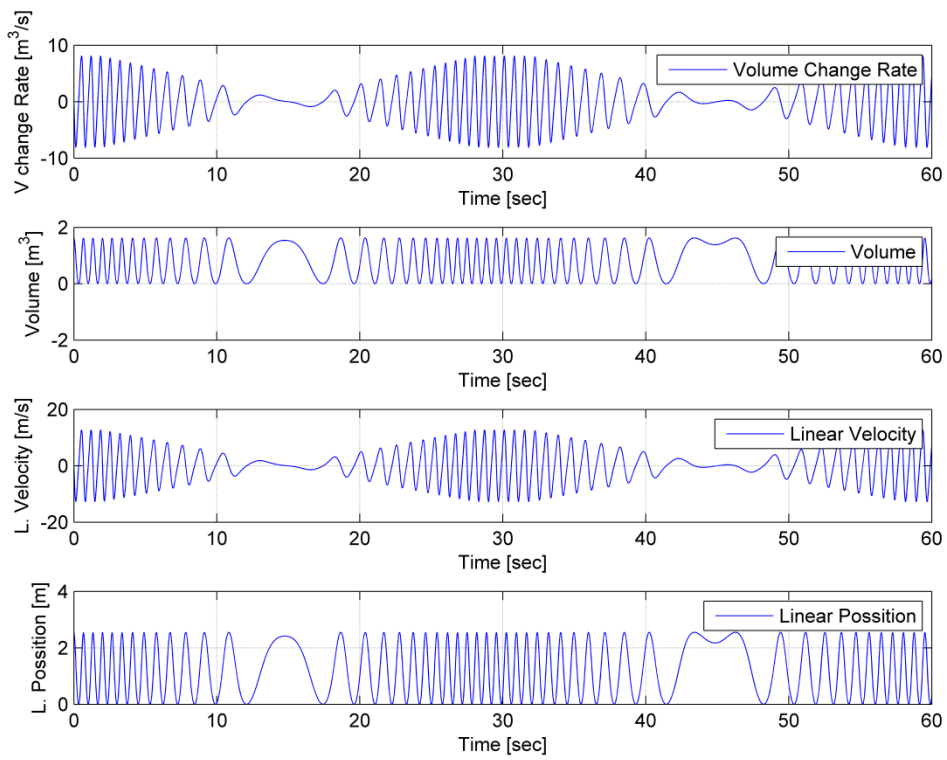


Fig. 4-13 Friction heat, temperature and cylinder's torque and polar inertia



**Fig. 4-14 Upper cylinder: volume change rate, volume, linear velocity and linear position**



**Fig. 4-15 Lower cylinder: volume change rate, volume, linear velocity and linear position**

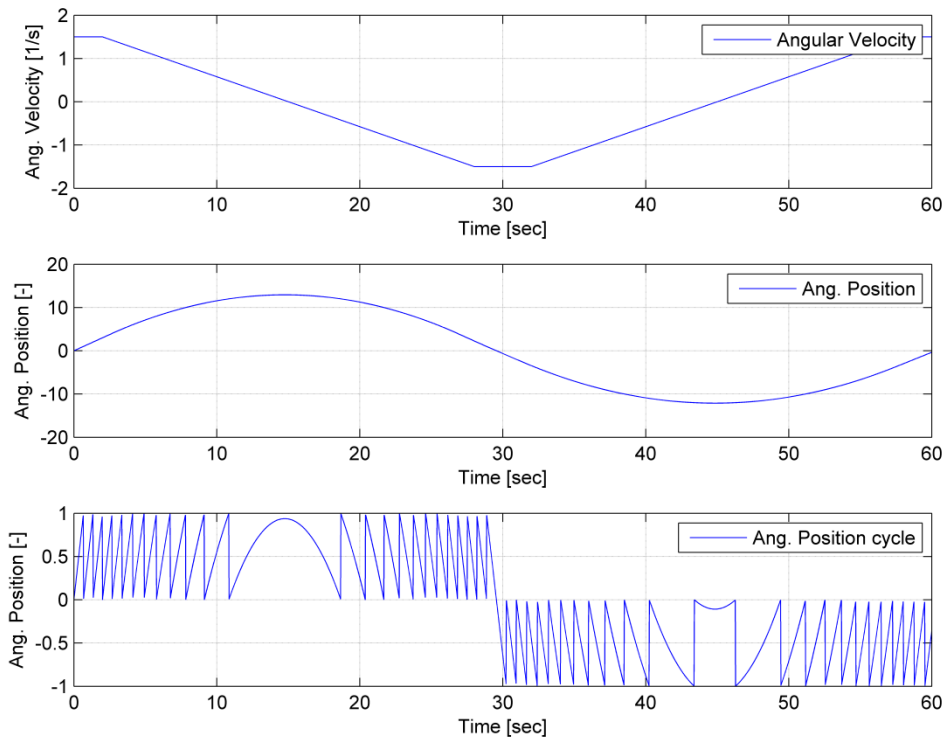


**Fig. 4-16 Crankshaft's angular velocity, angular position and angular position based on engine's cycle**



#### 4.1.4 Compressor and Intercooler test

In this example, a compressor is coupled with an intercooler heat exchanger and both of them are fitted between a gas container with infinite volume and a gas container with finite volume. The purpose of this example is mainly to validate the results of the compressor and secondary check the operation of the intercooler block. The configuration of the example is shown in Fig. 4-17. The input of the radial compressor is connected to a gas container which is so large that can keep the thermodynamic properties of the contained gas constant. The compressor is connected to a shaft that provides the necessary mechanical power to the compressor (in a turbocharger block the moment is provided by the rotation of the turbine). The output of the compressor is connected to a heat exchanger which cools the compressed gas before entering the downstream gas container. This container is insulated; therefore no heat flux is possible through the boundary wall. The infinite volume (upstream) is implemented using the fixed fluid block connected to the gas properties block. The container is implemented using the open thermodynamic system block and the gas properties blocks which controls the properties of the fluid inside the container. It is connected to a heat source that provides the insulation condition (heat flux equal to zero) and a geometry source that provides the geometrical data of the container.

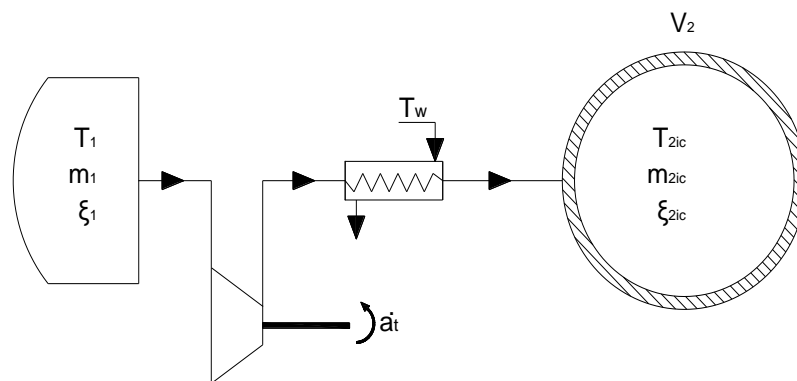


Fig. 4-17 Compressor and heat exchanger coupled between an infinite volume gas and a gas container

The compressor is implemented using the compressor block which is connected to the fixed fluid block that is the upstream state and downstream to the open thermodynamic system block. The compressor is also connected to a heat source that provides the insulation condition and a mechanical sink which provides the torque required by the compressor.

The heat exchanger is implemented using a heat exchanger (intercooler) block which is connected downstream to the open thermodynamic system and to a heat sink that absorbs the rejected from the intercooler heat. The configuration can be found in Fig. 4-22, while the data used in the example are shown in Table 4-9 and the compressor values of the map are located in Appendix A.

## Building block representation of the example

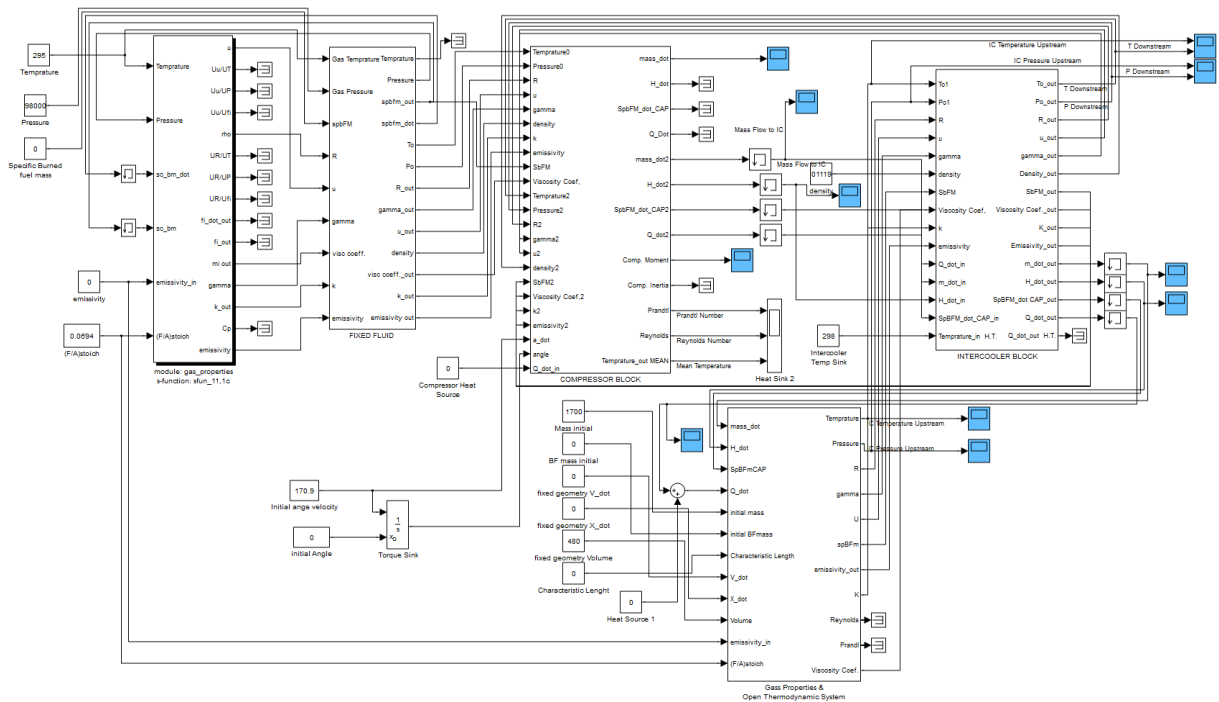


Fig. 4-18 Compressor Intercooler fitted between infinite volume and gas container

## Data used in the example

Table 4-9 Data for Open thermodynamic system, fixed fluid and geometry of the container

Open Thermodynamic System Block	Geometry Block of gas container one	Fixed Fluid Block
$m_{ic} = 1700 \text{ kg}$	$\dot{V} = 0 \text{ m}^3$	$p = 98000 \text{ N/m}^2$
$T_{ic} = 300 \text{ K}$	$V = 480 \text{ m}^3$	$T = 295 \text{ K}$
$\xi_{ic} = 0.01 \text{ -}$	$\dot{x} = 0 \text{ m/s}$	$\xi_{ic} = 0.01 \text{ -}$
$B = 0 \text{ m}$	$x = 0 \text{ m}$	

The compressor map used corresponds to MAN NA70/TO9098 Turbocharger. The basic dimensions are presented in Table 4-10.

Table 4-10 Dimensions of MAN NA70/TO9098 Turbocharger

Compressor impeller tip diameter	$D_c$	0.840 m
Turbine impeller tip Diameter	$D_T$	0.761 m
Turbine Diffuse outlet area	$A_{td}$	1 m <sup>2</sup>
Turbocharger Polar Moment of Inertia	$I_p$	13kg m <sup>2</sup>
Rotational Speed at design point	n	10700 RPM

The heat exchanger efficiency was each time interpolated between 0.80 and 0.82, due to mass flow, while the pressure drop was interpolated also between the values of 0 and 18000Pa. The temperature of cooling water was set equal to 298 K. The rotational speed of the compressor was set  $170.9 \text{ sec}^{-1}$  while the initial angular position was set zero.

### Results

The simulation run for 10 seconds. When the simulation started, the pressure at the gas container was found equal to 363234.4 Pascal. In the following graphs the expected behavior is observed, meaning that due to the compressor action, mass flows from the upstream infinite volume (atmosphere) to the finite gas container, which results in temperature and pressure increase due to the added mass at constant volume (fixed geometry container) and subsequently causes the mass flow rate to decrease over time. This increase is shown in Fig. 4-19. As a result Fig. 4-20 shows the downstream temperature after the intercooler where a temperature and pressure decrease is observed. Fig. 4-21 shows the map mass flow of the compressor, the efficiency and the pressure ratio that compressor was working and finally the required torque (torque absorbed) in order to work.

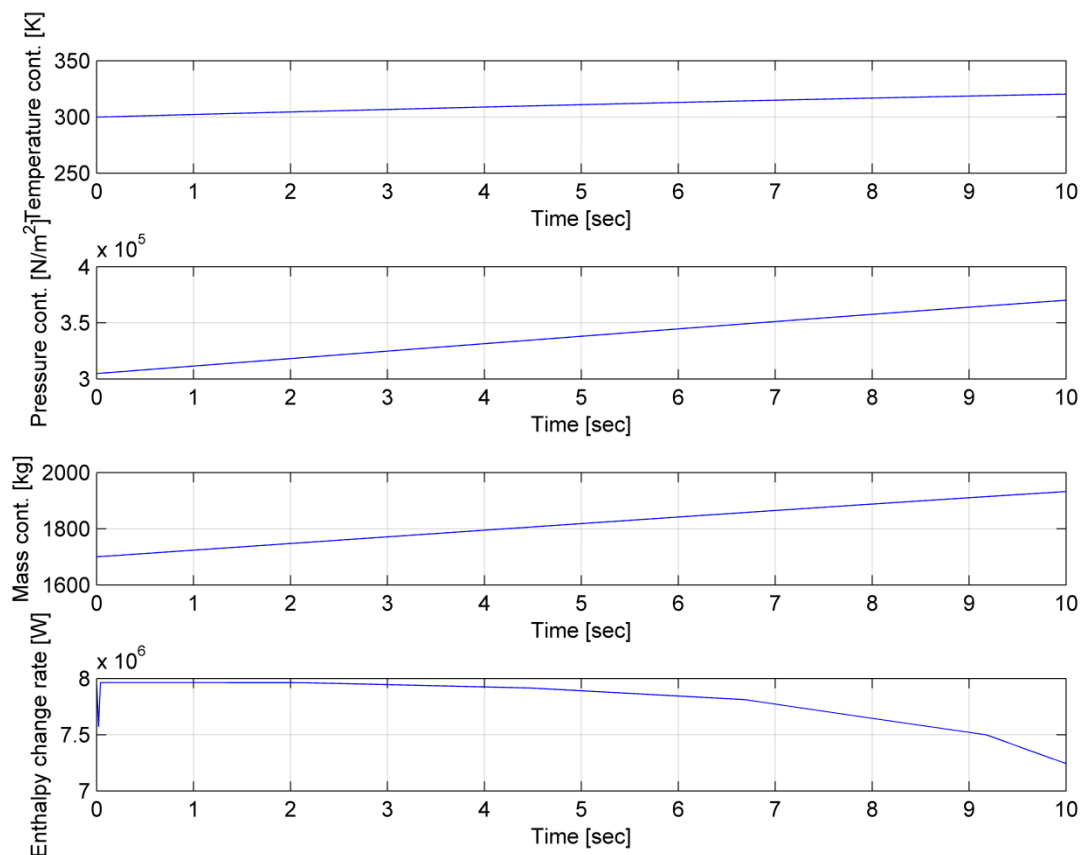


Fig. 4-19 temperature, pressure, mass increase and Enthalpy change rate of gas container

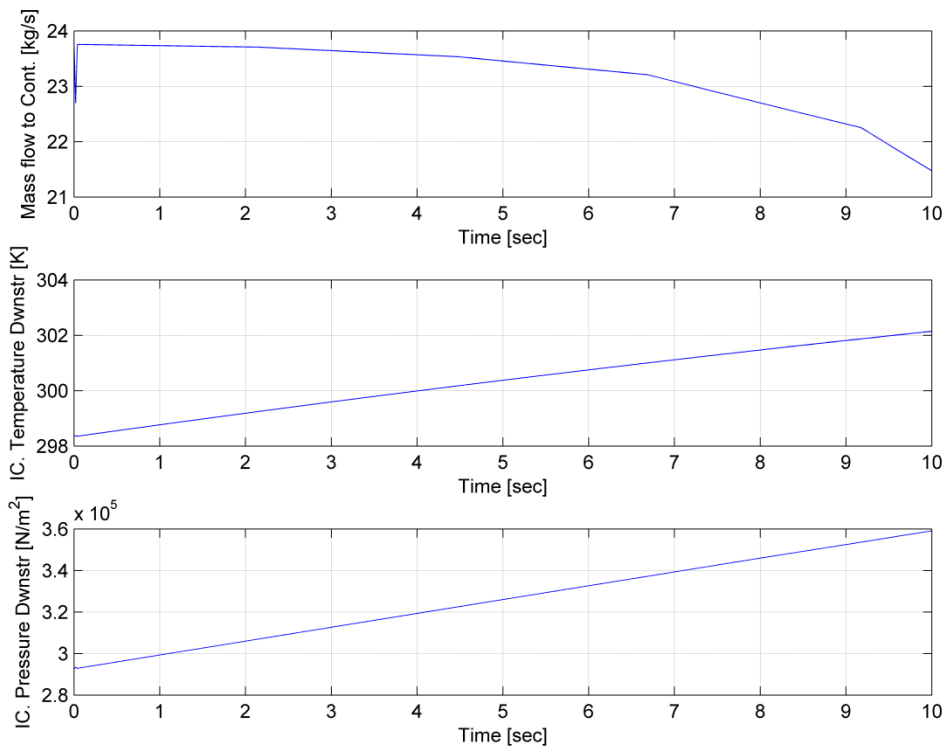


Fig. 4-20 Intercooler's downstream temperature, pressure and mass flow to container

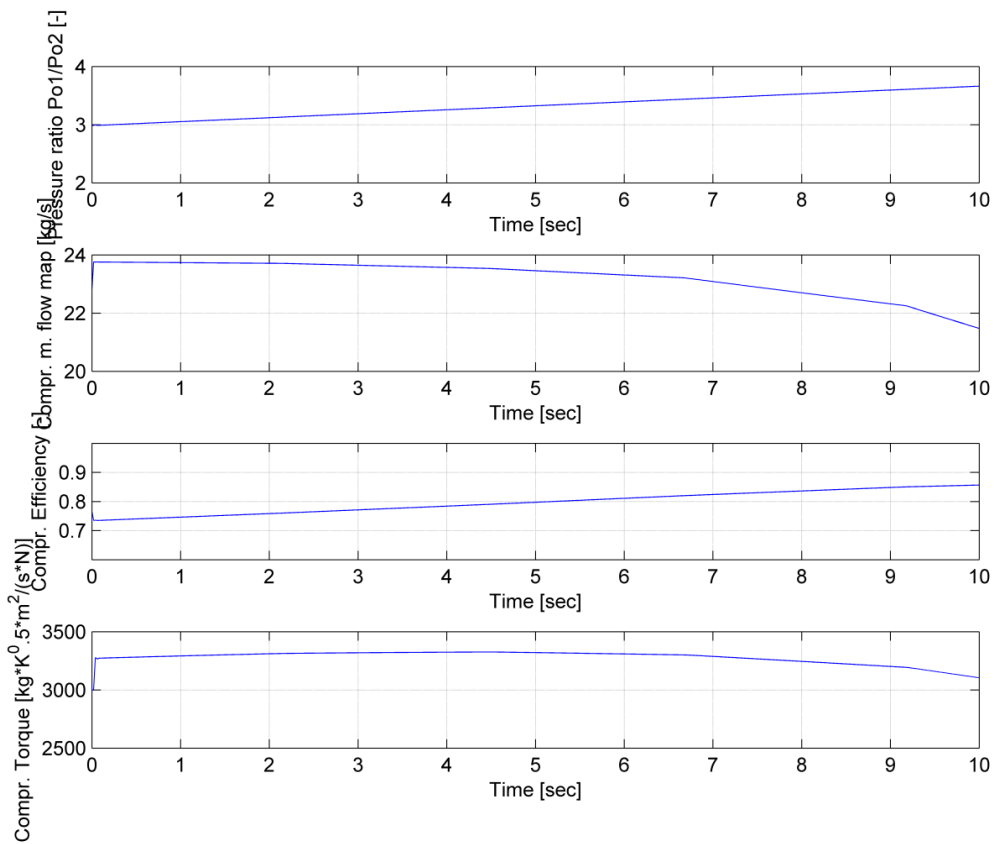


Fig. 4-21 Compressor's Pressure Ratio, mass flow, efficiency and Torque absorbed

### 4.1.5 Turbine test

In this test a turbine is fitted between a container of gas and an infinite volume. The purpose of this example is mainly to validate the turbine block. The configuration used in the example is shown in Fig. 4-22. The input of the axial turbine is connected with a finite volume gas container which is insulated (no heat transfer is possible), while the output of the compressor is connected with a gas container which is so large that can keep the thermodynamic properties of the contained gas constant. The turbine is connected to a shaft which absorbs the mechanical power from the turbine. The turbine is also insulated meaning no heat transfer between the passing gas and the turbine casing is possible.

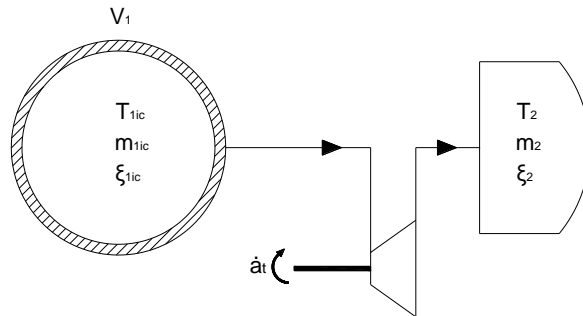


Fig. 4-22 Configuration of turbine fitted between gas container and infinite volume

The finite volume of gas container is implemented using the open thermodynamic system block which is connected to the gas properties block that provides the necessary thermodynamic properties of the contained gas, a heat source which provides the insulation condition (heat flux equal to zero) and a geometry source which provides the geometry of the container (volume). The infinite downstream volume gas container is modeled using a fixed fluid block connected to gas properties block which provides the thermodynamic properties of the contained gas. The turbine is modeled using the turbine block which is connected upstream to the finite volume and downstream to the infinite volume. The turbine is also connected to a heat sink source that provides the insulation condition (heat flux equal to zero) and a mechanical sink which absorbs the torque produced by the turbine.

### Building block representation of the example

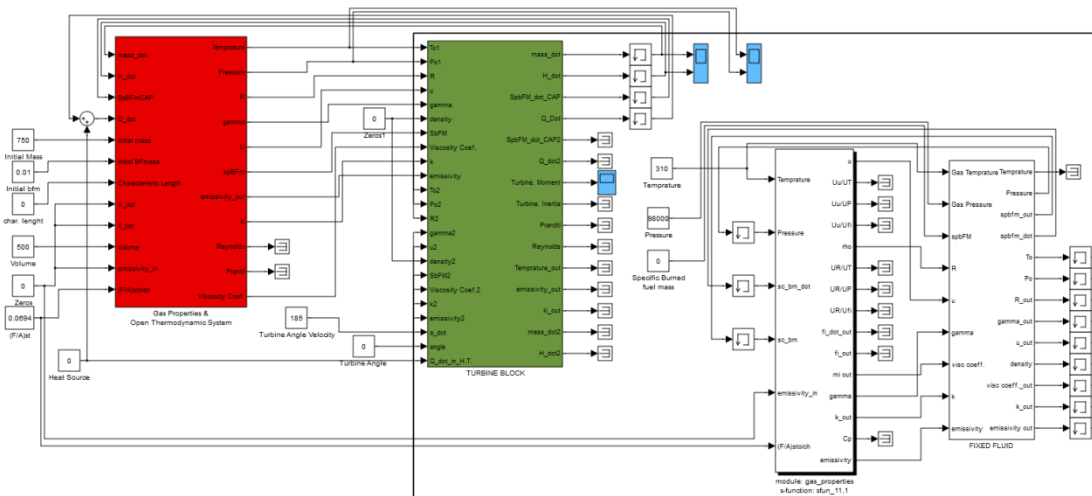


Fig. 4-23 Turbine connected to finite and infinite volumes

### Data used in the example

The data used in the open thermodynamic system, in the fixed fluid block and in the fixed geometry block are presented in Table 4-11.

Open Thermodynamic System Block	Geometry Block of gas container one	Fixed Fluid Block
$m_{ic} = 750 \text{ kg}$	$\dot{V} = 0 \text{ m}^3$	$p = 98000 \text{ N/m}^2$
$T_{ic} = 810 \text{ K}$	$V = 500 \text{ m}^3$	$T = 310 \text{ K}$
$\xi_{ic} = 0.01 \text{ -}$	$\dot{x} = 0 \text{ m/s}$	$\xi_{ic} = 0.01 \text{ -}$
$B = 0 \text{ m}$	$x = 0 \text{ m}$	

Table 4-11 Data used in the example

The swallowing capacity map of the turbine is illustrated in Fig. 4-24, while the turbine efficiency is illustrated in Fig. 4-25. For simpler results, it is assumed that turbine efficiency is constant.

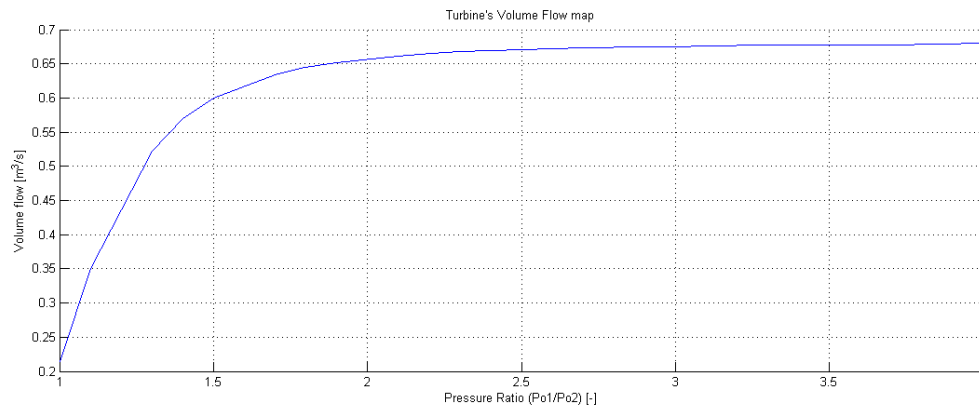


Fig. 4-24 Turbine swallowing capacity map versus pressure ratio

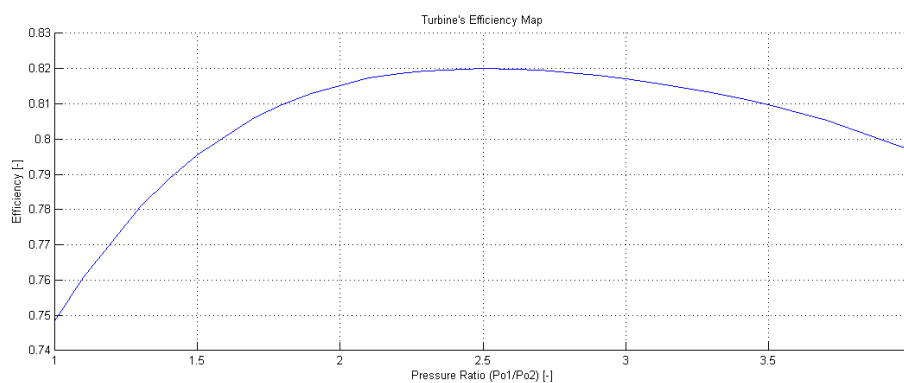
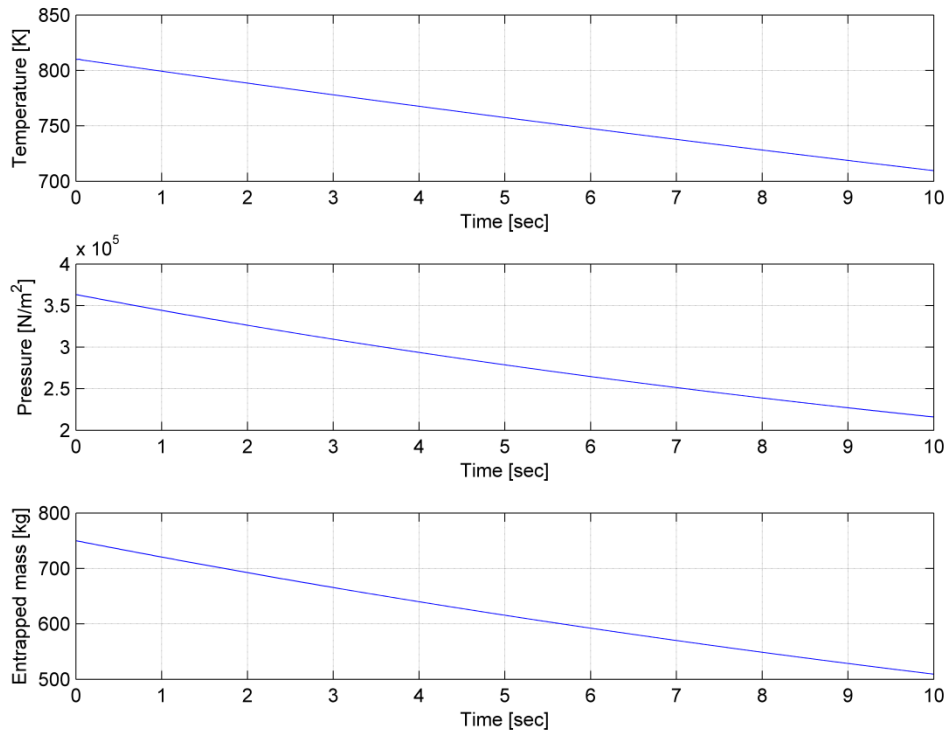


Fig. 4-25 Turbine stagnation to static isentropic efficiency map

### Results

The duration of the simulation was 10 seconds. When the simulation started ( $t=0s$ ) the gas pressure in the container one was equal to  $p_1 = 348847 \text{ N/m}^2$ . Due to the turbine operation, mass flows from the upstream container to the downstream container. This results to a temperature, mass decrease for the upstream container. Since the upstream

container has finite volume, due to mass flow the pressure in this container drops, Fig. 4-26. Fig. 4-27 shows the mean temperature of the turbine, the actual temperature increase and Enthalpy change rate of gas container 1. The Turbine's efficiency, map mass flow and torque developed are shown in Fig. 4-28.



**Fig. 4-26 Temperature, Pressure and Entrapped Mass drop of gas container 1**

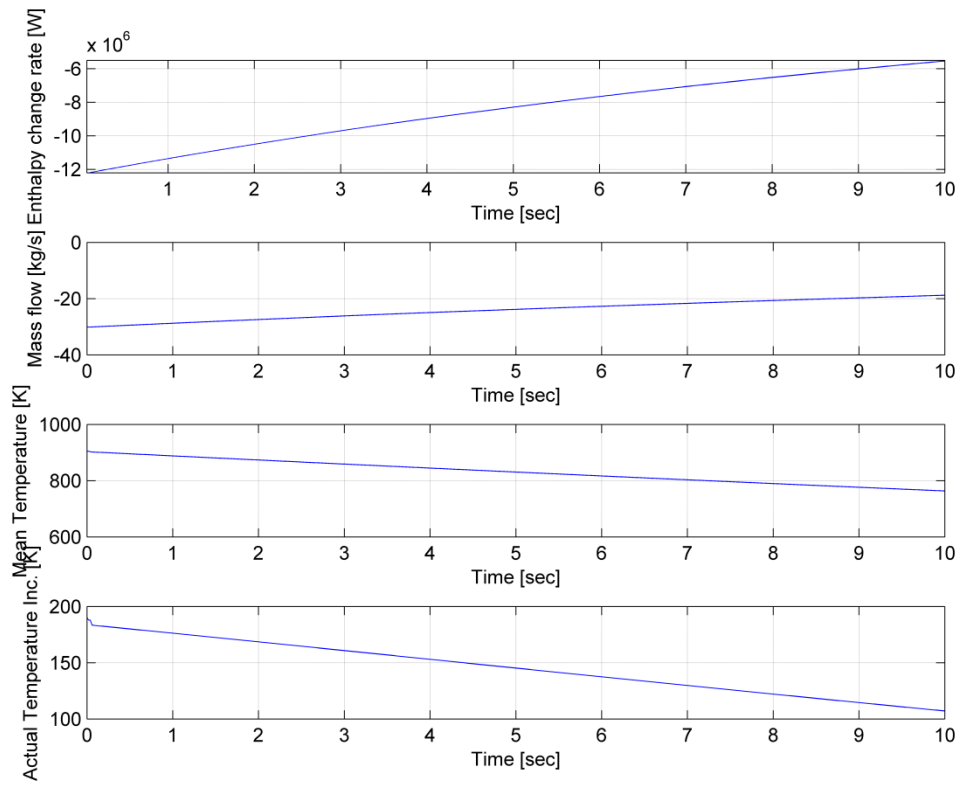


Fig. 4-27 Enthalpy change rate, mass flow to container 1, mean and Actual Temperature Increase

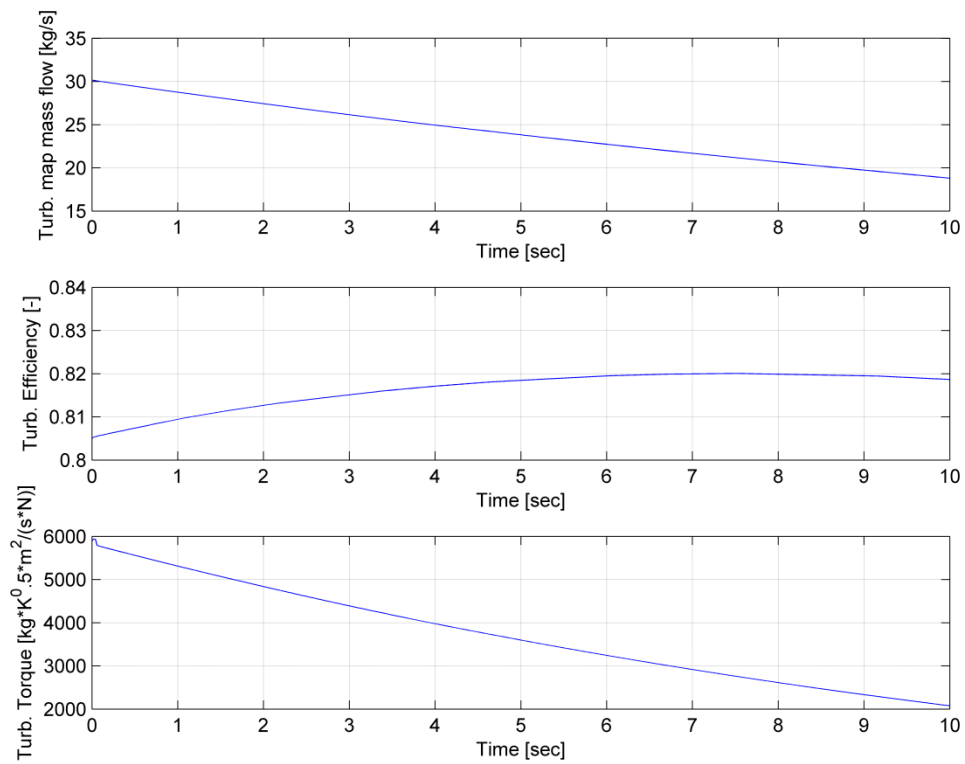


Fig. 4-28 Turbine's mass flow, efficiency and torque developed



## 4.2 One cylinder engine example

Although the modeling in the present thesis targeted towards the complete engine, time constraints of data input and submodel refinement, compelled to produce simulation results of adequate quality to compare to available experimental data only for the single cylinder case. These are presented below.

The model for the complete engine (8 cylinders, 3 turbochargers) is presented in Appendix B.

### Building block representation of the one cylinder engine closed cycle

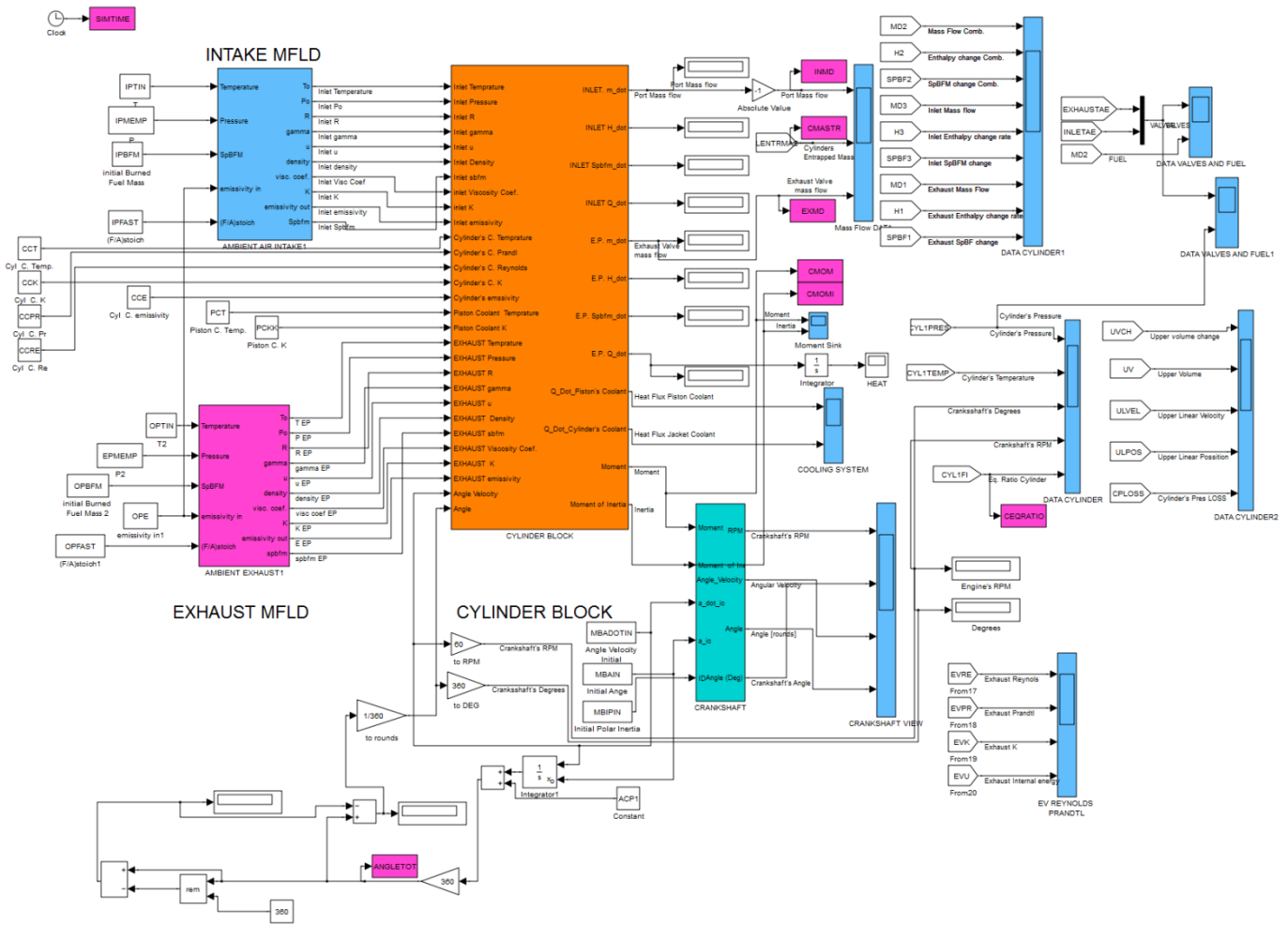


Fig. 4-29 One cylinder engine configuration

### ***One cylinder simulation results***

In this section, the results from the simulation of the one cylinder of the above mentioned engine are presented. These results were compared with the simulation program MoTher developed at LME. Motor Thermodynamics (MoTher), is a general purpose engine performance prediction program based on the thermodynamic control volume principle. The first version of this program was released in 1985. Since then it has been under continuous development, and in its present form is designed for the current needs of the engine designers and manufacturers (LME, 2008).

In order to divide the engine cycle to phases, Table 4-12 is introduced.

**Table 4-12 Phase of phenomenon versus crank angle**

<b>Angle</b>	<b>Phase</b>
<b>0.0° – 44.8°</b>	Combustion Period
<b>44.8° – 110.8°</b>	Expansion Period
<b>110.8° – 247.2°</b>	Gas Exchange Period
<b>247.2° – 360.0°</b>	Compression Period

Simulations were performed at 90% load at 100.5 RPM crankshaft angular velocity, at 75% load at 94.6 RPM and at 50% load at 82.5 RPM crankshaft angular velocity. The results are presented below.

**Case: 90% load at 100.5 RPM**

Fig. 4-30 shows the pressure developed inside the engine cylinder along with the temperature, in crank angle.

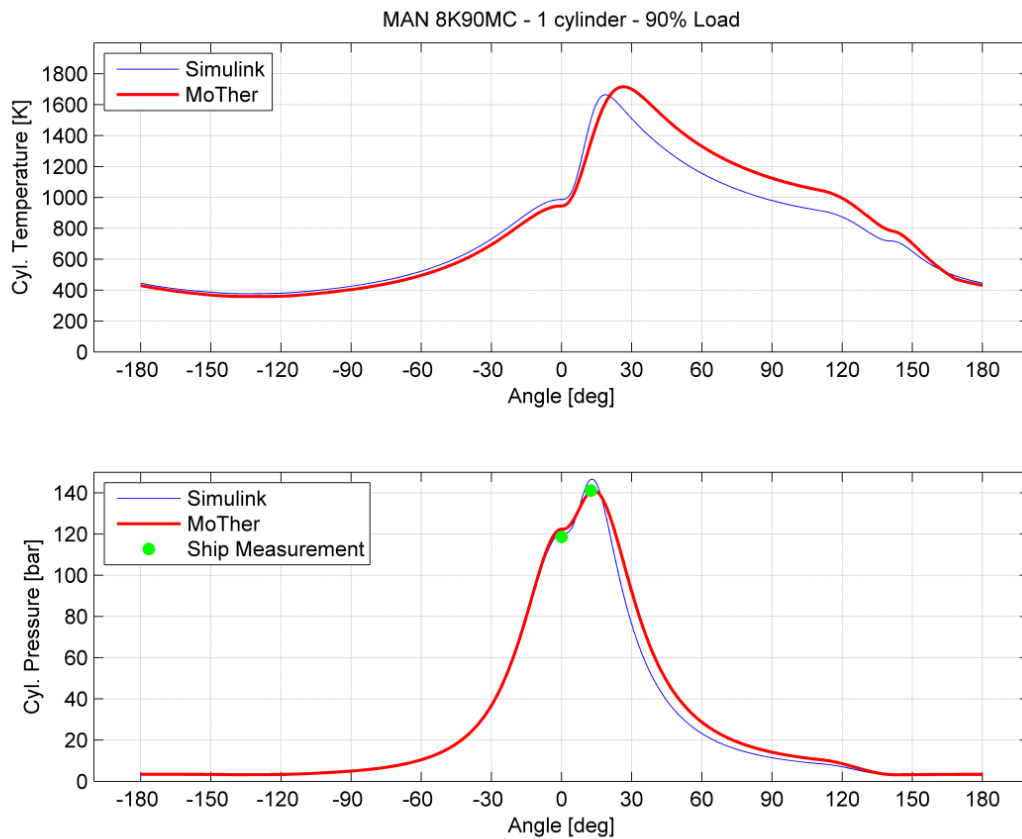


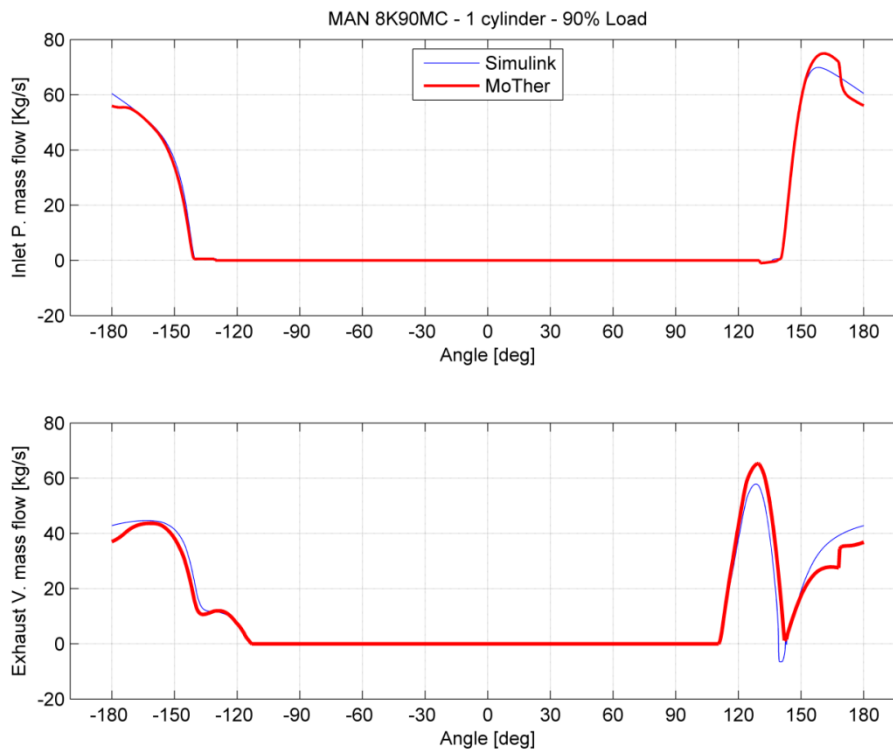
**Fig. 4-30 Simulation temperature (top) and pressure of cylinder**

As it is shown in Fig. 4-30, pressure trace of the Simulink run has an insignificant error in the compression period as compared MoTher. When the piston reaches the top dead center (TDC), the result of pressure at TDC, namely compression pressure, has a deviation from MoTher results, while it is slightly greater than the measured value<sup>3</sup>. As it is shown, the Simulink pressure trace is smaller compared to MoTher due to the fact that the cylinder has less entrapped mass (showed in Fig. 4-33). This deviation can be explained with the fact that during the gas exchange period, Simulink gives different temperature than MoTher. Simulink implementation of cooling system utilizes approximate values for the properties of the materials of the engine. Also, Simulink model has different approach in the model of heat transfer than the one of MoTher. Therefore it is not clear which constants have to be adjusted in order to compare the same simulation problem. This temperature difference results less instantaneous mass flow inside the cylinder. When the compression period ends and the combustion process occurs, a deviation is observed from MoTher. This can be explained from the fact that this thesis utilizes a very simple model of combustion. When applying the constants to form the S – Curve (section 2.7) it is not accurate to

<sup>3</sup> As measured on board ship. Data available at L.M.E.

speculate the appropriate constants (Gunter, Schwarz, Stiesch, & Otto, 2006) and adjust the S – Curve so that it matches the different combustion model of MoTher. The latter utilizes the Woschni – Ansits model. For more accurate results, the method of a Heat Release map which the engine manufacturer could provide, is proposed.

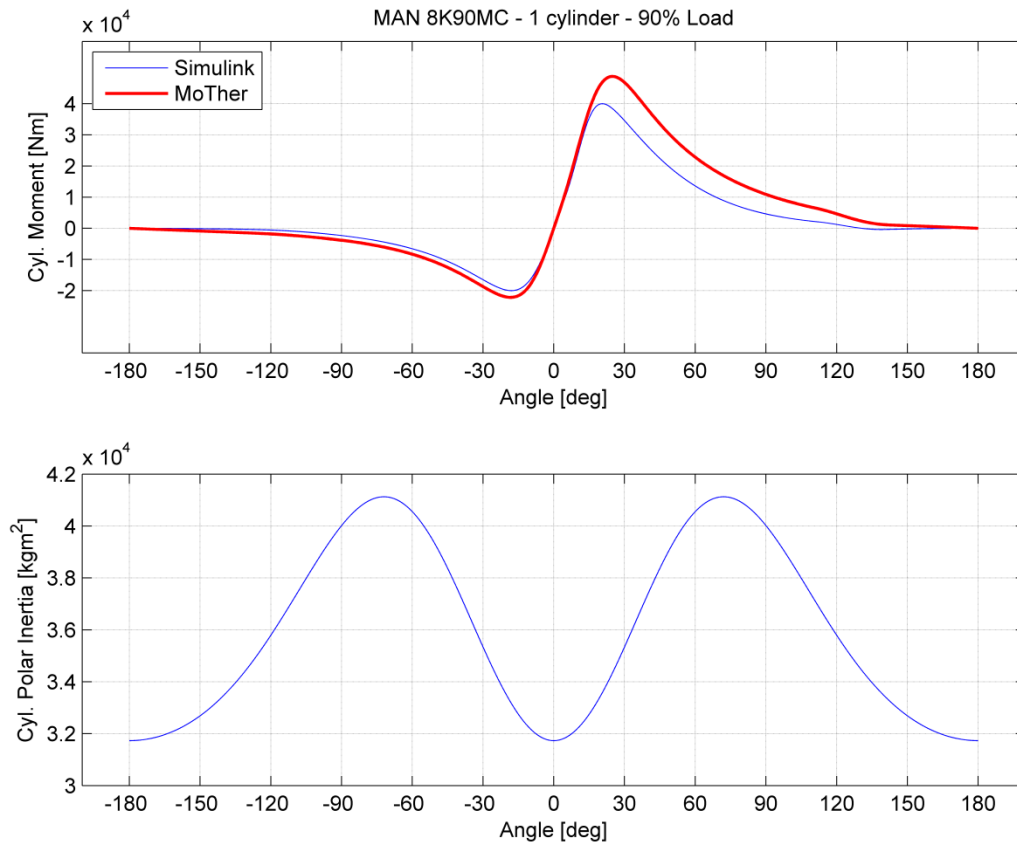
Fig. 4-31 shows the mass flow from inlet port to the cylinder chamber. Also it presents the mass flow from cylinder to exhaust manifold, when the exhaust valve opens.



**Fig. 4-31 Inlet port (top) and exhaust valve mass flow to or from cylinder**

Comparing the two simulation traces, it is observed that Simulink model produces a smaller trace of mass flow in and out of the cylinder. This is explained by the fact that higher pressure inside the cylinder is observed at the overlapping period. According to the equations of mass flow through restrictions, the amount of mass transferred is a function of pressure ratio before and after the restriction, of temperature before the restriction and of effective area of valve. Assuming the fact that the timing maps provided are identical to both models and on-site measurements of valve opening are correct, the error of two percent is rather acceptable.

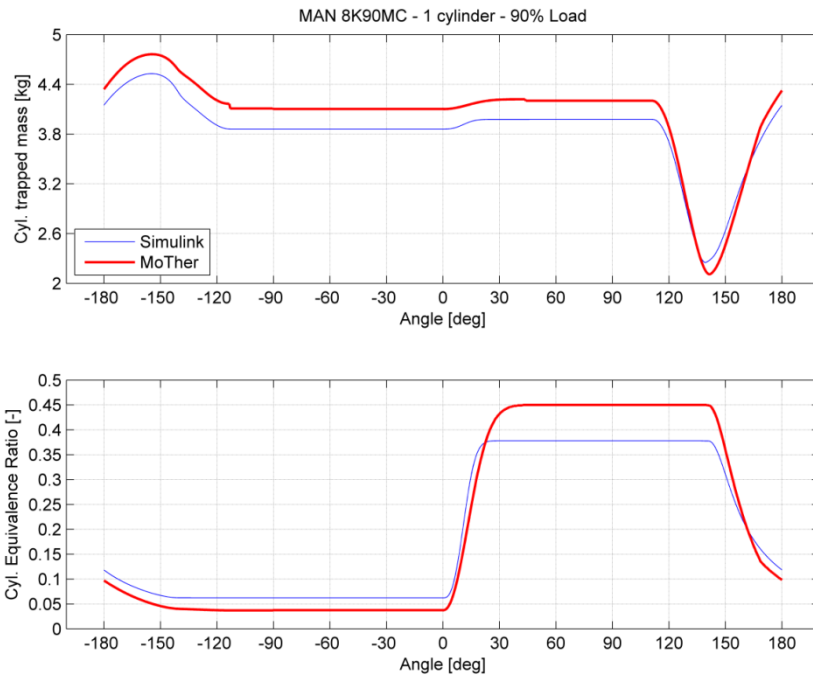
Fig. 4-32 shows the work produced by engine cylinder in one cycle versus crank angle.



**Fig. 4-32 Cylinder developed torque (top) and moment of inertia**

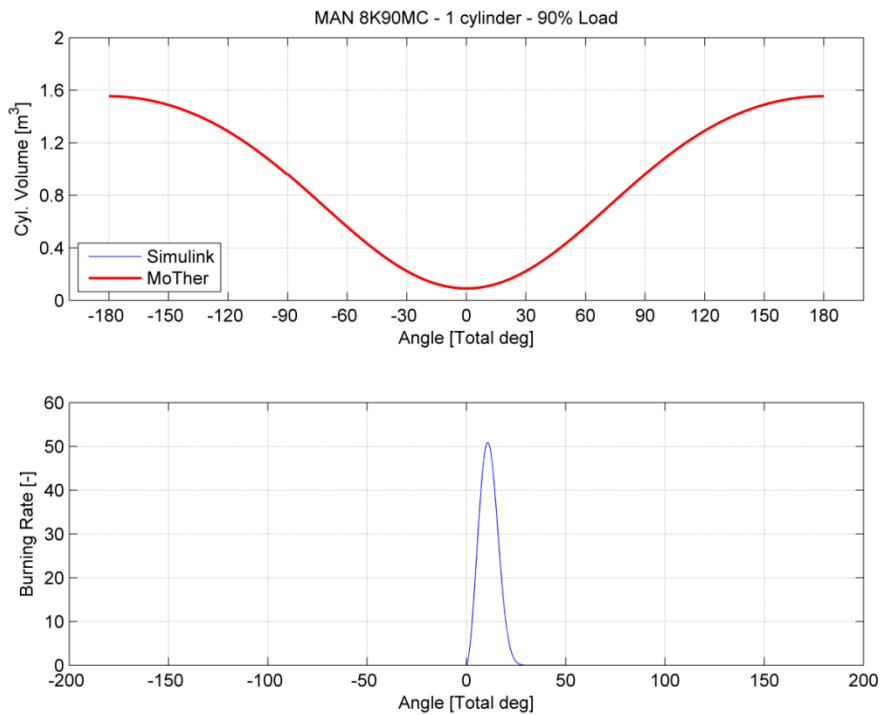
A significant deviation is observed in angles  $20^\circ$  to  $150^\circ$  due to the fact that cylinder pressure during and after the combustion is significantly different. According to equations described in chapter 2, section 2.9, the force developed by the piston movement is the difference of pressures (the gas pressure inside the engine cylinder minus the pressure applied below piston) multiplied by the area of the piston. This difference of gas pressure entrains the force and therefore the piston developed torque.

Fig. 4-33 presents the trapped mass inside the engine cylinder and also shows the change of equivalence ratio,  $\Phi$ , in one cycle.



**Fig. 4-33 Cylinder trapped mass (top) and equivalence ratio**

As mentioned before the trapped mass is below the value of MoTher almost seven percent. This causes an overall error in the simulation results. In order to validate the assumption that the Simulink model describes best the volume change rate, Fig. 4-34, is presented.



**Fig. 4-34 Instantaneous volume of cylinder (top) and burning fuel rate of combustion**

As shown in Fig. 4-34, the instantaneous volume of the cylinder is the same for Simulink model with the results of MoTher. This figure allows considering the mechanical model of the Simulink successful.

**Table 4-13 Inlet and exhaust manifold temperature, pressure at 90% load**

	<b>Temperature (Kelvin)</b>	<b>Pressure (bar)</b>
<b>Inlet</b>	314	3.445
<b>Exhaust</b>	643.7	3.19

**Case: 75% load at 94.6 RPM**

In this case, the results of Simulink simulation at 75% at 94.6 RPM are presented. Comparison between MoTher and Simulink was not able due to lack of MoTher data for this particular load point. The results of the non parametric run at 75% are shown in Fig. 4-35, Fig. 4-36, Fig. 4-37 and Fig. 4-38, while the data<sup>3</sup> of inlet and exhaust conditions during the measurements are presented in

Table 4-14.

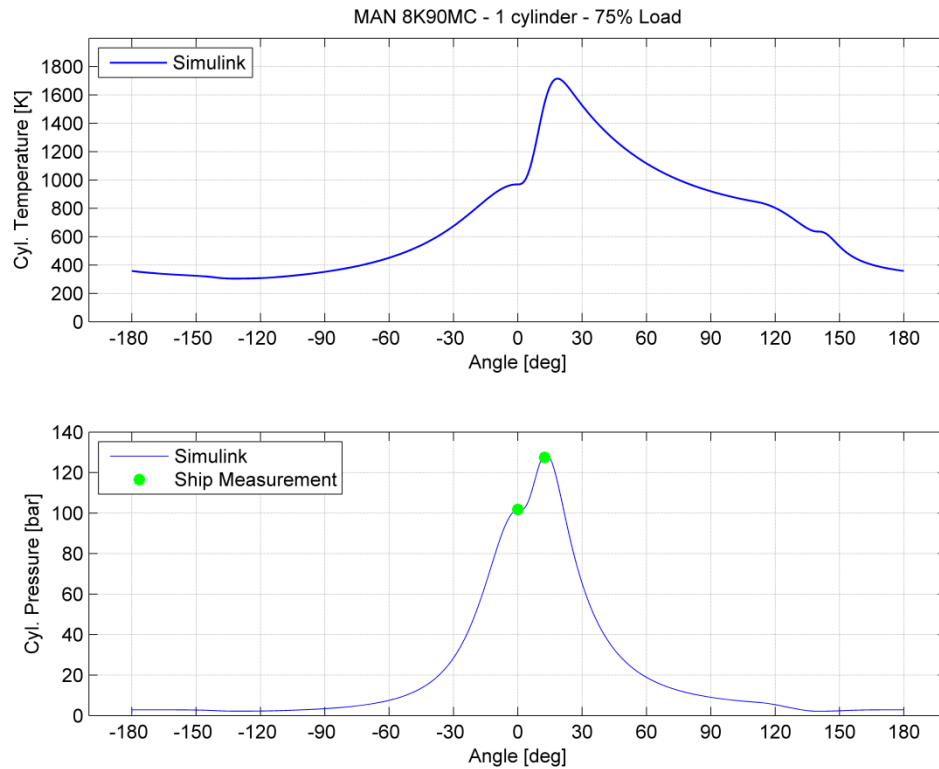


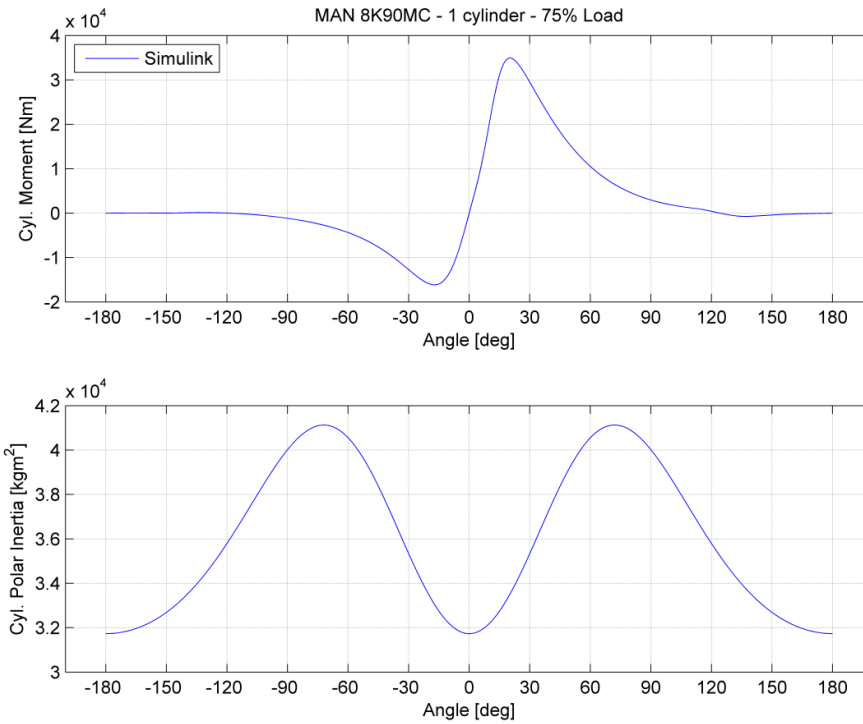
Fig. 4-35 Simulated temperature (top) and pressure of cylinder (75%)

Table 4-14 Inlet and exhaust manifold temperature and pressure at 75% load measured<sup>3</sup>

	Temperature (Kelvin)	Pressure (bar)
<b>Inlet</b>	306.7	2.93
<b>Exhaust</b>	621.3	2.70

Fig. 4-36 presents the torque developed per cycle by cylinder. In comparison with the values of 90% and 50%, the max value calculated in 75% is between the other two max values. This allows believing that consistency in results exists.





**Fig. 4-36 Torque (top) and polar inertia developed by cylinder (75%)**

In Fig. 4-37 mass flow from inlet port and the mass flow from exhaust valve is presented while Fig. 4-38 presents the trapped mass inside the cylinder and the equivalence ratio.

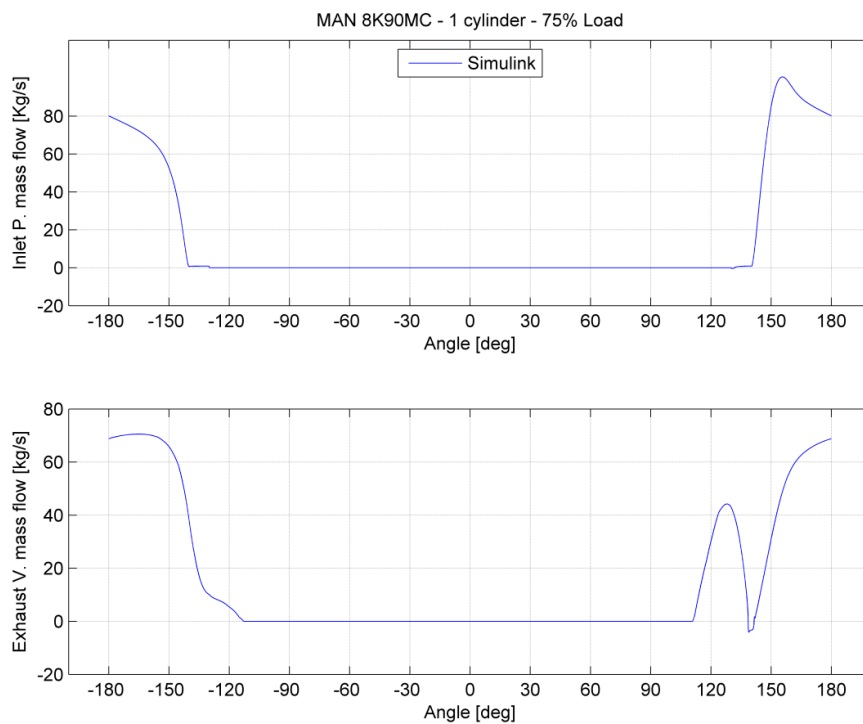


**Fig. 4-37 Inlet port (top) and exhaust valve mass flow to or from cylinder (75%)**

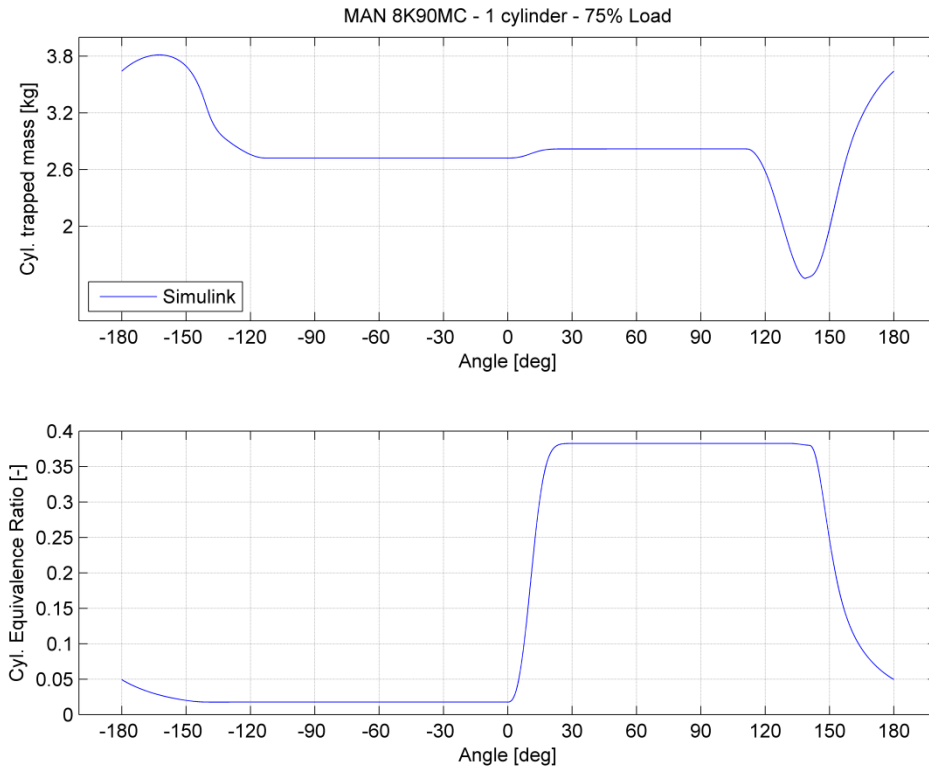


**Fig. 4-38 Trapped mass and equivalence ratio inside cylinder (75%)**

**Case: 50% load at 82.5 RPM**

Here are presented the results for partial load of the engine at 50% and at 82.5 RPM. Fig. 4-39 shows the temperature developed inside the engine cylinder along with the pressure, in crank angle.

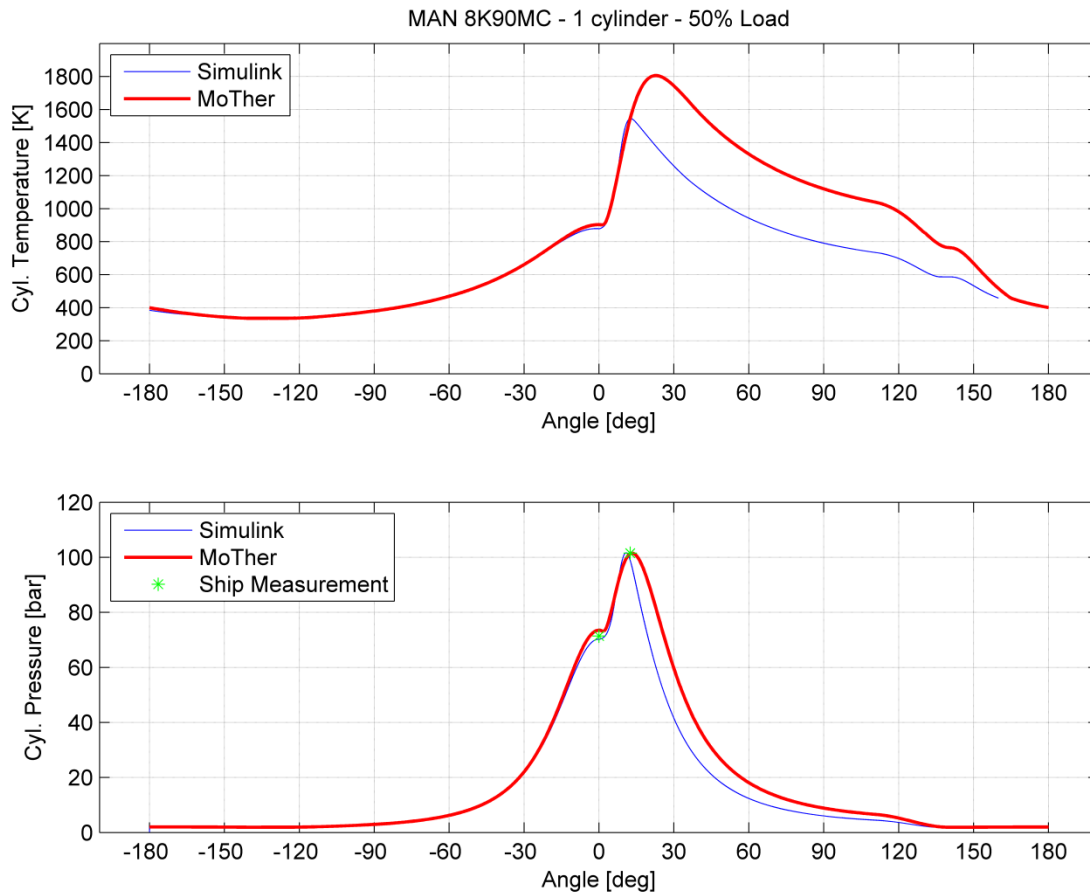


**Fig. 4-39 Simulation temperature (top) and pressure of cylinder (50%)**

As compared to 90% load, in the case of 50%, larger deviation in pressure is observed. As a result, lower values of temperature are calculated from Simulink simulation.

Fig. 4-40 shows the mass flow from inlet port to the cylinder chamber. Also it presents the mass flow from cylinder to exhaust manifold, when the exhaust valve opens.

**Table 4-15 Inlet and exhaust manifold temperature, pressure at 50% load**

	Temperature (Kelvin)	Pressure (bar)
<b>Inlet</b>	301	2.05
<b>Exhaust</b>	605	1.86

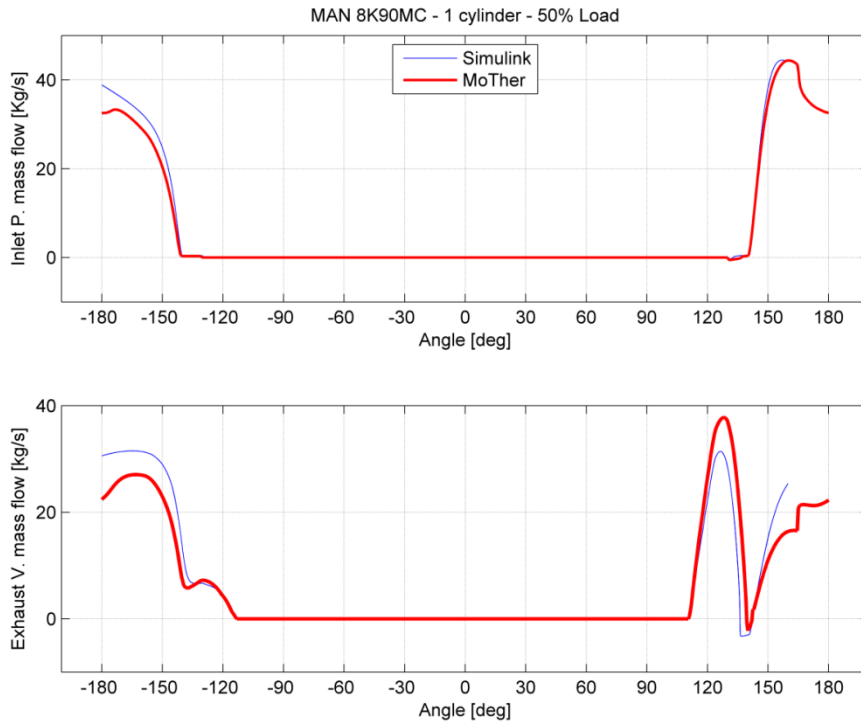


Fig. 4-40 Inlet port (top) and exhaust valve mass flow to or from cylinder (50%)

Fig. 4-41 shows the work produced by engine cylinder in one cycle versus crank angle.

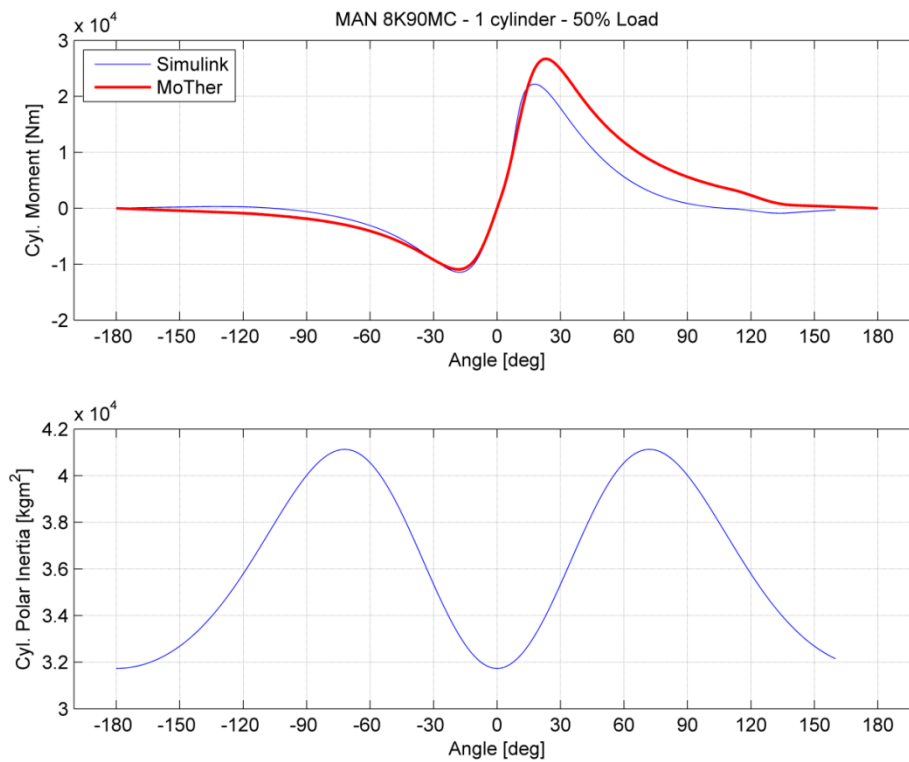
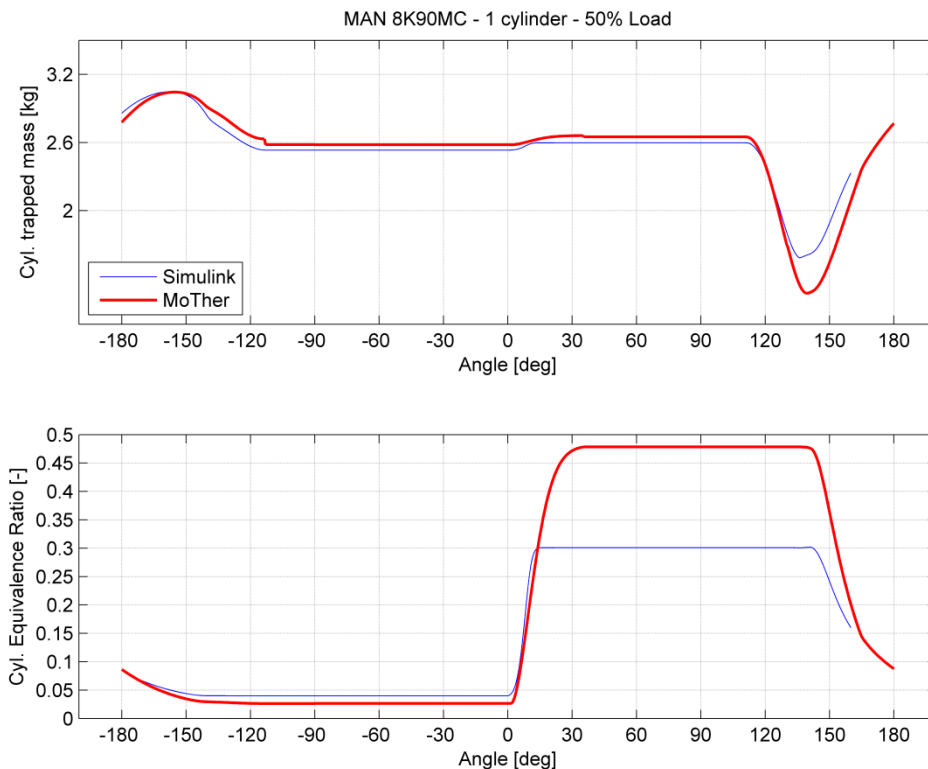


Fig. 4-41 Cylinder developed torque (top) and moment of inertia (50%)

A significant deviation is observed in angles  $20^{\circ}$  to  $150^{\circ}$  due to the fact that cylinder pressure during and after the combustion is significant different. According to equations described in chapter 2 section 2.9, the force developed by the piston movement is the difference of pressures (the one applied below the piston equal to the compressed air and the gas pressure inside the engine cylinder multiplied with the area of the piston). This difference of gas pressure entrains the force and therefore the piston developed torque.

Fig. 4-42 presents the trapped mass inside the engine cylinder in one cycle and also it shows the change of equivalence ratio,  $\Phi$ , in one cycle.



**Fig. 4-42 Cylinder trapped mass (top) and equivalence ratio (50%)**

As it is seen in Fig. 4-42, the equivalence ratio inside the cylinder shows a decreased value of 0.17 as compared to MoTher, due to the fact that different temperature is measured inside the engine cylinder. This deviation in temperature has resulted in different mixture phenomenon inside cylinder volume (Fig. 4-42). Different equivalent ratio changes the whole parameters of the system.

Combustion constants greatly affect simulation results. The sets of the constants that affected the Simulink model are shown in Table 4-16. Only the results of the last three sets are presented in Fig. 4-43 and in Fig. 4-39. Fig. 4-43 shows that although maximum pressure remains the same for set 7 and set 8, the temperature trace has great deviation among the various sets and MoTher.

On the other hand, when adjusting the S curve parameters (set 2, 3 and 5) it was observed that  $P_{max}$  value and the shape of pressure trace changed (not shown here). In

addition, when adjusting the constants to set 4, the temperature was found greater than MoTher while the pressure trace was the same with the one of MoTher.

This deviation of traces, allows considering that a more complex and fine tuned combustion model, could converge towards the results of MoTher.

Table 4-16 Constant sets for combustion model

Variables <sup>4</sup>	Cases							
	Set 1	Set 2	Set 3	Set 4	Set 5	Set 6	Set 7	Set 8
$a_r$	0	0	4	2	2	-0.5	4	4
$a_s$	8	11	8.41	8	8	2.41	8.4	4
$C_1$	3	2.8	600	120	280	3.8	500	6
$C_2$	1	1	5	5	5	1	5	1

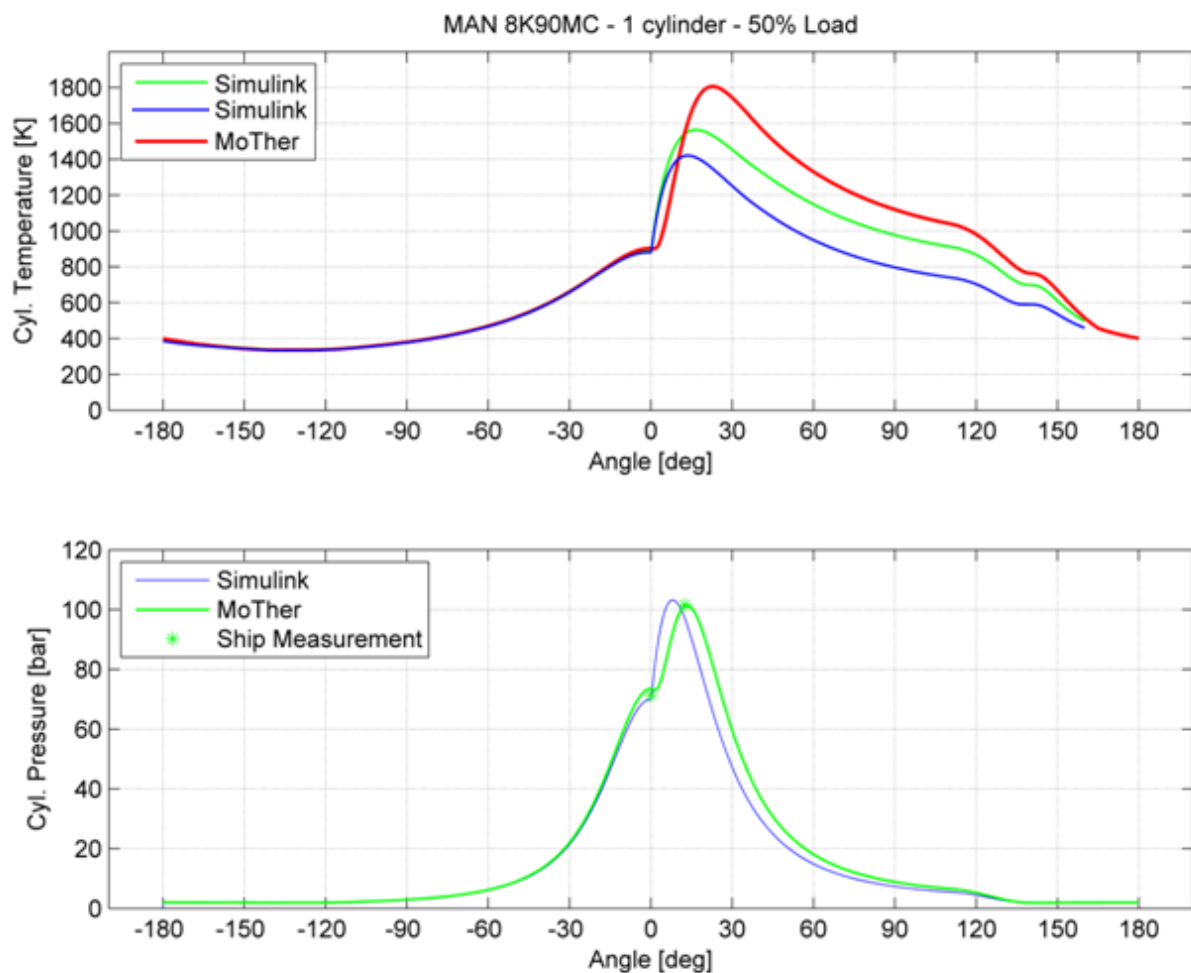


Fig. 4-43 Temperature (top) and pressure traces for different combustion parameters

<sup>4</sup> See section 2.7

### Parametric runs for 75% load at 94.6 RPM

Parametric simulations were run at 75% load. In the first set of parameters, values like,  $S$  – curve constants, start and duration of combustion that change the fuel burning rate, were tested (Table 4-17). In the other two simulations that were performed (case 1 and 2), the injected percent of fuel was changed while the other constant values were kept constant. In the final simulation (case 3 and 4), the injected fuel and combustion elements remained constant and the clearance volume was changed. Table 4-17 presents the sets of factors that change the simulated model.

Table 4-17 Constant values for parametric runs at 75% load

Variables	Cases		
	Case 1	Case 2	Case 3
$a_r$	0	2	4
$C_1$	30	26.7	15.6
$C_2$	2.7	2	2

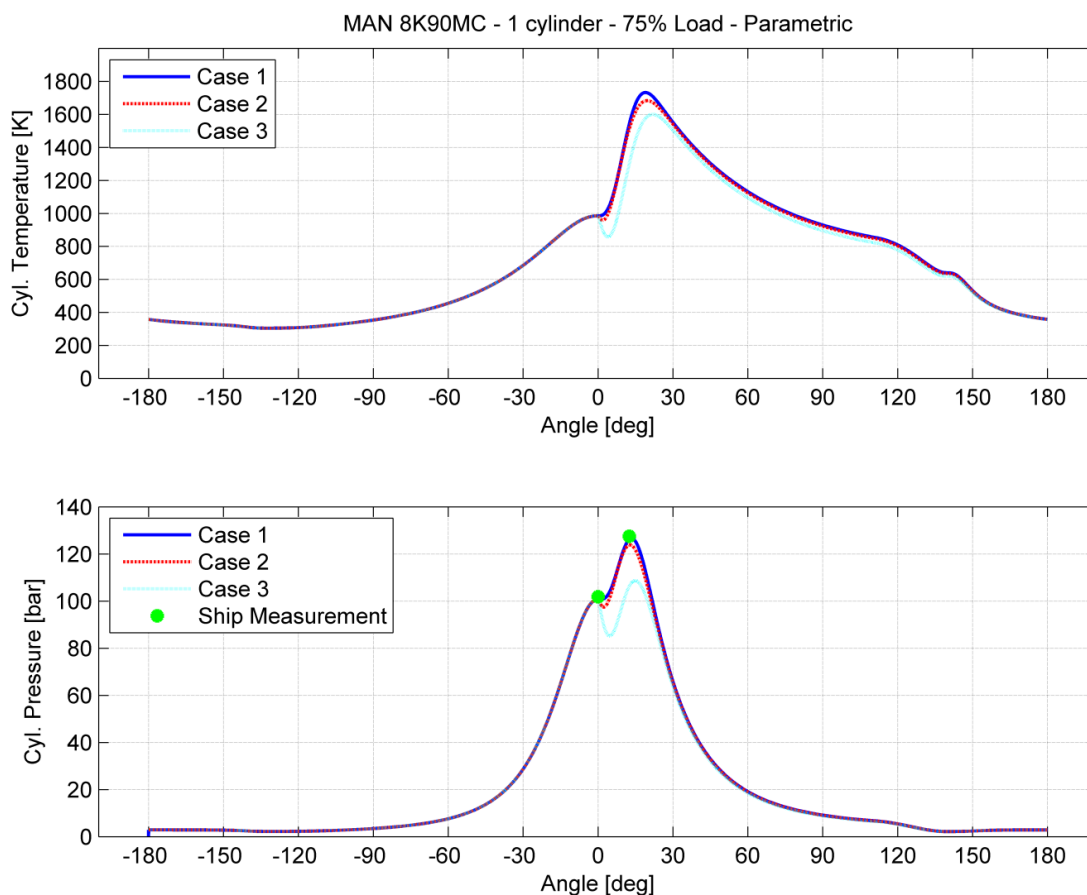
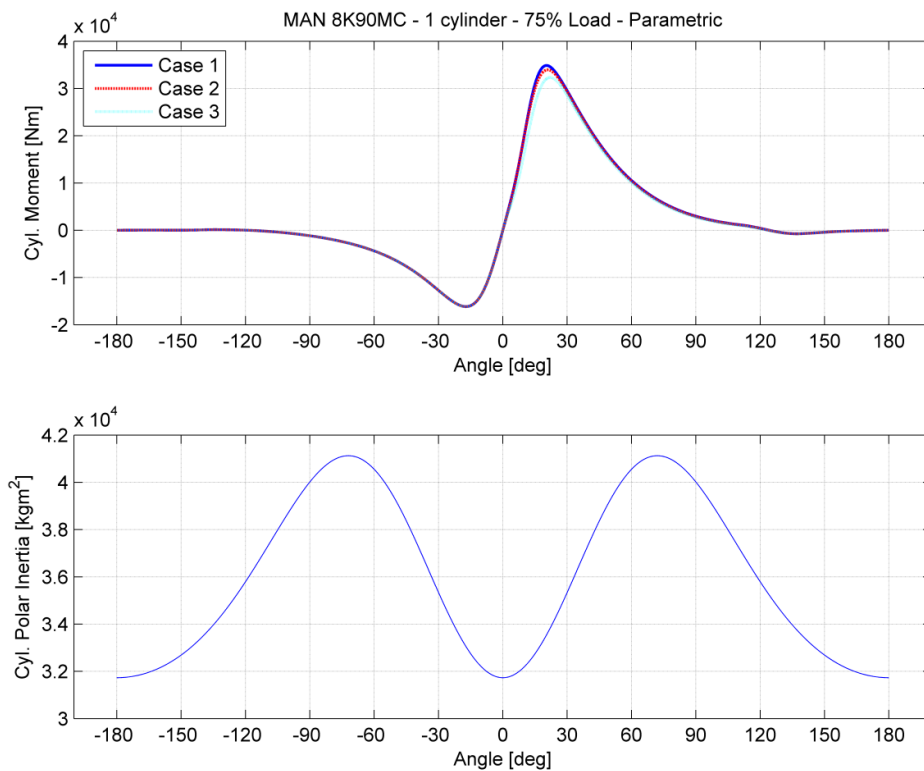


Fig. 4-44 Temperature (top), pressure traces for different combustion constants

Fig. 4-44 shows temperature and pressure traces for different  $S$  - curve constants but also for different start angle of combustion. As it is shown, for the  $4^\circ$  degrees start of combustion, the piston is moved significantly from the top dead center and occurred to a

non negligible pressure drop (case 3). As a result, the cylinder cannot achieve the maximum pressure per cycle. The trace for case 2 is almost the same as with case 1 but again cylinder cannot achieve the maximum pressure. This is a significant error in the burning process and consequently the torque developed per cycle is less than in case 1. This difference is shown in Fig. 4-45. Fig. 4-46 shows the torque traces per cycle in greater detail.

While the different cases change the already mentioned traces, the traces of mass flow from inlet port and from exhaust valve slightly change (Fig. 4-45 and Fig. 4-46) This can be explained by the fact that in gas exchange period the pressure trace is almost the same for all the cases while the total trapped mass inside the cylinder has a small deviation.



**Fig. 4-45 Torque developed per cycle (top) and moment of inertia**



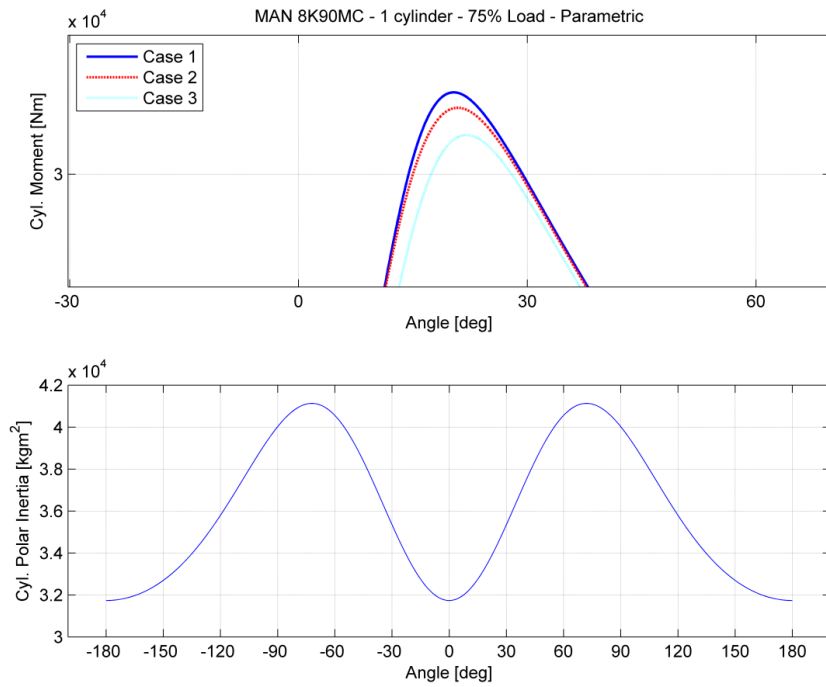


**Fig. 4-46 greater detail (top) of figure Fig. 4-45**

This can be explained due to the fact that mass is added to the system from the openings, as mentioned in chapter 2 section 2.3, pressure difference is responsible for the mass flow through a restriction. If this difference is almost zero between the three cases in the same periods, no great difference can be observed. This slight difference can be observed in Fig. 4-49. It must be taken into account that same amount of fuel is injected per cycle.

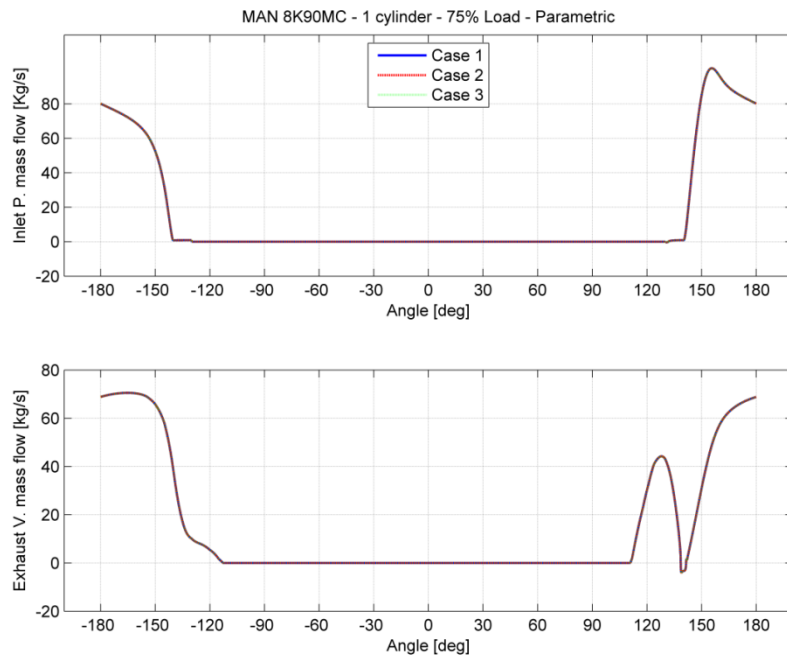


**Fig. 4-47 Mass flow from inlet port (top) and exhaust valve**

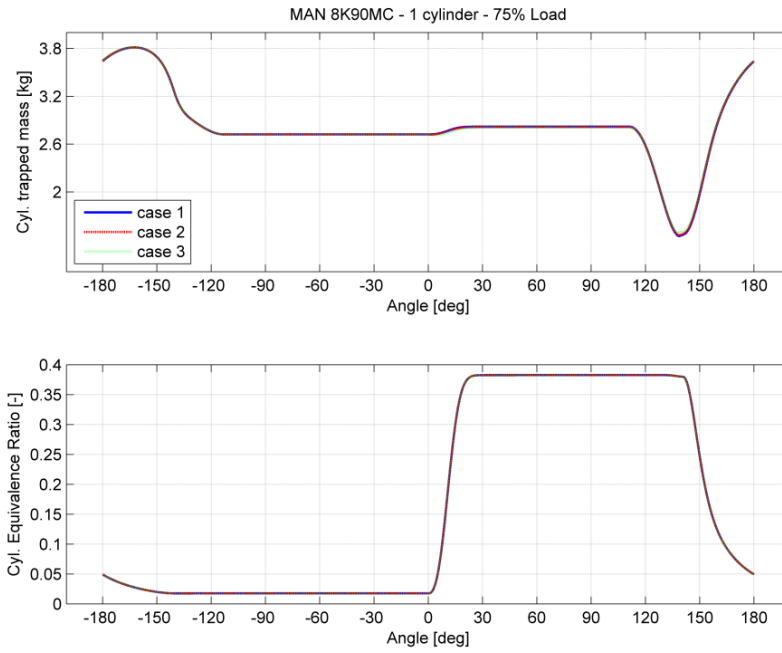


**Fig. 4-48 Trapped mass inside cylinder (top) and equivalence ratio**

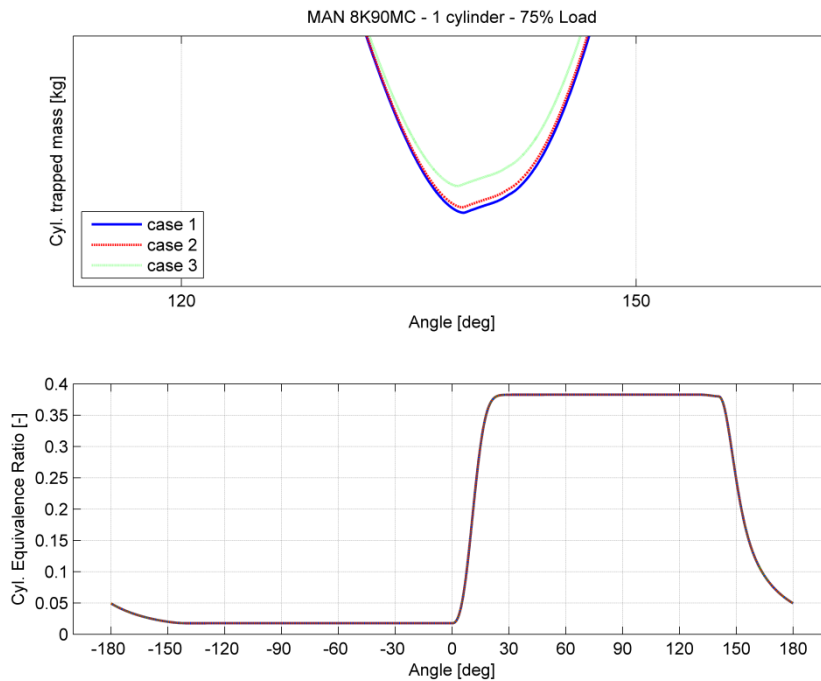


**Fig. 4-49 Details of Fig. 4-48 (top) and equivalence ratio**

Finally, for case 1 and 2, the mass of fuel modified. The data are presented in Table 4-18. For the cases 3 and 4, the clearance volume of the cylinder was modified. The data are presented in Table 4-19.

Table 4-18 Combustion constants and fuel injected per cycle

Variables	Cases	
	Case 1	Case 2
$a_r$	0	0
$C_1$	30	30
$C_2$	2.7	2.7
Mass of fuel	0.090	0.102

Table 4-19 Combustion constants and clearance volume of cylinder

Variables	Cases	
	Case 3	Case 4
$a_r$	0	0
$C_1$	30	30
$C_2$	2.7	2.7
Clearance Volume	0.089	0.093

Comparison is made for pressure and temperature traces for the two set of cases.

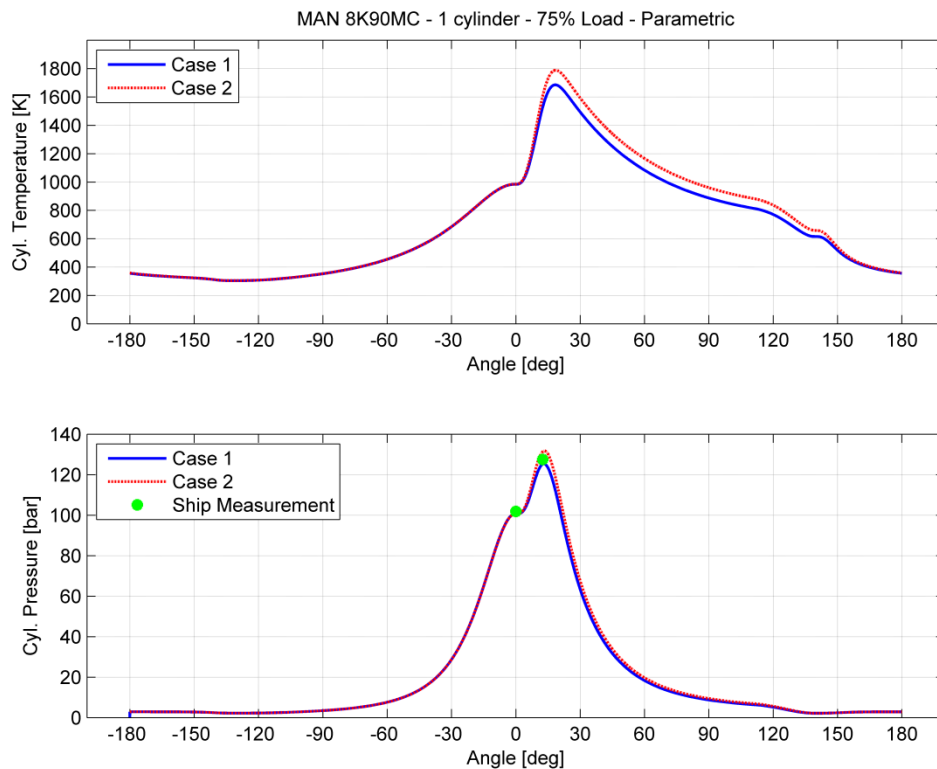


Fig. 4-50 Temperature (top) and pressure trace for one cylinder, for different values of injected fuel

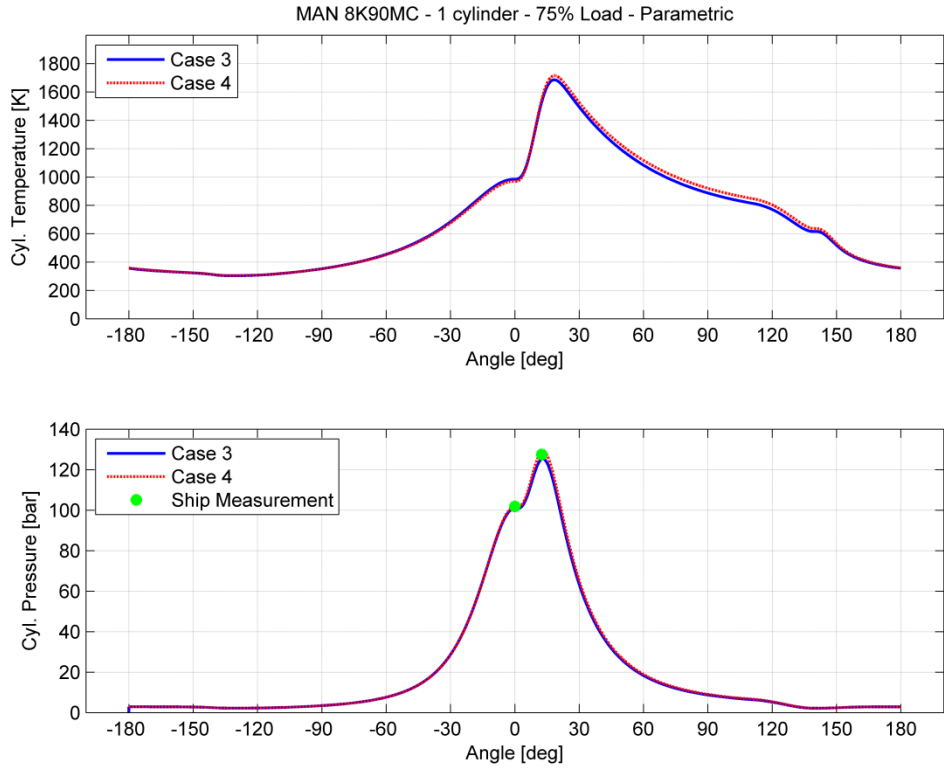


Fig. 4-51 Temperature (top) and pressure trace for one cylinder, for different values of clearance volume

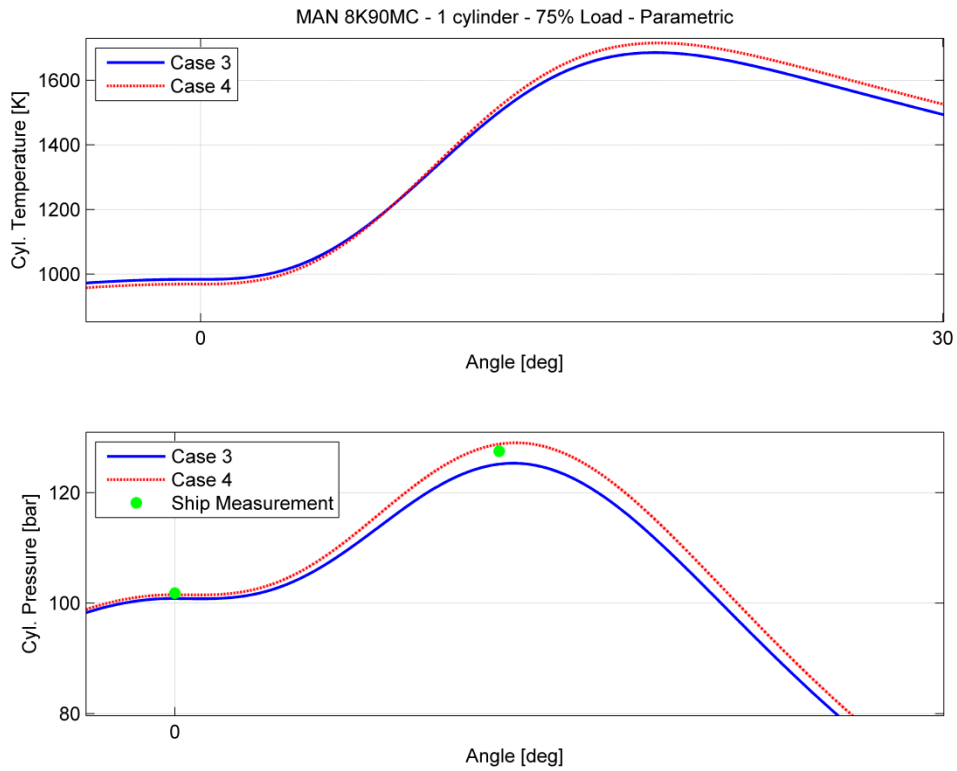


Fig. 4-52 greater detail of Fig. 4-51

As shown in Fig. 4-50, the compression pressure trace is the same for case 1 and in case 2. Due to the fact that more fuel is injected per cycle and combustion constants were kept the same, maximum pressure in case two is greater than in case one. This can be explained by the fact that burning fuel rate is different and as more fuel is injected more energy is released and this results in temperature and pressure increase while the volume change rate is the same in every case.

As shown in Fig. 4-51, the compression pressure trace changes, due to the fact that clearance volume is less than the original in case 3 and greater in case 4. As a result, having same trapped mass inside cylinder's clearance volume, pressure and temperature is less than the original when clearance volume is greater than the original and greater when the clearance volume is less than the original. This example shows the advantages of the simulation platform; the easy modification of engine parameters, during a parametric run which will allow for conclusions on the sensitivity of the tuning of certain operating variables.

## 5 Conclusions

This thesis attempts to illustrate a method for implementing a modular simulation of a marine propulsion installation. According to this concept, the approach was to create a library with scalable and extendable building blocks with an easy and well defined interface between the various sub - blocks of the model.

The essential governing thermodynamic equations of the whole engine were implemented. The basic engine configuration of one – cylinder in closed loop configuration was eventually simulated.

In the simulation tests, various numerical integration methods were used, like Euler, Heun, Runge - Kutta 4<sup>th</sup> order and Dorman Prince, with variable and fixed step integration. Variable step integration methods are not suitable for simulation of quasi steady engine models. The results obtained from the first two methods introduced significant errors, while Runge - Kutta 4<sup>th</sup> order method with 0.002 second time step, produced better results than the others but not a stable solution. In order to find the proper time step for the simulation, a wide range of values was tested. Using steps equal to 0.002 seconds, spikes were observed and very high or very low peaks caused the simulation to fail several times. Finally, based on observations of the unsteady simulation occurred by the wrong integration time step, it was found that time a step of 0.0001 second is optimum for simulation with the Runge - Kutta 4<sup>th</sup> order method, in the MATLAB/Simulink platform.

This text is intended to introduce a new simulation package to simulate marine propulsion installations with an easily extendable manner with adequate accuracy. A lot of work is required to be done, in order to simulate a complete engine model. Also mathematical models for the blocks already presented in this thesis can be introduced. For example a more complex combustion model like Woschni - Ansits or a multi zone injection system can be implement and inserted to the block library, so that a wide variety of internal combustion engines can be modeled.

## 6 References

- Borman, G. L., & Krieger, R. B. (1966). The computation of Apparent Heat Release for Internal Combustion Engines. *American Society of Mechanical Engineers (ASME), 66WA/DPG-11* .
- Dabney, J. B., & Harman, T. L. (2004). *Mastering Simulink*. Upper Saddle River, NJ 0745: Pearson Prentice Hall.
- Gunter, M. P., Schwarz, C., Stiesch, G., & Otto, F. (2006). *Simulating Combustion*. Berlin: Springer.
- Heywood, J. B. (1988). *Internal Combustion Engine Fundamentals*. Massachusetts U.S.A.: MacGraw-Hill.
- Kyrtatos, N. (1993). *Marine Diesel Engines*. Athens: Simetria.
- Lambropoulos, V. P. (2000, March). Modular Simulation of Marine Propulsion Systems. *Ph.D. Thesis* . Athens.
- LME. (2008). Motor Thermodynamics Users Manual version 1.7. Athens, Greece.
- Mathworks. (2002). Building an S - Function. Mathworks Inc.
- Metz, J., Urben, A., & Steiger, A. (1967). Determination of Woschni Coefficients. *IMechE Vol 182* , pp. 89-90.
- Newhall, H. K., & Starkman, E. S. (1963). Thermodynamic Properties of Octane and Air for Engine Performance. *SAE Technical Paper Series 633G* .
- Watson, N., & Janota, M. (1982). *Turbocharging the internal combustion engines*. London: Macmillan.

## Appendices



## — Appendix A

In this appendix MATLAB® code is presented that implements the mathematical equations of chapter 2. Table 0-1 contains the functions used.

**Table 0-1 Developed S - Functions**

Name of Block:	Function Name:
<b>Gas Properties</b>	sfun_13cgas(t,x,u,flag) sfun_1c(t,x,u,flag)
<b>Open Thermodynamic System</b>	OTS_cylinder1_50(t,x,u,flag)
<b>Valve</b>	sfun_2test3(t,x,u,flag)
<b>Compressor</b>	sfunctioncompr1(t,x,u,flag) sfunctioncompr2(t,x,u,flag,TCTREF)
<b>Intercooler</b>	sfunctionintercooler(t,x,u,flag)
<b>Turbine</b>	sfunctionturl1(t,x,u,flag) sfunctionturb2(t,x,u,flag) sfunctionturb3(t,x,u,flag)
<b>Conduction</b>	sfun_061(t,x,u,flag)
<b>Convection</b>	sfun_062(t,x,u,flag)
<b>Radiation</b>	sfun_063(t,x,u,flag)
<b>Combustion (S – Curve)</b>	sfun_05_1(t,x,u,flag)
<b>Cylinder Geometry</b>	sfun_3(t,x,u,flag)
<b>Geometrical Energy Loss</b>	sfun_4(t,x,u,flag)

### *Gas Properties*

```
function [sys,x0,str,ts] = sfun_13cgas(t,x,u,flag)

sizes.NumContStates = 0;
sizes.NumDiscStates = 0;
sizes.NumOutputs    = 8;
sizes.NumInputs     = 3;
sizes.DirFeedthrough = 1;
sizes.NumSampleTimes = 1;

function sys=mdlOutputs(t,x,u)

T=u(1);
fi=u(3);
p=u(2)/10^5;

% Values for R0 and U0 according to Krieger Borman

R0=0.287-0.02*fi;
k1=0.692*T+(39.17*10^-6*T^2)+(52.9*10^-9*T^3)-(228.62*10^-13*T^4)+(227.58*10^-17*T^5);
k2=3049.39-(5.7*10^-2)*T-(9.5*10^-5*T^2)+(21.53*10^-9*T^3)-(200.26*10^-14*T^4);
U0=k1-k2*fi;

if (T<=1333 && fi<1.0) % Dissociation effect negligible
```

```

k1=(0.692*T)+((39.17*10^-6)*T^2)+((52.9*10^-9)*T^3)-((228.62*10^-
13)*T^4)...
+((227.58*10^-17)*T^5);

k2=3049.39-(5.7*10^-2)*T-((9.5*10^-5)*T^2)+((21.53*10^-9)*T^3)...
-(200.26*10^-14)*T^4;

y1=(k1-k2*fi)*10^3;      %U J/kg
%y1=k1-k2*fi;          %U kJ/kg

%θu/θT
y2=-fi*((-5.7*10^-2)-((2*9.5*10^-5)*T)+((3*21.53*10^-9)*T^2)...
-((4*200.26*10^-14)*T^3))+0.692+(2*39.17*10^-
6)*T)+((3*52.9*10^-9)*T^2)...
-((4*228.62*10^-13)*T^3)+((5*277.58*10^-17)*T^4);
%θu/θp
y3=0;

%θu/θφ
y4=-k2;

% R
y5=(0.287-0.02*fi)*10^3; %R J/kg*K
%y5=0.287-0.02*fi; % R kJ/kg*K

%θP/θT
y6=0;

%θP/θp
y7=0;

%θP/θφ
y8=-0.02;

end
if (T>1333 && fi<1.0) % Dissociation effect not negligible

% U and U partial derivatives approximation:

C1=10.41066+7.85125*fi-3.71257*fi^3;
C2=(-27.00107-28.5087*fi+17.30375*fi^3)*1800/T;
C3=((0.154226*fi^3)-(0.38656*fi)-0.10329+(0.21289*fi-
0.026574)*1800/T)*log(14.5*p);

C=C1+C2+C3;

C1_dotT=0;
C2_dotT=-(-27.00107-(28.5087*fi)+(17.30375*fi^3))*1800/(T^2);
C3_dotT=-((0.21289*fi-0.026574)*1800/T^2)*log(14.5*p);

C_dotT=C1_dotT+C2_dotT+C3_dotT;

y2=((-fi*((-5.7*10^-2)-((2*9.5*10^-5)*T)+((3*21.53*10^-
9)*T^2)...
-((4*200.26*10^-14)*T^3))+0.692+(2*39.17*10^-
6)*T)+((3*52.9*10^-9)*T^2)...
-((4*228.62*10^-13)*T^3)+((5*277.58*10^-
17)*T^4))+2.326*(C_dotT)*exp(C);

```

```

C1_dotp=0;
C2_dotp=0;
C3_dotp=(0.154226*fi^3-0.38656*fi-0.10329+(0.21289*fi-
0.026574)*1800/T)*((1/(14.5*p))*14.5);
C_dotp=C1_dotp+C2_dotp+C3_dotp;

y3=(0+2.326*(C_dotp)*exp(C));

C1_dotfi=7.85125-3*3.71257*fi^2;
C2_dotfi=(-28.5087+3*17.30375*fi^2)*1800/T;
C3_dotfi=(3*0.154226*fi^2-
0.38656+(0.21289)*1800/T)*log(14.5*p);

C_dotfi= C1_dotfi+ C2_dotfi+ C3_dotfi;

y4=(-(3049.39-(5.7*10^-2)*T-((9.5*10^-5)*T^2)+(21.53*10^-
9)*T^3)...
-(200.26*10^-14)*T^4)+2.326*(C_dotfi)*exp(C));

y1=(U0+2.326*exp(C))*10^3;

% R and R partial derivatives approximation:

A=(11.98-45.796*(1800/T)-
0.4354*log(14.5*p))*fi+0.2977*log(fi);

y5=(R0*10^3+4.1868*exp(A));

A_dotT=(45.796*(1800/T^2))*fi;
A_dotP=(-14.5*0.4354*(1/(14.5*p)))*fi;
A_dotfi=(11.98-45.796*(1800/T)-
0.4354*log(14.5*p))+0.2977*(1/fi);

y6=10^-3*(0+4.1868*A_dotT*exp(A));

y7=10^-3*(0+4.1868*A_dotP*exp(A));

y8=10^-3*(-0.02*10^3+4.1868*A_dotfi*exp(A));

end
if (T<1333 && fi>1.0)
y1=(-2888.78+595.25*(fi-1)+0.66854*T+2.71304*10^-4*T^2-
7.40325*10^-8*T^3+0.25107*(fi-1)*T)*10^3;
y2=0.66854+2*2.71304*10^-4*T-3*7.40325*10^-8*T^2+0.25107*(fi-
1);
y3=0;
y4=595.25+0.25107*T;

y6=0;
y7=0;
y8=0.063438+2*(-3.33005*10^-3)*fi;
y5=(0.22751+0.063438*fi-3.33005*10^-3*fi^2)*10^3;
end
if (T>1333 && fi>1.1)

```

```

        y1=(-3466.2+903.84*(fi-1)+0.65898*T-3.79924*10^-4*T^2-
8.23288*10^-8*T^3)*10^3;
        y2=0.65898-2*3.79924*10^-4*T-3*8.23288*10^-8*T^2;
        y3=0;
        y4=903.84;
        y6=0;
        y7=0;
        y8=0.063438+2*(-3.33005*10^-3)*fi;
        y5=(0.22751+0.063438*fi-3.33005*10^-3*fi^2)*10^3;
end
if(T>1333 && fi<1.1 && 1.0<fi)
    uu1=-3466.2+903.84*(fi-1)+0.65898*T-3.79924*10^-4*T^2-
8.23288*10^-8*T^3;
    y1=(uu1+14.2029*((T-1388.89)^4.5371))*((11-
10*fi)/p^0.46024))*10^3;
    y2=0.65898-2*3.79924*10^-4*T-
3*8.23288*10^-8*T^2+...
    14.2029*4.5371*((T-1388.89)^(4.5371-1));
y3=(-14.2029*((T-1388.89)^4.5371))*((11-10*fi))^0.46024*p^(0.46024-
1))/(p^(2*0.46024));
    y4=14.2029*((T-1388.89)^4.5371)*(-10)/(p^0.46024);
    y6=0;
    y7=0;
    y8=0.063438+2*(-3.33005*10^-3)*fi;
    y5=(0.22751+0.063438*fi-3.33005*10^-3*fi^2)*10^3;
end

```

end

```
sys = [y1, y2, y3, y4, y5, y6, y7, y8]; % muxed outputs
```

```
function [sys,x0,str,ts] = sfun_1c(t,x,u,flag)
```

```

sizes.NumContStates = 0;
sizes.NumDiscStates = 0;
sizes.NumOutputs    = 6;
sizes.NumInputs     = 8;
sizes.DirFeedthrough = 1;
sizes.NumSampleTimes = 1;

```

```
function sys=mdlOutputs(t,x,u)
```

```

y1=(u(3)/((1-u(4))^2*u(6))); %fi_dot
y2=(u(4)/((1-u(4))*u(6))); %fi
miair=3.3*10^-7*u(8)^0.7; %miair calculation
y3=miair/(1+0.027*y2); %Isentropic Coefficient
y6=u(1)+u(2)*u(8)+u(7); %Cp Calculation
y4=y6/u(1); %gamma calculation
y5=((9*y4-5)/4)*y3*u(1); %k calculation

```

```
sys = [y1, y2, y3, y4, y5, y6]; % muxed outputs
```

### Open Thermodynamic System

```
function [sys,x0,str,ts] = OTS_cylinder1_50(t,x,u,flag)
```

```

sizes.NumContStates = 2;
sizes.NumDiscStates = 0;
sizes.NumOutputs    = 4;

```

```

sizes.NumInputs      = 24;
sizes.DirFeedthrough = 1;
sizes.NumSampleTimes = 1;

function sys=mdlDerivatives(t,x,u)

A=1-(x(2)/u(5))*u(7);
B=(1/x(1))+(1/u(5))*u(6);
C=(1/u(5))*u(8)*u(9)+(1/u(20))*u(18)-(1/u(21))*u(22);
D=u(16)-(x(2)*u(22))+u(17); %not u(15), correction: 10/7/2009

arithmitis=((D-u(1)*u(18))/u(20))-(u(3)*(C/A)*x(2))-u(4)*u(9);

paronomastis=u(2)+u(3)*(B/A)*x(2);

y1=arithmitis/paronomastis; % Temperature Dot Calculation
y2=(B*y1+C)*x(2)/A;         %Pressure Dot Calculation
sys = [y1,y2];
function sys=mdlOutputs(t,x,u)
mps=2*(100.5/60)*2.3; %mean piston speed 2*n*stroke
%reference values taken from MOTHER
Vd=2.3*pi*(0.9^2)/4; %cylinders volume m^3
Tr=365.081;          %Kelvin
pr=3.68502*10^2;     %Kpa
Vr=1.22489;          %m^3
pm=14.5*10^2;        %Kpa
%Paddle=3.33;
if (0.5575<u(25) && u(25)<=2.3)
    %gas exchange period
    C1=6.18;
    C2=0;
    %    C3=0.417;
end
if (0<=u(25) && u(25)<0.2870) %0.2875
    %combustion period
    C1=2.28;
    C2=3.24*10^-3;
    C3=0.308;
end
if (0.2870<=u(25) && u(25)<=0.5575)
    %compression period
    C1=2.28;
    C2=0;
    %    C3=0.308;
end

%w=C1*mps+C3*Paddle+C2*(Vd*Tr/(pr*Vr))* (x(2)-pm);
w=C1*mps+C2*(Vd*Tr/(pr*Vr))* (x(2)-pm);
r=u(20)/u(21); %Density
y3=r*w*u(23)/u(10); %Reynolds

Cp=u(6)*x(1)+u(2)+u(5); %Cp calculation
y4=Cp*u(10)/u(12); %Prandtl

sys = [x(1), x(2), y3, y4]; % muxed outputs

```

*Valve*

```

function [sys,x0,str,ts] = sfun_2test3(t,x,u,flag)
sizes.NumContStates = 0;
sizes.NumDiscStates = 0;
sizes.NumOutputs = 6;
sizes.NumInputs = 10;
sizes.DirFeedthrough = 1;
sizes.NumSampleTimes = 1;

function sys=mdlOutputs(t,x,u)

Pcr=u(2)*(2/(u(5)+1))^(u(5)/(u(5)-1));
% Downstream mass flow calculation

if (u(3)<=Pcr) %Subsonic Flow, subsonic when the pressure is less
than the Pcr

%MOTHER
y1=u(9)*u(2)*sqrt((u(5)/(u(4)*u(1)))*((2/(u(5)+1))^(u(5)+1)/(u(5)-
1))));
end

if (u(3)>Pcr) % sonic flow or ultrasonic

%MoTher mass flow calculation
K1=u(9)*u(2);
K2=(2*u(5)/((u(5)-1)*u(4)*u(1)));
K3=(u(3)/u(2))^(2/u(5));
K4=(u(3)/u(2))^(u(5)+1)/u(5);
y1=K1*sqrt(K2*(K3-K4));

end

h=u(6)+u(4)*u(1); %h calculation
y2=(h*y1+u(10)); %Downstream Enthalpy flow
y3=-h*y1; %Upstream Enthalpy flow
y4=-y1; %Upstream mass Flow
y5=0; %Upstream sp_bm_dot_Capital
y6=y1*(u(7)-u(8)); %Downstream bm_dot_Capital
%y6=y1*(u(7)-0); %Downstream bm_dot_Capital

sys = [y1, y2, y3, y4, y5, y6]; % muxed outputs

function [sys,x0,str,ts] = sfun_2a(t,x,u,flag)
sizes.NumContStates = 0;
sizes.NumDiscStates = 0;
sizes.NumOutputs = 2;
sizes.NumInputs = 6;
sizes.DirFeedthrough = 1;
sizes.NumSampleTimes = 1;

function sys=mdlOutputs(t,x,u)

y1=(2*u(1))/(u(2)*sqrt(pi*u(6)));
Cp=(u(3)*u(5))/(u(3)-1);
y2=Cp*u(2)/u(4);

```

### Compressor

```
function [sys,x0,str,ts] = sfunctioncompr1(t,x,u,flag)
sizes.NumContStates = 0;
sizes.NumDiscStates = 0;
sizes.NumOutputs    = 5;
sizes.NumInputs     = 13;
sizes.DirFeedthrough = 1;
sizes.NumSampleTimes = 1;

function sys=mdlOutputs(t,x,u)

Cp=(u(2)*u(4)/(u(4)-1));
y1=Cp*u(6)/u(7); %Prandtl Number Calculation
y2=u(10)*4/(pi*u(11)*u(6)); %Reynolds Number Calculation
y3=u(3)+(u(2)*u(1)); % Specific Enthalpy Calculation
y4=u(10)*(u(5)-u(9)); % Specific Burned Fuel Mass Calc.
y5=u(10)*Cp*u(12)/(2*pi*u(13)); % Moment Calculation OK

sys = [y1,y2,y3,y4,y5]; % muxed outputs
```

```
function [sys,x0,str,ts] = sfunctioncompr2(t,x,u,flag,TCTREF)
sizes.NumContStates = 0;
sizes.NumDiscStates = 0;
sizes.NumOutputs    = 4;
sizes.NumInputs     = 8;
sizes.DirFeedthrough = 1;
sizes.NumSampleTimes = 1;
```

```
function sys=mdlOutputs(t,x,u)
```

```
function sys=mdlOutputs(t,x,u,TCTREF)
```

```
y1=(u(1)/u(6))*(((u(8)/u(2))^(u(4)-1)/u(4)))-1; %Actual
Temperature increase Calculation
y2=u(1)+y1/2; %Mean Temperature Calculation
To2=u(1)+y1; %Actual Stagnation Temp.
UpsteamCalculation
y3=u(5)+u(3)*To2; %Specific enthalpy Calculation
%y4=u(7)*sqrt(u(1)); % a_dot for map Calculation
y4=u(7)*60*sqrt(TCTREF/u(1)); %RPS----> RPMcorrected
sys = [y1,y2,y3,y4]; % muxed outputs
```

### Intercooler

```
function [sys,x0,str,ts] = sfunctionintercooler(t,x,u,flag)
sizes.NumContStates = 0;
sizes.NumDiscStates = 0;
sizes.NumOutputs    = 4;
sizes.NumInputs     = 8;
sizes.DirFeedthrough = 1;
sizes.NumSampleTimes = 1;
```

```

function sys=mdlOutputs(t,x,u)
%1 is the OUTPUT and 2 is the INPUT
T1=(u(7)*u(8)-u(4))/(u(7)-1);
y1=u(1)/(u(2)*T1);
Cp=(u(5)/(u(5)-1))*u(2);
Cv=Cp/u(5);
y2=u(3)+Cv*(T1-u(4));
y3=T1;
y4=u(6)*Cp*(T1-u(4));
sys = [y1,y2,y3,y4]; % muxed outputs

```

### Turbine

```

function [sys,x0,str,ts] = sfunctionturl(t,x,u,flag)
sizes.NumContStates = 0;
sizes.NumDiscStates = 0;
sizes.NumOutputs = 6;
sizes.NumInputs = 13;
sizes.DirFeedthrough = 1;
sizes.NumSampleTimes = 1;

```

```

function sys=mdlOutputs(t,x,u)

Cp=(u(4)*u(2)/(u(4)-1)); %Cp Calculation
y1=Cp*u(6)/u(7); %Prandtl Number Calculation
y2=u(10)*4/(pi*u(11)*u(6)); %Reynolds Number Calculation
y3=u(3)+(u(2)*u(1)); % Specific Enthalpy Calculation
y4=u(10)*(u(5)-u(9)); % Specific Burned Fuel Mass
Calculation
y5=u(10)*Cp*u(12)/(2*pi*u(13)); % Moment Calculation
y6=Cp;
sys = [y1,y2,y3,y4,y5,y6]; % muxed outputs

```

```

function [sys,x0,str,ts] = sfunctionturb2(t,x,u,flag)
sizes.NumContStates = 0;
sizes.NumDiscStates = 0;
sizes.NumOutputs = 5;
sizes.NumInputs = 14;
sizes.DirFeedthrough = 1;
sizes.NumSampleTimes = 1;

```

```

function sys=mdlOutputs(t,x,u)

% $\dot{m}=u(12)*(u(2)/\sqrt{u(1)})$ ;
m_dot=u(12); %Already Corrected mass flow
ud=(m_dot*u(3)*u(9))/(u(11)*u(8));
y1=u(13)*u(10); %Actual Temperature increase
 $\Delta T_{oa}$  OK
To2=u(1)-y1;
T2=To2-((ud^2)/(2*u(6)));
y2=u(1)+((u(1)-T2)/2); %Mean Temperature
Ts2=u(1)*(u(2)/u(8))^(1-u(4)/u(4));
DTois=u(1)-Ts2;
y5=pi*u(14)*u(7)/sqrt(2*u(6)*DTois); %U/C
ho2=u(5)+u(3)*To2; %Stagnation specific Enthalpy
OK

```



```

y4=m_dot;
y3=m_dot*ho2; % Stagnation Enthalpy change
Rate OK
sys = [y1,y2,y3,y4,y5]; % muxed outputs

function [sys,x0,str,ts] = sfunctionturb3(t,x,u,flag)
sizes.NumContStates = 0;
sizes.NumDiscStates = 0;
sizes.NumOutputs = 3;
sizes.NumInputs = 9;
sizes.DirFeedthrough = 1;
sizes.NumSampleTimes = 1;

function sys=mdlOutputs(t,x,u)

m_dot=u(8)*(u(2)/sqrt(u(1)));

DToi=u(1)*(1-(u(2)/u(7))^(1-u(4)/u(4)));
y3=u(9)*DToi; %Actual Temperature increase
To2=u(1)-y3;
ud=(m_dot*u(3)*To2)/(u(5)*u(7));
T2=To2-((ud^2)/(2*u(6)));
y1=u(7)*(T2/To2)^(u(4)/(u(4)-1)); %Pressure 2
y2=T2; %Downstream static Temperature

sys = [y1,y2,y3]; % muxed outputs

```

### **Conduction**

```

function [sys,x0,str,ts] = sfun_061(t,x,u,flag)
sizes.NumContStates = 0;
sizes.NumDiscStates = 0;
sizes.NumOutputs = 2;
sizes.NumInputs = 7;
sizes.DirFeedthrough = 1;
sizes.NumSampleTimes = 1;

function sys=mdlOutputs(t,x,u)
L=u(2)*u(3)*u(7)*u(4)/(u(2)*u(3)+u(7)*u(4));
Tc=(u(2)*u(3)*u(1)+u(7)*u(4)*u(6))/(u(2)*u(3)+u(7)*u(4));

%y1=u(2)*u(3)*u(5)*(Tc-u(1)); % equation 5.14 flow from 2 to 1
% Alternatly
y1=L*u(5)*(u(6)-u(1));
y2=-y1;
sys = [y1, y2]; % muxed outputs

```

### **Convection**

```

function [sys,x0,str,ts] = sfun_062(t,x,u,flag)
sizes.NumContStates = 0;
sizes.NumDiscStates = 0;
sizes.NumOutputs = 2;
sizes.NumInputs = 12;
sizes.DirFeedthrough = 1;

```

```
sizes.NumSampleTimes = 1;
```

```
function sys=mdlOutputs(t,x,u)
```

```
%k1=ks and k2=kf
```

```
Nu=u(5)*(u(11)^(u(6)))*(u(12)^(u(7)));  
h=Nu*u(10)/u(8);  
L=u(2)*u(3)*h/(u(2)*u(3)+h);  
Tc=(u(2)*u(3)*u(1)+h*u(9))/(u(2)*u(3)+h);
```

```
%y1=h*u(4)*(u(9)-Tc); % equation 5.18 flow from 2 to 1  
%y1=h*u(4)*(Tc-u(1)); % equation 5.18 flow from 2 to 1  
% Alternately  
y1=L*u(4)*(u(9)-u(1));  
y2=-y1;  
sys = [y1, y2]; % muxed outputs
```

### ***Radiation***

```
function [sys,x0,str,ts] = sfun_063(t,x,u,flag)
```

```
sizes.NumContStates = 0;  
sizes.NumDiscStates = 0;  
sizes.NumOutputs = 2;  
sizes.NumInputs = 7;  
sizes.DirFeedthrough = 1;  
sizes.NumSampleTimes = 1;
```

```
function sys=mdlOutputs(t,x,u)
```

```
% Stephan Boltzman Law for energy radiation  
% si is stephans boltzman's constant  
si=5.6697*10^-8; % Watt/K^4*m^2  
Eb=si*((u(1)^4)-(u(6)^4)); % from 1 to 2 else u(6)^4-u(1)^4  
c1=(1-u(7))/(u(7)*u(5));  
c2=(1-u(2))/(u(2)*u(4));  
c3= 1/(u(4)*u(3));  
  
y1=Eb/(c1+c2+c3);  
y2=-y1;  
  
sys = [y1, y2]; % muxed outputs
```

### ***Combustion (S - Curve)***

```
function [sys,x0,str,ts] = sfun_05_1(t,x,u,flag)
```

```
sizes.NumContStates = 0;  
sizes.NumDiscStates = 0;  
sizes.NumOutputs = 6;  
sizes.NumInputs = 11;  
sizes.DirFeedthrough = 1;  
sizes.NumSampleTimes = 1;
```

```

function sys=mdlOutputs(t,x,u)
a1=rem(u(8),u(10))+u(7);
fs_dot=u(3)*u(4)*(u(11)/u(2))*...
    exp(-u(3)*((a1-u(1))/u(2))^u(4))*((a1-u(1))/u(2))^(u(4)-1);
sp_bm=1;
y1=fs_dot*u(6);           %m_dot
y2=u(5)*fs_dot*u(6);     %Enthalpy Change Rate
y3=y1*(sp_bm-u(9));      %Specific Burned Fuel Mass Fraction Capital
y4=0;                    % Q_dot
y5=0;                    %Moment
y6=0;                    %Inertia

sys = [y1, y2, y3, y4, y5, y6]; % muxed outputs

```

### Cylinder Geometry

```

function [sys,x0,str,ts] = sfun_3(t,x,u,flag)
sizes.NumContStates = 0;
sizes.NumDiscStates = 0;
sizes.NumOutputs    = 11;
sizes.NumInputs     = 12;
sizes.DirFeedthrough = 1;
sizes.NumSampleTimes = 1;

```

```

function sys=mdlOutputs(t,x,u)

    a1=rem(u(10),u(7));
    y11=a1;

w=cos(2*pi*a1);
h=sin(2*pi*a1);
E=u(2)*sqrt(1-(u(1)*h/u(2))^2);
xu_dot=u(1)*h*2*pi*u(9)*(1+(u(1)*w)/E);
d=u(2)-u(1)*w-E;
Fp=u(6)*(u(11)-u(12));

y1=xu_dot*u(6);
y2=u(4)+((u(1)+d)*u(6)); % OK
y3=xu_dot;
y4=u(1)+d;
y5=Fp*u(1)*h*(1+(u(1)*w)/E); % Torque OK

%Ip Caclulation equation 4.20 page 81
if (u(9)~= 0) % a_dot not zero
    y6=u(8)*u(1)^2+u(5)*(xu_dot)^2/((2*pi*u(9))^2);
else
    y6=u(8)*u(1)^2;
end

y7=-y1;
y8=u(3)+((u(1)-d)*u(6)); % x2
y9=-y3;
y10=u(1)-d;

```

```
sys = [y1, y2, y3, y4, y5, y6, y7, y8, y9, y10, y11]; % muxed
outputs
```

### *Geometrical Energy Loss*

```
function [sys,x0,str,ts] = sfun_4(t,x,u,flag)
sizes.NumContStates = 0;
sizes.NumDiscStates = 0;
sizes.NumOutputs = 10;
sizes.NumInputs = 8;
sizes.DirFeedthrough = 1;
sizes.NumSampleTimes = 1;
```

```
function sys=mdlOutputs(t,x,u)
```

```
if (u(4) ~= 0)
    pf=u(6)*abs(u(1))+u(7)*abs(u(4))+u(8);
    y8=u(6)*abs(u(1)); %pf1
    y9=u(7)*abs(u(4)); %pf2
    y10=u(8); %ps
```

```
else
    pf=u(6)*abs(u(1))+u(7)*abs(u(4));
    y8=u(6)*abs(u(1)); %pf1
    y9=u(7)*abs(u(4)); %pf2
    y10=u(8); %ps
```

```
end
```

```
if (u(4) >= 0)
    y1=u(1)-pf;
```

```
else
    y1=u(1)+pf;
```

```
end
```

```
y2=u(2);
y3=u(3);
y4=u(4);
y5=u(5);
y6=abs(u(2))*pf;
y7=pf;
```

```
sys = [y1, y2, y3, y4, y5, y6, y7,y8, y9, y10]; % muxed outputs
```

## — Appendix B

### Complete engine example

The engine is equipped with a single inlet manifold (plenum) where the three compressors of the turbochargers supply it with air. From the single inlet plenum, all the engine cylinders are supplied with compressed air through the inlet port of each cylinder. As already stated in previous chapters of this thesis, the inlet plenum is implemented using an open thermodynamic system block which is connected to the downstream side to the engine cylinders and to the upstream side to the heat exchanger located at the downstream side of the compressors of the turbochargers. The open thermodynamic system is connected to the gas properties block which provides the open thermodynamic system block with the thermodynamic properties of the compressed air. All the atmospheric conditions and also the conditions that were measured during manufacturer at shop tests were provided as input of the simulation process. The configuration is shown in Fig. 0-1.

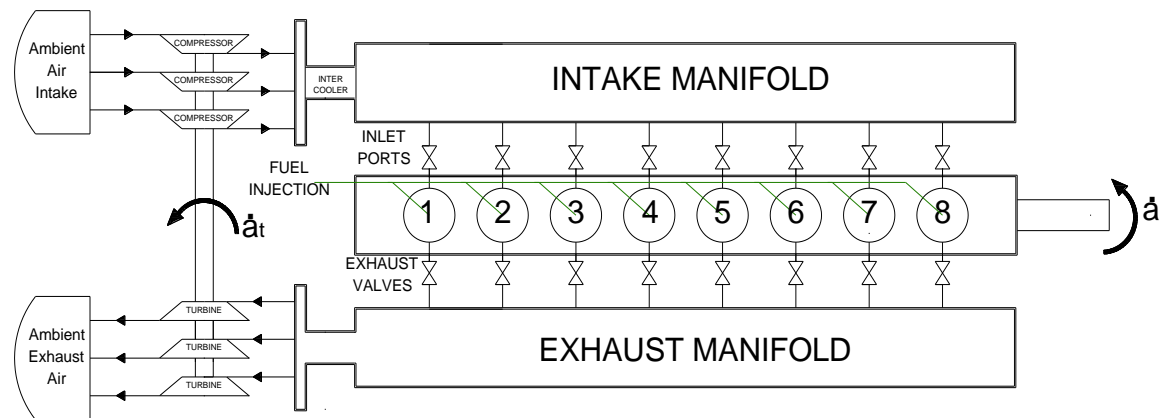


Fig. 0-1 Engine Configuration

Table 0-2 contains the data used in the open thermodynamic system block representing the inlet plenum and the geometrical volume of inlet manifold.

Table 0-2 Inlet Plenum geometry and gas properties

Open Thermodynamic System Block	Geometry Block
$m_{ic} = 113.5 \text{ kg}$	$\dot{V} = 0 \text{ m}^3$
$T_{ic} = 314 \text{ K}$	$V = 29.6 \text{ m}^3$
$\xi_{ic} = 0.029 -$	$\dot{x} = 0 \text{ m/s}$
$B = 1.68 \text{ m}$	$x = 0 \text{ m}$

The inlet manifold is considered insulated; therefore no heat transfer is possible. In this type of engine, the heat transfer taking place in the inlet manifold is very small and does not

affect the performance of the engine, thus the open thermodynamic system block is connected to a heat source that provides zero heat flux (insulation condition).

The engine is equipped with a single exhaust manifold (plenum) where all the exhaust valves of the engine cylinders are connected. The exhaust manifold provides exhaust gas to the turbines. As already stated in previous chapters of this thesis, the exhaust plenum is implemented using an open thermodynamic system block which is connected to the thermodynamic properties of the exhaust gas. Table 0-3 contains the data used in the open thermodynamic system block representing the exhaust plenum and the geometrical volume of exhaust manifold.

**Table 0-3 Exhaust Plenum geometry and gas properties**

Open Thermodynamic System Block		Geometry Block	
$m_{ic} = 82.7$	$kg$	$\dot{V} = 0$	$m^3$
$T_{ic} = 643.7$	$K$	$V = 42.7$	$m^3$
$\xi_{ic} = 0.29$	$-$	$\dot{x} = 0$	$m/s$
$B = 1.68$	$m$	$x = 0$	$m$

The heat transfer taking place in the exhaust plenum cannot be ignored due the higher temperature of the exhaust gas relative to the environment and the impact at the performance of the engine cannot be neglected. A simple heat transfer model is used using a convection heat flux block between the exhaust gas and the exhaust manifold and a convection heat flux block between the exhaust manifold and the ambient air. The data used in the simulation are presented in Table 0-4.

**Table 0-4 Heat transfer Convection Data for Exhaust Casing**

Convection Block Data 1		Convection Block Data 2	
$A_c = 95$	$m^2$	$A_c = 95$	$m^2$
$S_s = 100$	$m^{-1}$	$S_s = 100$	$m^{-1}$
$D = 2.1$	$m$	$D = 2.1$	$m$
$a = 0.03$	$-$	$a = 0.02$	$-$
$b = 0.8$	$-$	$b = 0.8$	$-$
$c = 0.4$	$-$	$c = 0.4$	$-$

The exhaust plenum manifold is implemented using a heat capacitor (data presented in Table 0-5) while the ambient air is implemented using a heat sink (data also presented in Table 0-5).

**Table 0-5 Exhaust Casing heat capacitor Data and Ambient Air's properties**

Heat Capacitor E. Manifold	Heat Sink Ambient Air
$m = 1250 \text{ kg}$	$T_{ic} = 290 \text{ K}$
$c_p = 465.0 \text{ J} / (\text{kg} \cdot \text{K})$	$Pr = 6.78 \text{ -}$
$T_{ic} = 640 \text{ K}$	$Re = 4592 \text{ -}$
$Pr = 0.0 \text{ -}$	$k = 0.604 \text{ W} / (\text{m} \cdot \text{K})$
$Re = 0.0 \text{ -}$	$\varepsilon = 0.95 \text{ -}$
$k = 54 \text{ W} / (\text{m} \cdot \text{K})$	
$\varepsilon = 0.8 \text{ -}$	

The air entering the turbocharger block is implemented using the fixed fluid block, representing the ambient air conditions. A pressure drop equal to  $500 \text{ N/m}^2$  ( $=0.005\text{Bar}$ ) is taken into account to compensate for air filter existence. The data used in the fixed fluid block is presented in Table 0-6.

**Table 0-6 Intake Ambient Air conditions**

Fixed Fluid Block Intake Ambient Air
$p = 101340 \text{ N} / \text{m}^2$
$T = 303.3 \text{ K}$
$\xi_{ic} = 0.00 \text{ -}$

The air leaving the turbocharger block is implemented using the fixed fluid block, representing the ambient air conditions. A pressure drop equal to  $2950 \text{ N/m}^2$  ( $=0.0295\text{Bar}$ ) is taken into account due to exhaust casing. The data used in the fixed fluid block is presented in Table 0-7.

**Table 0-7 Exhaust Ambient Air conditions**

Fixed Fluid Block Exhaust Ambient Air
$p = 103460 \text{ N} / \text{m}^2$
$T = 298 \text{ K}$
$\xi_{ic} = 0.48 \text{ -}$

The crank shaft block is a rigid shaft used for the transmission of the power produced by the engine cylinders. In general it is not a weightless shaft, but may include the equivalent polar moment of inertia of the engine moving parts. Since the polar moment of inertia of each

cylinder is included in the piston geometry blocks, the rest of the system polar moment of inertia is included. The crank shaft may be connected to other shaft element through mechanical connections such as a gear box (for 4stroke medium speed engines) or a clutch, or may be connected to any number of shaft loads.

The data used for the stiff shaft block representing the crankshaft is presented in Table 0-8.

**Table 0-8 Crank shafts Data**

Data used for Stiff shaft representing the crank shaft of the ship	
$I$	$= 10 \quad kg \cdot m^2$
$\dot{a}_{ic}$	$= 1.675 \quad s^{-1}$
$a_{ic}$	$= 0 \quad -$

In the following graphs, the contact area of the heat transfer blocks is illustrated. The contact area is given versus the piston linear position. Also the following tables contain the thermal properties of all materials that form the engine's cylinder. Thus the used contact area graphs are shown in Fig. 0-2, Fig. 0-3, Fig. 0-4, Fig. 0-5 and Fig. 0-6.

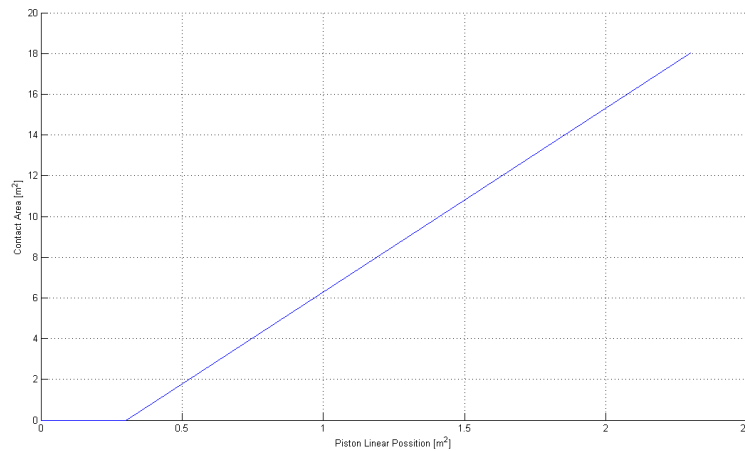


**Fig. 0-2 Heat Transfer area versus piston position for convection HTB2**



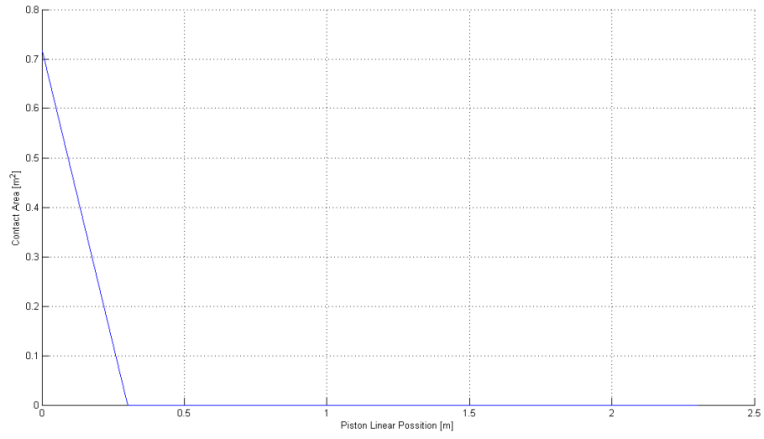


**Fig. 0-3 Heat Transfer area versus piston position for convection HTG2**

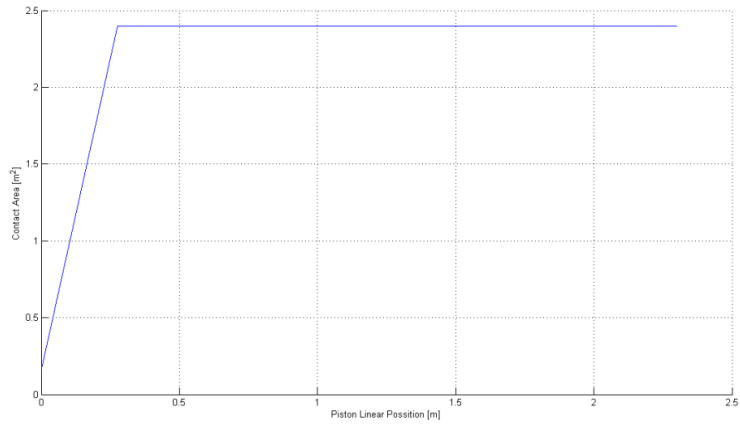


**Fig. 0-4 Heat Transfer area versus piston position for conduction HTA3**

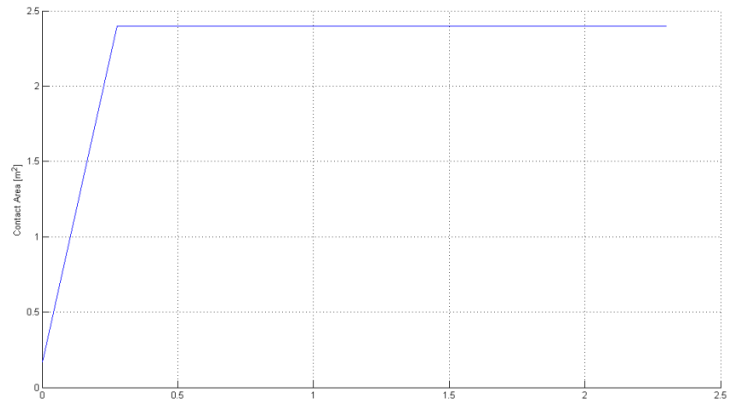


**Fig. 0-5 Heat Transfer area versus piston position for convection HTB2**

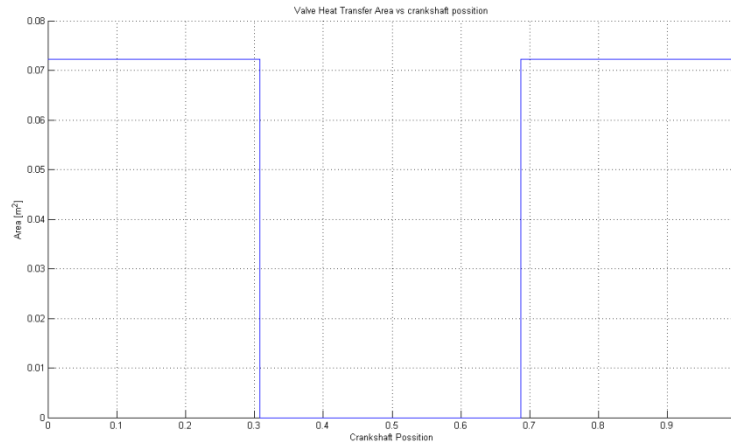


**Fig. 0-6 Heat Transfer area versus crankshaft position between the exhaust valve disk and cylinder head EVA2**

**Table 0-9 Abbreviation for Heat Transfer Elements**

Abbreviation	
<b>G</b>	Working Gas
<b>H</b>	Cylinder's Head
<b>UL</b>	Upper cylinder Liner
<b>LL</b>	Lower cylinder Liner
<b>PC</b>	Piston Crown
<b>PS</b>	Piston Skirt
<b>JC</b>	Jacket Coolant
<b>OC</b>	Oil Coolant

**Table 0-10 Data used in radiation heat flux Blocks**

Item	Units	HTD1R	HTB1R	HTG1R	HTA1R
<b>A<sub>1</sub></b>	m <sup>2</sup>	0.47	graph	graph	0.8
<b>A<sub>2</sub></b>	m <sup>2</sup>	0.47	graph	graph	0.8
<b>F<sub>(1-2)</sub></b>	-	0.95	0.95	0.95	0.95

**Table 0-11 Data used in the conduction heat flux controllers**

Item	Units	HTA4	HTA3	HTB2	EVA2	EVA3	EVB2
<b>A<sub>c</sub></b>	m <sup>2</sup>	0.108	graph	graph	graph	0.005	0.25
<b>S<sub>1</sub></b>	m <sup>-1</sup>	5.6	10	10	34	1.33	40
<b>S<sub>2</sub></b>	m <sup>-1</sup>	13.5	50	50	34	50	40

Table 0-12 Data used in the convection heat flux controllers

Item	Units	HTD1	HTB1	HTG1	HTA1	HTA2	HTD2	HTG2	HTG3	EVA3	EVA1	EVA5	EVB1	EVB3
$A_c$	$m^2$	0.47	graph	graph	0.8	0.5	0.8	2.4	15	0.18	0.18	0.054	0.1875	0.628
$S_s$	$m^{-1}$	50	50	50	50	50	50	50	50	100	50	34	40	30
$D$	$m$	0.9	0.9	0.9	0.9	0.25	0.15	0.05	0.1	0.45	0.45	0.3	0.75	1
$a$	-	0.035	0.035	0.035	0.035	0.5	0.5	0.5	0.5	0.5	0.025	0.025	0.025	0.025
$b$	-	0.8	0.8	0.8	0.8	0.8	0.8	0.8	0.8	0.8	0.8	0.8	0.8	0.8
$c$	-	0	0	0	0	0.333	0.333	0.333	0.333	0.333	0.333	0.333	0.333	0.333

Table 0-13 Data used in the heat capacitors

Item	Units	PS	PC	UL	LL	H	VD	VS	SG
$m$	$kg$	305	747	763	2976	1600	70	59	500
$c_p$	$J/kg K$	465	465	465	465	465	465	465	465
$T_{ic}$	$K$	390	655	510	400	515	520	380	365
$Pr$	-	1	1	1	1	1	1	1	1
$Re$	-	0	0	0	0	0	0	0	0
$k$	$W/m K$	54	54	54	54	54	54	54	54
$\epsilon$	-	0.8	0.8	0.8	0.8	0.8	0.8	0.8	0.8

Table 0-14 Data used in the Open Thermodynamic system Block representing cylinder

Item	Units	Cyl 1	Cyl 2	Cyl 3	Cyl 4	Cyl 5	Cyl 6	Cyl 7	Cyl 8
$m_{ic}$	$kg$	4.41	6.04	4.41	3.30	4.46	4.42	4.51	4.53
$T_{ic}$	$K$	395	1077	421	856	908	562	1077	344
$P$	$Bar$	5.15	48.94	3.4	5.71	118	18.7	14.34	3.15
$\xi_{ic}$	-	0.0029	0.0393	0.0096	0.0393	0.0029	0.0029	0.0393	0.0029
$B$	$m$	0.9	0.9	0.9	0.9	0.9	0.9	0.9	0.9

## Building block Representation of the MAN 8K90MC-C6 marine diesel engine

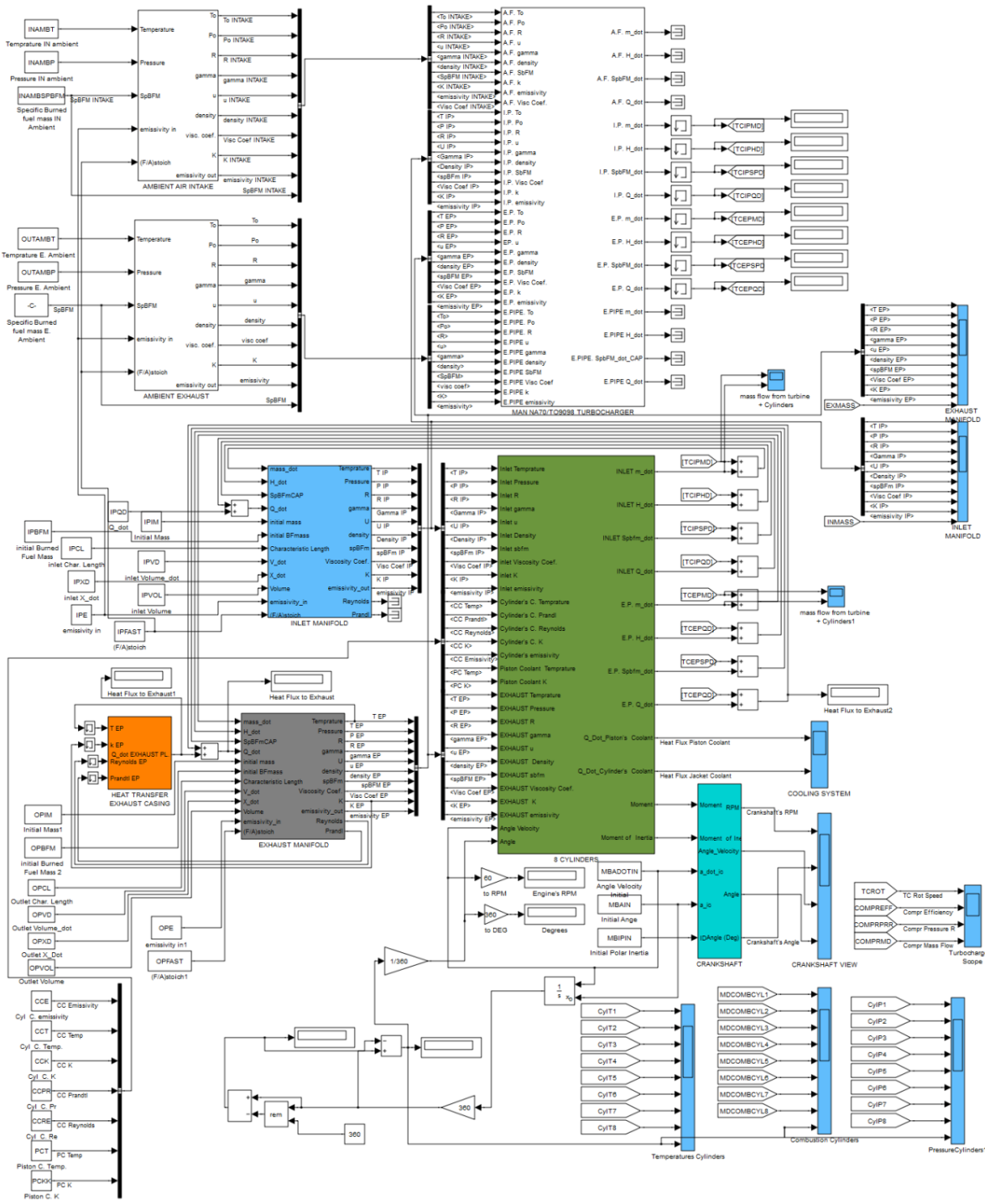


Fig. 0-7 MAN 8K90MC-C6 implementation

## — **Appendix C**

Simulink block library is presented in this appendix in greater detail. Also the Simulink model of the closed cycle period of one cylinder of large marine diesel engine MAN K90MC-C6 is presented. In addition, the proposed implementation of the MAN 8K90MC-C6 Marine Diesel engine is shown in this appendix.

- A) Simulink block library
- B) MAN 8K90MC-C6 implementation
- C) One cylinder engine configuration
- D) Presents the cylinder layout
- E) Exhaust valve model
- F) Cylinder heat transfer

## — Appendix D

In this appendix, the compressor map of NA70/TO9098 MAN turbocharger is presented.

### *Compressor map*

RPM	Pressure Ratio	Volume flow(m <sup>3</sup> /s)	Efficiency
2842	1.081	8.12	0.73
3410	1.103	8.75	0.73
3979	1.155	9.56	0.73
4547	1.2145	10.53	0.73
5116	1.312	11.64	0.73
5684	1.4185	12.9588	0.73
6253	1.5379	14.6123	0.73
6821	1.683	16.281	0.73
7389	1.832	18.1384	0.73
7958	2.0135	19.823	0.73
8526	2.2124	21.7957	0.73
9095	2.4236	23.919	0.73
9663	2.6792	25.584	0.73
10254	2.9614	27.5054	0.73
10800	3.2966	28.9433	0.73
11368	3.5037	29.5418	0.73
2842	1.104	7.93	0.76
3410	1.132	8.56	0.76
3979	1.193	9.2607	0.76
4547	1.2556	10.2566	0.76
5116	1.3498	11.4218	0.76
5684	1.4628	12.739	0.76
6253	1.5851	14.3112	0.76
6821	1.7402	15.8812	0.76
7389	1.8969	17.7918	0.76
7958	2.0796	19.5354	0.76
8526	2.3093	21.4947	0.76
9095	2.5559	23.6759	0.76

9663	2.8221	25.4197	0.76
10254	3.129	27.44	0.76
10800	3.4949	28.8778	0.76
11368	3.7244	29.4973	0.76
2842	1.137	7.68	0.79
3410	1.1823	8.19	0.79
3979	1.2324	8.9214	0.79
4547	1.3029	9.7962	0.79
5116	1.3937	10.8767	0.79
5684	1.5065	12.1405	0.79
6253	1.6319	13.7221	0.79
6821	1.7933	15.285	0.79
7389	1.9594	17.2779	0.79
7958	2.1546	19.0912	0.79
8526	2.4003	21.086	0.79
9095	2.6662	23.3439	0.79
9663	2.9544	25.1463	0.79
10254	3.2877	27.2389	0.79
10800	3.6755	28.7679	0.79
11368	3.8478	29.4529	0.773
2842	1.16	7.2	0.82
3410	1.208	7.76	0.82
3979	1.258	8.3457	0.82
4547	1.339	9.22	0.82
5116	1.4205	10.2019	0.82
5684	1.5377	11.4321	0.82
6253	1.6727	12.9641	0.82
6821	1.8417	14.5322	0.82
7389	2.0232	16.4907	0.82
7958	2.243	18.2729	0.82
8526	2.4924	20.3814	0.82
9095	2.763	22.7664	0.82
9663	3.0806	24.6364	0.82

10254	3.4376	26.8625	0.82
10800	3.8915	28.3681	0.82
11368	3.9316	29.4085	0.785
2842	1.176	6.58	0.815
3410	1.2144	7.28	0.822
3979	1.2663	7.6	0.825
4547	1.359	8.11	0.828
5116	1.4401	9.31	0.83
5684	1.5638	10.3683	0.835
6253	1.7021	11.9836	0.847
6821	1.8813	13.6905	0.85
7389	2.0663	15.531	0.85
7958	2.3045	17.2559	0.85
8526	2.5685	19.3896	0.85
9095	2.8515	21.6816	0.85
9663	3.2087	23.5595	0.85
10254	3.6052	25.7566	0.85
10800	4.0065	27.9262	0.84
11368	3.9888	29.3875	0.79
2842	1.177	6	0.81
3410	1.216	6.65	0.82
3979	1.269	6.61	0.83
4547	1.365	6.88	0.835
5116	1.45	8.668	0.836
5684	1.5684	9.8937	0.84
6253	1.712	11.3137	0.845
6821	1.9036	12.8489	0.85
7389	2.0846	14.6046	0.855
7958	2.331	16.0589	0.858
8526	2.6051	18.264	0.86
9095	2.8911	20.7301	0.86
9663	3.2734	22.2918	0.86
10254	3.6932	24.3399	0.86



10800	4.0549	27.5709	0.847
11368	4.068	29.3641	0.795
2842	1.18	5.04	0.794
3410	1.221	5.17	0.796
3979	1.269	5.76	0.8
4547	1.365	6.1377	0.82
5116	1.457	7.4165	0.838
5684	1.5815	8.8206	0.84
6253	1.7202	10.4443	0.842
6821	1.9078	12.0516	0.845
7389	2.091	13.9573	0.85
7958	2.3357	15.8812	0.858
8526	2.6159	17.6998	0.864
9095	2.9129	19.6687	0.8687
9663	3.2947	21.672	0.866
10254	3.7197	23.8091	0.86
10800	4.0903	27.2833	0.85
11368	4.209	29.1887	0.815
2842	1.185	3.97	0.7456
3410	1.229	4.28	0.75
3979	1.2771	4.65	0.775
4547	1.375	4.92	0.795
5116	1.475	6.22	0.81
5684	1.5815	7.2706	0.828
6253	1.7204	9.0949	0.832
6821	1.9078	11.1211	0.838
7389	2.0948	12.6694	0.842
7958	2.3445	14.5766	0.85
8526	2.6262	16.5176	0.855
9095	2.9264	18.2519	0.86
9663	3.3147	20.6396	0.859
10254	3.7463	23.0329	0.858
10800	4.1387	26.6193	0.855

11368	4.324	29.0111	0.82
2842	1.187	3.63	0.73
3410	1.235	3.93	0.74
3979	1.289	4.2057	0.76
4547	1.38	4.58	0.78
5116	1.484	5.91	0.8
5684	1.5861	7.004	0.82
6253	1.7213	8.4776	0.82
6821	1.9036	9.9498	0.82
7389	2.0958	11.8674	0.83
7958	2.3445	13.9781	0.83
8526	2.6297	15.7356	0.84
9095	2.9395	17.6978	0.85
9663	3.3233	20.0824	0.85
10254	3.7551	22.5677	0.85
10800	4.1741	25.9787	0.85
11368	4.3766	28.6791	0.79





ΕΘΝΙΚΟ ΜΕΤΣΟΒΙΟ ΠΟΛΥΤΕΧΝΕΙΟ  
ΣΧΟΛΗ ΝΑΥΠΗΓΩΝ ΜΗΧΑΝΟΛΟΓΩΝ ΜΗΧΑΝΙΚΩΝ

**ΣΠΟΝΔΥΛΩΤΗ ΘΕΡΜΟΔΥΝΑΜΙΚΗ  
ΠΡΟΣΟΜΟΙΩΣΗ ΤΟΥ ΚΛΕΙΣΤΟΥ  
ΚΥΚΛΟΥ ΕΝΟΣ ΚΥΛΙΝΔΡΟΥ  
ΜΕΓΑΛΟΥ ΝΑΥΤΙΚΟΥ ΚΙΝΗΤΗΡΑ  
DIESEL**

ΔΙΠΛΩΜΑΤΙΚΗ ΕΡΓΑΣΙΑ

Εκτενής περίληψη του αγγλικού κειμένου

**ΕΛΕΥΘΕΡΙΟΣ ΔΕΔΕΣ**

ΕΠΙΒΛΕΠΩΝ: ΚΑΘΗΓΗΤΗΣ ΝΙΚΟΛΑΟΣ ΚΥΡΤΑΤΟΣ

ΙΟΥΛΙΟΣ 2009

## Περιεχόμενα

1	Εισαγωγή .....	3
2	Μαθηματικά μοντέλα .....	5
2.1	Ιδιότητες αερίων .....	5
2.2	Ανοικτό θερμοδυναμικό σύστημα .....	6
2.3	Βαλβίδα .....	8
2.4	Μοντέλο καύσης σύμφωνα με την S – Curve .....	8
2.5	Μοντέλα μεταφοράς θερμότητας.....	9
2.6	Γεωμετρία κυλίνδρου .....	9
2.7	Ενεργειακές Απώλειες.....	11
3	Simulink Blocks .....	12
3.1	Θυρίδα εισαγωγής και Βαλβίδα εξαγωγής .....	12
3.2	Ανοικτό Θερμοδυναμικό Σύστημα και ιδιότητες Αερίων .....	15
3.3	Σταθερές Ιδιότητες και Ιδιότητες Αερίων .....	16
3.4	Μεταφορά θερμότητας στον κύλινδρο .....	17
3.5	Καύση .....	19
3.6	Κύλινδρος .....	20
3.7	Μοντέλο οκτώ κυλίνδρων .....	21
4	Αποτελέσματα προσομοίωσης .....	22
5	Συμπεράσματα .....	33
6	Βιβλιογραφία.....	34

## Πίνακας Εικόνων

Εικόνα 3-1 Πραγματικό άνοιγμα Θυρίδας εισαγωγής συναρτήσει στροφαλογωνίας .....	13
Εικόνα 3-2 Πραγματικό άνοιγμα Βαλβίδας εξαγωγής συναρτήσει στροφαλογωνίας .....	13
Εικόνα 3-3 Block: Βαλβίδα Εξαγωγής.....	14
Εικόνα 3-4 Block: Ανοικτό θερμοδυναμικό σύστημα .....	15
Εικόνα 3-5 Block: Σταθερές ιδιότητες και Ιδιότητες Αερίου .....	16
Εικόνα 3-6 Μοντέλο μεταφοράς θερμότητας μέσα στον κύλινδρο .....	17
Εικόνα 3-7 Παράδειγμα χάρτη μεταβλητής επιφάνειας επαφής .....	18
Εικόνα 3-8 Block: μεταφορά θερμότητας στον κύλινδρο .....	18
Εικόνα 3-9 Block: S - curve .....	19
Εικόνα 3-10 Block: Ένας κύλινδρος .....	20
Εικόνα 3-11 Κύλινδροι MAN 8K90MC-C6 .....	21
Εικόνα 4-1 Διάταξη προσομοίωσης .....	22
Εικόνα 4-2 Ίχνος θερμοκρασίας (πάνω) και πίεσης μέσα στον κύλινδρο .....	23
Εικόνα 4-3 Μεταφορά μάζας από την θυρίδα εισαγωγής (πάνω) και από την βαλβίδα εξαγωγής .....	24
Εικόνα 4-4 Αναπτυσσόμενη ροπή (πάνω) και πολική ροπή αδρανείας κυλίνδρου .....	24
Εικόνα 4-5 Αναπτυσσόμενη θερμοκρασία (πάνω) και πίεση στον κύλινδρο (75%) .....	25
Εικόνα 4-6 Αναπτυσσόμενη θερμοκρασία (πάνω) και πίεση μέσα στον κύλινδρο (50%) .....	26
Εικόνα 4-7 Μεταφορά μάζας από τις θυρίδες εισαγωγής (πάνω) και τη βαλβίδα εξαγωγής	27
Εικόνα 4-8 Αναπτυσσόμενη ροπή (πάνω) και πολική ροπή αδρανείας κυλίνδρου .....	27
Εικόνα 4-9 Αναπτυσσόμενη θερμοκρασία (πάνω) και πίεση στον κύλινδρο για περιπτώσεις .....	28
Εικόνα 4-10 Αναπτυσσόμενη ροπή (πάνω) και πολική ροπή αδρανείας παραμετρικών προσομοιώσεων.....	29
Εικόνα 4-11 Εστίαση σε περιοχή της εικόνας 4-10 .....	30
Εικόνα 4-12 Αναπτυσσόμενη θερμοκρασία (πάνω) και πίεση στον κύλινδρο για διαφορετική μάζα εγχυόμενου καυσίμου .....	31
Εικόνα 4-13 Αναπτυσσόμενη θερμοκρασία (πάνω) και πίεση στον κύλινδρο για διαφορετικό επιζήμιο όγκο .....	31
Εικόνα 4-14 Μεγαλύτερη ακρίβεια της εικόνας 4-13 .....	32

## Πίνακας Πινάκων

Πίνακας 1 Ομαδοποίηση Blocks.....	12
Πίνακας 2 Φάσεις κύκλου .....	23
Πίνακας 3 Σταθερές καύσης για διάφορες περιπτώσεις .....	28
Πίνακας 4 Σταθερές καύσης και μάζα εγχυόμενου καυσίμου .....	30
Πίνακας 5 Σταθερές καύσης και επιζήμιος όγκος.....	30

# 1 Εισαγωγή

Στις μέρες μας, όταν η προστασία του περιβάλλοντος αλλά και η χαμηλή κατανάλωση καυσίμου, αποτελούν πρωταρχικούς στόχους για την υλοποίηση μίας κατασκευής, ο ρόλος της προσομοίωσης λειτουργίας, γίνεται επιτακτικός. Η προσομοίωση βοηθά τον κατασκευαστή των μηχανών σε όλα τα στάδια της σχεδίασης της, όπως είναι η κατασκευή της με βάση το βέλτιστο δυνατό τρόπο, η παρακολούθηση της εύρυθμης λειτουργίας μετά την παράδοση και παραλαβή της από τον πελάτη αλλά και παράλληλα, η συνεχής ρύθμιση της, με απώτερο στόχο την βελτιστοποίηση των παραμέτρων. Επίσης η προσομοίωση, επιτρέπει τον έλεγχο των βαθμών ελευθερίας του συστήματος και λόγω της αλληλεπίδρασης όλων των κομματιών που απαρτίζουν το σύστημα μεταξύ τους να βελτιστοποιούνται τελικά όλα μαζί.

Η χρήση της προσομοίωσης, επιτρέπει τη βαθύτερη κατανόηση των φυσικών διεργασιών μέσα στο σύστημα. Καθώς αυτή λειτουργεί, οι ερευνητές μπορούν να βλέπουν ανά πάσα στιγμή της επιδράσεις στο σύστημα. Συνεπώς, είναι πολύ πιο εύκολο να βρεθούν και να διορθωθούν στοιχεία τα οποία θα βελτιστοποιήσουν το σύστημα.

Στις μέρες μας, κυριαρχούν τρεις κατηγορίες λογισμικού για την μοντελοποίηση προσομοίωση και ανάλυση της δυναμικής των συστημάτων. Στην πρώτη κατηγορία ανήκουν οι γλώσσες προγραμματισμού όπως είναι η FORTRAN, C, C++. Στη δεύτερη κατηγορία εντάσσονται τα πακέτα προσομοίωσης όπως είναι το παλαιότερο ACSL και η γνωστή πλατφόρμα MATLAB/Simulink. Στην τρίτη κατηγορία, εντάσσονται τα πακέτα πολυδιαστασιακής ανάλυσης όπως είναι η Μέθοδος των Πεπερασμένων Στοιχείων.

Το Simulink είναι ένα πρόγραμμα μοντελοποίησης και προσομοίωσης λειτουργίας με εύκολο γραφικό περιβάλλον. Διαθέτει βιβλιοθήκη με έτοιμα blocks υπολογισμού, ενώ αλληλεπιδρά συνεχώς με τις ρουτίνες του MATLAB. Υποστηρίζει μεθόδους ολοκλήρωσης σταθερού ή μεταβλητού βήματος ενώ μοντελοποιεί διακριτά ή συνεχή συστήματα.

Η Μέθοδος Πεπερασμένων Στοιχείων, είναι μία αριθμητική μέθοδος για την εύρεση προσεγγιστικών λύσεων των μερικών διαφορικών εξισώσεων. Η λύση τους βασίζεται στην τεχνική της μείωσης της διαφορικής εξίσωσης ή της μετατροπής της σε συνήθη διαφορική εξίσωση όπου μπορεί και να λυθεί με τις γνωστές μεθόδους αριθμητικής ολοκλήρωσης όπως η Runge – Kutta, Euler κλπ. Στην ναυπηγική βιομηχανία η μέθοδος των πεπερασμένων στοιχείων χρησιμοποιείται στη μοντελοποίηση του θαλάμου καύσης, προκειμένου να προβλεφτούν οι θερμικές και οι μηχανικές καταπονήσεις σε δυναμικές φορτίσεις αλλά και να προσομοιαστεί ο θόρυβος και οι ταλαντώσεις των μηχανικών μερών του.

Η συγκεκριμένη διπλωματική εργασία, χρησιμοποιεί τα μοντέλα μηδενικής διάστασης (zero dimensional models), τα οποία περιλαμβάνουν πιο απλές διαφορικές εξισώσεις στη μοντελοποίηση τους, έχουν λιγότερους βαθμούς ελευθερίας, ενώ απαιτούν μικρότερη υπολογιστική ισχύ, προκειμένου να προσομοιαστούν. Θεωρούνται οι εξισώσεις αυτές ως θερμοδυναμικά μοντέλα διότι δεν απαιτούν γνώση της γεωμετρικής κατανομής του αερίου μέσα στον όγκο ελέγχου. Γενικότερα τα μοντέλα που χρησιμοποιούνται στη μοντελοποίηση είναι τα θερμοδυναμικά, ενώ σε άλλες περιπτώσεις μοντελοποίησης χρησιμοποιείται και της δυναμικής των αερίων. Η διαφορά των δύο μοντέλων έγκειται στο

γεγονός ότι οι βασικές εξισώσεις που περιγράφουν το μοντέλο, προκύπτουν από την αρχή διατήρησης της μάζας ενώ στην δεύτερη προκύπτει από την πλήρη ανάλυση της κίνησης του ρευστού μέσα στους όγκους της μηχανής (Κυρτάτος, 1993). Στη παρούσα εργασία η μοντελοποίηση θα γίνει με το θερμοδυναμικό μοντέλο. Επίσης η μοντελοποίηση γίνεται με την μέθοδο πλήρωσης και απόπλυσης (emptying and filling method) (Heywood, 1988). Οι σχετοί εισαγωγής και εξαγωγής όπως επίσης και του μεταβλητού όγκου του κυλίνδρου, θεωρούνται πεπερασμένοι όγκοι. Επίσης η συνολική μηχανή μπορεί να μοντελοποιηθεί ως ένα σύνολο όγκων οι οποίοι περιέχουν στενώσεις (π.χ. θυρίδες, βαλβίδες). Ο κάθε όγκος πλέον μπορεί να θεωρηθεί ως όγκος ελέγχου όπου το περιεχόμενο αέριο θεωρείται ότι έχει ομοιόμορφες ιδιότητες σε όλο τον χώρο που καταλαμβάνει. Οι νόμοι της διατήρησης της ενέργειας και της μάζας ισχύουν, υπό την προϋπόθεση της γνώσης της μεταφερόμενης μάζας από και προς το σύστημα, προκειμένου να γνωρίζεται η κατάσταση του αερίου την κάθε χρονική στιγμή.

Η εργασία αυτή διαρθρώνεται σε 3 κεφάλαια.

Το κεφάλαιο 2 περιγράφει όλες τις μαθηματικές εξισώσεις των μοντέλων που χρησιμοποιήθηκαν.

Το κεφάλαιο 3 περιλαμβάνει τα βασικά blocks που μοντελοποιήθηκαν και έχουν ομαδοποιηθεί με βάση τη λειτουργικότητα τους

Το κεφάλαιο 4 περιλαμβάνει τα αποτελέσματα διατάξεων επαλήθευσης αποτελεσμάτων και τα αποτελέσματα προσομοίωσης για φορτία 90%, 75% και 50% της μέγιστης ισχύος του κινητήρα, για έναν κύλινδρο. Συγκρίσεις με το πρόγραμμα του εργαστηρίου ναυτικής μηχανολογίας και παραμετρικές προσομοιώσεις, βρίσκονται και αυτές στο κεφάλαιο 4.

Σκοπός της εργασίας αυτής ήταν να εισάγει ένα νέο εργαλείο μοντελοποίησης όπως είναι η πλατφόρμα του MATLAB/Simulink, για την εφαρμογή της σε ναυτικά συστήματα πρόωσης, έχοντας ικανοποιητική ακρίβεια. Μελλοντική δουλειά απαιτείται για να ολοκληρωθεί η μοντελοποίηση της πλήρους ναυτικής μηχανής. Παρόλο που αρκετά μαθηματικά μοντέλα εισήχθησαν στην παρούσα διπλωματική εργασία, πιο πολύπλοκες εξισώσεις σε κάποια μοντέλα πρέπει να αντικαταστήσουν τις υπάρχουσες προκειμένου να έχουμε πιο ακριβή αποτελέσματα στην προσομοίωση των φυσικών διεργασιών που παρατηρούνται σε έναν ναυτικό κινητήρα Diesel.



## 2 Μαθηματικά μοντέλα

Στο συγκεκριμένο κεφάλαιο παρουσιάζονται οι εξισώσεις που μοντελοποιούν τα συστήματα των παρακάτω κομματιών:

- Ιδιότητες αερίων
- Ανοικτό θερμοδυναμικό σύστημα
- Βαλβίδα
- Μοντέλο καύσης σύμφωνα με την S – curve
- Μεταφορά θερμότητας
  - Αγωγή
  - Συναγωγή
  - Ακτινοβολία
- Γεωμετρία κυλίνδρου
- Ενεργειακές απώλειες

### 2.1 Ιδιότητες αερίων

Στο κεφάλαιο αυτό, περιγράφονται οι εξισώσεις υπολογισμού των ιδιοτήτων των αερίων. Προκειμένου να υπολογιστούν οι ιδιότητες των εργαζόμενων μέσων, χρησιμοποιούνται τα πολυώνυμα υπολογισμού της σταθεράς των αερίων και της εσωτερικής ενέργειας όπως προέκυψαν από τους Krieger και Borman (Borman & Krieger, 1966) όπου ανέλυσαν τα διαγράμματα των Newhall και Starkman (Newhall & Starkman, 1963).

$$u = f_u(T, p, \phi) \quad (2.1)$$

$$R = f_R(T, p, \phi) \quad (2.2)$$

Για φτωχό μίγμα ( $\Phi < 1$ ) και για  $T > 1333$  K οι εξισώσεις προκύπτουν από

$$u = K_1(T) - K_2(T) \text{ [kJ / kg]} \quad (2.3)$$

όπου,

$$K_1(T) = 0.692 \cdot T + 39.17 \cdot 10^{-6} \cdot T^2 + 52.9 \cdot 10^{-9} \cdot T^3 - 228.62 \cdot 10^{-13} \cdot T^4 + 277.58 \cdot 10^{-17} \cdot T^5 \quad (2.4)$$

καθώς και

$$K_2(T) = 3049.39 + 5.7 \cdot 10^{-2} \cdot T + 9.5 \cdot 10^{-5} \cdot T^2 - 21.53 \cdot 10^{-9} \cdot T^3 + 200.26 \cdot 10^{-14} \cdot T^4 \quad (2.5)$$

Η σταθερά του αερίου δίδεται από τον τύπο

$$R = 0.285 - 0.02 \cdot \phi \text{ [kJ / Kg} \cdot \text{K]} \quad (2.6)$$

Ενώ για θερμοκρασίες μεγαλύτερες των 1333 K, προστίθεται διορθωτικός συντελεστής, καθώς η διάσπαση των μορίων μετά τη καύση δεν μπορεί να αγνοηθεί

$$u = u_0 + 2.326 \cdot e^C \quad (2.7)$$

όπου το C είναι ίσο με

$$C = C_1 + C_2 + C_3 \quad (2.8)$$

και οι συντελεστές είναι ίσοι με

$$C_1 = 10.4166 + 7.85125 \cdot \phi - 3.71257 \cdot \phi^3 \quad (2.9)$$

$$C_2 = \left( -27.00107 - 28.5087 \cdot \phi - 17.30375 \cdot \phi^3 \right) \cdot \frac{1800}{T} \quad (2.10)$$

$$C_3 = (0.154226 \cdot \phi^3 - 0.38656 \cdot \phi - 0.10329 + (0.21289 \cdot \phi - 0.026574) \cdot \frac{1800}{T}) \cdot \ln(14.5 \cdot p) \quad (2.11)$$

Η σταθερά των αερίων δίδεται από τον τύπο

$$R = R_0 + 4.1868 \cdot e^{A \cdot 10^{-3}} \quad (2.12)$$

ενώ το A από

$$A = \left( 11.98 - 45.796 \cdot \frac{1800}{T} - 0.4354 \cdot \ln(14.5 \cdot p) \right) \cdot \phi + 0.2977 \cdot \ln(\phi) \quad (2.13)$$

Σε ότι αφορά τα υπόλοιπα μεγέθη, αξίζει να αναφερθεί η σχέση υπολογισμού του λόγου ισοδυναμίας

$$\phi = \frac{\xi}{(1 - \xi) \cdot (F/A)_{st}} \quad (2.14)$$

## 2.2 Ανοικτό θερμοδυναμικό σύστημα

Στη παρούσα ενότητα περιγράφονται οι εξισώσεις υπολογισμού της πίεσης και της θερμοκρασίας των αερίων σε κάθε χρονικό βήμα της ολοκλήρωσης. Στο ανοικτό θερμοδυναμικό σύστημα ισχύει η διατήρηση της μάζας όπως επίσης και ο ενεργειακός ισολογισμός, λαμβάνοντας υπ' όψιν την εναλλαγή ενέργειας με το υπόλοιπο περιβάλλον. Επομένως,

$$m = \int_0^t \dot{m} dt + m_{ic} \quad (2.15)$$

$$\xi = \int_0^t \dot{\xi} + \xi_{ic} \quad (2.16)$$

$$P \cdot V = m \cdot R \cdot T \quad (2.17)$$

$$\dot{p} = \frac{m \cdot R}{V} \cdot \dot{T} + \frac{m \cdot T}{V} \cdot \left( \frac{\partial R}{\partial T} \cdot \dot{T} + \frac{\partial R}{\partial p} \cdot \dot{p} + \frac{\partial R}{\partial \phi} \cdot \dot{\phi} \right) + \frac{R \cdot T}{V} \cdot \dot{m} - \frac{m \cdot R \cdot T}{V^2} \cdot \dot{V} \quad (2.18)$$

Για απλούστευση της σχέσης (2.18) αντικαθιστούμε σύμφωνα με τις παρακάτω σταθερές

$$A = \left( 1 - \frac{p \cdot \partial R}{R \cdot \partial p} \right) \quad (2.19)$$

$$B = \left( \frac{1}{T} + \frac{\partial R}{R \cdot \partial T} \right) \quad (2.20)$$

$$C = \frac{\partial R}{R \cdot \partial \phi} \cdot \dot{\phi} + \frac{1}{m} \cdot \dot{m} - \frac{1}{V} \cdot \dot{V} \quad (2.21)$$

Επομένως η σχέση (2.18) μετασχηματίζεται σε

$$\dot{p} = \frac{(B \cdot \dot{T} + C) \cdot p}{A} \quad (2.22)$$

Για τον υπολογισμό της θερμοκρασίας ισχύει η σχέση

$$\dot{U} = \dot{Q} - \dot{W} + \dot{H} \quad (2.23)$$

Επομένως

$$\dot{u} \cdot m + u \cdot \dot{m} = \sum_{i=1}^n \dot{Q}_i + \sum_{j=1}^n \dot{Q}_j - p \cdot \dot{V} + \sum_{i=1}^n (h_i \cdot \dot{m}_i) \quad (2.24)$$

Όπου και τελικά προκύπτει η θερμοκρασία, αντικαθιστώντας και πάλι τις σταθερές (εξισώσεις (2.19 – 2.21))

$$\dot{T} = \frac{\frac{D - u \cdot \dot{m}}{m} - \frac{\partial u \cdot C}{\partial p \cdot A} \cdot p - \frac{\partial u}{\partial \phi} \cdot \dot{\phi}}{\frac{\partial u}{\partial T} + \frac{\partial u}{\partial p} \cdot \frac{B}{A} \cdot p} \quad (2.25)$$

### 2.3 Βαλβίδα

Οι ροή ρευστού μέσα από στένωση περιγράφεται από τις ακόλουθες εξισώσεις. Όταν η ροή είναι ηχητική, ο αριθμός Mach είναι ίσος με τη μονάδα. Η πίεση για την οποία ο αριθμός Mach γίνεται ίσος με τη μονάδα, καλείται κρίσιμη πίεση.

Για ηχητική ροή η παροχή μάζας μέσα από την βαλβίδα γίνεται από την εξίσωση

$$\dot{m} = \frac{A \cdot p_0}{\sqrt{R \cdot T_0}} \cdot \sqrt{\frac{2 \cdot \gamma}{\gamma} \cdot \left[ \left( \frac{p}{p_0} \right)^{\frac{2}{\gamma}} - \left( \frac{p}{p_0} \right)^{\frac{\gamma+1}{\gamma}} \right]} \quad (2.26)$$

Ενώ για την υποηχητική ροή, όταν η πίεση είναι ίση με την κρίσιμη πίεση (εξίσωση 2.27)

$$\frac{p}{p_0} = \left( 1 + \frac{\gamma-1}{2} \right)^{\frac{-\gamma}{\gamma-1}} \quad (2.27)$$

η παροχή μάζας δίδεται από τον τύπο

$$\dot{m} = \frac{\gamma \cdot A \cdot p_0}{\sqrt{\gamma \cdot R \cdot T_0}} \cdot \left( \frac{2}{\gamma+1} \right)^{\frac{(\gamma+1)}{2(\gamma-1)}} \quad (2.28)$$

### 2.4 Μοντέλο καύσης σύμφωνα με την S – Curve

Στην ενότητα αυτή χρησιμοποιείται το μοντέλο της S – curve για την μοντελοποίηση του εκλυόμενου ρυθμού καύσης για την απευθείας έγχυση στον κύλινδρο. Για ευκολία, έχει χρησιμοποιηθεί η χρονική παράγωγος της S – Curve. Έτσι, για το βασικό της μοντέλο έχουμε,

$$f_s = 1 - e^{-C_1 \cdot x^{C_2}} \quad (2.29)$$

ενώ για μηχανές ε μονή έγχυση ο όρος x είναι ίσος με

$$\frac{\alpha - \alpha_r}{\Delta \alpha} \quad (2.30)$$

Όπου α είναι η γωνία του στροφάλου, α<sub>r</sub> είναι η γωνία έναρξης της καύσης και Δα είναι η διάρκεια της καύσης. Επομένως η σχέση (2.29) γίνεται:

$$f_s = 1 - e^{-C_1 \cdot \frac{\alpha - \alpha_r}{\Delta \alpha}^{C_2}} \quad (2.31)$$

Η χρονική παράγωγος της σχέσης (2.31) είναι η εξής

$$\dot{f}_s = C_1 \cdot C_2 \cdot \frac{\dot{\alpha}}{\Delta \alpha} \cdot e^{-C_1 \cdot \frac{\alpha - \alpha_r}{\Delta \alpha}^{C_2}} \cdot \left( \frac{\alpha - \alpha_r}{\Delta \alpha} \right)^{C_2-1} \quad (2.32)$$

όπου C1 και C2 είναι σταθερές που ρυθμίζουν το σχήμα της.

## 2.5 Μοντέλα μεταφοράς θερμότητας

Στη παρούσα ενότητα, θα περιγραφούν οι εξισώσεις που περιγράφουν τα τρία βασικά είδη μεταφοράς θερμότητας όπως είναι η αγωγή, η συναγωγή και η ακτινοβολία.

### Αγωγή

Η αγωγή εμφανίζεται όταν δύο ή περισσότερα σώματα βρίσκονται σε επαφή, όπου το σώμα με την μεγαλύτερη θερμοκρασία προκαλεί μεταφορά ενέργειας σε αυτό με τη μικρότερη θερμοκρασία σύμφωνα με τον νόμο του Fourier.

$$\dot{Q}_{cd(2-1)} = \frac{K_1}{\delta_1} \cdot A_c \cdot (T_c - T_1) = \frac{K_2}{\delta_2} \cdot A_c \cdot (T_2 - T_c) = -\dot{Q}_{cd(1-2)} \quad (2.33)$$

### Συναγωγή

Η μεταφορά θερμότητας με συναγωγή συμβαίνει όταν έρχονται σε επαφή ένα στερεό και ένα υγρό ρευστό με θερμοκρασιακή μεταξύ τους διαφορά. Το ποσοστό της ενέργειας που μεταφέρεται δίδεται από τον νόμο του Newton.

$$\dot{Q}_{cv(2-1)} = S_s \cdot A_c \cdot (T_c - T_s) = h \cdot A_c \cdot (T_f - T_c) \quad (2.34)$$

### Ακτινοβολία

Η ακτινοβολία είναι η τρίτη βασική μορφή μεταφοράς θερμότητας. Εμφανίζεται όταν το σώμα δεν είναι σε επαφή με κάποιο άλλο, αλλά ακτινοβολεί ως μέλαν σώμα ενέργεια. Σύμφωνα με τη θεωρία των Steffan - Boltzman η σχέση υπολογισμού είναι η ακόλουθη

$$\dot{Q}_{rd(1-2)} = \frac{\sigma \cdot (T_1^4 - T_2^4)}{\left( \frac{(1-\varepsilon_1)}{\varepsilon_1 \cdot A_1} + \frac{1}{(A_1 \cdot F_{(1-2)})} + \frac{(1-\varepsilon_2)}{\varepsilon_2 \cdot A_2} \right)} \quad (2.35)$$

## 2.6 Γεωμετρία κυλίνδρου

Ο κύλινδρος αποτελείται από δύο μεταβλητούς όγκους για τους οποίους το μέγεθος τους καθορίζεται κάθε στιγμή από τη θέση του εμβόλου. Επιπλέον του όγκου σαρώσεως, υπάρχει και ο επιζήμιος όγκος, όγκος ο οποίος παραμένει παρόλο που το έμβολο βρίσκεται στο ΑΝΣ (Άνω Νεκρό Σημείο).

$$V_U = V_{cU} + V_{dU} \quad (2.36)$$

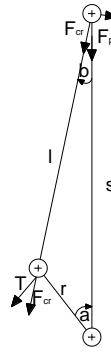
όπου,

$$V_{dU} = A_{cs} \cdot x_U \quad (2.37)$$

και

$$A_{cs} = \pi \cdot \frac{B^2}{4} \quad (2.38)$$

Εκτελώντας πράξεις στη γεωμετρία του κυλίνδρου και κάνοντας χρήση του σχήματος 1



Σχήμα 1 Γεωμετρικά στοιχεία κυλίνδρου – εμβόλου

Προκύπτουν οι παρακάτω εξισώσεις

$$E = l \cdot \sqrt{1 - \frac{r^2}{l^2} \cdot \sin^2(2 \cdot \pi \cdot a)} \quad (2.39)$$

ενώ για ευκολία αντικαθιστούμε τους παρακάτω όρους με σταθερές

$$\begin{aligned} \cos(2 \cdot \pi \cdot a) &= w \\ \sin(2 \cdot \pi \cdot a) &= h \end{aligned} \quad (2.40)$$

Έτσι για την ταχύτητα του εμβόλου ισχύει η σχέση

$$\dot{x}_U = r \cdot h \cdot 2 \cdot \pi \cdot \dot{a} \cdot \left(1 + \frac{r \cdot w}{E}\right) \quad (2.41)$$

ενώ για την αναπτυσσόμενη ροπή ισχύει

$$M_p = F_p \cdot r \cdot h \cdot \left(1 + \frac{r \cdot w}{E}\right) \quad (2.42)$$

όπου η δύναμη που αναπτύσσεται στον κύλινδρο δίδεται από τη σχέση

$$F_p = A_{cs} \cdot p_U - A_{cs} \cdot p_L = A_{cs} \cdot (p_U - p_L) \quad (2.43)$$

Εκτελώντας πράξεις για την διατήρηση της ενέργειας προκύπτει ότι η πολική ροπή αδρανείας δίδεται από τη σχέση

$$I_p = \begin{cases} m_r \cdot r^2 + \frac{m_l \cdot \dot{x}_U^2}{(2 \cdot \pi \cdot \dot{a})^2} & \text{if } \dot{a} \neq 0 \\ m_r \cdot r^2 & \text{if } \dot{a} = 0 \end{cases} \quad (2.44)$$

## 2.7 Ενεργειακές Απώλειες

Οι ενεργειακές απώλειες στον κύλινδρο οφείλονται σε τρεις παραμέτρους. Στην ύπαρξη των ελατηρίων στεγανοποίησης, στην ταχύτητα του εμβόλου αλλά και γενικές απώλειες ως ποσοστό της συνολικής αναπτυσσόμενης πίεσης. Η σχέση υπολογισμού είναι η παρακάτω

$$p_f = \begin{cases} \eta_f \cdot |p_2| + C \cdot |\dot{x}_2| + p_s & \text{if } \dot{x}_2 \neq 0 \\ \eta_f \cdot |p_2| + C \cdot |\dot{x}_2| & \text{if } \dot{x}_2 = 0 \end{cases} \quad (2.45)$$

ενώ η πίεση δίδεται αναλόγως της ταχύτητας του εμβόλου,

$$p_1 = \begin{cases} p_2 - p_f & \text{if } \dot{x}_2 \geq 0 \\ p_2 - p_f & \text{if } \dot{x}_2 < 0 \end{cases} \quad (2.46)$$

Για την ενέργεια που απελευθερώνεται από το σύστημα ισχύει ότι

$$\dot{Q}_f = |\dot{V}| \cdot p_f \quad (2.47)$$

### 3 Simulink Blocks

Στη ενότητα αυτή, περιγράφονται μερικά σύνθετα blocks. Τα blocks αυτά είναι:

- Θερμοδυναμική ομάδα
- Γεωμετρική ομάδα
- ομάδα Μεταφοράς Θερμότητας

Η ιδέα της ύπαρξης των σύνθετων blocks οφείλεται στο γεγονός της απλούστευσης των συνδέσεων σε ένα πολύπλοκο μοντέλο, καθώς συγκεκριμένα blocks μεταξύ τους εμφανίζονται πάντα συνδεδεμένα μαζί σε πολλές περιπτώσεις.

Τα σύνθετα Blocks που εμφανίζονται σε αυτή τη διπλωματική εργασία είναι τα ακόλουθα:

- Θυρίδες Εισαγωγής, Βαλβίδα Εξαγωγής
- Ανοικτό Θερμοδυναμικό Σύστημα και Ιδιοτήτων Αερίων
- Σταθερών Ιδιοτήτων ρευστό και Ιδιοτήτων Αερίων
- Μεταφορά Θερμότητας Κυλίνδρου μηχανής
- Καύση
- Μονοκύλινδρο σύστημα
- Μοντέλο σύνδεσης πολλών κυλίνδρων

Ποιο συγκεκριμένα ο Πίνακας 1 περιλαμβάνει τα ονόματα των blocks που ομαδοποιούνται στις προαναφερθέντες ομάδες.

Πίνακας 1 Ομαδοποίηση Blocks

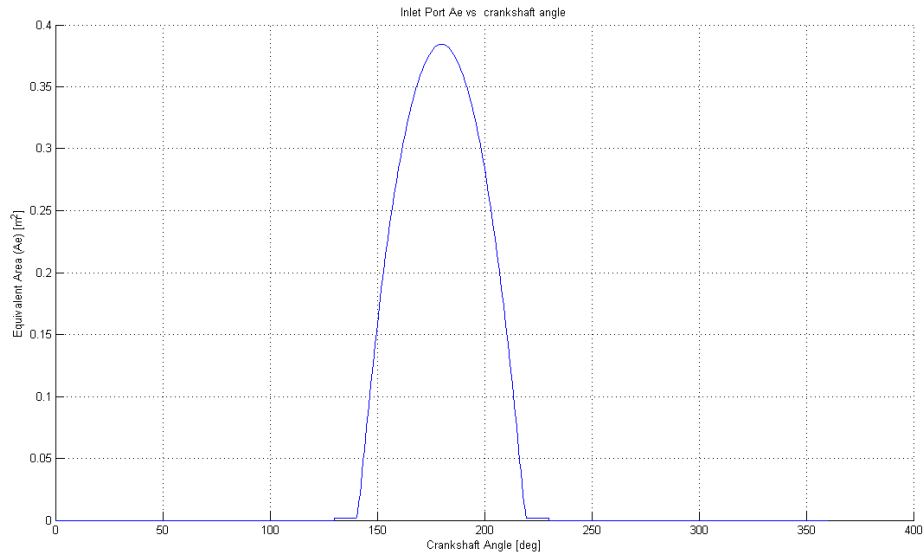
Ομάδα	Blocks
<b>Θερμοδυναμική</b>	Ιδιότητες Αερίου, Σταθερές Ιδιότητες Αερίου, Ανοικτό Θερμοδυναμικό σύστημα, Συμπιεστής, Εναλλάκτης Θερμότητας, Στρόβιλος, Καύση S – Curve, Υπερπληρωτής, Υπερπληρωτής MAN NA70/TO78, 8 Κύλινδροι, Ένας Κύλινδρος
<b>Γεωμετρική</b>	Γεωμετρία κυλίνδρου, ενεργειακές απώλειες, μη ελαστικός άξονας
<b>Μεταφοράς Θερμότητας</b>	Αγωγή, Συναγωγή, Ακτινοβολία, Μεταφορά θερμότητας κυλίνδρου

#### 3.1 Θυρίδα εισαγωγής και Βαλβίδα εξαγωγής

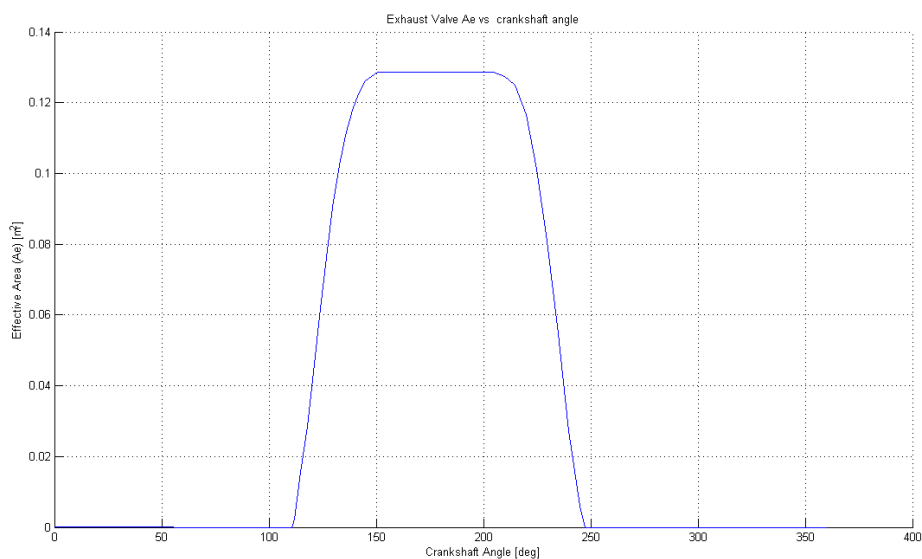
Σε πολλά σημεία της μηχανής το ρευστό ρέει μέσα από στενώσεις. Χαρακτηριστικές περιπτώσεις είναι όταν ο κρύος συμπιεσμένος αέρας εισαγωγής, εισέρχεται μέσω των θυρίδων στον κύλινδρο, αλλά και της περίπτωσης όπου το θερμό καυσαέριο εξέρχεται από τον κύλινδρο, κατευθυνόμενο στον οχετό εξαγωγής. Μία ροή ρευστού ιδανικά θεωρείται αδιαβατική και αναστρέψιμη. Επειδή στην πραγματικότητα δεν συναντιέται τέτοια περίπτωση, χρησιμοποιείται αντί για το πραγματικό άνοιγμα της βαλβίδα, ισοδύναμη επιφάνεια (effective area).



Οι θυρίδες εισαγωγής δεν περιλαμβάνουν συνδέσεις για τα μοντέλα της μεταφοράς θερμότητας καθώς θεωρείται ότι δεν έχουμε ανταλλαγή θερμότητας που να επηρεάζει τα αποτελέσματα της προσομοίωσης. Αντιθέτως όμως, δεν γίνεται να αγνοηθούν τέτοια φαινόμενα στη βαλβίδα εξαγωγής.

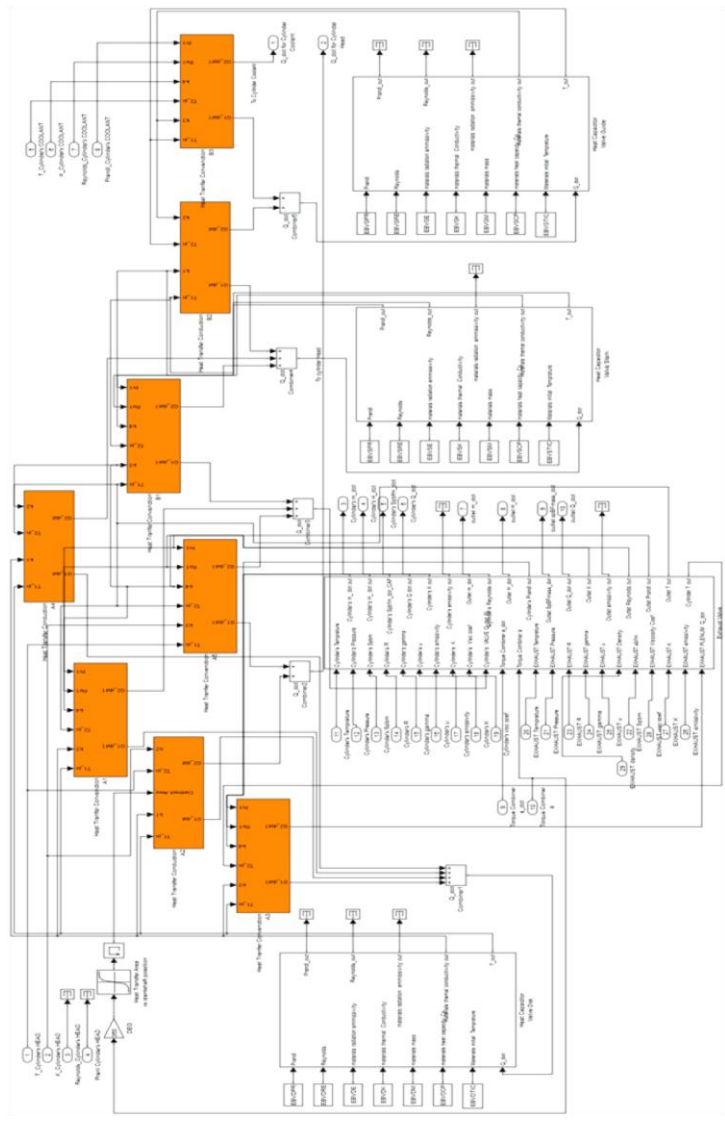


**Εικόνα 3-1** Πραγματικό άνοιγμα Θυρίδας εισαγωγής συναρτήσει στροφαλογωνίας



**Εικόνα 3-2** Πραγματικό άνοιγμα Βαλβίδας εξαγωγής συναρτήσει στροφαλογωνίας

Στην Εικόνα 3-1 και στην Εικόνα 3-2, απεικονίζεται ο χρονισμός των θυρίδων και της βαλβίδας εξαγωγής συναρτήσει της γωνίας του στροφάλου. Στην Εικόνα 3-3, απεικονίζεται η αναπαράσταση της βαλβίδα εξαγωγής, συνδεδεμένη με τα μοντέλα μεταφοράς θερμότητας σε MATLAB/Simulink.

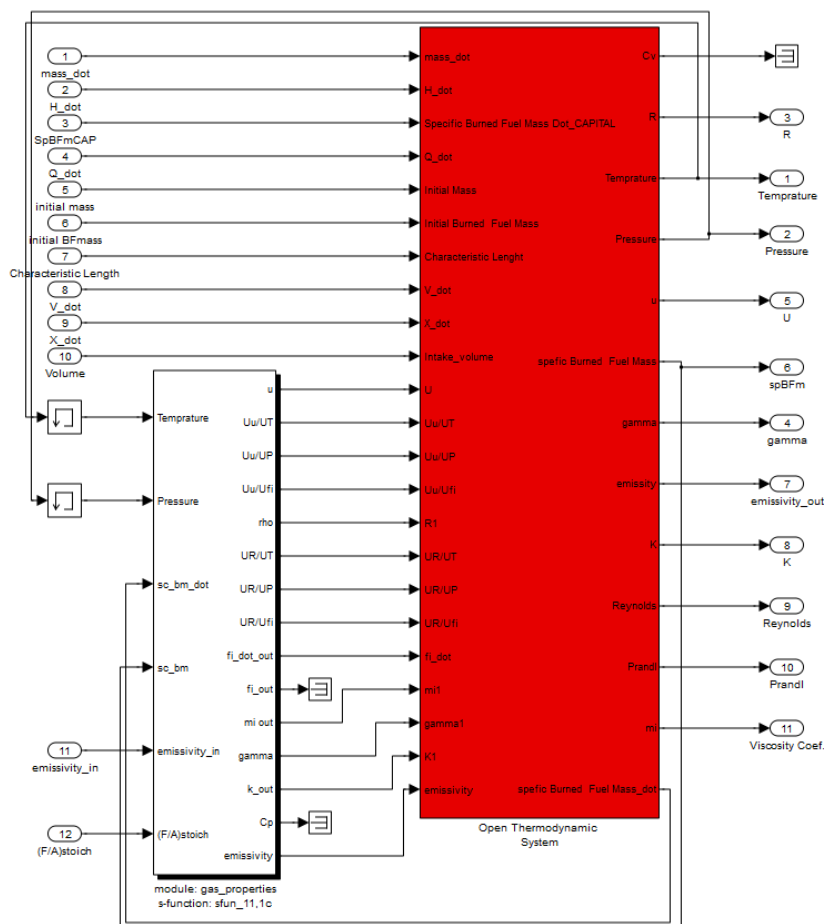


Εικόνα 3-3 Block: Βαλβίδα Εξαγωγής

### 3.2 Ανοικτό Θερμοδυναμικό Σύστημα και ιδιότητες Αερίων

Το μοντέλο αυτό περιλαμβάνει τα μοντέλα των ιδιοτήτων αερίων καθώς και τις εξισώσεις υπολογισμού της πίεσης και της θερμοκρασίας, όπως αυτές συναντιούνται στο κεφάλαιο 2 και περιγράφουν τα φαινόμενα που απαρτίζουν ένα ανοικτό θερμοδυναμικό σύστημα. Συγκεκριμένα παραδείγματα χρήσης αυτού του σύνθετου block είναι οι σχετοί εισαγωγής και εξαγωγής, αλλά και ο μεταβλητής γεωμετρίας όγκος του κυλίνδρου λόγω της κίνησης του εμβόλου.

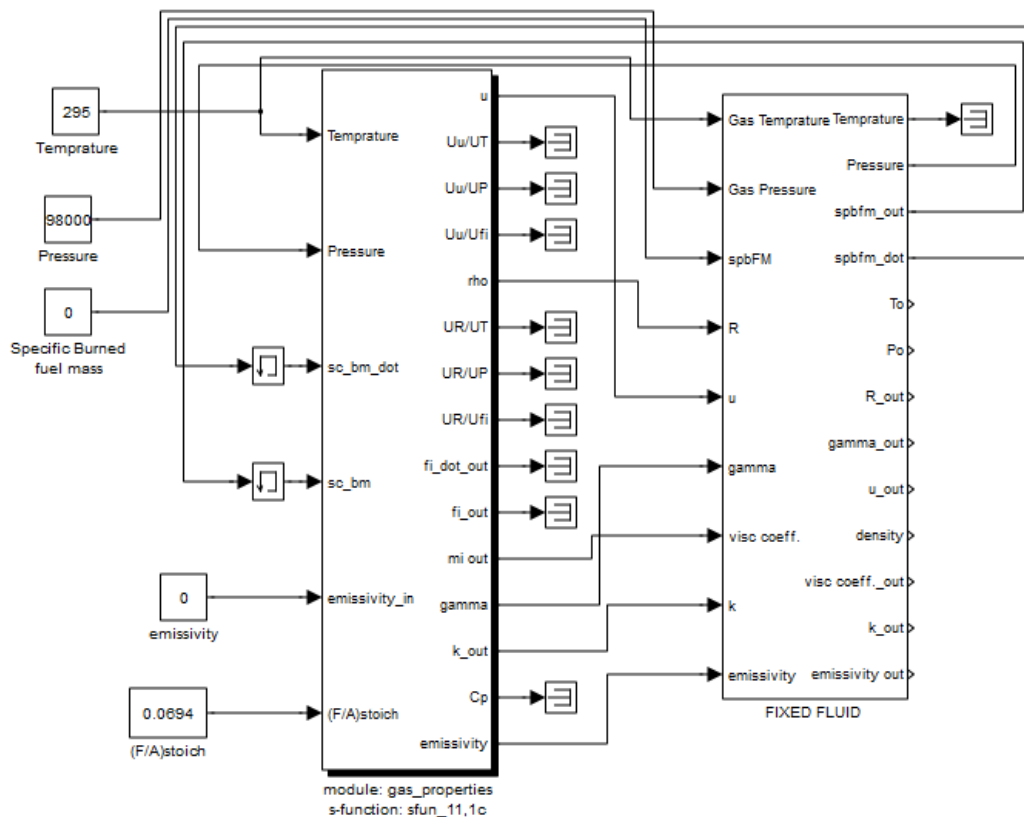
Το μοντέλο του ανοικτού θερμοδυναμικού συστήματος έχει δώδεκα εισόδους και τέσσερις εξόδους ενώ συνδέεται μέσα στο μεγάλο block με το μοντέλο των ιδιοτήτων του αερίου. Τα στοιχεία που απαιτούν τα μοντέλα μεταφοράς θερμότητας υπολογίζονται και τροφοδοτούνται σε αυτά μέσω των κατάλληλων συνδέσεων.



Εικόνα 3-4 Block: Ανοικτό θερμοδυναμικό σύστημα

### 3.3 Σταθερές Ιδιότητες και Ιδιότητες Αερίων

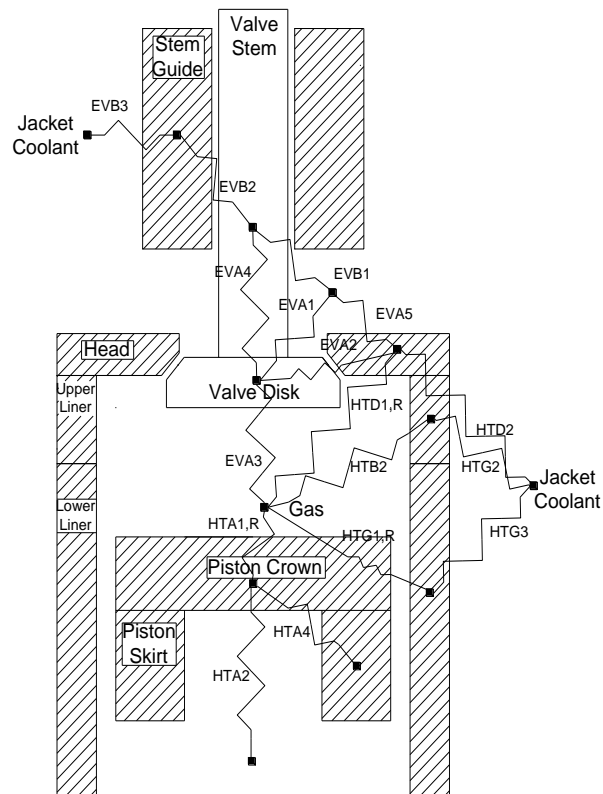
Στην ίδια φιλοσοφία με την παράγραφο 0 κινείται και το συγκεκριμένο σύνθετο block. Η ουσιαστική διαφορά τους είναι ότι το συγκεκριμένο, δεν λαμβάνει υπ' όψιν του όλες τις παραμέτρους που υπολογίζει το μοντέλο των ιδιοτήτων του αερίου. Αυτό συμβαίνει γιατί το συγκεκριμένο μοντέλο των σταθερών ιδιοτήτων χρησιμοποιείται για τη μοντελοποίηση αερίων που οποιαδήποτε προσθήκη ενέργειας σε αυτά λόγω του απείρου όγκου που καταλαμβάνουν, δεν θα τους επιδράσει σε καμία ιδιότητα τους. Παραδείγματα που χρησιμοποιείται αυτό το σύνθετο block είναι οι συνθήκες στο φίλτρο του συμπιεστή (ατμοσφαιρικός αέρας) ή μετά την έξοδο του στροβίλου (φουγάρο και ατμόσφαιρα). Η σχηματική αναπαράσταση του συγκεκριμένου block γίνεται στην Εικόνα 3-5.



Εικόνα 3-5 Block: Σταθερές ιδιότητες και Ιδιότητες Αερίου

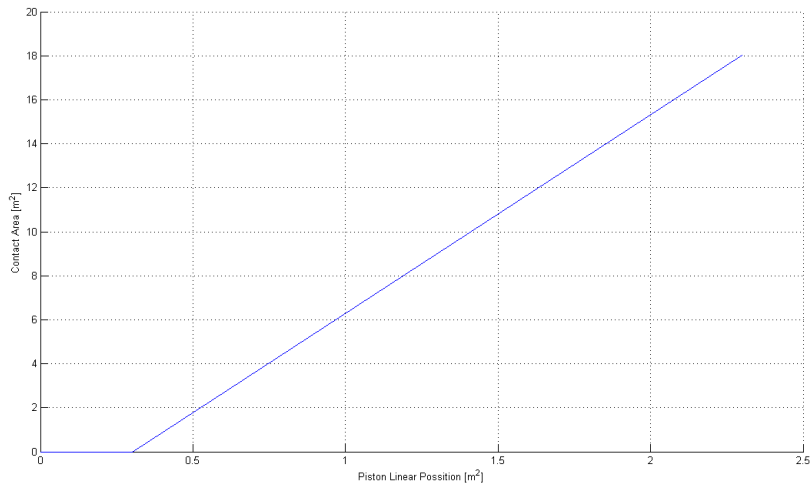
### 3.4 Μεταφορά θερμότητας στον κύλινδρο

Μέσα στον κύλινδρο εμφανίζονται και οι τρεις τρόποι μεταφοράς θερμότητας. Λόγω της καύσης το ζεστό αέριο θερμαίνει τα τοιχώματα του κυλίνδρου (χιτώνιο), τη κεφαλή του εμβόλου, το καπάκι καθώς και τη βάση και το υπόλοιπο στέλεχος της βαλβίδας εξαγωγής. Σχηματικά το μοντέλο, όπως αυτό προκύπτει από την ανάλυση του σύμφωνα με τη θεωρία των θερμικών αντιστάσεων φαίνεται στην Εικόνα 3-6.

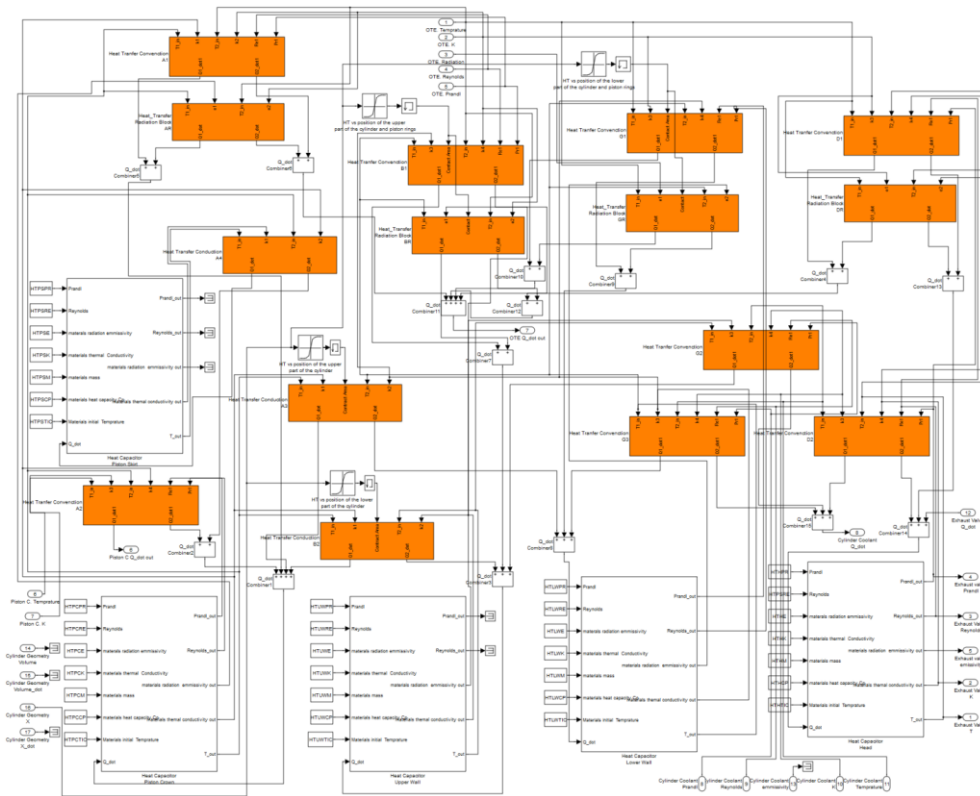


Εικόνα 3-6 Μοντέλο μεταφοράς θερμότητας μέσα στον κύλινδρο

Λόγω του ότι το έμβολο αλλάζει συνεχώς θέση, η επιφάνεια επαφής μεταβάλλεται συνεχώς. Έτσι οποιοδήποτε μοντέλο απαιτεί τη επιφάνεια, διαβάζει κάποιον χάρτη με τη μεταβολή της κάνοντας όποτε απαιτηθεί γραμμική παρεμβολή. Ένα χαρακτηριστικό παράδειγμα τέτοιου χάρτη δίδεται στην Εικόνα 3-7 ενώ η μοντελοποίηση της μεταφοράς θερμότητας μέσα στον κύλινδρο φαίνεται στην Εικόνα 3-8.



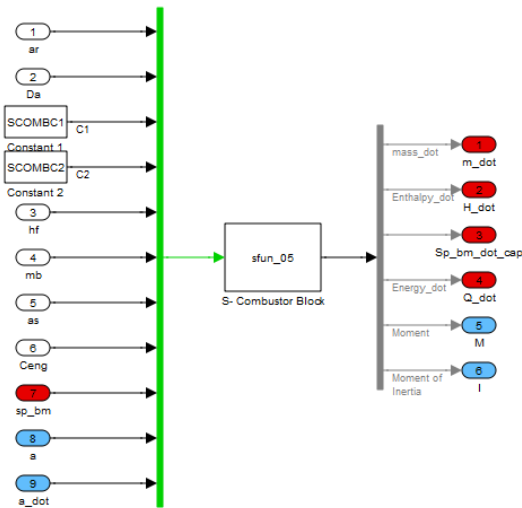
Εικόνα 3-7 Παράδειγμα χάρτη μεταβλητής επιφάνειας επαφής



Εικόνα 3-8 Block: μεταφορά θερμότητας στον κύλινδρο

### 3.5 Καύση

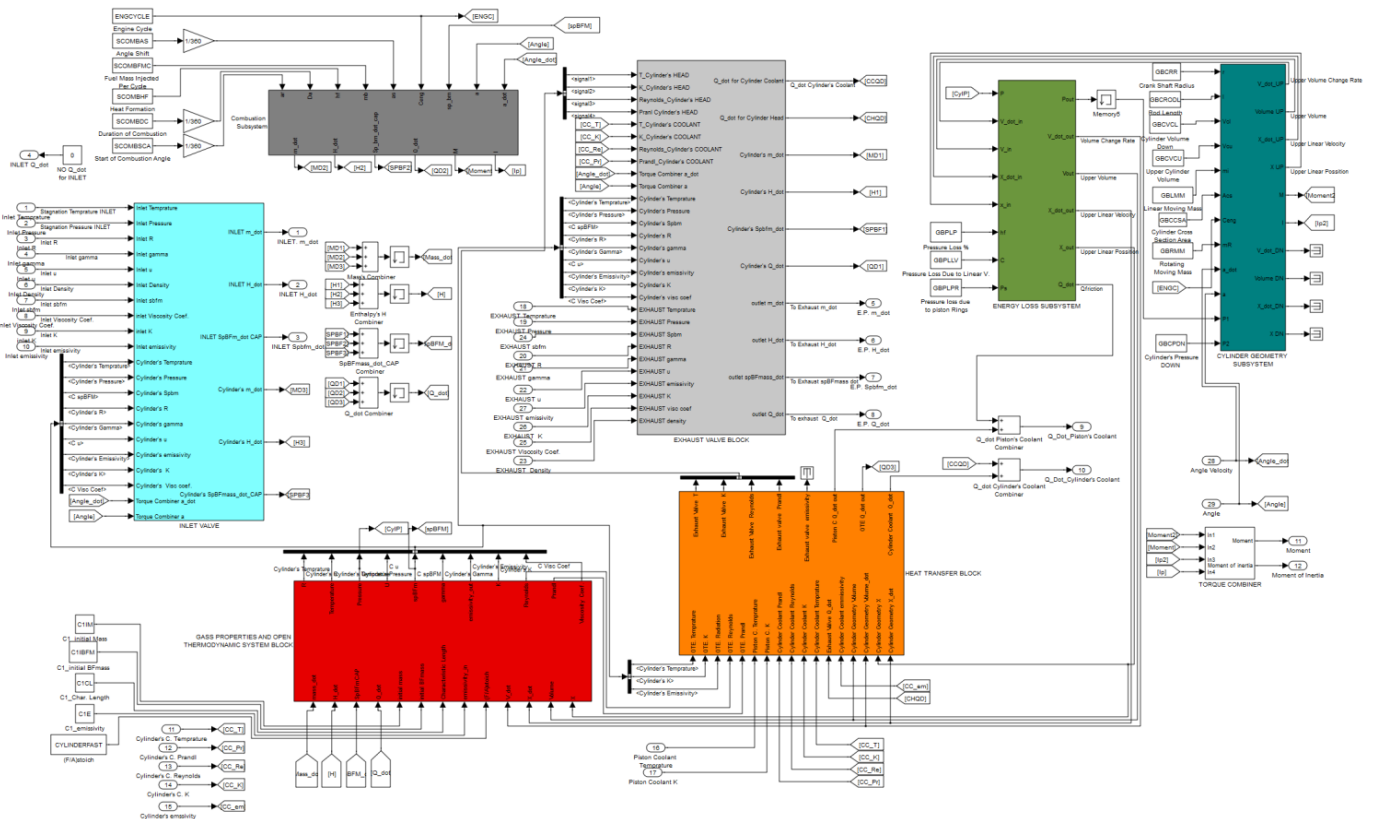
Το μοντέλο καύσης που χρησιμοποιείται σε αυτή τη διπλωματική εργασία είναι απλοϊκό και στηρίζεται στην S – curve. Το μοντέλο αυτό είναι τυπικά μία καμπύλη απελευθέρωσης θερμότητας. Απαιτεί σαν μοντέλο στοιχεία όπως η ενθαλπία των καυσαερίων (προϊόντα της καύσης), μάζα εγχυόμενου καυσίμου αλλά και της γωνίες έναρξης και λήξης της καύσης. Προσδιορίζεται από δύο σταθερές οι οποίες δίνουν σχήμα στην καμπύλη, μεταβάλλοντας τα χαρακτηριστικά της καύσης. Η σχηματική αναπαράσταση του μοντέλου γίνεται στην Εικόνα 3-9.



Εικόνα 3-9 Block: S - curve

### 3.6 Κύλινδρος

Το μοντέλο του κυλίνδρου περιλαμβάνει όλα τα μηχανικά μέρη όπως είναι το ποδάρι, το κομβίο, η κεφαλή του εμβόλου, το χιτώνιο, οι θυρίδες, ο εγχυτήρας και η βαλβίδα εξαγωγής. Ο όγκος του κυλίνδρου περιγράφεται από το ανοικτό θερμοδυναμικό σύστημα, καθώς μάζα μεταφέρεται από και προς αυτό από τη βαλβίδα και τις θυρίδες αντίστοιχα. Η μεταφορά μάζας συμβαίνει εξαιτίας του γεγονότος όπου η πίεση μέσα στον κύλινδρο είναι διαφορετική από τις πιέσεις που επικρατούν στους οχετούς εισαγωγής και εξαγωγής. Λόγω της διαφοράς αυτής από τη θυρίδα εισέρχεται στο σύστημα συμπιεσμένος κρύος αέρας που διώχνει τα καυσαέρια ενώ παραμένει και μέρος του προκειμένου να συμπιεστεί ώστε να αναμιχθεί με το καύσιμο αργότερα. Μέσα στον κύλινδρο λόγω της καύσης αυξάνεται η ενέργεια του και παράγεται μηχανικό έργο που εμφανίζεται ως δύναμη στο έμβολο. Η μεταφορά θερμότητας γίνεται μέσω του μοντέλου 0. Η Εικόνα 3-10 παρουσιάζει το μοντέλο του κυλίνδρου.



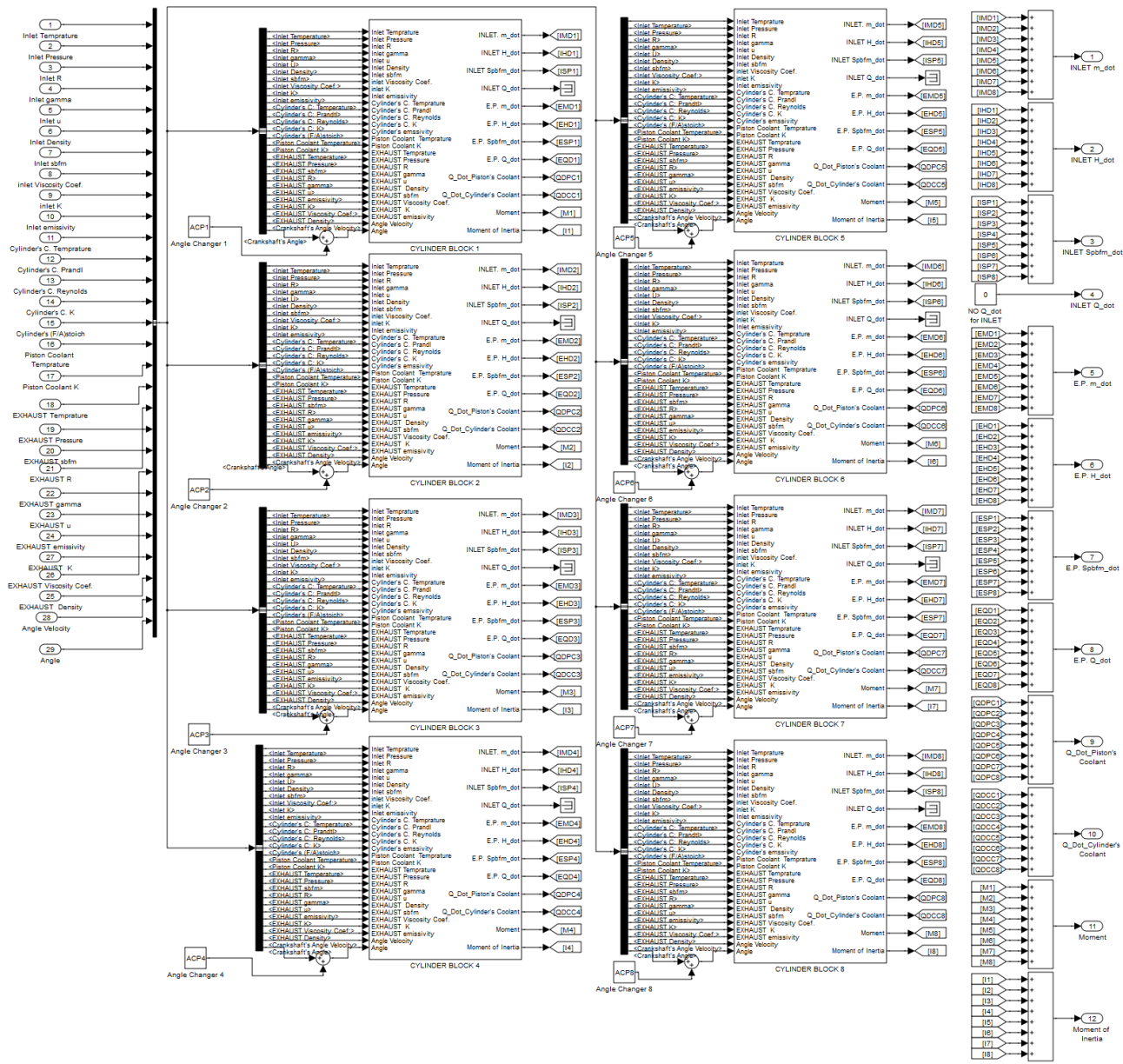
Εικόνα 3-10 Block: Ένας κύλινδρος



### 3.7 Μοντέλο οκτώ κυλίνδρων

Σε μία πραγματική προσομοίωση, η λειτουργία μίας πολύ-κύλινδρης μηχανής προσομοιάζεται. Για αυτή τη περίπτωση ένα μοντέλο για τους κυλίνδρους της MAN 8K90MC-C6 αναπτύχθηκε.

Η διαφορά στους κυλίνδρους έγκειται μόνο στο γεγονός ότι ο κάθε ένας λειτουργεί σε με διαφορετική γωνία φάσης ως προς τον στροφαλοφόρο. Στην συγκεκριμένη ναυτική μηχανή η φάση των οκτώ κυλίνδρων είναι 45 μοίρες και αυτό γίνεται προκειμένου να υπάρχει μία ομαλή παραγωγή ροπής αλλά και ταυτόχρονα να αποσβένονται οι ταλαντώσεις που αναπτύσσονται λόγω της παλινδρομικής κίνησης των εμβόλων. Στην Εικόνα 3-11, παρουσιάζεται το μοντέλο των οκτώ κυλίνδρων.

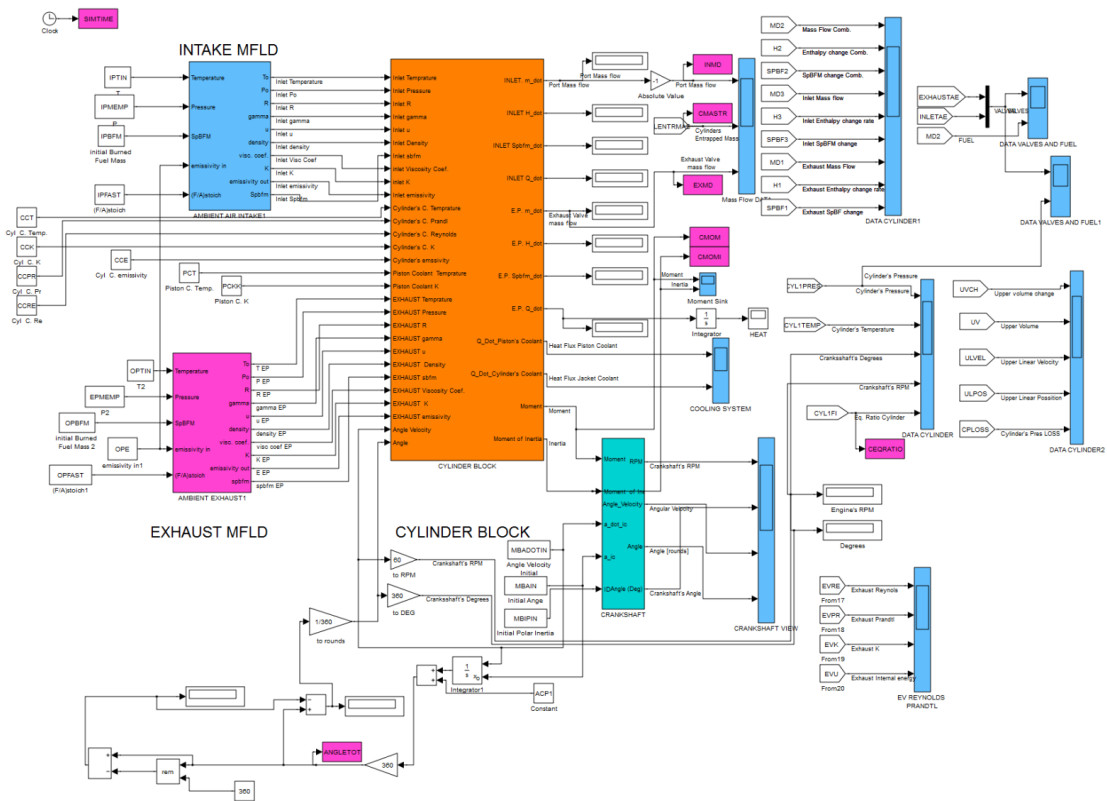


Εικόνα 3-11 Κύλινδροι MAN 8K90MC-C6

## 4 Αποτελέσματα προσομοίωσης ενός κυλίνδρου

Αν και ο αρχικός στόχος της διπλωματικής εργασίας ήταν να μοντελοποιηθεί και να προσομοιωθεί η λειτουργία της 8 κύλινδρης μηχανής, συνδεδεμένη με τους 3 υπερπληρωτές, η προσομοίωση δεν στάθηκε δυνατή λόγω χρονικών περιορισμών στην επεξεργασία των δεδομένων εισόδου αλλά και στην βελτιστοποίηση των διαφόρων υπό-μοντέλων. Έτσι λοιπόν, πραγματοποιήθηκαν προσομοιώσεις για ένα κύλινδρο κατά τον κλειστό κύκλο, για το 90% του φορτίου στις 100.5 ΣΑΛ, για το 75% του φορτίου στις 92.4 ΣΑΛ και για το 50% του φορτίου στις 82.5 ΣΑΛ.

### Σχέδιο διάταξης προσομοίωσης ενός κυλίνδρου



Εικόνα 4-1 Διάταξη προσομοίωσης

### Αποτελέσματα προσομοίωσης ενός κυλίνδρου

Σε αυτή την ενότητα, παρουσιάζονται τα αποτελέσματα από την προσομοίωση του ενός κυλίνδρου της μηχανής. Τα αποτελέσματα συγκρίθηκαν με το πρόγραμμα MoTher αναπτυγμένο από το E.N.M.. Motor Thermodynamics, είναι ένα πρόγραμμα για την προσομοίωση και την πρόβλεψη των επιδόσεων μηχανών, σύμφωνα με την αρχή των όγκων ελέγχου. Το πρόγραμμα αυτό βρίσκεται υπό συνεχή βελτίωση από το 1985 (LME, 2008).

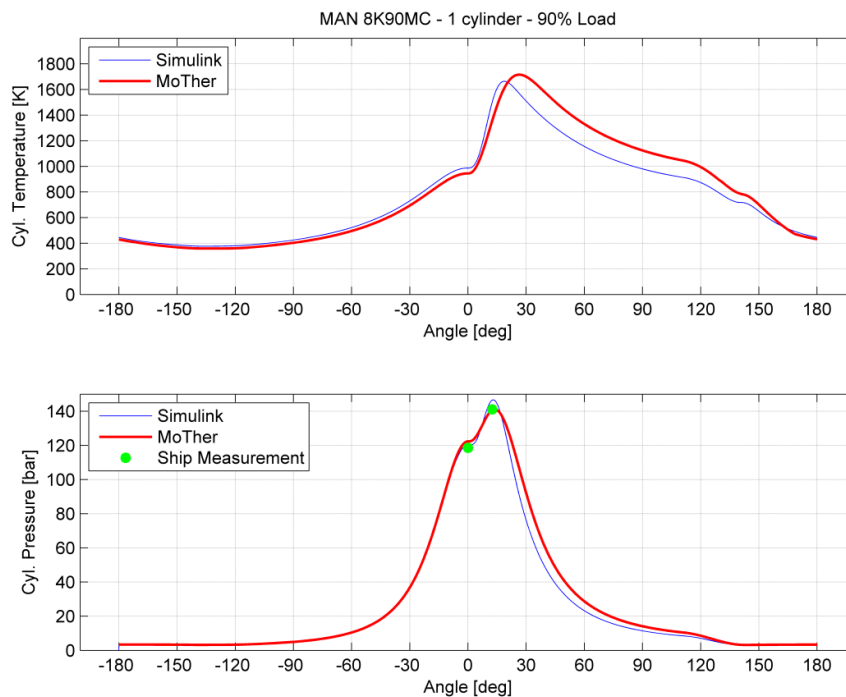
Προκειμένου να χωριστεί ο κύκλος της μηχανής σε φάσεις, εισάγεται ο Πίνακας 2.

Πίνακας 2 Φάσεις κύκλου

Γωνία	Φάση
0.0° – 44.8°	Καύση
44.8° – 110.8°	Αποτόνωση
110.8° – 247.2°	Εναλλαγή Αερίων
247.2° – 360.0°	Συμπίεση

### Περίπτωση 1<sup>η</sup>: 90% φορτίου στις 100.5 ΣΑΑ

Η Εικόνα 4-2 δείχνει την αναπτυσσόμενη θερμοκρασία και πίεση στον κύλινδρο συναρτήσει της γωνίας στροφάλου.

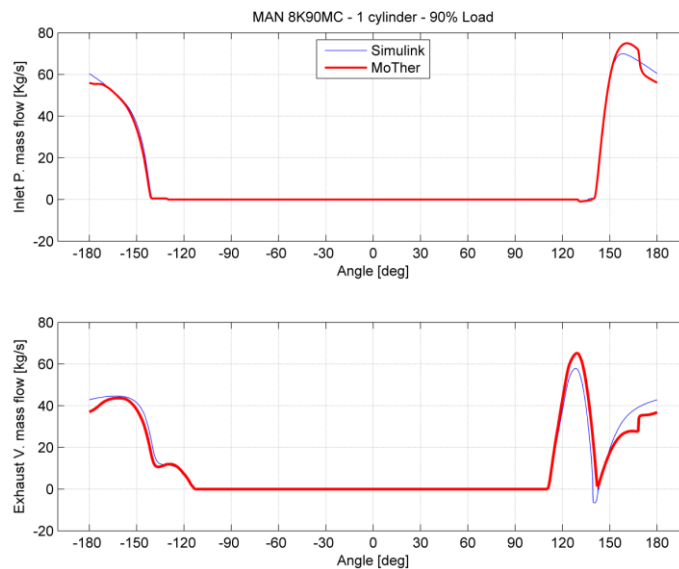


Εικόνα 4-2 Ίχνος θερμοκρασίας (πάνω) και πίεσης μέσα στον κύλινδρο

Όπως φαίνεται στο διάγραμμα αυτό, το ίχνος της πίεσης του Simulink έχει μία πολύ μικρή απόκλιση κατά τη διάρκεια της περιόδου της συμπίεσης σε σύγκριση με το MoTher. Όταν το έμβολο φτάνει το άνω νεκρό σημείο (ΑΝΣ), η πίεση (πίεση συμπίεσης αφού αναπτύσσεται εξαιτίας των μηχανικών μερών του κυλίνδρου), έχει απόκλιση από αυτή του MoTher ενώ είναι λίγο μεγαλύτερη από αυτή της μέτρησης<sup>1</sup>. Όπως φαίνεται από το διάγραμμα αυτό, η υπολογιζόμενη πίεση από το Simulink είναι μικρότερη από αυτή του MoTher, εξαιτίας του γεγονότος ότι ο κύλινδρος έχει μικρότερη εγκλωβισμένη μάζα. Η απόκλιση αυτή οφείλεται στο γεγονός ότι κατά τη διάρκεια της εναλλαγής των αερίων το Simulink υπολογίζει μεγαλύτερες θερμοκρασίες από ότι το MoTher. Η μοντελοποίηση της μεταφοράς θερμότητας στο Simulink δεν γίνεται με τις ίδιες σταθερές με του MoTher, καθώς το δεύτερο χρησιμοποιεί διαφορετικά μοντέλα. Εκτός αυτού, οι σταθερές στο

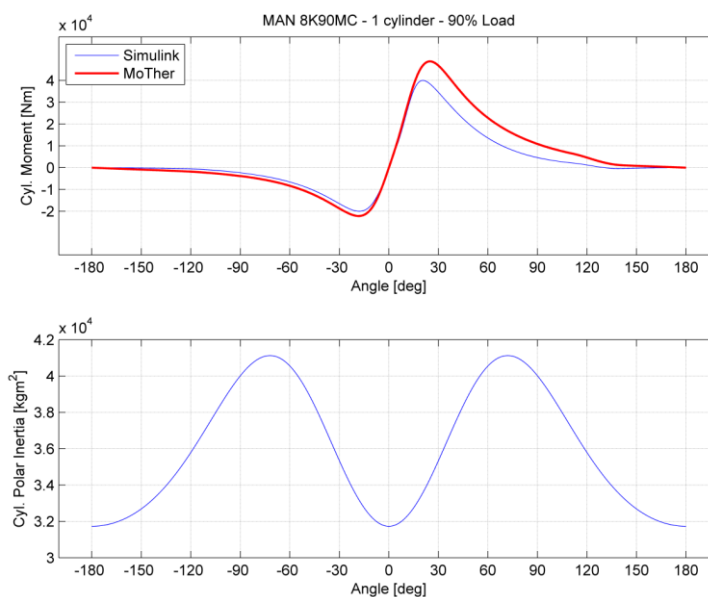
<sup>1</sup> Όπως μετρήθηκε πάνω στο πλοίο. Τα δεδομένα είναι διαθέσιμα στο E.N.M.

Simulink, έχουν ρυθμιστεί με εμπειρικό τρόπο, κάτι που προκαλεί διαφορές με τα αποτελέσματα του MoTher. Επίσης, παρατηρήθηκε απόκλιση κατά τη διάρκεια αλλά και μετά τη καύση, κάτι το οποίο οδηγεί στο συμπέρασμα ότι το μοντέλο της καύσης που αναπτύχθηκε και χρησιμοποιήθηκε δεν προσομοιάζει σωστά την φυσική διεργασία στον κινητήρα. Επίσης παρατηρήθηκε και μικρή διαφορά στην εναλλαγή των μαζών κάτι το οποίο επηρεάζει την ποσότητα της εγκλωβισμένης μάζας, που μειώνει την πίεση συμπίεσης κατ' επέκταση. Η διαφορά αυτή φαίνεται στην Εικόνα 4-3.



**Εικόνα 4-3 Μεταφορά μάζας από την θυρίδα εισαγωγής (πάνω) και από την βαλβίδα εξαγωγής**

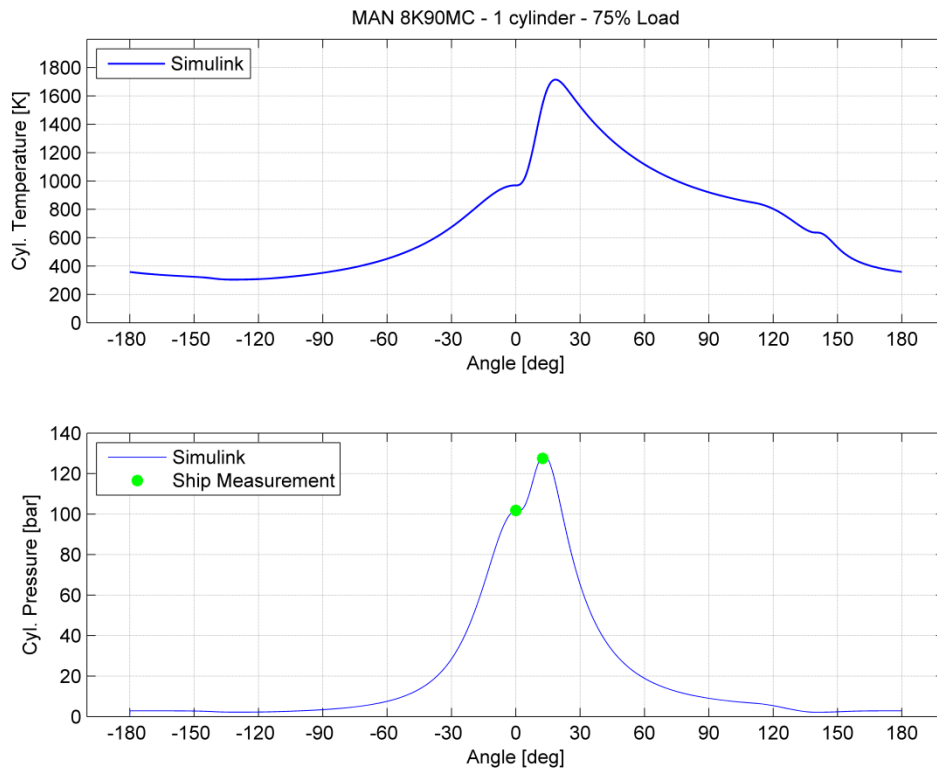
Οι διαφορές στην πίεση, έχουν άμεσο αποτέλεσμα στην αναπτυσσόμενη ροπή. Έτσι λόγω του ότι η προσομοίωση με το Simulink, δίνει χαμηλότερο ίχνος πίεσης, η αναπτυσσόμενη ροπή από τον κύλινδρο είναι μικρότερη, όπως φαίνεται στην Εικόνα 4-4.



**Εικόνα 4-4 Αναπτυσσόμενη ροπή (πάνω) και πολική ροπή αδρανείας κυλίνδρου**

### Περίπτωση 2<sup>η</sup>: 75% φορτίου στις 94.6 ΣΑΛ

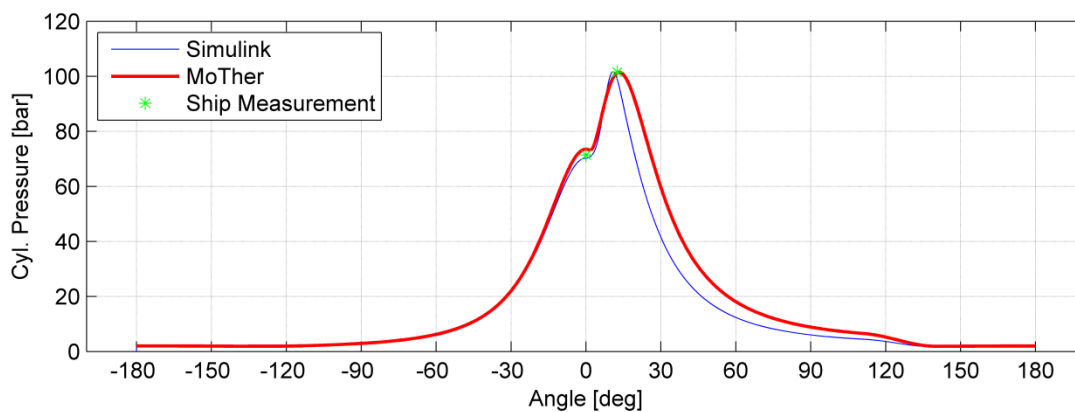
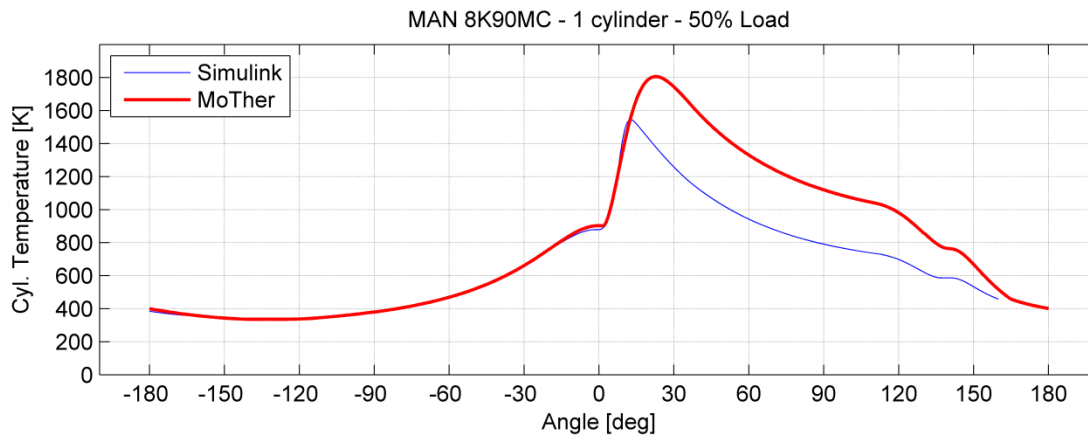
Σε αυτή τη περίπτωση παρουσιάζονται τα αποτελέσματα της προσομοίωσης για το 75% του φορτίου στις 94.6 ΣΑΛ. Η σύγκριση με τα δεδομένα του MoTher δεν ήταν δυνατή λόγω της έλλειψης δεδομένων για αυτό το φορτίο. Τα αποτελέσματα για τη μη παραμετρική προσομοίωση παρουσιάζονται στην Εικόνα 4-5.



Εικόνα 4-5 Αναπτυσσόμενη θερμοκρασία (πάνω) και πίεση στον κύλινδρο (75%)

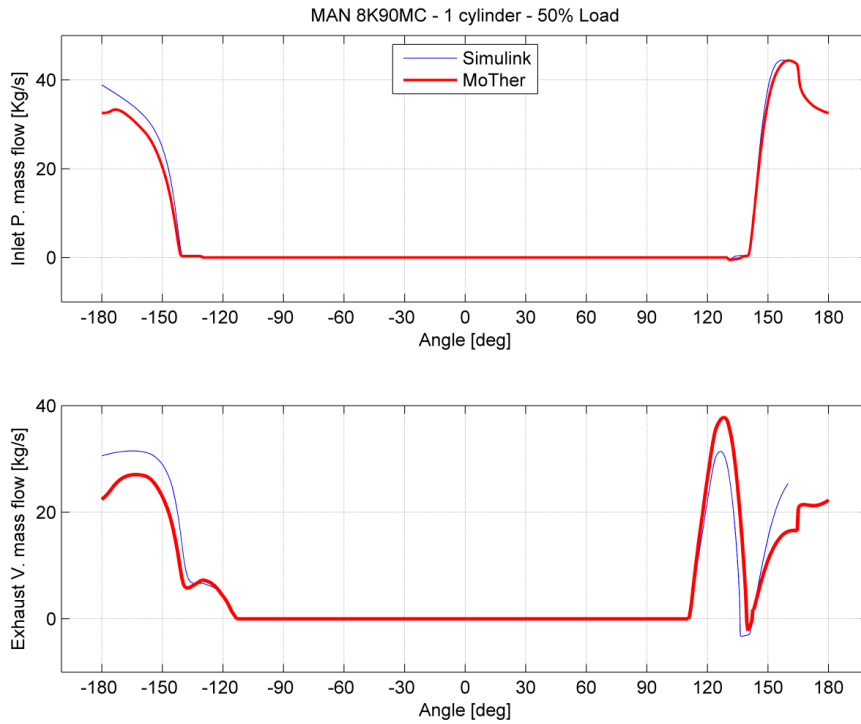
### Περίπτωση 3<sup>η</sup>: 50% φορτίου στις 82.5 ΣΑΛ

Σε αυτή την ενότητα παρουσιάζονται τα αποτελέσματα για το μερικό φορτίο της μηχανής (50%) στις 82.5 ΣΑΛ. Η Εικόνα 4-6 δείχνει την θερμοκρασία και την πίεση που αναπτύσσεται στον κύλινδρο συναρτήσει της γωνίας στροφάλου για το Simulink και το MoTher.

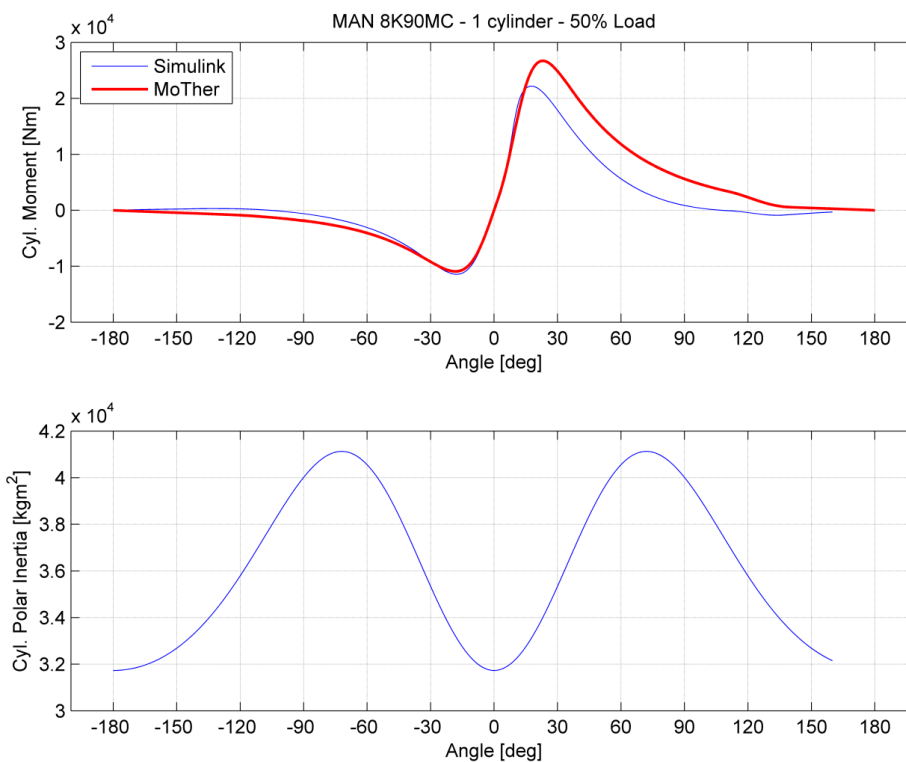


Εικόνα 4-6 Αναπτυσσόμενη θερμοκρασία (πάνω) και πίεση μέσα στον κύλινδρο (50%)

Συγκρίνοντας τα παραπάνω ίχνη, παρατηρείται ότι υπάρχει μεγαλύτερη απόκλιση στα αποτελέσματα του 50% φορτίου σε σχέση με το 90%. Λόγω του ότι το ίχνος της πίεσης είναι σημαντικά χαμηλότερο κυρίως στη φάση της αποτόνωσης, η θερμοκρασία σε αυτή τη φάση είναι πολύ χαμηλότερη για τη προσομοίωση του Simulink. Στις Εικόνα 4-7 και Εικόνα 4-8, παρουσιάζονται τα ίχνη της μεταφοράς μάζας από τις θυρίδες εισαγωγής και τη βαλβίδα εξαγωγής όπως επίσης και η αναπτυσσόμενη ροπή και η πολική ροπή αδρανείας του κυλίνδρου. Σημαντική απόκλιση παρατηρείται στις γωνίες 20° μέχρι 150° λόγω της διαφοράς πίεσης μετά τη καύση. Όπως έχει περιγραφεί στο κεφάλαιο 2 ενότητα 2.4 η διαφορά στην αναπτυσσόμενη πίεση συμπαρασύρει την αναπτυσσόμενη ροπή καθώς η δύναμη που αναπτύσσεται στο έμβολο ορίζεται ως η διαφορά της αναπτυσσόμενης πίεσης από το αέριο μείον τη πίεση του συμπιεσμένου αέρα που περνάει από τις θυρίδες εκείνη τη στιγμή κάτω από το έμβολο.



Εικόνα 4-7 Μεταφορά μάζας από τις θυρίδες εισαγωγής (πάνω) και τη βαλβίδα εξαγωγής



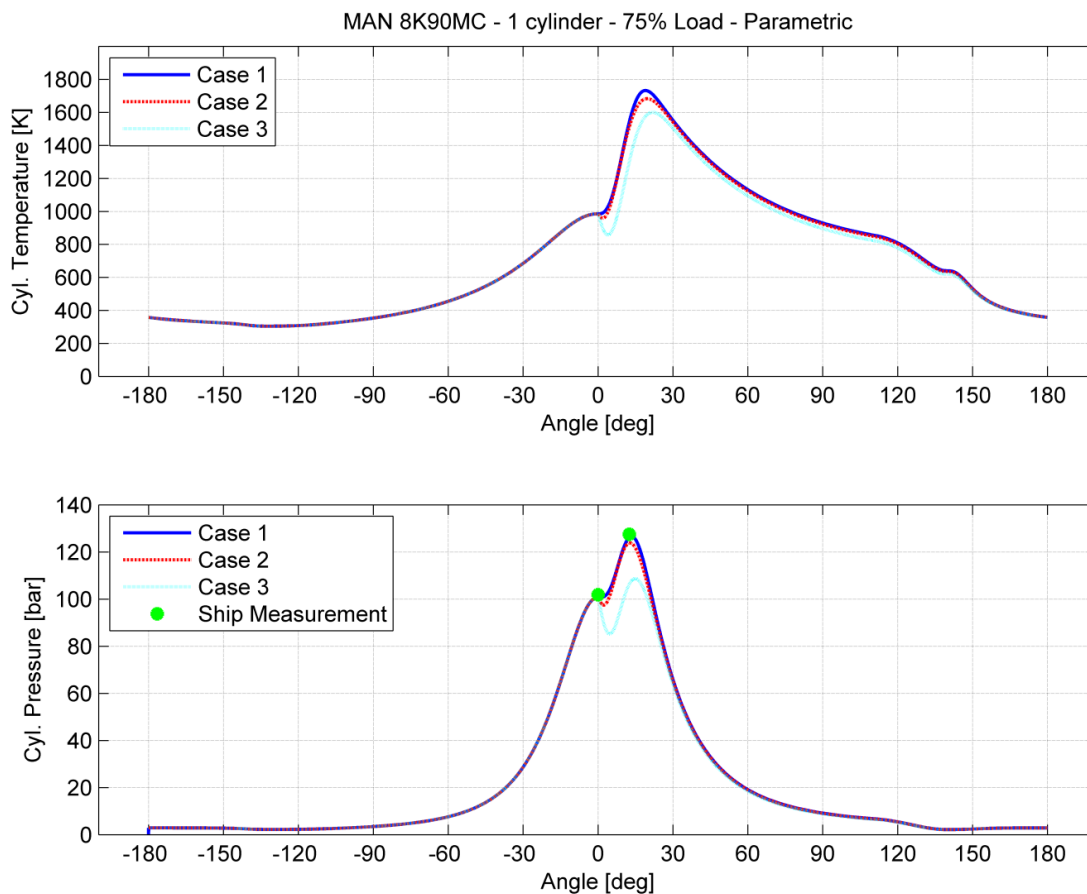
Εικόνα 4-8 Αναπτυσσόμενη ροπή (πάνω) και πολική ροπή αδρανείας κυλίνδρου

### Παραμετρικές προσομοιώσεις για το 75% φορτίου στις 94.6 ΣΑΛ

Παραμετρικές προσομοιώσεις πραγματοποιήθηκαν στο 75% του φορτίου. Στη πρώτη ομάδα παραμέτρων, τροποποιήθηκαν τιμές όπως οι σταθερές της καύσης, η αρχή και το η διάρκεια της συμπίεσης, που επηρεάζουν το ρυθμό της καύσης όπως φαίνεται στον Πίνακα 3. Οι άλλες δύο προσομοιώσεις πραγματοποιήθηκαν με τροποποιημένη την ποσότητα εγχυόμενου καυσίμου (Περίπτωση 1 και 2), με σταθερές τις υπόλοιπες παραμέτρους (Πίνακας 4). Στην τελευταία προσομοίωση (περίπτωση 3 και 4), η μάζα του εγχυόμενου καυσίμου παρέμεινε σταθερή ενώ τροποποιήθηκε ο επιζήμιος όγκος (Πίνακας 5).

Πίνακας 3 Σταθερές καύσης για διάφορες περιπτώσεις

Μεταβλητές	Περιπτώσεις		
	Περίπτωση 1	Περίπτωση 2	Περίπτωση 3
$a_r$	0	2	4
$C_1$	30	26.7	15.6
$C_2$	2.7	2	2

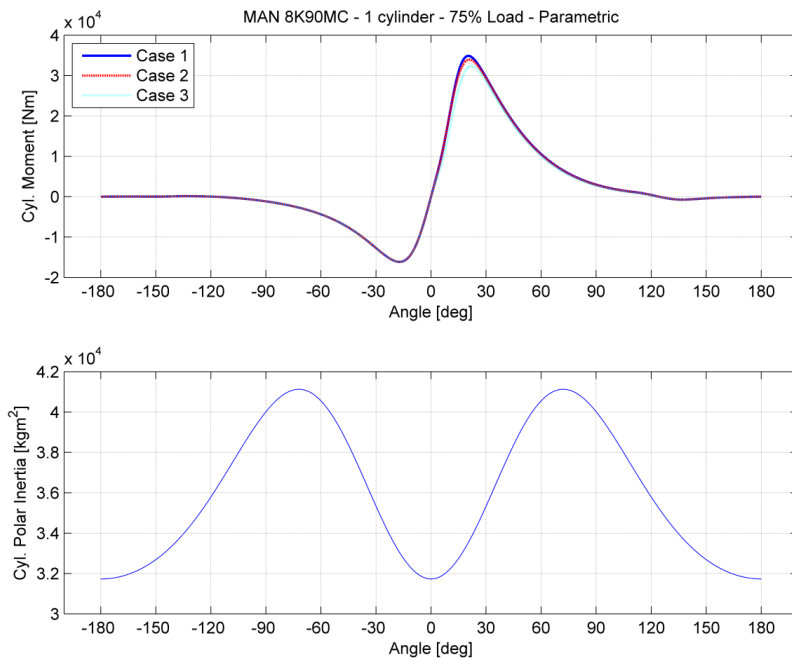


Εικόνα 4-9 Αναπτυσσόμενη θερμοκρασία (πάνω) και πίεση στον κύλινδρο για περιπτώσεις

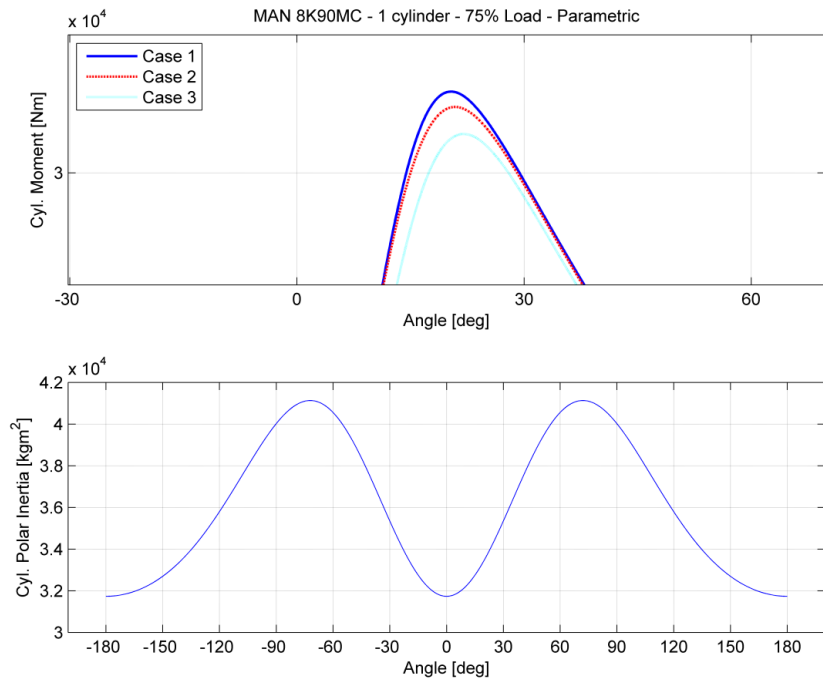
Η Εικόνα 4-9 δείχνει την αναπτυσσόμενη θερμοκρασία και πίεση για διαφορετικές σταθερές καύσης αλλά και για διαφορετικές γωνίες έναρξης καύσης. Όπως φαίνεται στο



σχήμα, οι 4 μίρες προκαλούν μία βύθιση στη πίεση λόγω του ότι πριν την έναυση το έμβολο έχει μετακινηθεί από το ΑΝΣ και η αποτόνωση που παρατηρείται δεν είναι αμελητέα. Αυτό έχει ως αποτέλεσμα ο κύλινδρος να μην μπορεί να επιτύχει τη μέγιστη πίεση ανά κύκλο. Για την περίπτωση 2, το ίχνος πίεσης είναι σαν το ίχνος της περίπτωσης 1, αλλά και πάλι δεν επιτυγχάνεται η μέγιστη πίεση. Οι διαφορές αυτές στην πίεση, οδηγούν και σε σφάλματα στον υπολογισμό της αναπτυσσόμενης ροπής, όπως φαίνεται στις εικόνες Εικόνα 4-10 και Εικόνα 4-11.



**Εικόνα 4-10 Αναπτυσσόμενη ροπή (πάνω) και πολική ροπή αδρανείας παραμετρικών προσομοιώσεων**



Εικόνα 4-11 Εστίαση σε περιοχή της Εικόνα 4-10

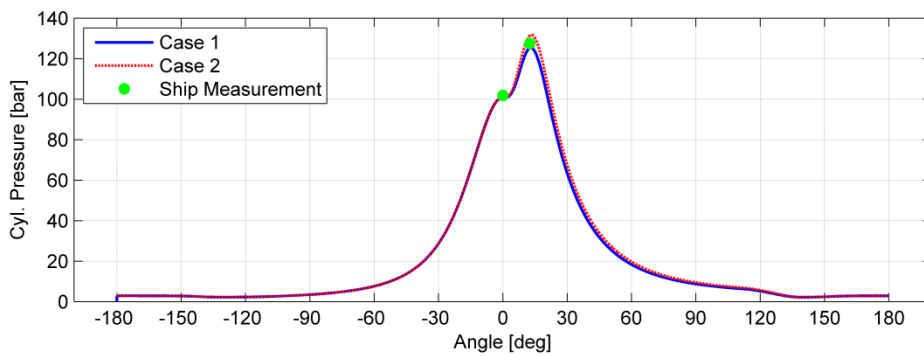
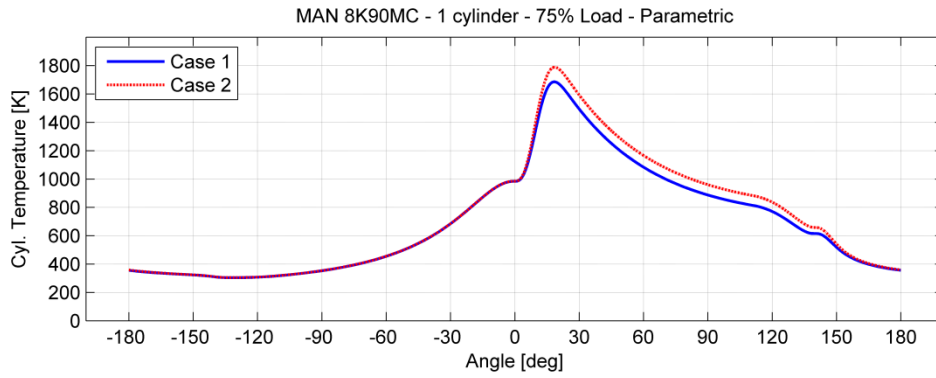
Πίνακας 4 Σταθερές καύσης και μάζα εγχυόμενου καυσίμου

Μεταβλητές	Περιπτώσεις	
	Περίπτωση 1	Περίπτωση 2
$a_r$	0	0
$C_1$	30	30
$C_2$	2.7	2.7
<b>Μάζα καυσίμου</b>	0.090	0.102

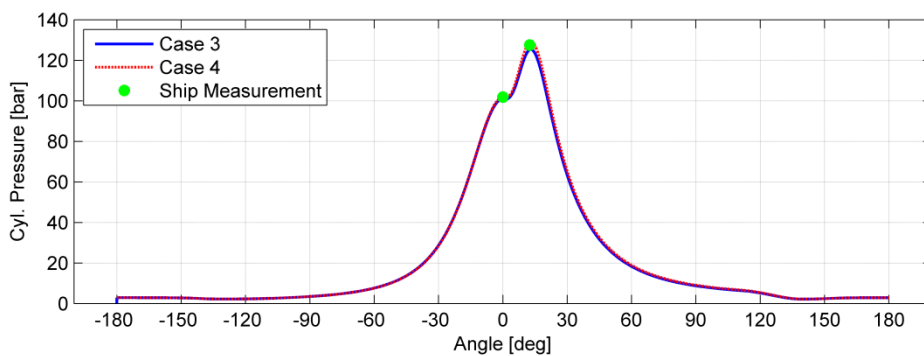
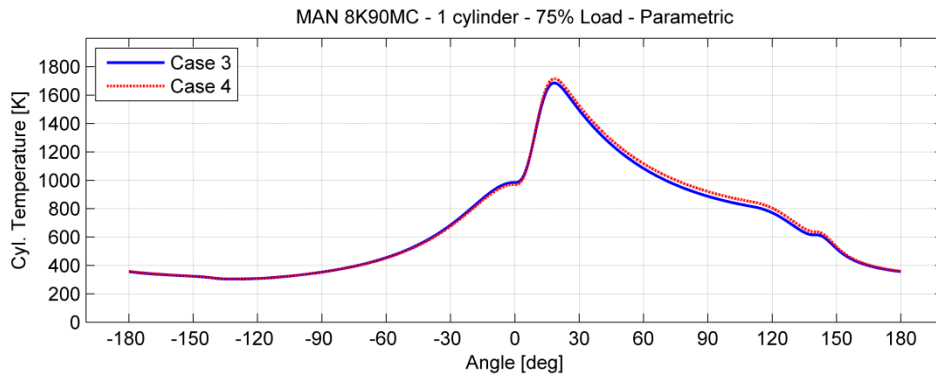
Πίνακας 5 Σταθερές καύσης και επιζήμιος όγκος

Μεταβλητές	Περιπτώσεις	
	Περίπτωση 3	Περίπτωση 4
$a_r$	0	0
$C_1$	30	30
$C_2$	2.7	2.7
<b>Επιζήμιος όγκος</b>	0.089	0.093

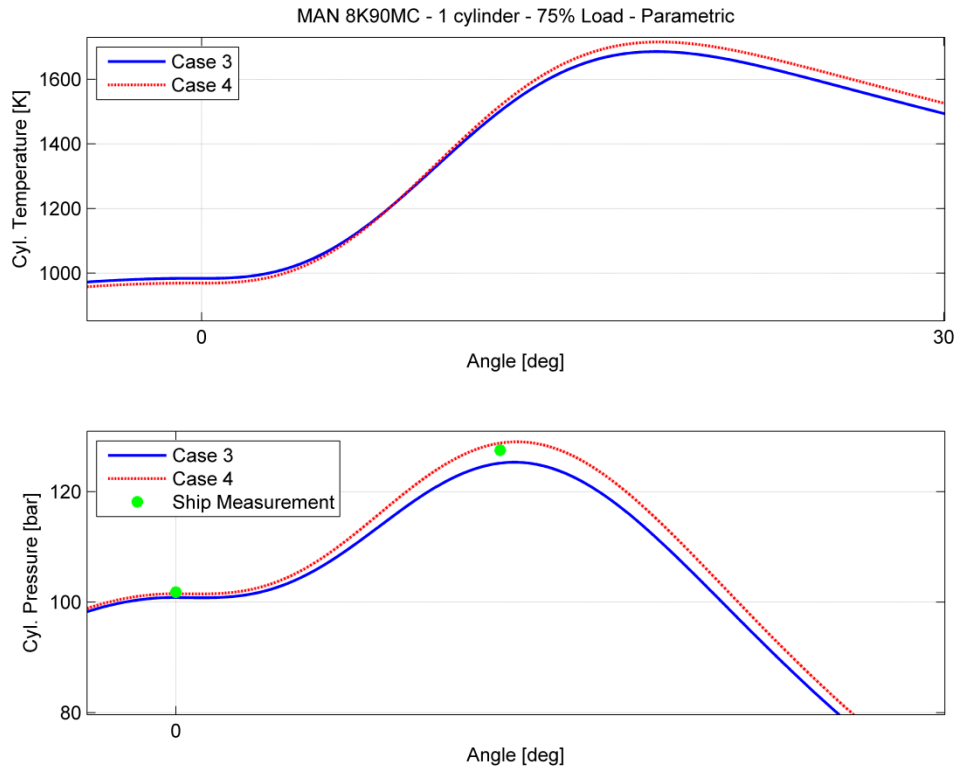
Ακολουθεί σύγκριση των αποτελεσμάτων για τις προσομοιώσεις των περιπτώσεων που βρίσκονται στους πίνακες 4,5.



**Εικόνα 4-12 Αναπτυσσόμενη θερμοκρασία (πάνω) και πίεση στον κύλινδρο για διαφορετική μάζα εγχυόμενου καυσίμου**



**Εικόνα 4-13 Αναπτυσσόμενη θερμοκρασία (πάνω) και πίεση στον κύλινδρο για διαφορετικό επιζήμιο όγκο**



**Εικόνα 4-14 Μεγαλύτερη ακρίβεια της Εικόνα 4-13**

Όπως φαίνεται στην Εικόνα 4-12 τα ίχνη της θερμοκρασίας και της πίεσης είναι τα ίδια για την περίπτωση 1 και 2. Επειδή όμως περισσότερη μάζα καυσίμου εγχύεται, προκαλείται αύξηση της μέγιστης πίεσης λόγω της καύσης. Αυτό εξηγείται από τον διαφορετικό ρυθμό καύσης λόγω της μεγαλύτερης μάζας ανά κύκλο που εγχύεται και επομένως εκλύεται μεγαλύτερη ενέργεια. Αυτό έχει ως άμεσο επακόλουθο σε δεδομένο όγκο να αυξηθεί η πίεση και η θερμοκρασία στο δοχείο.

Όπως φαίνεται στην Εικόνα 4-13 τα ίχνη πίεσης και θερμοκρασίας διαφέρουν από τα ίχνη που προέκυψαν από τα αντίστοιχα διαγράμματα για τον αρχικό (και πραγματικό) επιζήμιο όγκο της μοντελοποιημένης μηχανής. Στη περίπτωση 3 όπου ο επιζήμιος όγκος είναι μικρότερος από τον πραγματικό, παρατηρείται μεγαλύτερη πίεση συμπίεσης. Ακριβώς το αντίθετο παρατηρείται όταν αυξάνουμε τον επιζήμιο όγκο. Αυτό εξηγείται από το γεγονός ότι για κάθε μία περίπτωση έχουμε την ίδια εγκλωβισμένη μάζα για μεγαλύτερο ή μικρότερο όγκο έχουμε μικρότερη ή μεγαλύτερη πίεση και θερμοκρασία αντίστοιχα.

Το παράδειγμα αυτό αποδεικνύει πόσο εύκολο είναι στη συγκεκριμένη πλατφόρμα εναλλαγή των δεδομένων και της γεωμετρίας της μηχανής. Ταυτόχρονα επισημαίνει πως τυχόν λάθη στα δεδομένα εισόδου μπορούν να οδηγήσουν σε μη αποδεκτά αποτελέσματα.

## 5 Συμπεράσματα

Σε αυτή τη διπλωματική εργασία πραγματοποιήθηκε σπονδυλωτή μοντελοποίηση μίας ναυτικής εγκατάστασης πρόωσης και να δημιουργήθηκε μία βιβλιοθήκη με κλιμακούμενα κομμάτια και υποσυστήματα, με τρόπο εύκολο και επεκτάσιμο.

Οι βασικές θερμοδυναμικές εξισώσεις της πλήρους μηχανής μοντελοποιήθηκαν. Παρ' όλα αυτά, μόνο η προσομοίωση του κλειστού κύκλου ενός κυλίνδρου προσομοιώθηκε.

Στις προσομοιώσεις που πραγματοποιήθηκαν, χρησιμοποιήθηκαν αρκετές μέθοδοι ολοκλήρωσης, είτε μεταβλητού είτε σταθερού βήματος. Οι μέθοδοι αυτές είναι οι Euler, Heun, Runge-Kutta 4<sup>ης</sup> τάξης και Dorman-Prince. Οι μέθοδοι ολοκλήρωσης με μεταβλητό βήμα δεν μπορούν να εφαρμοστούν με επιτυχία σε αυτού του είδους τα μαθηματικά μοντέλα και στη θεώρηση της ομοιομορφίας των ιδιοτήτων (quasi steady models). Τα αποτελέσματα δε που προέκυψαν από τις δύο πρώτες μεθόδους ολοκλήρωσης κρίθηκαν μη αποδεκτά. Αντιθέτως η μέθοδος Runge - Kutta 4<sup>ης</sup> τάξης με αρχικό βήμα 0.02 δευτερόλεπτα, παρήγαγε καλύτερα αποτελέσματα αλλά μη σταθερή λύση. Μετά από σειρά δοκιμών, το συμπέρασμα που αντλήθηκε ήταν ότι βήμα 0.0001 δευτερολέπτων με μέθοδο ολοκλήρωσης Runge-Kutta 4<sup>ης</sup> τάξης είναι το βέλτιστο για την πλατφόρμα του MATLAB/Simulink για αυτού του είδους της προσομοιώσεις.

Αυτό το κείμενο είχε ως σκοπό να εμβαθύνει στην δουλειά που είχε γίνει σχετικά με την σπονδυλωτή προσομοίωση ναυτικών υποσυστημάτων πρόωσης, του Λαμπρόπουλου (Lambrououlos, 2000). Επιπλέον είχε ως σκοπό να εισάγει μία νέα πλατφόρμα προσομοιώσεων, ικανοποιητικής ακρίβειας, για ναυτικά συστήματα πρόωσης.

Απαιτείται ακόμα αρκετή δουλειά, προκειμένου να προσομοιωθεί η λειτουργία μίας πλήρους μηχανής. Επίσης τα μαθηματικά μοντέλα που αναπτύχθηκαν στη διπλωματική εργασία επιδέχονται προσθήκες και πιθανές αντικαταστάσεις με μερικά πιο σύνθετα, όπως για παράδειγμα στην περίπτωση ενός σύνθετου μοντέλου καύσης. Η εισαγωγή του μοντέλου των Woschni - Ansits όπως και η μοντελοποίηση έγχυσης καυσίμου πολλαπλών ζωνών, μπορεί να εισαχθεί στην βιβλιοθήκη, προκειμένου να μπορεί να προσομοιωθεί μεγαλύτερος αριθμός μηχανών εσωτερικής καύσης.

## 6 Βιβλιογραφία

- Borman, G. L., & Krieger, R. B. (1966). The computation of Apparent Heat Release for Internal Combustion Engines. *American Society of Mechanical Engineers (ASME), 66WA/DPG-11* .
- Dabney, J. B., & Harman, T. L. (2004). *Mastering Simulink*. Upper Saddle River, NJ 0745: Pearson Prentice Hall.
- Gunter, M. P., Schwarz, C., Stiesch, G., & Otto, F. (2006). *Simulating Combustion*. Berlin: Springer.
- Heywood, J. B. (1988). *Internal combustion Engine Fundamentals*. Massachusetts: Mc Graw Hill.
- Lambropoulos, V. P. (2000, March). Modular Simulation of Marine Propulsion Systems. *Ph.D. Thesis* . Athens.
- LME. (2008). Motor Thermodynamics Users Manual version 1.7. Athens, Greece.
- Mathworks. (2002). Building an S - Function. Mathworks Inc.
- Metz, J., Urban, A., & Steiger, A. (1967). Determination of Woschni Coefficients. *IMechE Vol 182* , σσ. 89-90.
- Newhall, H. K., & Starkman, E. S. (1963). Thermodynamic Properties of Octane and Air for Engine Performance. *SAE Technical Paper Series 633G* .
- Watson, N., & Janota, M. (1982). *Turbocharging the internal combustion engines*. London: Macmillan.
- Κυρτάτος, Ν. (1993). *Ναυτικοί κινητήρες Diesel*. Συμμετρία.